3SM - Impacts of 1.5ºC Global Warming on Natural and Human Systems
Supplemantary Material

Coordinating Lead Authors: Ove Hoegh-Guldberg (Australia), Daniela Jacob (Germany), Michael Taylor (Jamaica)

Lead Authors: Marco Bindi (Italy), Sally Brown (United Kingdom), Ines Camilloni (Argentina), Arona Diedhiou (Senegal), Riyanti Djalante (Indonesia), Kristie L. Ebi (United States of America), Francois Engelbrecht (South Africa), Joel Guiot (France), Yasuaki Hijioka (Japan), Shagun Mehrotra (United States of America/India), Antony Payne (United Kingdom), Sonia I. Seneviratne (Switzerland), Adelle Thomas (Bahamas), Rachel Warren (United Kingdom), Guangsheng Zhou (China)

Contributing Authors: Sharina Abdul Halim (Malaysia), Michelle Achlatis (Greece), Lisa V. Alexander (Australia), Myles Allen (United Kingdom), Peter Berry (Canada), Christopher Boyer (United States of America), Lorenzo Brilli (Italy), Marcos Buckeridge (Brazil), Edward Byers (Austria/Brazil), William Cheung (Canada), Marlies Craig (South Africa), Neville Ellis (Australia), Jason Evans (Australia), Hubertus Fisher (Switzerland), Klaus Fraedrich (Germany), Sabine Fuss (Germany), Anjani Ganase (Trinidad and Tobago), Jean Pierre Gattuso (France), Peter Greve (Germany/Austria), Tania Guillén Bolaños (Germany/Nicaragua), Naota Hanasaki (Japan), Tomoko Hasegawa (Japan), Katie Hayes (Canada), Annette Hirsch (Australia/Switzerland), Chris Jones (United Kingdom), Thomas Jung (Germany), Makku Kanninen (Finland), Gerhard Krinner (France), David Lawrence (United States of America), Tim Lenton (United Kingdom), Debora Ley (Guatemala/Mexico), Diana Liverman (United States of America), Natalie Mahowald (United States of America), Kathleen McInnes (Australia), Katrin J. Meissner (Australia), Richard Millar (United Kingdom), Katja Mintenbeck (Germany), Dann Mitchell (United Kingdom), Alan C. Mix (United States), Dirk Notz (Germany), Leonard Nurse (Barbados), Andrew Okem (Nigeria), Lennart Olsson (Sweden), Michael Oppenheimer (United States of America), Shlomit Paz (Israel), Juliane Petersen (Germany), Jan Petzold (Germany), Swantje Preuschmann (Germany), Mohammad Feisal Rahman (Bangladesh), Joeri Rogelj (Austria/Belgium), Hanna Scheuffele (Germany), Carl-Friedrich Schleussner (Germany), Daniel Scott (Canada), Roland Séférian (France), Jana Sillmann (Germany/Norway), Chandni Singh (India), Raphael Slade (United Kingdom), Kimberly Stephensen (Jamaica), Tannecia Stephenson (Jamaica), Mouhamadou B. Sylla (Senegal), Mark Tebboth (United Kingdom), Petra Tschakert (Australia), Robert Vautard (France), Richard Wartenburger (Germany/Switzerland), Michael Wehner (United States of America), Nora M. Weyer (Germany), Felicia Whyte (Jamaica), Gary Yohe (United States of America), Xuebin Zhang (Canada), Robert B. Zougmoré (Burkina Faso/Mali)

Review Editors: Jose Antonio Marengo (Brazil), Joy Pereira (Malaysia), Boris Sherstyukov (Russian Federation)

Chapter Scientist: Tania Guillén Bolaños (Germany/Nicaragua)

Note: this version is subject to final layout and proof read.

This Supplementary Material should be cited as:

O. Hoegh-Guldberg, D. Jacob, M. Taylor, M. Bindi, S. Brown, I. Camilloni, A. Diedhiou, R. Djalante, K. L. Ebi, F. Engelbrecht, J. Guiot, Y. Hijioka, S. Mehrotra, A. Payne, S. I. Seneviratne, A. Thomas, R. Warren, G. Zhou, 2018, Impacts of 1.5ºC Global Warming on Natural and Human Systems Supplementary Material. In: *Global warming of 1.5°C. An IPCC Special Report on the impacts of global warming of 1.5°C above pre-industrial levels and related global greenhouse gas emission pathways, in the context of strengthening the global response to the threat of climate change, sustainable development, and efforts to eradicate poverty* [V. Masson-Delmotte, P. Zhai, H. O. Pörtner, D. Roberts, J. Skea, P.R. Shukla, A. Pirani, W. Moufouma-Okia, C. Péan, R. Pidcock, S. Connors, J. B. R. Matthews, Y. Chen, X. Zhou, M. I. Gomis, E. Lonnoy, T. Maycock, M. Tignor, T. Waterfield (eds.)]. Available from https://www.ipcc.ch/sr15

3.SM.1 Supplementary information to Section 3.2

3.SM.1.1 Climate Models and Associated Simulations Available for the Present Assessment

Climate models allow for policy-relevant calculations such as the assessment of the levels of carbon dioxide (CO_2) and other greenhouse gas (GHG) emissions compatible with a specified climate stabilization target, such as the 1.5°C or 2°C global warming scenarios. Climate models are numerical models that can be of varying complexity and resolution (e.g., Le Treut et al. 2007). Presently, global climate models are typically Earth System Models (ESMs), in that they entail a comprehensive representation of Earth system processes, including biogeochemical processes.

In order to assess the impact and risk of projected climate changes on ecosystems or human systems, typical ESM simulations have a resolution that is too coarse – 100 km or more in many cases. Different approaches can be used to derive higher-resolution information. In some cases, ESMs can be run globally with very-high resolution; however, such simulations are cost-intensive and thus very rare. Another approach is to use regional climate models (RCM) to dynamically downscale the ESM simulations. RCMs are limited-area models with representations of climate processes comparable to those in the atmospheric and land surface components of the global models but with a higher resolution than 100 km – generally down to 10–50 km (e.g., Coordinated Regional Climate Downscaling Experiment, CORDEX; Giorgi and Gutowski 2015; Jacob et al. 2014; Cloke et al. 2013; Erfanian et al. 2016; Barlow et al. 2016) and in some cases even higher (convection permitting models, i.e., less than 4 km, e.g., Kendon et al. 2014; Ban et al. 2014; Prein et al. 2015). Statistical downscaling is another approach for downscaling information from global climate models to higher resolution. Its underlying principle is to develop statistical relationships that link large-scale atmospheric variables with local/regional climate variables, and to apply them to coarser-resolution models (Salameh et al. 2009; Su et al. 2016). Nonetheless, at the time of writing, there are only very few studies for 1.5°C climate that use regional climate models or statistical downscaling. One exception is an extension of the IMPACT2C project for Europe (see below).

There are various sources of climate model information available for the present assessment. There are global simulations that have been used in previous IPCC assessments and which were computed as part of the World Climate Research Programme (WCRP) Coupled Model Intercomparison Project (CMIP). The IPCC Fourth Assessment Report (AR4) and Special Report on Managing the Risks of Extreme Events and Disasters to Advance Climate Change Adaptation (SREX) were mostly based on simulations from the CMIP3 experiment, while the AR5 was mostly based on simulations from the CMIP5 experiment. Simulations of the CMIP3 and CMIP5 experiments were found to be very similar (e.g., Knutti and Sedláček 2012; Mueller and Seneviratne 2014).

In addition to the CMIP3 and CMIP5 experiments, there are results from CORDEX which are available for different regions (Giorgi and Gutowski 2015). For instance, assessments based on publications from an extension of the IMPACT2C project (Vautard et al. 2014; Jacob and Solman 2017) have recently become available for projections associated with global warming of 1.5°C.

Simulations from the Half a degree Additional warming, Prognosis and Projected Impacts (HAPPI) multimodel experiment have also been run to specifically assess climate changes at 1.5°C versus 2°C global warming (Mitchell et al. 2017). The HAPPI protocol consists of coupled land-atmosphere initial condition ensemble simulations with prescribed sea surface temperatures (SSTs), sea ice, GHG and aerosol concentrations and solar and volcanic activity that coincide with three forced climate states: present-day (2006–2015), future (2091–2100) and either with 1.5°C or 2°C global warming (prescribed from the modified SST conditions).

Beside climate models, other models are available to assess changes in regional and global climate systems (e.g., models for sea level rise, models for floods, droughts and freshwater input to oceans, cryosphere/snow models, models for sea ice, as well as models for glaciers and ice sheets). Analyses of impacts in 1.5°C and 2°C warmer climates (relative to the pre-industrial period) using such models include, for example, Schleussner et al. (2016) and publications from the Inter-Sectoral Impact Model Intercomparison Project (ISIMIP) (Warszawski et al. 2014), which have recently derived new analyses dedicated to assessments for responses to 1.5ºC and 2ºC global warming.

3.SM.1.2 Methods for the Attribution of Observed Changes in Climate and Their Relevance for Assessing Projected Changes at 1.5°C or 2°C Global Warming

As highlighted in previous IPCC reports, detection and attribution is an approach which is typically applied to assess impacts of GHG forcing on observed changes in climate (e.g., Hegerl et al. 2007; Seneviratne et al. 2012; Bindoff et al. 2013). For more background on this topic, the reader is referred to these past IPCC reports, as well as to the IPCC Good Practice Guidance Paper on Detection and Attribution related to Anthropogenic Climate Change (Hegerl et al. 2010). It is noted that in the IPCC Working Group I (WGI) framework, 'attribution' is focused on the 'attribution to anthropogenic greenhouse gas forcing' (e.g., Bindoff et al. 2013b). In past IPCC Working Groups II (WGII) reports, attribution of observed impacts were also made to regional changes in climate, but without consideration of whether the patterns of changes in regional climate had had a detectable influence from GHG forcing. As noted in Section 3.2.2, a recent study (Hansen and Stone 2016) shows that most of the detected temperature-related impacts that were reported in AR5 (Cramer et al. 2014) can be attributed to anthropogenic climate change, while the signals for precipitation-induced responses are more ambiguous.

Attribution to anthropogenic GHG forcing is an important field of research for the assessments of projected changes at 1.5°C and 2°C global warming in this report (see Section 3.3, and in particular Table 3.2). Indeed, observed global warming compared to the pre-industrial conditions up to the 2006–2015 decade was 0.87°C, and approximately 1ºC at around 2017 (Chapter 1; Section 3.2). Thus, 'climate at 1.5°C global warming' corresponds to the addition of approximately half a degree of global warming compared to present-day temperatures, and observed regional climate changes and impacts associated with a ca. 0.5°C global warming can be inferred from the historical record (although there could be non-linear changes at higher levels of warming, see Sections 3.2.1 and 3.2.2). This means that methods applied in the attribution of climate changes to human influences can be relevant for assessments of changes in climate with 1.5°C global warming, especially in cases where no climate model simulations or analyses are available for the conducted assessments. Indeed, impacts at 1.5°C global warming can be assessed in part from regional and global climate changes that have already been detected and attributed to human influence (e.g., Schleussner et al. 2017). This is because changes that could already be ascribed to anthropogenic GHG forcing pinpoint components of the climate system which are most responsive to this forcing, and thus will continue to be under 1.5°C or 2°C global warming. For this reason, when specific projections are missing for 1.5°C global warming, some of the assessments provided in Section 3.3 (in particular in Table 3.2) build upon joint assessments of (i) changes that were observed and attributed to human influence up to present, that is, for 1°C global warming or less, and (ii) projections for higher levels of warming (e.g., 2°C, 3°C or 4°C) to assess the most likely changes at 1.5°C. Such assessments are for transient changes only (Section 3.2.1). Evidence from attribution analyses can also be considered in the assessment of the reliability of climate projections for 1.5°C and 2°C global warming.

3.SM.1.3 The Propagation of Uncertainties from Climate Forcings to Impacts on the Ecosystems

The uncertainties associated with future projections of climate change are calculated using ensembles of model simulations (Flato et al. 2013). However, models are not fully independent, and the use of model spread as an estimator of uncertainty has been called into question (Annan and Hargreaves 2017). Many studies have been devoted to this issue, which is highly relevant to policymakers. The sources of uncertainty are diverse (Rougier and Goldstein 2014), and they must be identified to better determine the limits of predictions. The following list includes several key sources of uncertainty:

1. Input uncertainties include a lack of knowledge about the boundary conditions and the noise affecting the forcing variables;
2. Parametric and structural uncertainties are related to the lack of knowledge about some processes (i.e., those that are highly complex or operate at very fine scales) and the lack of clear information about the parameterisations used in models and the differences among the models. It has also been shown that different combinations of parameters can yield plausible simulations (Mauritsen et al. 2012);
3. Observational errors include noise and the unknown covariance structure in the data used;
4. Scale uncertainty originates from the fact that impact studies require a finer scale than ESM outputs can provide (Khan and Coulibaly 2010);
5. The offline coupling of climate-impact models introduces uncertainty because this coupling permits only a limited number of linkage variables and does not allow the representation of key feedbacks. This procedure may cause a lack of coherence between the linked climate and impact models (Meinshausen et al. 2011);
6. Important biases also include the consequences of tuning using a restricted range of climate states, that is, the periods from which climate data are available. Large biases in projections may be produced when future forcings are very different to those used for tuning; and
7. It is also assumed that ESMs yield adequate estimates of climate, except for an unknown translation (Rougier and Goldstein 2014). Usually this translation is estimated by performing an anomaly correction (the difference between the control simulation and the observed field). Such correction represents an additional uncertainty that is often ignored in the final estimate of the error bars.

Due to these uncertainties in the formulation, parametrisation and initial states of models, any individual simulation represents only one step in the pathway followed by the climate system (Flato et al. 2013). The assessment of these uncertainties must therefore be done in a probabilistic way. It is particularly important when the signal to noise ratio is weak, as it could be when assessing the difference of risks between 1.5°C and 2°C global warming.

References

Annan, J. D., and J. C. Hargreaves, 2017: On the meaning of independence in climate science. Earth Syst. Dyn., 8, 211–224, doi:10.5194/esd-8-211-2017.

Ban, N., J. Schmidli, and C. Schär, 2014: Evaluation of the convection-resolving regional climate modeling approach in decade-long simulations. J. Geophys. Res. Atmos., 119, 7889–7907, doi:10.1002/2014JD021478. http://doi.wiley.com/10.1002/2014JD021478 (Accessed April 6, 2017).

Barlow, M., and Coauthors, 2016: A Review of Drought in the Middle East and Southwest Asia. J. Clim., 29, 8547–8574, doi:10.1175/JCLI-D-13-00692.1. http://journals.ametsoc.org/doi/10.1175/JCLI-D-13-00692.1 (Accessed March 22, 2017).

Bindoff, N. L., and Coauthors, 2013a: Detection and Attribution of Climate Change: from Global to Regional - Supplementary Material. Climate Change 2013: The Physical Science Basis. Contribution of Working Group I to the Fifth Assessment Report of the Intergovernmental Panel on Climate Change, T.F. Stocker et al., Eds., p. 25 http://www.climatechange2013.org/.

——, and Coauthors, 2013b: Detection and Attribution of Climate Change: from Global to Regional. Climate Change 2013: The Physical Science Basis. Contribution of Working Group I to the Fifth Assessment Report of the Intergovernmental Panel on Climate Change, T.F. Stocker et al., Eds., 867–952.

Cloke, H. L., F. Wetterhall, Y. He, J. E. Freer, and F. Pappenberger, 2013: Modelling climate impact on floods with ensemble climate projections. Q. J. R. Meteorol. Soc., 139, 282–297, doi:10.1002/qj.1998. http://doi.wiley.com/10.1002/qj.1998 (Accessed March 22, 2017).

Cramer, W., and Coauthors, 2014: Detection and Attribution of Observed Impacts. Climate Change 2014: Impacts, Adaptation, and Vulnerability. Part A: Global and Sectoral Aspects. Contribution of Working Group II to the Fifth Assessment Report of the Intergovernmental Panel on Climate Change, C.B. Field, V.R. Barros, D.J. Dokken, K.J. Mach, and M.D. Mastrandrea, Eds., Cambridge University Press, Cambridge, United Kingdom and New York, NY, USA, 979–1037 http://ebooks.cambridge.org/ref/id/CBO9781107415379A039 (Accessed June 25, 2017).

Erfanian, A., G. Wang, M. Yu, and R. Anyah, 2016: Multimodel ensemble simulations of present and future climates over West Africa: Impacts of vegetation dynamics. J. Adv. Model. Earth Syst., 8, 1411–1431,

doi:10.1002/2016MS000660. http://doi.wiley.com/10.1002/2016MS000660 (Accessed March 22, 2017).
Flato, G., and Coauthors, 2013: Evaluation of Climate Models. Climate Change 2013: The Physical Science Basis. Contribution of Working Group I to the Fifth Assessment Report of the Intergovernmental Panel on Climate Change, T.F. Stocker et al., Eds., Cambridge University Press, Cambridge, United Kingdom and New York, NY, USA, 741–866.
Giorgi, F., and W. J. Gutowski, 2015: Regional Dynamical Downscaling and the CORDEX Initiative. Annu. Rev. Environ. Resour., 40, 467–490, doi:10.1146/annurev-environ-102014-021217. http://www.annualreviews.org/doi/10.1146/annurev-environ-102014-021217 (Accessed July 14, 2017).
Hansen, G., and D. Stone, 2016: Assessing the observed impact of anthropogenic climate change. Nat. Clim. Chang., 6, 532–537, doi:10.1038/nclimate2896.
Hegerl, G. C., and Coauthors, 2007: Understanding and Attributing Climate Change. Climate Change 2007: The Physical Science Basis. Contribution of Working Group I to the Fourth Assessment Report of the Intergovernmental Panel on Climate Change, S. Solomon, D. Qin, M. Manning, Z. Chen, M. Marquis, K.B. Averyt, M. Tignor, and H.L. Miller, Eds., Cambridge University Press, Cambridge, United Kingdom and New York, NY, USA, 663–745.
——, O. Hoegh-Guldberg, G. Casassa, M. P. Hoerling, R. S. Kovats, C. Parmesan, D. W. Pierce, and P. A. Stott, 2010: Good Practice Guidance Paper on Detection and Attribution Related to Anthropogenic Climate Change. Meeting Report of the Intergovernmental Panel on Climate Change Expert Meeting on Detection and Attribution of Anthropogenic Climate Change, T.F. Stocker, C.B. Field, D. Qin, V. Barros, G.-K. Plattner, M. Tignor, P.M. Midgley, and K.L. Ebi, Eds., IPCC Working Group I Technical Support Unit, University of Bern, Bern, Switzerland, p. 9 http://www.ipcc-wg2.awi.de/guidancepaper/IPCC_D&A_GoodPracticeGuidancePaper.pdf.
Jacob, D., and S. Solman, 2017: IMPACT2C – An introduction. Clim. Serv., 7, 1–2, doi:https://doi.org/10.1016/j.cliser.2017.07.006. http://www.sciencedirect.com/science/article/pii/S2405880717300870.
——, and Coauthors, 2014: EURO-CORDEX: new high-resolution climate change projections for European impact research. Reg. Environ. Chang., 14, 563–578, doi:10.1007/s10113-013-0499-2. http://link.springer.com/10.1007/s10113-013-0499-2 (Accessed March 22, 2017).
Kendon, E. J., N. M. Roberts, H. J. Fowler, M. J. Roberts, S. C. Chan, and C. A. Senior, 2014: Heavier summer downpours with climate change revealed by weather forecast resolution model. Nat. Clim. Chang., 4, 570–576, doi:10.1038/nclimate2258. http://www.nature.com/doifinder/10.1038/nclimate2258 (Accessed April 6, 2017).
Khan, M. S., and P. Coulibaly, 2010: Assessing Hydrologic Impact of Climate Change with Uncertainty Estimates: Bayesian Neural Network Approach. J. Hydrometeorol., 11, 482–495, doi:10.1175/2009JHM1160.1.
Knutti, R., and J. Sedláček, 2012: Robustness and uncertainties in the new CMIP5 climate model projections. Nat. Clim. Chang., 3, 369–373, doi:10.1038/nclimate1716. http://www.nature.com/doifinder/10.1038/nclimate1716.
Mauritsen, T., and Coauthors, 2012: Tuning the climate of a global model. J. Adv. Model. Earth Syst., 4, 1–18, doi:10.1029/2012MS000154.
Meinshausen, M., T. M. L. Wigley, and S. C. B. Raper, 2011: Emulating atmosphere-ocean and carbon cycle models with a simpler model, MAGICC6 - Part 2: Applications. Atmos. Chem. Phys., 11, 1457–1471, doi:10.5194/acp-11-1457-2011.
Mitchell, D., and Coauthors, 2017: Half a degree additional warming, prognosis and projected impacts (HAPPI): background and experimental design. Geosci. Model Dev., 10, 571–583, doi:10.5194/gmd-10-571-2017. www.geosci-model-dev.net/10/571/2017/ (Accessed April 6, 2017).
Mueller, B., and S. I. Seneviratne, 2014: Systematic land climate and evapotranspiration biases in CMIP5 simulations. Geophys. Res. Lett., 41, 128–134, doi:10.1002/2013GL058055. http://doi.wiley.com/10.1002/2013GL058055 (Accessed July 7, 2017).
Prein, A. F., and Coauthors, 2015: A review on regional convection-permitting climate modeling: Demonstrations, prospects, and challenges. Rev. Geophys., 53, 323–361, doi:10.1002/2014RG000475. http://doi.wiley.com/10.1002/2014RG000475 (Accessed April 6, 2017).
Rougier, J., and M. Goldstein, 2014: Climate Simulators and Climate Projections. Annu. Rev. Stat. Its Appl., 1, 103–123, doi:10.1146/annurev-statistics-022513-115652.
Salameh, T., P. Drobinski, M. Vrac, and P. Naveau, 2009: Statistical downscaling of near-surface wind over complex terrain in southern France. Meteorol. Atmos. Phys., 103, 253–265, doi:10.1007/s00703-008-0330-7. http://link.springer.com/10.1007/s00703-008-0330-7 (Accessed March 22, 2017).
Schleussner, C.-F., and Coauthors, 2016: Differential climate impacts for policy-relevant limits to global warming: The case of 1.5°C and 2°C. Earth Syst. Dyn., 7, 327–351, doi:10.5194/esd-7-327-2016.

Schleussner, C.-F., P. Pfleiderer, and E. M. Fischer, 2017: In the observational record half a degree matters. Nat. Clim. Chang., 7, 460–462. https://www.nature.com/articles/nclimate3320.
Seneviratne, S. I., and Coauthors, 2012: Changes in Climate Extremes and their Impacts on the Natural Physical Environment. Managing the Risks of Extreme Events and Disasters to Advance Climate Change Adaptation. A Special Report of Working Groups I and II of IPCC Intergovernmental Panel on Climate Change, C.B. Field et al., Eds., Cambridge University Press, Cambridge, United Kingdom and New York, NY, USA, 109–230 https://www.ipcc.ch/pdf/special-reports/srex/SREX-Chap3_FINAL.pdf.
Su, B., J. Huang, M. Gemmer, D. Jian, H. Tao, T. Jiang, and C. Zhao, 2016: Statistical downscaling of CMIP5 multi-model ensemble for projected changes of climate in the Indus River Basin. Atmos. Res., 178–179, 138–149, doi:10.1016/j.atmosres.2016.03.023. http://linkinghub.elsevier.com/retrieve/pii/S0169809516300850 (Accessed March 22, 2017).
Le Treut, H., R. Somerville, U. Cubasch, Y. Ding, C. Mauritzen, A. Mokssit, T. Peterson, and M. . Prathe, 2007: Historical Overview of Climate Change. Climate Change 2007: The Physical Science Basis. Contribution of Working Group I to the Fourth Assessment Report of the Intergovernmental Panel on Climate Change, S. Solomon, D. Qin, M. Manning, Z. Chen, M. Marquis, K.B. Averyt, M. Tignor, and H.L. Miller, Eds., Cambridge University Press, Cambridge, United Kingdom and New York, NY, USA, 93–128 https://www.ipcc.ch/pdf/assessment-report/ar4/wg1/ar4-wg1-chapter1.pdf.
Vautard, R., and Coauthors, 2014: The European climate under a 2 °C global warming. Environ. Res. Lett., 9, 034006, doi:10.1088/1748-9326/9/3/034006. http://stacks.iop.org/1748-9326/9/i=3/a=034006?key=crossref.3587f26000b4f1e5cccbcb7c216cfea4 (Accessed July 22, 2017).
Warszawski, L., K. Frieler, V. Huber, F. Piontek, O. Serdeczny, and J. Schewe, 2014: The Inter-Sectoral Impact Model Intercomparison Project (ISI-MIP): project framework. Proc. Natl. Acad. Sci. U. S. A., 111, 3228–3232, doi:10.1073/pnas.1312330110. http://www.ncbi.nlm.nih.gov/pubmed/24344316 (Accessed July 20, 2017).

3.SM.2 Supplementary Information to Section 3.3

3.SM.2.1 Change in Global Climate

The Global Mean Surface Temperature (GMST) increase reached approximately 1°C above pre-industrial levels in 2017 (Haustein et al. 2017; see also Chapter 1). At the time of writing the AR5 WGI report (i.e., for time frames up to 2012; Stocker et al. 2013), Hartmann et al. (2013) assessed that the globally averaged combined land and ocean surface temperature data as calculated by a linear trend showed a warming of 0.85°C (0.65°C–1.06°C) over the period 1880–2012, when multiple independently produced datasets existed, and about 0.72°C (0.49°C –0.89°C) over the period 1951–2012. Hence most of the global warming has occurred since 1950, and it has continued substantially in recent years. The above values are for global mean warming; however, regional trends can be much more varied (Figure S3.1). With few exceptions, most land regions display stronger trends in the global mean warming, and by 2012, that is, with a warming of about 0.85°C (see above), some land regions already displayed warming higher than 1.5°C (Figure 3.SM.1).

It should be noted that more recent evaluations of the observational record suggest that the estimates of global warming at the time of the AR5 may have been underestimated (Cowtan and Way, 2014; Richardson et al., 2016). Indeed, as highlighted in Section 3.3.1 and also discussed in Chapter 1, sampling biases and different approaches to estimate GMST (e.g., using water versus air temperature over oceans) can sensibly impact estimates of GMST increase as well as differences between model simulations and observations-based estimates (Richardson et al., 2016). It should be noted that studies analyzing projected changes in extremes as a function of GMST generally use surface air temperature on both land and oceans (e.g., Fischer and Knutti, 2015; Seneviratne et al., 2016; Mitchell et al., 2017; Wartenburger et al., 2017; Kharin et al., 2018) rather than a blend of ocean surface temperature and surface air temperature over land (Chapter 1).

As highlighted in Chapter 1, an area in which substantial new literature has become available since the AR5 is the GMST trend over the period 1998–2012, which has been referred to by some as the 'global warming hiatus' (Stocker et al., 2013; Karl et al., 2015; Lewandowsky et al., 2016; Medhaug et al., 2017). This term was used to refer to an apparent slowdown of GMST increase over that time period (although other climate variables continued to display unabated changes during that period, including a particular intense warming of hot extremes over land; Seneviratne et al. 2014). Medhaug et al. (2017) noted that from a climate point of view, with 2015 and 2016 being the two warmest years on record in early 2017 (based on GMST), the question of whether 'global warming has stopped' was no longer present in the public debate. Nonetheless, the related literature is relevant for the assessment of changes in climate at 1.5°C global warming, since this event illustrates the possibility that the global temperature response may be decoupled from the radiative forcing over short time periods. While this may be associated with cooler global temperatures as experienced during the incorrectly labeled hiatus period, this implies that there could also be time periods with global warming higher than 1.5°C even if the radiative forcing would be consistent with a global warming of 1.5°C in the long-term average. Recent publications have highlighted that the 'slow down' in global temperature warming that occurred in the time frame of the hiatus episode was possibly overestimated at the time of the AR5 due to issues with data corrections, in particular related to coverage (Cowtan and Way 2014; Karl et al. 2015; Figure 3.SM.2). This has some relevance for the definition of a '1.5°C climate' (see Chapter 1 and Cross-Chapter Box 8 in Chapter 3 on 1.5°C warmer worlds). Overall, the issue of internal climate variability is the reason why a 1.5°C warming level needs to be determined in terms of 'human-induced warming' (see Chapter 1 for additional background on this issue).

A large fraction of the detected global warming has been attributed to anthropogenic forcing (Bindoff et al., 2013b). The AR5 (Bindoff et al., 2013b) assessed that it is *virtually certain* that human influence has warmed the global climate system and that it is *extremely likely* that human activities caused more than half of the observed increase in GMST from 1951 to 2010 (supplementary Figure 3.SM.3). The AR5 (Bindoff et al., 2013b) assessed that GHGs contributed a GMST increase *likely* to be between

0.5°C and 1.3°C over the period 1951–2010, with the contributions from other anthropogenic forcings *likely* to lie between –0.6°C and 0.1°C, from natural forcings *likely* to be between –0.1°C and 0.1°C, and from internal variability *likely* to be between –0.1°C and 0.1°C. Regarding observed global changes in temperature extremes, reports from the AR5 cycle assessed that since 1950 it is *very likely* that there has been an overall decrease in the number of cold days and nights and an overall increase in the number of warm days and nights at the global scale, that is, for land areas with sufficient data (Seneviratne et al., 2012; Hartmann et al., 2013). This assessment is confirmed as part of the present report and highlights that further decreases in cold extremes and increases in hot extremes are projected for a global warming of 1.5°C.

Observed global changes in the water cycle, including precipitation, are more uncertain than observed changes in temperature (Hartmann et al., 2013; Stocker et al., 2013). The AR5 assessed that it is *very likely* that global near surface and tropospheric air specific humidity have increased since the 1970s (Hartmann et al., 2013). However, AR5 also highlighted that during recent years the near surface moistening over land has abated (*medium confidence*), and that as a result, there have been fairly widespread decreases in relative humidity near the surface over the land in recent years (Hartmann et al., 2013). With respect to precipitation, some regional precipitation trends appear to be robust (Stocker et al., 2013), but when virtually all the land area is filled in using a reconstruction method, the resulting time series of global mean land precipitation shows little change since 1900. Hartmann et al. (2013) highlight that confidence in precipitation change averaged over global land areas since 1901 is low for years prior to 1951 and medium after 1951. However, for averages over the mid-latitude land areas of the Northern Hemisphere, Hartmann et al. (2013) assessed that precipitation had likely increased since 1901 (*medium confidence* before and *high confidence* after 1951). For other latitudinal zones, area-averaged long-term positive or negative trends have *low confidence* due to data quality, data completeness or disagreement amongst available estimates (Hartmann et al., 2013). For heavy precipitation, the AR5 assessed that in land regions where observational coverage was sufficient for assessment, there was *medium confidence* that anthropogenic forcing had contributed to a global-scale intensification of heavy precipitation over the second half of the 20th century (Bindoff et al., 2013b).

Figures 3.SM.4 and 3.SM.5 display the same analyses as the left-hand panels of Figures 3.3 and 3.4 in the main text, but based on Representative Concentration Pathway (RCP)2.6 simulations instead of RCP8.5.

3.SM.2.2 Regional Temperature on Land, Including Extremes

3.SM.2.2.1 Observed and Attributed Changes in Regional Temperature Means and Extremes

While the quality of temperature measurements obtained through ground observational networks tend to be high compared to that of measurements for other climate variables (Seneviratne et al., 2012), it should be noted that some regions are undersampled. Cowtan and Way (2014) highlighted issues regarding undersampling being concentrated at the Poles and over Africa, which may lead to biases in estimated changes in GMST (see also Section 3.3.2 and Chapter 1). This undersampling also affects the confidence of assessments regarding regional observed and projected changes in both mean and extreme temperature.

Despite this partly limited coverage, the attribution chapter of the AR5 (Bindoff et al., 2013b) and recent papers (e.g., Sun et al. 2016; Wan et al. 2018) assessed that over every continental region and in many sub-continental regions, anthropogenic influence has made a substantial contribution to surface temperature increases since the mid-20th century. For Antarctica, while changes are occurring, statistical assessment (presumably to 95% confidence) has not been achieved due primarily to the large natural variability in the weather that occurs there and the comparatively short observational record.

Regarding observed regional changes in temperature extremes, the AR5 (Hartmann et al. 2013) provided the following assessment based in part on the IPCC Special Report on Managing the Risks of

Extreme Events and Disasters to Advance Climate Change Adaptation (SREX - Seneviratne et al., 2012):

- *Likely (high confidence)* overall increases in warm days and warm nights, and decreases in cold days and cold nights in North America and Central America, Europe and Mediterranean region, in Asia, in Southeast Asia and Oceania (including Australia), and in southern Africa
- *Medium confidence* overall increases in warm days and warm nights, and decreases in cold days and cold nights in South America, and North Africa and Middle East
- *Low to medium confidence* in some African regions lacking observations, but locations with observations display increases in warm days and warm nights, and decreases in cold days and cold nights.

Further, the IPCC SREX (Seneviratne et al. 2012) assessed that globally, in many (but not all) regions with sufficient data there is *medium confidence* that the length and the number of warm spells or heat waves has increased since the middle of the 20th century, and that it is *likely* that anthropogenic influences have led to warming of extreme daily minimum and maximum temperatures at the global scale.

Hence, observed and attributed changes in both mean and extreme temperature consistently point to a widespread influence of human-induced warming in most land regions. Also, there are new publications regarding observed trends in temperature and precipitation means and extremes in Africa (e.g., Ringard et al. 2016; Moron et al. 2016; Omondi et al. 2013; MacKellar et al. 2014), which may allow an increase in the confidence regarding observed changes on this continent.

Specific attribution statements for changes associated with a global warming of 0.5°C are currently not available on a regional scale from the literature, unlike global assessments (Schleussner et al. 2017), although preliminary results suggest that a 0.5°C global warming can also be identified for temperature extremes in a few large regions (Europe, Asia, Russia, North America; see supplementary material of Schleussner et al. 2017).

As highlighted in Section 3.2, the observational record can be used to assess past changes associated with a global warming of 0.5°C, with this type of assessment being considered as an analogue for the difference between a scenario at 1.5°C and at 2°C global warming. This approach has its limitations. For example, the methodology does not account for non-linearity in responses, including possible regional or global tipping points. Nonetheless, it can provide a first assessment of aspects of the climate system that have been identified as being sensitive to a global warming change of this magnitude. Schleussner et al. (2017), using this approach, assessed observed changes in extreme indices for the 1991–2010 versus the 1960–1979 period, which corresponds to about 0.5°C GMST difference in the observed record (based on the Goddard Institute for Space Studies Surface Temperature Analysis GISTEMP dataset, Hansen et al. 2010). They found that substantial changes due to 0.5°C warming are apparent for indices related to hot and cold extremes, as well as for the Warm Spell Duration Indicator (WSDI). Some results are displayed in Figures S3.6 and S3.7. Using two well-established observational datasets – Hadley Centre Global Climate Extremes Index 2 (HadEX2) and Global Historical Climatology Network (GHCN)-Daily climate Extremes (GHCNDEX); Donat et al. (2013a,b) – these analyses show that one quarter of the land has experienced an intensification of hot extremes (annual maximum value of daily maximum temperature; TXx) by more than 1°C and a reduction of the intensity of cold extremes by at least 2.5°C (annual minimum value of daily minimum temperature; TNn). Half of the global land mass has experienced changes in WSDI of more than six days, and the emergence of extremes outside the range of natural variability is particularly pronounced for this duration-based indicator (Figure 3.7). Results for TXx based on reanalysis products are similar for the 20th century reanalysis (20CR) product, but even more pronounced for the European Centre for Medium-Range Weather Forecasts (ECMWF) reanalyses (referred to as “ERA”), as noted by Schleussner et al. 2017; however, results based on reanalysis products need to be considered with caution since they are partly a modelling product, and also assimilate datasets of different length. Overall, based on the analysis of Schleussner et al. (2017), the observational record suggests that a 0.5°C change in global warming has noticeable global impacts on temperature extremes.

3.SM.2.2.2 Projected Changes at 1.5°C versus 2°C in Regional Temperature Means and Extremes

This supplementary information provides more detailed material as background for the assessment of Section 3.3.2.2.

As noted in Section 3.3.2.2., there is a stronger warming of the regional land-based hot extremes compared to the mean global temperature warming in most land regions (also discussed in Seneviratne et al. 2016). The regions displaying the stronger contrast are central North America, eastern North America, Central Europe, southern Europe/Mediterranean, western Asia, Central Asia and southern Africa. As highlighted in Vogel et al. (2017), these regions are characterized by transitional climate regimes between dry and wet climates, which are associated with strong soil-moisture–temperature coupling (related to a transitional soil-moisture regime; Koster et al. 2004; Seneviratne et al. 2010). Several of these regions display enhanced drying under enhanced GHG forcing (see Section 3.3.4), which leads to a decrease of evaporative cooling and an additional regional warming compared to the global temperature response. In a recent study, Karmalkar and Bradley (2017) also found consistent results for the contiguous United States, with all subregions projected to reach 2°C approximately between 10 and 20 years before the global mean temperature.

In general, these transitional climate regions also show the largest spread in temperature extremes response, likely related to the impact of the soil-moisture–temperature coupling for the overall response. This spread is due to both intermodel variations in the representation of drying trends (see also Section 3.3.4; Orlowsky and Seneviratne 2013; Greve and Seneviratne 2015) and to differences in soil-moisture–temperature coupling in climate models (Seneviratne et al., 2013; Stegehuis et al., 2013; Sippel et al., 2016), whereby feedbacks with clouds and surface radiation are also relevant (Cheruy et al., 2014). Furthermore, in some regions internal climate variability can also explain the spread in projections (Deser et al., 2012). Regions with the most striking spread in projections of hot extremes include Central Europe, with projected regional TXx warming at 1.5°C, ranging from 1°C to 5°C warming, and central North America, which displays projected changes at 1.5°C global warming, ranging from no warming to 4°C warming.

Regarding results from regional studies, Vautard et al. (2014) report that most of Europe will experience higher warming than the global average with strong distributional patterns across Europe for global warming of 2°C, which is consistent with the present assessment for 1.5°C warming (Jacob et al., 2018). For instance, a north–south (west–east) warming gradient is found for summer (winter) along with a general increase and summer extreme temperatures.

It should be noted that recent evidence suggests that climate models overestimate the strength of soil-moisture–temperature coupling in transitional climate regions, although it is not clear if this behaviour would lead to an overestimation of projected changes in hot temperatures (Sippel et al., 2016). In addition, there are discrepancies in projections from regional versus global climate models in Europe, possibly due to differences in prescribed aerosol concentrations (Bartók et al., 2017).

While the above-mentioned hot spots of changes in temperature extremes are located in transitional climate regimes between dry and wet climates, a recent study has also performed a separate analysis of changes in temperature extremes between 'drylands' and 'humid' lands, defining the first category based on mean precipitation lower than 600 mm and the ratio of mean Precipitation to Potential Evapo-Transpiration (P/PET) being lower than 0.65 (Huang et al., 2017). This study identifies that warming is much greater in 'drylands' compared to 'humid lands' (by 44%), although the latter are mostly responsible for GHG emissions that underlie this change.

Figure 3.5 in Chapter 3 displays projected changes in the TXx as a function of GMST for the main regions as specified in the IPCC SREX (see Figure 3.2 for a description of the regions) using Empirical Scaling Relationships (ESR; Section 3.2). The underlying model projections include

Coupled Model Intercomparison Project Phase 5 (CMIP5) multimodel global climate simulations (based on the analyses of Wartenburger et al. 2017 and Seneviratne et al. 2016) and simulations from the 'Half a degree Additional warming, Prognosis and Projected Impacts' (HAPPI) multimodel experiments (Mitchell et al. 2017; based on analyses presented in Seneviratne et al. 2018). The CMIP5 analyses provide continuous estimates of the dependency of the analysed climate extremes as functions of GMST, while the HAPPI-derived estimates are only available for the estimation of responses at two global warming levels, 1.5°C and 2°C. The CMIP5-based ESR analyses are computed from historical and RCP8.5 simulations from 26 CMIP5 global climate models (including up to 10 ensemble members per model). For the HAPPI analyses, changes in the indices and in the corresponding global mean temperatures (as indicated in the map and in the bar plots shown in the figures) are based on the 100 first ensemble members (#1 to #100) from five models (following Seneviratne et al. 2018): Canadian 4th generation Atmospheric global climate Model (CanAM4); Community Atmosphere Model version 4 (CAM4); European Center Hamburg model version 6-3-Default (Low) Resolution (ECHAM6-3-LR); Model for Interdisciplinary Research On Climate version 5 (MIROC5); and Norwegian Earth System Model version 1-HAPPI (NorESM1-HAPPI). For each of the HAPPI models and the two experiments considered (1.5°C relative to pre-industrial and 2°C relative to pre-industrial), differences were computed of the indices (scenario period – reference period, consisting of 10 years of data each per ensemble member); the reader is referred to the referenced publications for more background on the analyses and databases. Note that the ESR analyses are based on land data only for all of the considered regions, that is, with a mask being applied to ocean data within the considered regions. (Ocean datapoints are, however, included for analyses for island regions provided in this Supplementary Material, i.e., a subset of the regions indicated asterisks (*) in Figure 3.2; see e.g., Figure 3.SM.9 and similar).

Figure 3.SM.8 displays similar analyses as Figure 3.5 but for TNn. The mean response of these cold extremes displays less discrepancy with the global levels of warming (often close to the 1:1 line in many regions), however, there is a clear amplified warming in regions with snow and ice cover. This is expected given the Arctic warming amplification (Serreze and Barry 2011; see also AR5 overview on 'polar amplification': Masson-Delmotte et al. 2013; IPCC 2013) which is to a large extent due to snow-albedo-temperature feedbacks (Hall and Qu, 2006). In some regions and for some model simulations, the warming of TNn at 1.5°C global warming can reach up to 8°C regionally (e.g., northern Europe, Figure 3.SM.8), and thus be much larger than the global temperature warming.

Figures 3.SM.9 and 3.SM.10 display the same analyses as Figures 3.5 (main text) and 3.SM.8 for the regions indicated with asterisks in Figure 3.2. It should be noted that for the island regions, the land fraction is often too small to be resolved by standard global climate models. For this reason, as mentioned above, the analyses for island regions (indicated with # sign) are based on both land and ocean air temperatures and are representative of average climate conditions in the areas in which they are located.

Figure 3.SM.13 displays maps of changes in the number of hot days (NHD) and number of frost days (NFD) at 1.5°C and 2°C GMST increase. These analyses reveal clear patterns of changes between the two warming levels, with decreases in frost days in many regions.

3.SM.2.3 Regional Precipitation on Land, Including Heavy Precipitation and Monsoons

3.SM.2.3.1 Observed and Attributed Changes in Regional Precipitation

There is overall *low confidence* in observed trends for monsoons because of insufficient evidence (consistent with a previous assessment in the IPCC SREX, Seneviratne et al. 2012). There are, nonetheless, a few new assessments available, although they do not report consistent trends in different monsoon regions (Singh et al., 2014; Taylor et al., 2017; Bichet and Diedhiou, 2018). For instance, Singh et al. (2014) use precipitation observations (1951–2011) of the South Asian summer monsoon and show that there have been significant decreases in peak-season precipitation over the core-monsoon region and significant increases in daily-scale precipitation variability. Furthermore, Taylor et al. (2017) showed that over the west African Sahel, the frequency of extreme storms tripled since 1982 in satellite observations and Bichet and Diedhiou (2018) confirm that the region has been wetter during the last 30 years but dry spells are shorter and more frequent with a decreasing precipitation intensity in the western part (over Senegal). However, there is not sufficient evidence to provide higher than *low confidence* in the assessment of observations in overall trends in monsoons.

3.SM.2.3.2 Projected Changes at 1.5°C and 2°C in Regional Precipitation

The AR5 assessed that the global monsoon, aggregated over all monsoon systems, is likely to strengthen (Christensen et al., 2013). There are a few publications that provide more recent evaluations on projections of changes in monsoons for high-emissions scenarios. Jiang and Tian (2013), who compared the results of 31 and 29 reliable climate models under the Special Report on Emissions Scenarios (SRES) A1B scenario or the RCP4.5 scenario, respectively, found weak projected changes in the East Asian winter monsoon as a whole relative to the reference period (1980–1999). Regionally, they found a weakening north of about 25°N in East Asia and a strengthening south of this latitude, which resulted from atmospheric circulation changes over the western north Pacific Ocean and northeast Asia. This is linked to the weakening and northward shift of the Aleutian Low, and from decreased northwest–southeast thermal and sea level pressure differences across northeast Asia. In summer, Jiang and Tian (2013) found a projected strengthening (albeit, slight) of monsoon in east China over the 21st century as a consequence of an increased land–sea thermal contrast between the East Asian continent and the adjacent western north Pacific Ocean and South China Sea. Using six CMIP5 model simulations of the RCP8.5 high-emissions scenario, Jones and Carvalho (2013) found a 30% increase in the amplitude of the South American Monsoon System (SAMS) from the current level by 2045–2050. They also found an ensemble mean onset date of the SAMS which was 17 days earlier, and a demise date 17 days later, by 2045–2050. The most consistent CMIP5 projections analysed confirmed the increase in the total precipitation over southern Brazil, Uruguay and northern Argentina. Given that scenarios at 1.5°C or 2°C would include a substantially smaller radiative forcing than those assessed in the studies of Jiang and Tian (2013) and Jones and Carvalho (2013), there is *low confidence* regarding changes in monsoons at these low global warming levels, as well as regarding differences in responses at 1.5°C versus 2°C.

Several analyses of global circulation models (GCM-RCM) simulations in the framework of the Coordinated Regional Climate Downscaling Experiment for Africa (CORDEX-AFRICA) were performed to capture changes in the African climate system in a warmer climate. Sylla et al. (2015, 2016) analysed the response of the annual cycle of high-intensity daily precipitation events over West Africa to anthropogenic GHG for the late 21st century. The late-21st-century projected changes in mean precipitation exhibit a delay of the monsoon season and a decrease in frequency, but an increase in intensity of very wet events, particularly in the pre-monsoon and early mature monsoon stages, more pronounced in RCP8.5 over the Sahel and in RCP4.5 over the Gulf of Guinea. The pre-monsoon season also experiences the largest changes in daily precipitation statistics, with increased risk of drought associated with a decrease in mean precipitation and frequency of wet days and an increased risk of flood associated with very wet events. Weber et al. (2018) assessed the changes in temperature- and rainfall-related climate change indices in a 1.5°C, 2°C and 3°C global warming world for the Africa continent. The results showed the daily rainfall intensity is also projected to increase for higher global warming scenarios, especially for the sub-Saharan coastal regions.

Figure 3.SM.14 displays the same analyses as Figure 3.9 for the regions indicated with asterisks in Figure 3.2. For the underlying methodology, a similar approach was used as for Figure 3.5 (see Section 3.3.2.2).

3.SM.2.4 Drought and Dryness

Figure 3.SM.15 displays the same analyses as Figure 3.12 for the regions indicated with asterisks in Figure 3.2. For the underlying methodology, a similar approach was used as for Figure 3.5 (see Section 3.SM.3.2.2).

Supplementary Figures

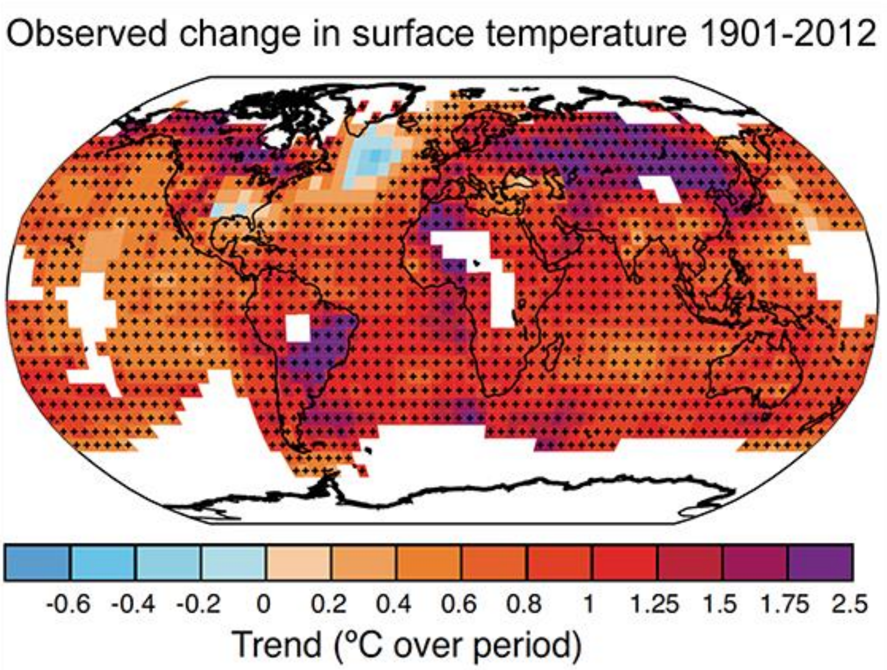

Figure 3.SM.1: Map of the observed surface temperature change from 1901 to 2012 derived from temperature trends determined by linear regression from one dataset. Trends have been calculated where data availability permits a robust estimate (i.e., only for grid boxes with greater than 70% complete records and more than 20% data availability in the first and last 10% of the time period). Other areas are white. Grid boxes where the trend is significant at the 10% level are indicated by a + sign. From Stocker et al. (2013).

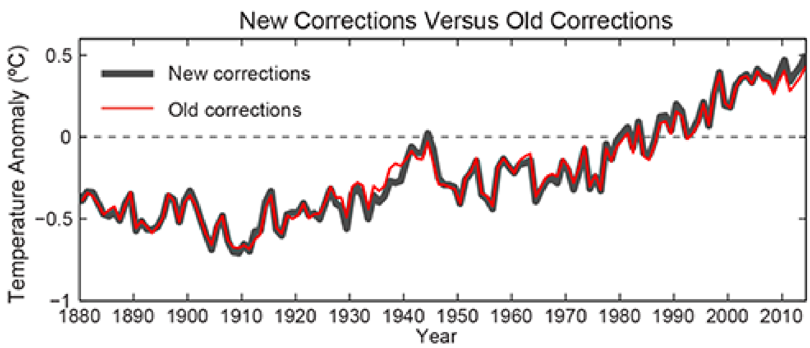

Figure 3.SM.2: Global temperature warming using older and newer corrections (Karl et al., 2015).

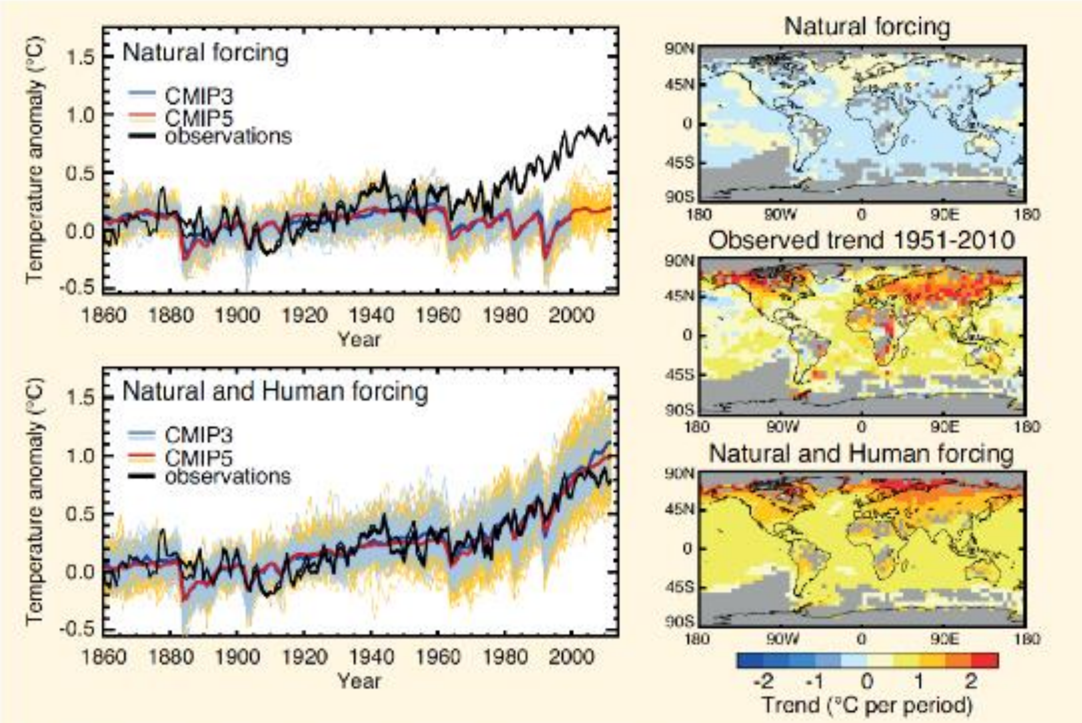

FAQ 10.1, Figure 1 | (Left) Time series of global and annual-averaged surface temperature change from 1860 to 2010. The top left panel shows results from two ensemble of climate models driven with just natural forcings, shown as thin blue and yellow lines; ensemble average temperature changes are thick blue and red lines. Three different observed estimates are shown as black lines. The lower left panel shows simulations by the same models, but driven with both natural forcing and human-induced changes in greenhouse gases and aerosols. (Right) Spatial patterns of local surface temperature trends from 1951 to 2010. The upper panel shows the pattern of trends from a large ensemble of Coupled Model Intercomparison Project Phase 5 (CMIP5) simulations driven with just natural forcings. The bottom panel shows trends from a corresponding ensemble of simulations driven with natural + human forcings. The middle panel shows the pattern of observed trends from the Hadley Centre/Climatic Research Unit gridded surface temperature data set 4 (HadCRUT4) during this period.

Figure 3.SM.3: Attribution of global warming change (from IPCC AR5, Bindoff et al., 2013)

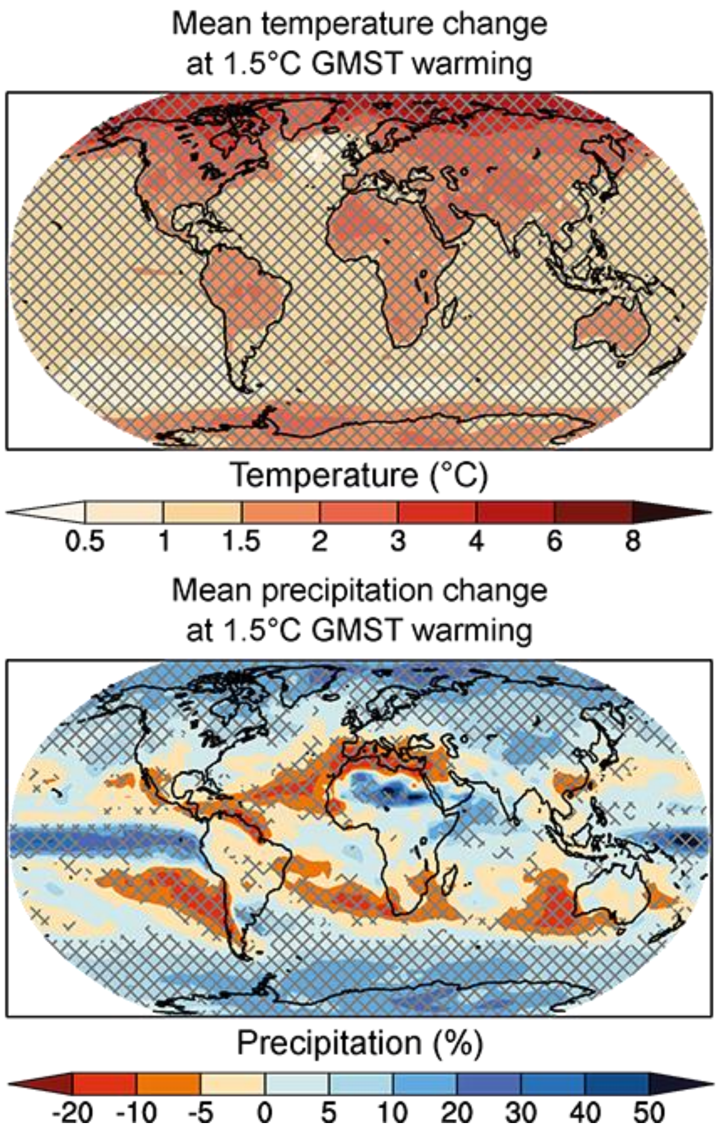

Figure 3.SM.4: Same as left-hand plots of Figure 3.3, but based on Representative Concentration Pathway (RCP)2.6 scenarios.

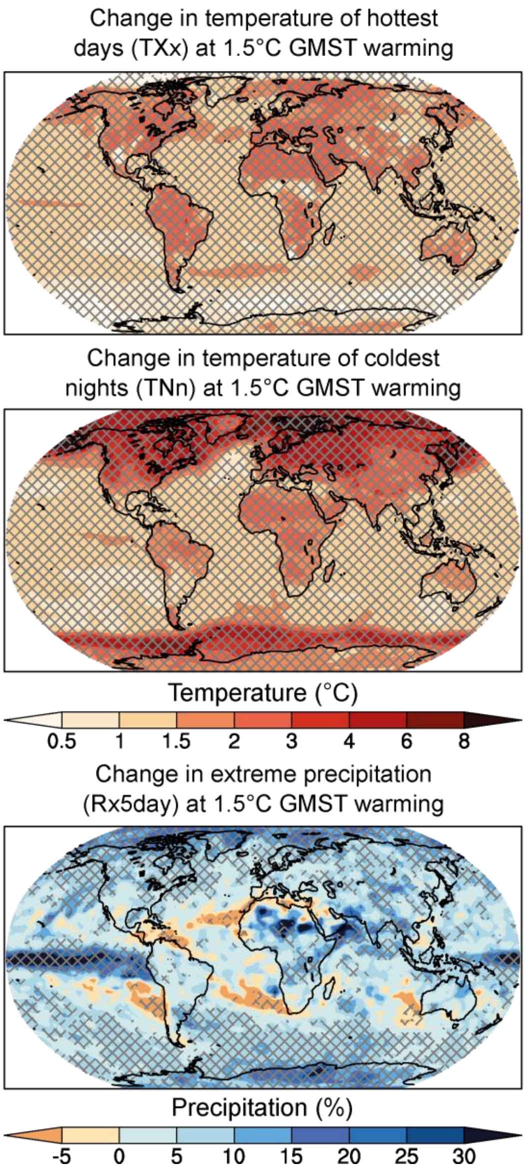

Figure 3.SM.5: Same as left-hand plot of Figure 3.4, but based on the Representative Concentration Pathway (RCP)2.6 scenarios.

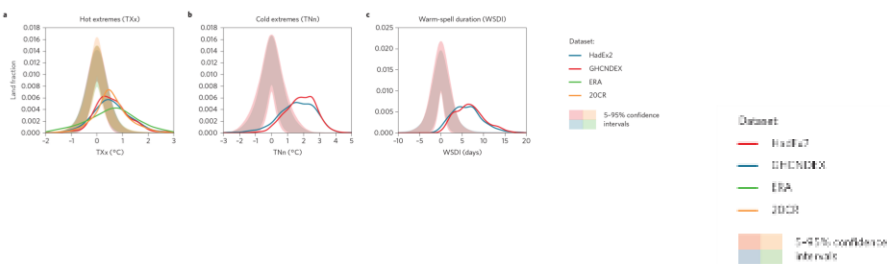

Figure 3.SM.6: Difference in extreme temperature event indices for 0.5°C warming over the observational record. Probability density functions show the globally aggregated land fraction that experienced a certain change between the 1991–2010 and 1960–1979 periods for the Hadley Centre Global Climate Extremes Index 2 (HadEX2) and Global Historical Climatology Network (GHCN)-Daily

climate Extremes (GHCNDEX) datasets. For annual maximum value of daily maximum temperature (TXx), the analysis also includes reanalysis data from the European Centre for Medium-Range Forecasts (ECMWF) (ECMWF Reanalysis 40 (ERA-40) and Interim (ERA-Interim), used as a combined dataset including ERA-40 until 1979 and ERA-Interim from 1979 onward) and the Twentieth Century Reanalysis (20CR) ERA and 20CR over the global land area. Light-coloured envelopes illustrate the changes expected by internal variability alone, estimated by statistically resampling individual years. From Schleussner et al. (2017).

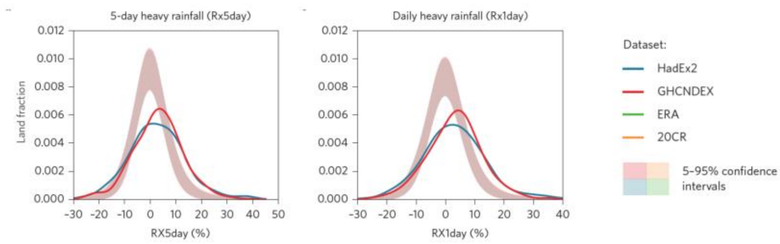

Figure 3.SM.7: Differences in extreme precipitation event indices for 0.5°C warming over the observational record. Probability density functions show the globally aggregated land fraction that experienced a certain change between the 1991–2010 and 1960–1979 periods for the HadEX2 and GHCNDEX datasets. Light-coloured envelopes illustrate the changes expected by internal variability alone, estimated by statistically resampling individual years. From Schleussner et al. (2017).

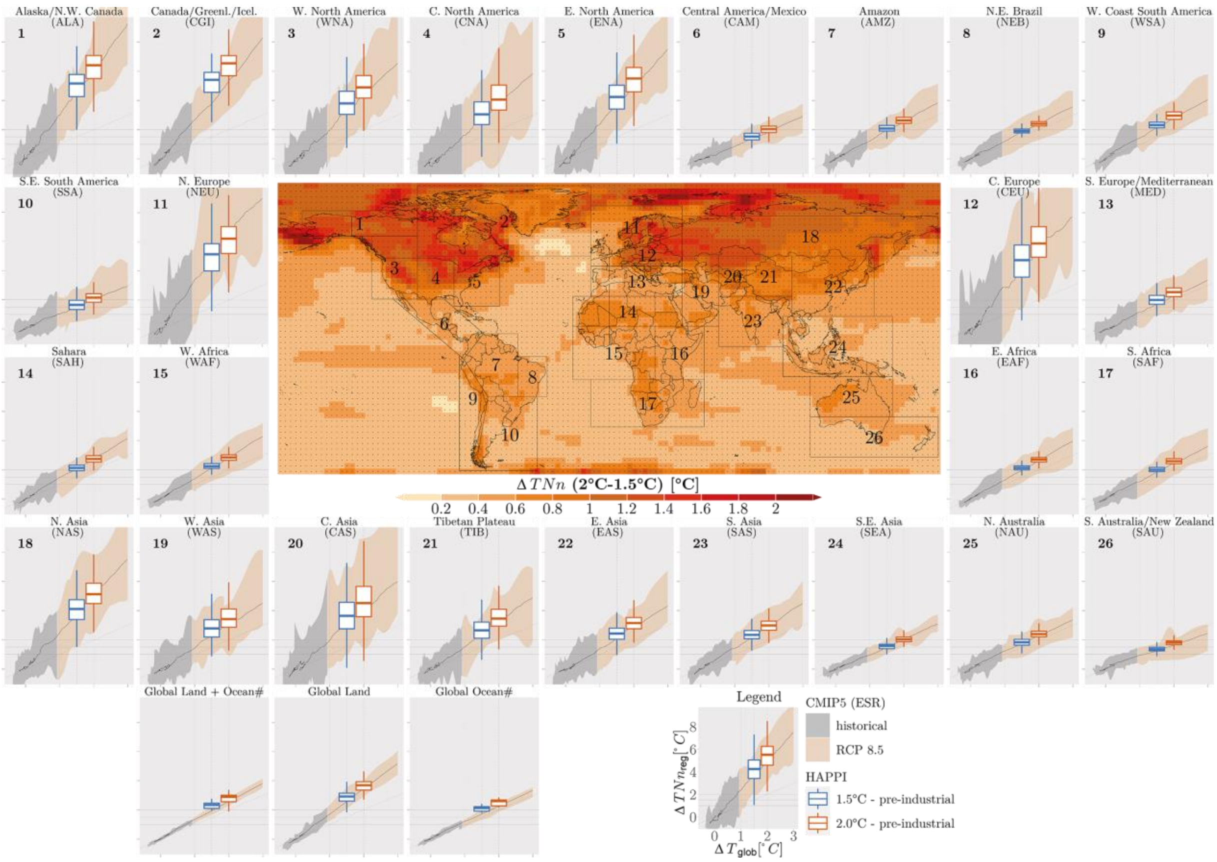

Figure 3.SM.8: Same analysis as Figure 3.5, but for the annual minimum value of daily minimum temperature (TNn). For more details on computation, see description of computation of Figure 3.5 in the present Annex, as well as Wartenburger et al. (2017), Seneviratne et al. (2016) and Seneviratne et al. (2018).

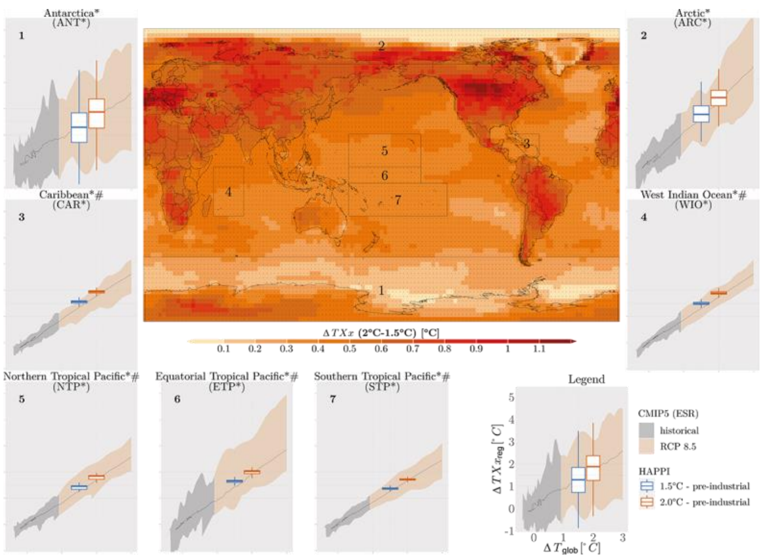

Figure 3.SM.9: Same analysis as Figure 3.5 (projected changes in annual maximum value of daily maximum temperature, TXx, as function of global temperature warming) for additional regions displayed with asterisks in Figure 3.2 (island regions, polar regions). Asterisks (*) indicate non-SREX reference regions (http://www.ipcc-data.org/guidelines/pages/ar5_regions.html). Hashtag (#) indicates island regions; for these regions, the ocean area was not masked out in the analyses. See description of computation of Figure 3.5 in the present Annex for more details.

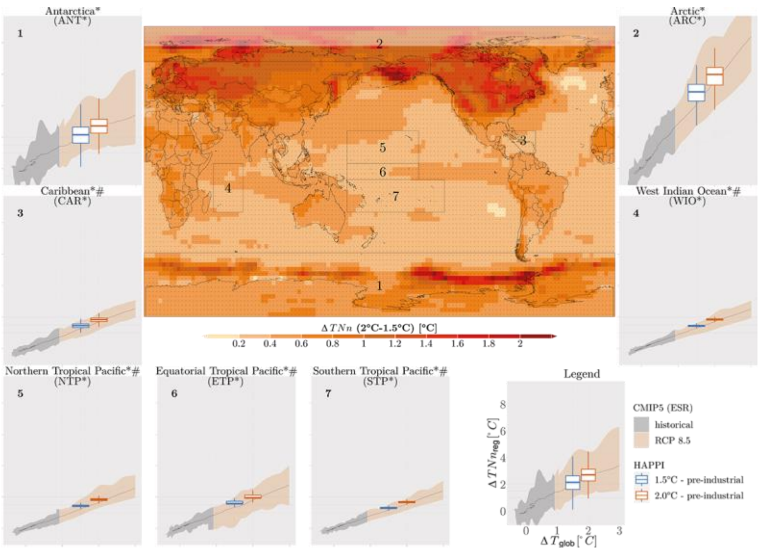

Figure 3.SM.10: Same analysis as Figure S3.8 (projected changes in TNn as function of global temperature warming) for additional regions displayed with asterisks in Figure 3.2 (island regions, polar regions). Asterisks (*) indicate non-SREX reference regions (http://www.ipcc-data.org/guidelines/pages/ar5_regions.html). Hashtag (#) indicates island regions; for these regions, the ocean area was not masked out in the analyses.

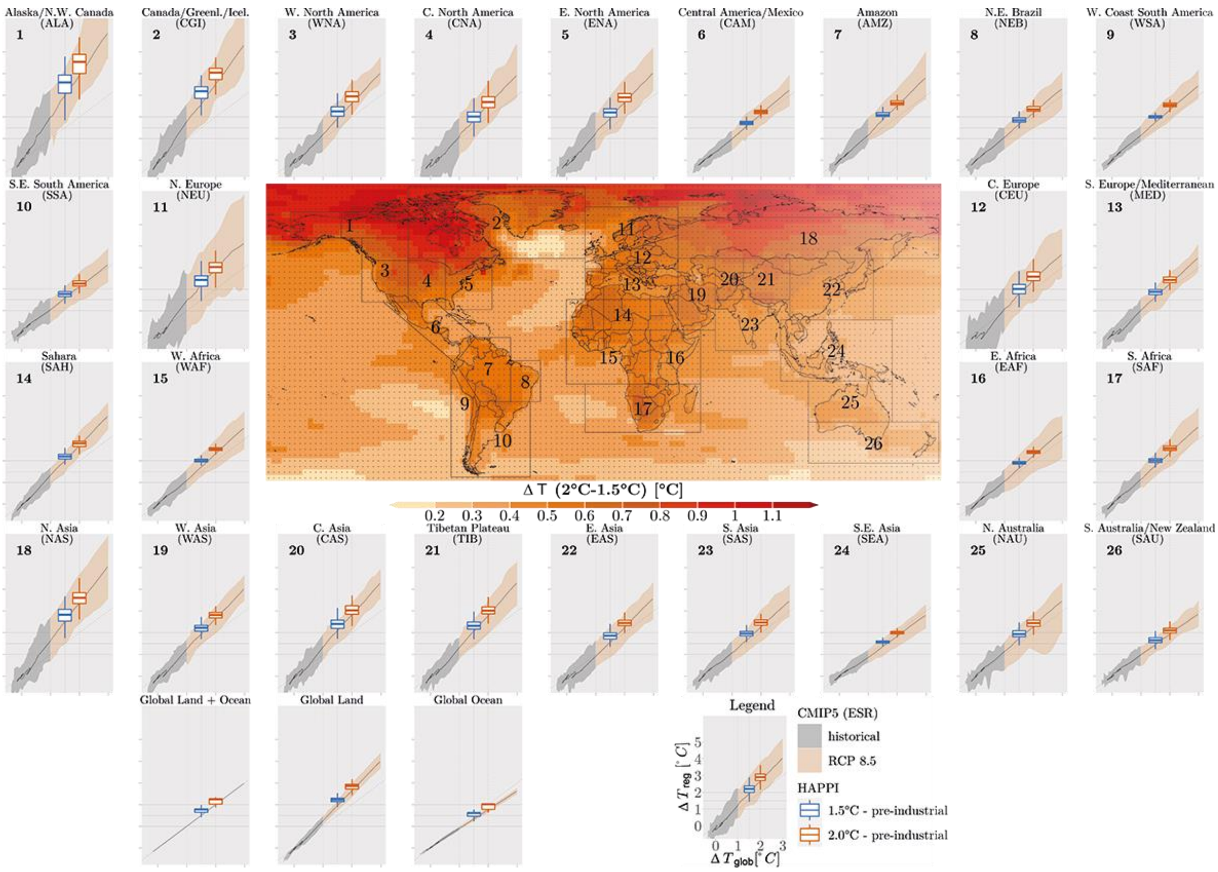

Figure 3.SM.11: Same analysis as Figure 3.5, but for the mean surface temperature (Tmean).

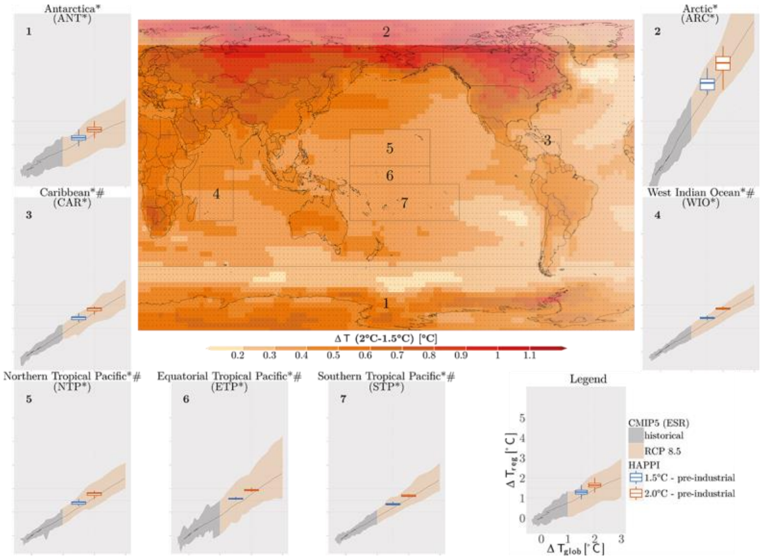

Figure 3.SM.12: Same analysis as Figure 3.SM.11 (projected in the changes in Tmean as function of the mean global temperature) for additional regions displayed with asterisks in Figure 3.2 (island regions, polar regions). Asterisks (*) indicate non-SREX reference regions (http://www.ipcc-data.org/guidelines/pages/ar5_regions.html). Hashtag (#) indicates island regions; for these regions, the ocean area was not masked out in the analyses.

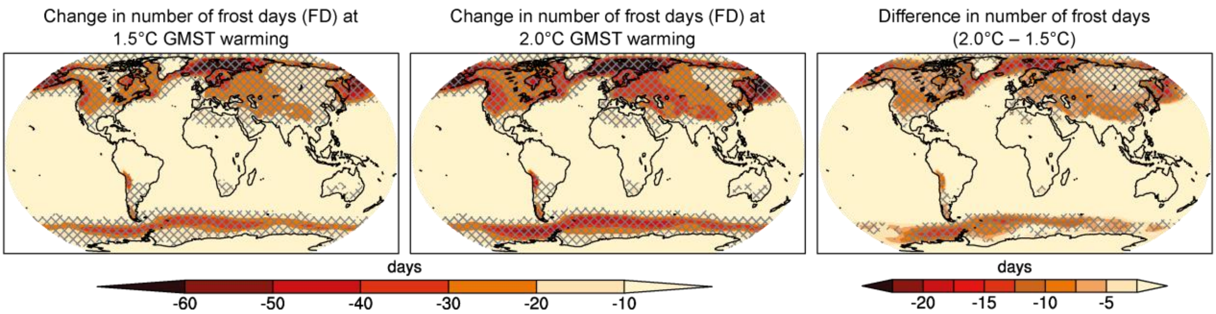

Figure 3.SM.13: Projected changes in number of frost days (days with T<0°C, bottom) at 1.5°C (left) and 2°C (middle) GMST increase, and their difference (right). Cross-hatching highlights areas in which at least 2/3rds of the models agree on the sign of change as a measure of robustness (18 or more out of 26). Adapted from Wartenburger et al. (2017).

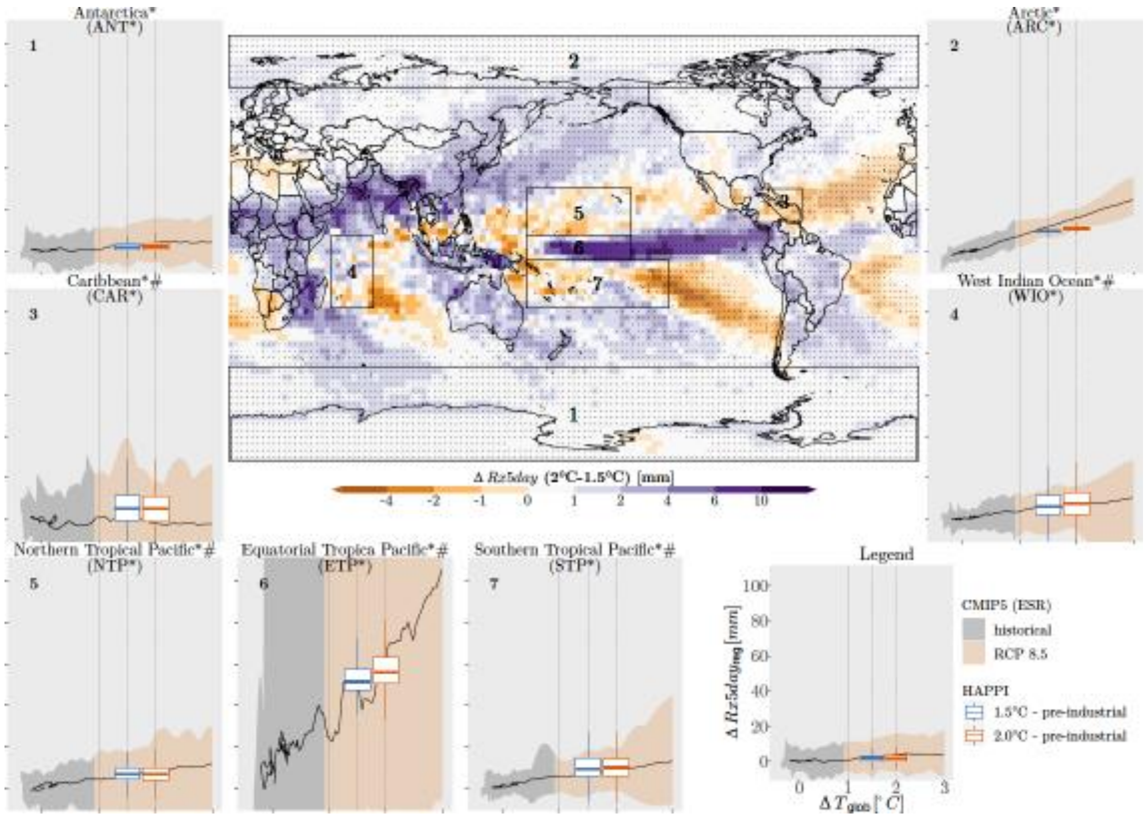

Figure 3.SM.14: Same analysis as Figure 3.9 for additional regions displayed with asterisks in Figure 3.2 (island regions, polar regions). Asterisks (*) indicate non-SREX reference regions (http://www.ipcc-data.org/guidelines/pages/ar5_regions.html). Hashtag (#) indicates island regions; for these regions, the ocean area was not masked out in the analyses.

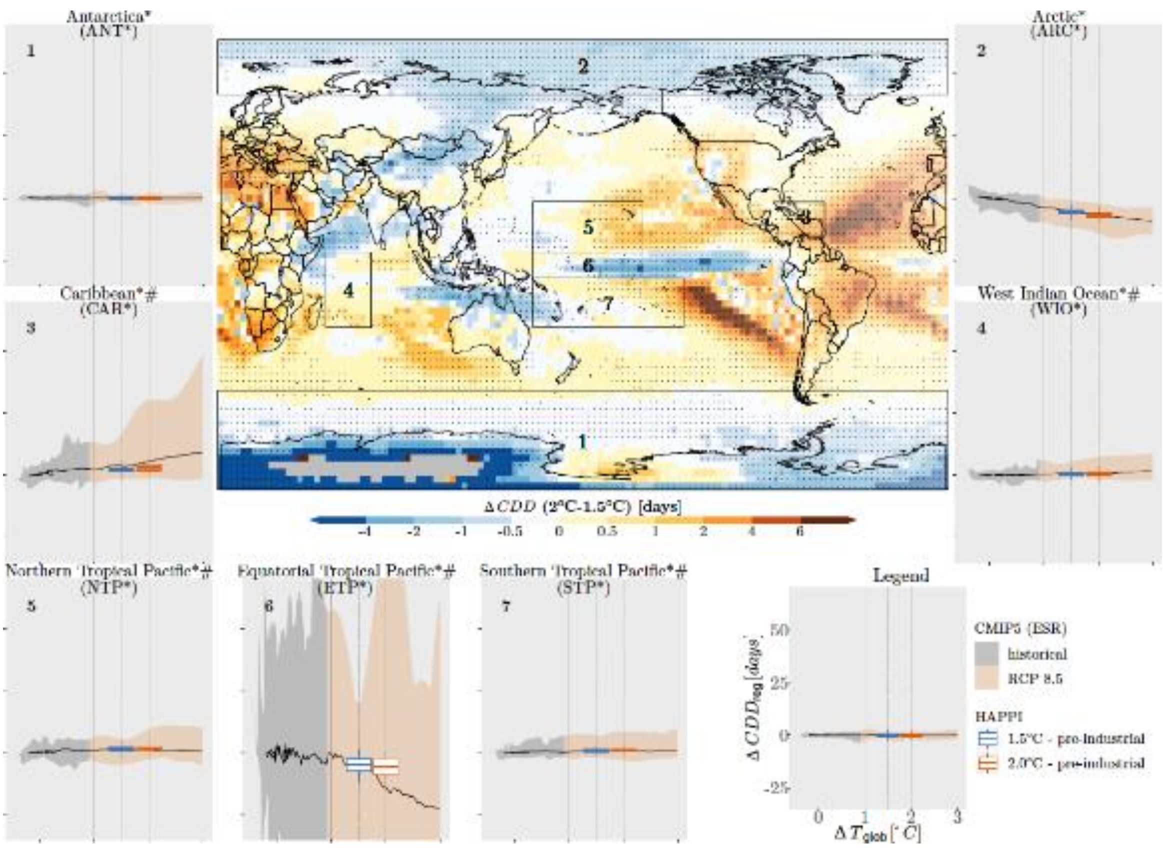

Figure 3.SM.15: Same analysis as Figure 3.12 for additional regions displayed with asterisks in Figure 3.2 (island regions, polar regions). Asterisks (*) indicate non-SREX reference regions (http://www.ipcc-data.org/guidelines/pages/ar5_regions.html). Hashtag (#) indicates island regions; for these regions, the ocean area was not masked out in the analyses.

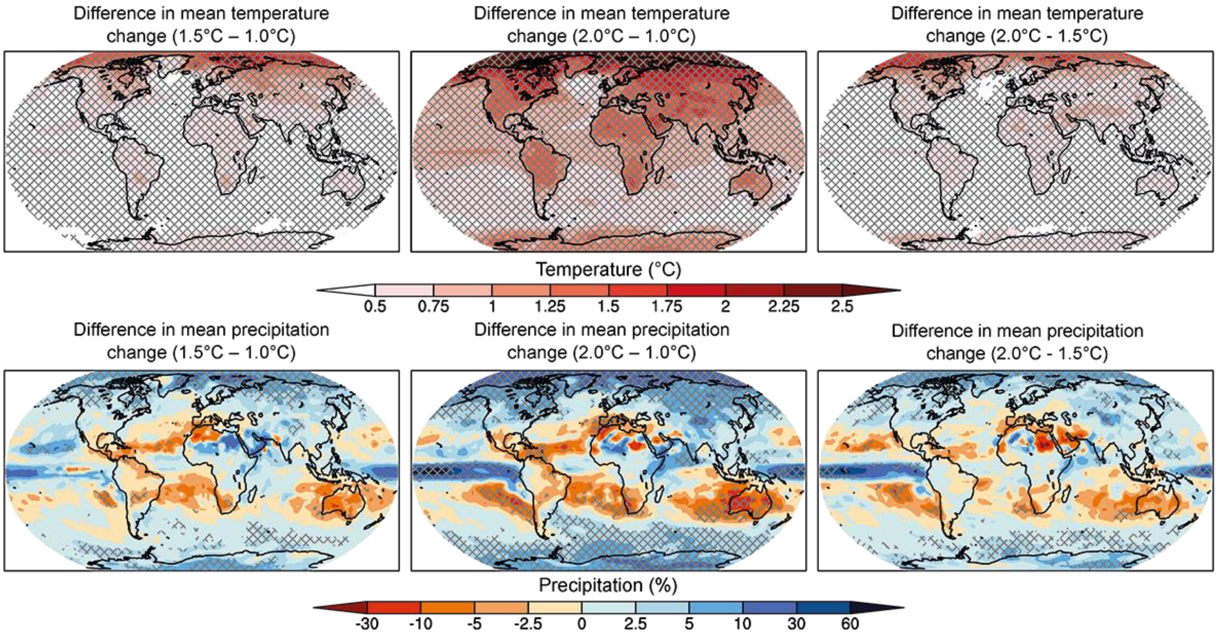

Figure 3.SM.16: Same as Figure 3.3 but for differences to 1°C global warming instead of pre-industrial conditions (left and middle plots).

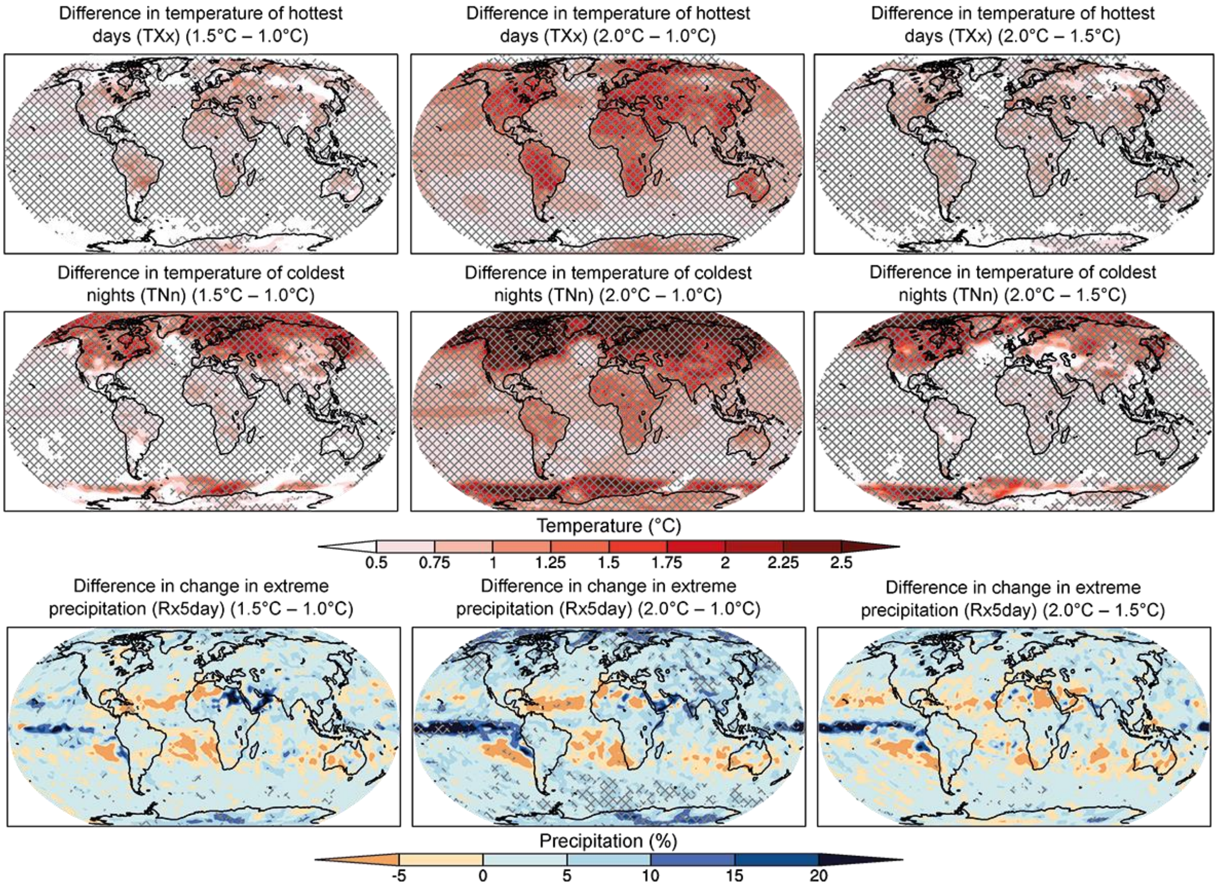

Figure 3.SM.17: Same as Figure 3.4 but for differences to 1°C global warming instead of pre-industrial conditions (left and middle plots).

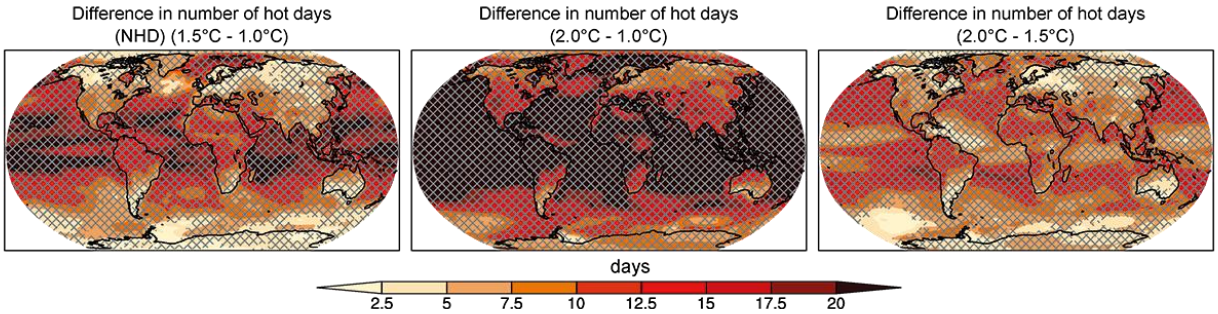

Figure 3.SM.18: Same as Figure 3.7 but for differences to 1°C global warming instead of pre-industrial conditions (left and middle plots).

References

Bartók, B., Wild, M., Folini, D., Lüthi, D., Kotlarski, S., Schär, C., et al. (2017). Projected changes in surface solar radiation in CMIP5 global climate models and in EURO-CORDEX regional climate models for Europe. Clim. Dyn. 49, 2665–2683. doi:10.1007/s00382-016-3471-2.

Bichet, A., and Diedhiou, A. (2018). West African Sahel becomes wetter during the last 30 years but dry spells are shorter and more frequent. Clim. Res. (in press). doi:10.3354/cr01515.

Bindoff, N. L., Stott, P. A., AchutaRao, K. M., Allen, M. R., Gillett, N., Gutzler, D., et al. (2013a). “Detection and Attribution of Climate Change: from Global to Regional,” in Climate Change 2013: The Physical Science Basis. Contribution of Working Group I to the Fifth Assessment Report of the Intergovernmental Panel on Climate Change, eds. T. F. Stocker, D. Qin, G.-K. Plattner, M. Tignor, S. K. Allen, J. Boschung, et al., 867–952.

Bindoff, N. L., Stott, P. A., AchutaRao, K. M., Allen, M. R., Gillett, N., Gutzler, D., et al. (2013b). “Detection and Attribution of Climate Change: from Global to Regional - Supplementary Material,” in Climate Change 2013: The Physical Science Basis. Contribution of Working Group I to the Fifth Assessment Report of the Intergovernmental Panel on Climate Change, eds. T. F. Stocker, D. Qin, G.-K. Plattner, M. Tignor, S. K. Allen, J. Boschung, et al., 25. Available at: http://www.climatechange2013.org/.

Cheruy, F., Dufresne, J. L., Hourdin, F., and Ducharne, A. (2014). Role of clouds and land-atmosphere coupling in midlatitude continental summer warm biases and climate change amplification in CMIP5 simulations. Geophys. Res. Lett. 41, 6493–6500. doi:10.1002/2014GL061145.

Christensen, J. H., Kumar, K. K., Aldrian, E., An, S.-I., Cavalcanti, I. F. A., Castro, M. de, et al. (2013). “Climate Phenomena and their Relevance for Future Regional Climate Change,” in Climate Change 2013: The Physical Science Basis. Contribution of Working Group I to the Fifth Assessment Report of the Intergovernmental Panel on Climate Change, eds. T. F. Stocker, D. Qin, G.-K. Plattner, M. Tignor, S. K. Allen, J. Boschung, et al. (Cambridge, United Kingdom and New York, NY, USA: Cambridge University Press).

Cowtan, K., and Way, R. G. (2014). Coverage bias in the HadCRUT4 temperature series and its impact on recent temperature trends. Q. J. R. Meteorol. Soc. 140, 1935–1944. doi:10.1002/qj.2297.

Deser, C., Knutti, R., Solomon, S., and Phillips, A. S. (2012). Communication of the role of natural variability in future North American climate. Nat. Clim. Chang. 2, 775–779. doi:10.1038/nclimate1562.

Donat, M. G., Alexander, L. V., Yang, H., Durre, I., Vose, R., Caesar, J., et al. (2013a). Global Land-Based Datasets for Monitoring Climatic Extremes. Bull. Am. Meteorol. Soc. 94, 997–1006. doi:10.1175/BAMS-D-12-00109.1.

Donat, M. G., Alexander, L. V., Yang, H., Durre, I., Vose, R., Dunn, R. J. H., et al. (2013b). Updated analyses of temperature and precipitation extreme indices since the beginning of the twentieth century: The HadEX2 dataset. J. Geophys. Res. Atmos. 118, 2098–2118. doi:10.1002/jgrd.50150.

Fischer, E. M., and Knutti, R. (2015). Anthropogenic contribution to global occurrence of heavy-precipitation and high-temperature extremes. Nat. Clim. Chang. 5, 560–564. doi:10.1038/nclimate2617.

Greve, P., and Seneviratne, S. I. (2015). Assessment of future changes in water availability and aridity. Geophys. Res. Lett. 42, 5493–5499. doi:10.1002/2015GL064127.

Hall, A., and Qu, X. (2006). Using the current seasonal cycle to constrain snow albedo feedback in future climate change. Geophys. Res. Lett. 33, L03502. doi:10.1029/2005GL025127.

Hansen, J., Ruedy, R., Sato, M., and Lo, K. (2010). Global surface temperature change. Rev. Geophys. 48,

RG4004. doi:10.1029/2010RG000345.
Hartmann, D. L., Tank, A. M. G. K., Rusticucci, M., Alexander, L. V., Brönnimann, S., Charabi, Y., et al. (2013). “Observations: Atmosphere and Surface,” in Climate Change 2013: The Physical Science Basis. Contribution of Working Group I to the Fifth Assessment Report of the Intergovernmental Panel on Climate Change, eds. T. F. Stocker, D. Qin, G.-K. Plattner, M. Tignor, S. K. Allen, J. Boschung, et al. (Cambridge, United Kingdom and New York, NY, USA: Cambridge University Press), 159–254.
Haustein, K., Allen, M. R., Forster, P. M., Otto, F. E. L., Mitchell, D. M., Matthews, H. D., et al. (2017). A real-time Global Warming Index. Sci. Rep. 7, 15417. doi:10.1038/s41598-017-14828-5.
Huang, J., Yu, H., Dai, A., Wei, Y., and Kang, L. (2017). Drylands face potential threat under 2 °C global warming target. Nat. Clim. Chang. 7, 417–422. doi:10.1038/nclimate3275.
IPCC (2013). Climate Change 2013: The Physical Science Basis. Working Group I Contribution to the Fifth Assessment Report of the Intergovernmental Panel on Climate Change. , eds. T. F. Stocker, D. Qin, G.-K. Plattner, M. Tignor, S. K. Allen, J. Boschung, et al. Cambridge, United Kingdom and New York, NY, USA: Cambridge University Press doi:http://www.ipcc.ch/report/ar5/wg1/.
Jacob, D., Kotova, L., Teichmann, C., Sobolowski, S. P., Vautard, R., Donnelly, C., et al. (2018). Climate Impacts in Europe Under +1.5°C Global Warming. Earth’s Futur. 6, 264–285. doi:10.1002/2017EF000710.
Jiang, D., and Tian, Z. (2013). East Asian monsoon change for the 21st century: Results of CMIP3 and CMIP5 models. Chinese Sci. Bull. 58, 1427–1435. doi:10.1007/s11434-012-5533-0.
Jones, C., and Carvalho, L. M. V. (2013). Climate change in the South American monsoon system: Present climate and CMIP5 projections. J. Clim. 26, 6660–6678. doi:10.1175/JCLI-D-12-00412.1.
Karl, T. R., Arguez, A., Huang, B., Lawrimore, J. H., McMahon, J. R., Menne, M. J., et al. (2015). Possible artifacts of data biases in the recent global surface warming hiatus. Science (80-.). 348. Available at: http://science.sciencemag.org/content/348/6242/1469 [Accessed April 6, 2017].
Karmalkar, A. V., and Bradley, R. S. (2017). Consequences of Global Warming of 1.5 °C and 2 °C for Regional Temperature and Precipitation Changes in the Contiguous United States. PLoS One 12, e0168697. doi:10.1371/journal.pone.0168697.
Kharin, V., Flato, G., Zhang, X., Gillett, N., Zwiers, F., and Anderson, K. (2018). Risks from climate extremes change differently from 1.5°C to 2.0°C depending on rarity. Earth’s Futur. doi:10.1002/2018EF000813.
Koster, R. D., Dirmeyer, P. A., Guo, Z., Bonan, G., Chan, E., Cox, P., et al. (2004). Regions of Strong Coupling Between Soil Moisture and Precipitation. Science (80-.). 305. Available at: http://science.sciencemag.org/content/305/5687/1138 [Accessed April 5, 2017].
Lewandowsky, S., Risbey, J. S., and Oreskes, N. (2016). The pause in global warming: Turning a routine fluctuation into a problem for science. Bull. Am. Meteorol. Soc. 97, 723–733. doi:10.1175/BAMS-D-14-00106.1.
MacKellar, N., New, M., and Jack, C. (2014). Observed and modelled trends in rainfall and temperature for South Africa: 1960-2010. S. Afr. J. Sci. 110, 1–13.
Masson-Delmotte, V., Schulz, M., Abe-Ouchi, A., Beer, J., Ganopolski, A., González Rouco, J. F., et al. (2013). “Information from Paleoclimate Archives,” in Climate Change 2013: The Physical Science Basis. Contribution of Working Group I to the Fifth Assessment Report of the Intergovernmental Panel on Climate Change, 383–464. doi:10.1017/CBO9781107415324.
Medhaug, I., Stolpe, M. B., Fischer, E. M., and Knutti, R. (2017). Reconciling controversies about the ‘global warming hiatus.’ Nature 545, 41–47. doi:10.1038/nature22315.
Mitchell, D., Achutarao, K., Allen, M., Bethke, I., Beyerle, U., Ciavarella, A., et al. (2017). Half a degree additional warming, prognosis and projected impacts (HAPPI): background and experimental design. Geosci. Model Dev. 10, 571–583. doi:10.5194/gmd-10-571-2017.
Moron, V., Oueslati, B., Pohl, B., Rome, S., and Janicot, S. (2016). Trends of mean temperatures and warm extremes in northern tropical Africa (1961–2014) from observed and PPCA-reconstructed time series. J. Geophys. Res. Atmos. 121, 5298–5319. doi:10.1002/2015JD024303.
Omondi, A., Joseph, L. A., Forootan, E., Laban, A. O., Barakiza, R., Gezahegn, B. G., et al. (2014). Changes in temperature and precipitation extremes over the Greater Horn of Africa region from 1961 to 2010. Int. J. Climatol. 34, 1262–1277. doi:10.1002/joc.3763.
Orlowsky, B., and Seneviratne, S. I. (2013). Elusive drought: uncertainty in observed trends and short- and long-term CMIP5 projections. Hydrol. Earth Syst. Sci. 17, 1765–1781. doi:10.5194/hess-17-1765-2013.
Richardson, M., Cowtan, K., Hawkins, E., and Stolpe, M. B. (2016). Reconciled climate response estimates from climate models and the energy budget of Earth. Nat. Clim. Chang. 6, 931. doi:10.1038/nclimate3066.
Ringard, J., Dieppois, B., Rome, S., Diedhiou, A., Pellarin, T., Konaré, A., et al. (2016). The intensification of thermal extremes in west Africa. Glob. Planet. Change 139, 66–77. doi:https://doi.org/10.1016/j.gloplacha.2015.12.009.
Schleussner, C.-F., Pfleiderer, P., and Fischer, E. M. (2017). In the observational record half a degree matters. Nat. Clim. Chang. 7, 460–462. Available at: https://www.nature.com/articles/nclimate3320.

Seneviratne, S. I., Corti, T., Davin, E. L., Hirschi, M., Jaeger, E. B., Lehner, I., et al. (2010). Investigating soil moisture-climate interactions in a changing climate: A review. Earth-Science Rev. 99, 125–161. doi:10.1016/j.earscirev.2010.02.004.
Seneviratne, S. I., Donat, M. G., Mueller, B., and Alexander, L. V. (2014). No pause in the increase of hot temperature extremes. Nat. Clim. Chang. 4, 161–163. doi:10.1038/nclimate2145.
Seneviratne, S. I., Donat, M. G., Pitman, A. J., Knutti, R., and Wilby, R. L. (2016). Allowable CO2 emissions based on regional and impact-related climate targets. Nature 529, 477–83. doi:10.1038/nature16542.
Seneviratne, S. I., Nicholls, N., Easterling, D., Goodess, C. M., Kanae, S., Kossin, J., et al. (2012). "Changes in Climate Extremes and their Impacts on the Natural Physical Environment," in Managing the Risks of Extreme Events and Disasters to Advance Climate Change Adaptation. A Special Report of Working Groups I and II of IPCC Intergovernmental Panel on Climate Change, eds. C. B. Field, V. Barros, T. F. Stocker, D. Qin, D. J. Dokken, K. L. Ebi, et al. (Cambridge, United Kingdom and New York, NY, USA: Cambridge University Press), 109–230. Available at: https://www.ipcc.ch/pdf/special-reports/srex/SREX-Chap3_FINAL.pdf.
Seneviratne, S. I., Wartenburger, R., Guillod, B. P., Hirsch, A. L., Vogel, M. M., Brovkin, V., et al. (2018). Climate extremes, land-climate feedbacks, and land-use forcing at 1.5°C. Philos. Trans. R. Soc. A Math. Phys. Eng. Sci. 376, 1–23. doi:10.1098/rsta.2016.0450.
Seneviratne, S. I., Wilhelm, M., Stanelle, T., van den Hurk, B., Hagemann, S., Berg, A., et al. (2013). Impact of soil moisture-climate feedbacks on CMIP5 projections: First results from the GLACE-CMIP5 experiment. Geophys. Res. Lett. 40, 5212–5217. doi:10.1002/grl.50956.
Serreze, M. C., and Barry, R. G. (2011). Processes and impacts of Arctic amplification: A research synthesis. Glob. Planet. Change 77, 85–96. doi:10.1016/j.gloplacha.2011.03.004.
Singh, D., Tsiang, M., Rajaratnam, B., and Diffenbaugh, N. S. (2014). Observed changes in extreme wet and dry spells during the South Asian summer monsoon season. Nat. Clim. Chang. 4, 456–461. doi:10.1038/nclimate2208.
Sippel, S., Zscheischler, J., Mahecha, M. D., Orth, R., Reichstein, M., Vogel, M., et al. (2016). Refining multi-model projections of temperature extremes by evaluation against land-atmosphere coupling diagnostics. Earth Syst. Dyn. Discuss., 1–24. doi:10.5194/esd-2016-48.
Stegehuis, A. I., Teuling, A. J., Ciais, P., Vautard, R., and Jung, M. (2013). Future European temperature change uncertainties reduced by using land heat flux observations. Geophys. Res. Lett. 40, 2242–2245. doi:10.1002/grl.50404.
Stocker, T. F., Qin, D., Plattner, G.-K., Alexander, L. V., Allen, S. K., Bindoff, N. L., et al. (2013). Technical Summary. , eds. T. F. Stocker, D. Qin, G.-K. Plattner, M. Tignor, S. K. Allen, J. Boschung, et al. Cambridge, United Kingdom and New York, NY, USA: Cambridge University Press Available at: https://www.ipcc.ch/pdf/assessment-report/ar5/wg1/WG1AR5_SummaryVolume_FINAL.pdf.
Sun, Y., Zhang, X., Ren, G., Zwiers, F. W., and Hu, T. (2016). Contribution of urbanization to warming in China. Nat. Clim. Chang. 6, 706. Available at: http://dx.doi.org/10.1038/nclimate2956.
Sylla, M. B., Elguindi, N., Giorgi, F., and Wisser, D. (2016). Projected robust shift of climate zones over West Africa in response to anthropogenic climate change for the late 21st century. Clim. Change 134, 241–253. doi:10.1007/s10584-015-1522-z.
Sylla, M. B., Giorgi, F., Pal, J. S., Gibba, P., Kebe, I., and Nikiema, M. (2015). Projected Changes in the Annual Cycle of High-Intensity Precipitation Events over West Africa for the Late Twenty-First Century. J. Clim. 28, 6475–6488. doi:10.1175/JCLI-D-14-00854.1.
Taylor, C. M., Belušić, D., Guichard, F., Parker, D. J., Vischel, T., Bock, O., et al. (2017). Frequency of extreme Sahelian storms tripled since 1982 in satellite observations. Nature 544, 475–478. doi:10.1038/nature22069.
Vautard, R., Gobiet, A., Sobolowski, S., Kjellström, E., Stegehuis, A., Watkiss, P., et al. (2014). The European climate under a 2 °C global warming. Environ. Res. Lett. 9, 034006. doi:10.1088/1748-9326/9/3/034006.
Vogel, M. M., Orth, R., Cheruy, F., Hagemann, S., Lorenz, R., van den Hurk, B. J. J. M., et al. (2017). Regional amplification of projected changes in extreme temperatures strongly controlled by soil moisture-temperature feedbacks. Geophys. Res. Lett. 44, 1511–1519. doi:10.1002/2016GL071235.
Wan, H., Zhang, X., and Zwiers, F. (2018). Human influence on Canadian temperatures. Clim. Dyn. doi:10.1007/s00382-018-4145-z.
Wartenburger, R., Hirschi, M., Donat, M. G., Greve, P., Pitman, A. J., and Seneviratne, S. I. (2017). Changes in regional climate extremes as a function of global mean temperature: an interactive plotting framework. Geosci. Model Dev. 10, 3609–3634. doi:10.5194/gmd-2017-33.
Weber, T., Haensler, A., Rechid, D., Pfeifer, S., Eggert, B., and Jacob, D. (2018). Analysing regional climate change in Africa in a 1.5°C, 2°C and 3°C global warming world. Earth's Futur. 6, 1–13. doi:10.1002/2017EF000714.

3.SM.3_ Supplementary information to Section 3.4

These tables document some of the quantitative projections of projected climate change impacts that are to be found in the literature cited in this report. They do not necessarily contain all of the quantitative projections that could be found in the literature, in particular where a single publication contains a large number of projections.

Table 3.SM.1: 3.4.2 Freshwater resources

Risk	Region	Metric (Unit)	Baseline Time Period against Which Change Measured	Socio-economic Scenario and Date	Baseline Global T above Pre-industrial	Climate Scenario Used	Transient (T) or Equilibrium (E)	Dynamic Model?	Projected Impact at 1.5°C above Pre-Industrial	2°C	3°C	4°C	Projected Impact at Delta T(°C)	Delta T Relative to Pre-Industrial	Delta T Relative to Baseline Temperature	Projected Impact (Reference Value)	Projected Impact (Unit)	Reference	GCM (e.g., MIROC5)	RCM	Future Period	Cited Part
Water scarcity	Global	%	1980-2009	N/A	N/A	19GCM from the CMIP3 archive, MAGICC6, SRES A1F1, RCP8.5, 2086–2115	N/A	Y	N/A	8	N/A	N/A	8	2	N/A	N/A	Million people	Gerten et al., 2013	19GCM from the CMIP3 archive	N/A	2086–2115	Table 1, Fig.4 (a)
Water scarcity	Global	Million people (<1000 m3 cap-1 y-1)	1980-2009	N/A	N/A	19GCM from the CMIP3 archive, MAGICC6, SRES A1F1, RCP8.5, 2086–2115	N/A	Y	N/A	1397	N/A	N/A	1397	2	N/A	Total 6012, affected 1267	Million people	Gerten et al., 2013	19GCM from the CMIP3 archive	N/A	2086–2115	Table 1
Water scarcity	Europe	Million people (<1000 m3 cap-1 y-1)	1980-2009	N/A	N/A	19GCM from the CMIP3 archive, MAGICC6, SRES A1F1, RCP8.5, 2086–2115	N/A	Y	N/A	118	N/A	N/A	118	2	N/A	Total 906, affected 110	Million people	Gerten et al., 2013	19GCM from the CMIP3 archive	N/A	2086–2115	Table 1
Water scarcity	Asia	Million people (<1000 m3 cap-1 y-1)	1980-2009	N/A	N/A	19GCM from the CMIP3 archive, MAGICC6, SRES A1F1, RCP8.5, 2086–2115	N/A	Y	N/A	Y	N/A	N/A	988	2	N/A	Total 3879, affected 870	Million people	Gerten et al., 2013	19GCM from the CMIP3 archive	N/A	2086–2115	Table 1
Water scarcity	Africa	Million people (<1000 m3 cap-1 y-1)	1980-2009	N/A	N/A	19GCM from the CMIP3 archive, MAGICC6, SRES A1F1, RCP8.5, 2086–2115	N/A	Y	N/A	115	N/A	N/A	115	2	N/A	Total 775, affected 115	Million people	Gerten et al., 2013	19GCM from the CMIP3 archive	N/A	2086–2115	Table 1
Water scarcity	North America	Million people (<1000 m3 cap-1 y-1)	1980-2009	N/A	N/A	19GCM from the CMIP3 archive, MAGICC6, SRES A1F1, RCP8.5, 2086–2115	N/A	Y	N/A	81	N/A	N/A	81	2	N/A	Total 479, affected 83	Million people	Gerten et al., 2013	19GCM from the CMIP3 archive	N/A	2086–2115	Table 1
Water scarcity	South America	Million people (<1000 m3 cap-1 y-1)	1980-2009	N/A	N/A	19GCM from the CMIP3 archive, MAGICC6, SRES A1F1, RCP8.5, 2086–2115	N/A	Y	N/A	82	N/A	N/A	82	2	N/A	Total 345, affected 77	Million people	Gerten et al., 2013	19GCM from the CMIP3 archive	N/A	2086–2115	Table 1
Water scarcity	Oceania	Million people (<1000 m3 cap-1 y-1)	1980-2009	N/A	N/A	19GCM from the CMIP3 archive, MAGICC6, SRES A1F1, RCP8.5, 2086–2115	N/A	Y	N/A	13	N/A	N/A	13	2	N/A	Total 29, affected 13	Million people	Gerten et al., 2013	19GCM from the CMIP3 archive	N/A	2086–2115	Table 1
Water resources	Global	%	1980-2010	SSP2	0.7	Transition of RCP8.5, 2090, 11 GHMs by 5 GCMs	T	Y	N/A	N/A	N/A	N/A	8	1.7	1	N/A	N/A	Schewe et al., 2014	HadGEM2-ES, IPSL-CM5A-LR, MIROC-ESM-CHEM, GFDL-ESM2M, NorESM1-M	N/A	2090	Fig.2, p3247 Table S1 (GCM) Table S2 (GHM)
Water resources	Global	%	1980-2010	SSP2	0.7	Transition of RCP8.5, 2090, 11 GHMs by 5 GCMs	T	Y	N/A	N/A	N/A	N/A	14	2.7	2	N/A	N/A	Schewe et al., 2014	HadGEM2-ES, IPSL-CM5A-LR, MIROC-ESM-CHEM, GFDL-ESM2M, NorESM1-M	N/A	2090	Fig.2, p3247 Table S1 (GCM) Table S2 (GHM)
Water scarcity, Increased water resources stress	Global	Million people	1961–1990	SSP1	0.3	Transition of RCP2.6 in 2050s, 19 CMIP5 GCMs	E	N/A	1330	N/A	N/A	N/A	1330 (379-2997)	Around 1.6	Around 1.3	Population in 2050, total 8411, water stressed 3286	Million people	Arnell and Lloyd-Hughes, 2014	CSIRO-Mk3-6-0, FIO-ESM, GFDL-CM3, GFDL-ESM2G, GFDL-ESM2M, GISS-E2-H, GISS-E2-R, HadGEM2-AO, HadGEM2-ES, IPSL-CM5A-LR, IPSL-CM5A-MR, MIROC-ESM, MIROC-ESM-CEM, MIROC5, MRI-CGCM3, NorESM1-M, NorESM1-ME, bcc-csm1-1, bcc-csm1-1-m	N/A	2070–2099	Table 2 Table 3 a) Fig.1 Supplementary Table 1 (GCM)
Water scarcity, Increased water resources stress	Global	Million people (<1000 m3 cap-1 y-1)	1961–1990	SSP1	0.3	Transition of RCP4.5 in 2050s, 19 CMIP5 GCMs	T	N/A	N/A	1514	N/A	N/A	1514 (810-2845)	Around 2	Around 1.7	Population in 2050, total 8411, water stressed 3286	Million people	Arnell and Lloyd-Hughes, 2014	CSIRO-Mk3-6-0, FIO-ESM, GFDL-CM3, GFDL-ESM2G, GFDL-ESM2M, GISS-E2-H, GISS-E2-R, HadGEM2-AO, HadGEM2-ES, IPSL-CM5A-LR, IPSL-CM5A-MR, MIROC-ESM, MIROC-ESM-CEM, MIROC5, MRI-CGCM3, NorESM1-M, NorESM1-ME, bcc-csm1-1, bcc-csm1-1-m	N/A	2070–2099	Table 2 Table 3 a) Fig.1
Water scarcity, Increased water resources stress	Global	Million people (<1000 m3 cap-1 y-1)	1961–1990	SSP2	0.3	Transition of RCP2.6 in 2050s, 19 CMIP5 GCMs	E	N/A	1575	N/A	N/A	N/A	1575 (473-3434)	Around 1.6	Around 1.3	Population in 2050, total 9245, water stressed 4079	Million people	Arnell and Lloyd-Hughes, 2014	CSIRO-Mk3-6-0, FIO-ESM, GFDL-CM3, GFDL-ESM2G, GFDL-ESM2M, GISS-E2-H, GISS-E2-R, HadGEM2-AO, HadGEM2-ES, IPSL-CM5A-LR, IPSL-CM5A-MR, MIROC-ESM, MIROC-ESM-CEM, MIROC5, MRI-CGCM3, NorESM1-M, NorESM1-ME, bcc-csm1-1, bcc-csm1-1-m	N/A	2070–2099	Table 2 Table 3 a) Fig.1
Water scarcity, Increased water resources stress	Global	Million people (<1000 m3 cap-1 y-1)	1961–1990	SSP2	0.3	Transition of RCP4.5 in 2050s, 19 CMIP5 GCMs	T	N/A	N/A	1794	N/A	N/A	1794 (881-3239)	Around 2	Around 1.7	Population in 2050, total 9245, water stressed 4079	Million people	Arnell and Lloyd-Hughes, 2014	CSIRO-Mk3-6-0, FIO-ESM, GFDL-CM3, GFDL-ESM2G, GFDL-ESM2M, GISS-E2-H, GISS-E2-R, HadGEM2-AO, HadGEM2-ES, IPSL-CM5A-LR, IPSL-CM5A-MR, MIROC-ESM, MIROC-ESM-CEM, MIROC5, MRI-CGCM3, NorESM1-M, NorESM1-ME, bcc-csm1-1, bcc-csm1-1-m	N/A	2070–2099	Table 2 Table 3 a) Fig.1

Risk	Region	Metric (Unit)	Baseline Time Period against Which Change Measured	Socio-economic Scenario and Date	Baseline Global T above Pre-industrial	Climate Scenario Used	Transient (T) or Equilibrium (E)	Dynamic Model?	Projected Impact at 1.5°C above Pre-Industrial	2°C	3°C	4°C	Projected Impact at Delta T(°C)	Delta T Relative to Pre-Industrial	Delta T Relative to Baseline Temperature	Projected Impact (Reference Value)	Projected Impact (Unit)	Reference	GCM (e.g., MIROC5)	RCM	Future Period	Cited Part
Water scarcity, Increased water resources stress	Global	Million people (<1000m3cap-1yr-1)	1961–1990	SSP3	0,3	Transition of RCP2.6 in 2050s, 19 CMIP5 GCMs	E	N/A	1887	N/A	N/A	N/A	1887 (626-4088)	Around 1.6	Around 1.3	Population in 2050, total 10233, water stressed 4774	Million people	Arnell and Lloyd-Hughes, 2014	CSIRO-Mk3-6-0, FIO-ESM, GFDL-CM3, GFDL-ESM2G, GFDL-ESM2M, GISS-E2-H, GISS-E2-R, HadGEM2-AO, HadGEM2-ES, IPSL-CM5A-LR, IPSL-CM5A-MR, MIROC-ESM, MIROC-ESM-CEM, MIROC5, MRI-CGCM3, NorESM1-M, NorESM1-ME, bcc-csm1-1, bcc-csm1-1-m	N/A	2070–2099	Table 2 Table 3 a) Fig.1
Water scarcity, Increased water resources stress	Global	Million people (<1000m3cap-1yr-1)	1961–1990	SSP3	0,3	Transition of RCP4.5 in 2050s, 19 CMIP5 GCMs	T	N/A	N/A	2157	N/A	N/A	2157 (1037-3975)	Around 2	Around 1.7	Population in 2050, total 10233, water stressed 4774	Million people	Arnell and Lloyd-Hughes, 2014	CSIRO-Mk3-6-0, FIO-ESM, GFDL-CM3, GFDL-ESM2G, GFDL-ESM2M, GISS-E2-H, GISS-E2-R, HadGEM2-AO, HadGEM2-ES, IPSL-CM5A-LR, IPSL-CM5A-MR, MIROC-ESM, MIROC-ESM-CEM, MIROC5, MRI-CGCM3, NorESM1-M, NorESM1-ME, bcc-csm1-1, bcc-csm1-1-m	N/A	2070–2099	Table 2 Table 3 a) Fig.1
Water scarcity, Increased water resources stress	Global	Million people (<1000m3cap-1yr-1)	1961–1990	SSP4	0,3	Transition of RCP2.6 in 2050s, 19 CMIP5 GCMs	E	N/A	1666	N/A	N/A	N/A	1666 (508-3481)	Around 1.6	Around 1.3	Population in 2050, total 9368, water stressed 4236	Million people	Arnell and Lloyd-Hughes, 2014	CSIRO-Mk3-6-0, FIO-ESM, GFDL-CM3, GFDL-ESM2G, GFDL-ESM2M, GISS-E2-H, GISS-E2-R, HadGEM2-AO, HadGEM2-ES, IPSL-CM5A-LR, IPSL-CM5A-MR, MIROC-ESM, MIROC-ESM-CEM, MIROC5, MRI-CGCM3, NorESM1-M, NorESM1-ME, bcc-csm1-1, bcc-csm1-1-m	N/A	2070–2099	Table 2 Table 3 a) Fig.1
Water scarcity, Increased water resources stress	Global	Million people (<1000m3cap-1yr-1)	1961–1990	SSP4	0,3	Transition of RCP4.5 in 2050s, 19 CMIP5 GCMs	T	N/A	N/A	1867	N/A	N/A	1867 (884-3444)	Around 2	Around 1.7	Population in 2050, total 9368, water stressed 4236	Million people	Arnell and Lloyd-Hughes, 2014	CSIRO-Mk3-6-0, FIO-ESM, GFDL-CM3, GFDL-ESM2G, GFDL-ESM2M, GISS-E2-H, GISS-E2-R, HadGEM2-AO, HadGEM2-ES, IPSL-CM5A-LR, IPSL-CM5A-MR, MIROC-ESM, MIROC-ESM-CEM, MIROC5, MRI-CGCM3, NorESM1-M, NorESM1-ME, bcc-csm1-1, bcc-csm1-1-m	N/A	2070–2099	Table 2 Table 3 a) Fig.1
Water scarcity, Increased water resources stress	Global	Million people (<1000m3cap-1yr-1)	1961–1990	SSP5	0,3	Transition of RCP2.6 in 2050s, 19 CMIP5 GCMs	T	N/A	1375	N/A	N/A	N/A	1375 (418-3033)	Around 1.6	Around 1.3	Population in 2050, total 8508, water stressed 3350	Million people	Arnell and Lloyd-Hughes, 2014	CSIRO-Mk3-6-0, FIO-ESM, GFDL-CM3, GFDL-ESM2G, GFDL-ESM2M, GISS-E2-H, GISS-E2-R, HadGEM2-AO, HadGEM2-ES, IPSL-CM5A-LR, IPSL-CM5A-MR, MIROC-ESM, MIROC-ESM-CEM, MIROC5, MRI-CGCM3, NorESM1-M, NorESM1-ME, bcc-csm1-1, bcc-csm1-1-m	N/A	2070–2099	Table 2 Table 3 a) Fig.1
Water scarcity, Increased water resources stress	Global	Million people (<1000m3cap-1yr-1)	1961–1990	SSP5	0,3	Transition of RCP4.5 in 2050s, 19 CMIP5 GCMs	T	N/A	N/A	1566	N/A	N/A	1566 (854-2879)	Around 2	Around 1.7	Population in 2050, total 8508, water stressed 3350	Million people	Arnell and Lloyd-Hughes, 2014	CSIRO-Mk3-6-0, FIO-ESM, GFDL-CM3, GFDL-ESM2G, GFDL-ESM2M, GISS-E2-H, GISS-E2-R, HadGEM2-AO, HadGEM2-ES, IPSL-CM5A-LR, IPSL-CM5A-MR, MIROC-ESM, MIROC-ESM-CEM, MIROC5, MRI-CGCM3, NorESM1-M, NorESM1-ME, bcc-csm1-1, bcc-csm1-1-m	N/A	2070–2099	Table 2 Table 3 a) Fig.1
Freshwater stress	Bahamas	FSI (freshwater stress index) = PCI (population change index) × ACI (aridity change index)	1986–2005 (climatology), 2010 (population)	SSP1–5	0,6	20GCM, CMIP5, 2030, RCP8.5, SSP2	T	Y	1,27	N/A	N/A	N/A	1,27	1,5	0,9	0,34	Million people (2010)	Karnauskas et al., 2018	access1-0, access1-3, bcc-csm1-1, csm1-1-m, cesm1-cam5, cnrm-cm5, csiro-mk3-6-0, gfdl-cm3, gfdl-esm2g, gfdl-esm2m, giss-e2-r, hadgem2-cc, hadgem2-es, inmcm4, ipsl-cm5a-lr, ipsl-cm5a-mr, miroc-esm, miroc-esm-chem, miroc5, mri-cgcm3	N/A	2100	Table 1
Freshwater stress	Bahamas	FSI (freshwater stress index) = PCI (population change index) × ACI (aridity change index)	1986–2005 (climatology), 2010 (population)	SSP1–5	0,6	20GCM, CMIP5, 2030, RCP8.5, SSP2	T	Y	N/A	1,27	N/A	N/A	1,27	2	1,4	0,34	Million people (2010)	Karnauskas et al., 2018	access1-0, access1-3, bcc-csm1-1, csm1-1-m, cesm1-cam5, cnrm-cm5, csiro-mk3-6-0, gfdl-cm3, gfdl-esm2g, gfdl-esm2m, giss-e2-r, hadgem2-cc, hadgem2-es, inmcm4, ipsl-cm5a-lr, ipsl-cm5a-mr, miroc-esm, miroc-esm-chem, miroc5, mri-cgcm3	N/A	2100	Table 1

Risk	Region	Metric (Unit)	Baseline Time Period against Which Change Measured	Socio-economic Scenario and Date	Baseline Global T above Pre-industrial	Climate Scenario Used	Transient (T) or Equilibrium (E)	Dynamic Model?	Projected Impact at 1.5°C above Pre-Industrial	2°C	3°C	4°C	Projected Impact at Delta T(°C)	Delta T Relative to Pre-Industrial	Delta T Relative to Baseline Temperature	Projected Impact (Reference Value)	Projected Impact (Unit)	Reference	GCM (e.g., MIROC5)	RCM	Future Period	Cited Part
Freshwater stress	Belize	FSI (freshwater stress index) = PCI (population change index) × ACI (aridity change index)	1986–2005 (climatology), 2010 (population)	SSP1–5	0,6	20GCM, CMIP5, 2030, RCP85, SSP2	T	Y	1,4	N/A	N/A	N/A	1,4	1,5	0,9	0,31	Million people (2010)	Karnauskas et al., 2018	access1-0,access1-3,bcc-csm1-1,csm1-1-m,cesm1-cam5,cnrm-cm5,csiro-mk3-6-0,gfdl-cm3,gfdl-esm2g,gfdl-esm2m,giss-e2-r,hadgem2-cc,hadgem2-es,inmcm4,ipsl-cm5a-lr,ipsl-cm5a-mr,miroc-esm,miroc-esm-chem,miroc5,mri-cgcm3	N/A	2100	Table 1
Freshwater stress	Belize	FSI (freshwater stress index) = PCI (population change index) × ACI (aridity change index)	1986–2005 (climatology), 2010 (population)	SSP1–5	0,6	20GCM, CMIP5, 2030, RCP85, SSP2	T	Y	N/A	1,41	N/A	N/A	1,41	2	1,4	0,31	Million people (2010)	Karnauskas et al., 2018	access1-0,access1-3,bcc-csm1-1,csm1-1-m,cesm1-cam5,cnrm-cm5,csiro-mk3-6-0,gfdl-cm3,gfdl-esm2g,gfdl-esm2m,giss-e2-r,hadgem2-cc,hadgem2-es,inmcm4,ipsl-cm5a-lr,ipsl-cm5a-mr,miroc-esm,miroc-esm-chem,miroc5,mri-cgcm3	N/A	2100	Table 1
Freshwater stress	Cabo Verde	FSI (freshwater stress index) = PCI (population change index) × ACI (aridity change index)	1986–2005 (climatology), 2010 (population)	SSP1–5	0,6	20GCM, CMIP5, 2030, RCP85, SSP2	T	Y	1,18	N/A	N/A	N/A	1,18	1,5	0,9	0,5	Million people (2010)	Karnauskas et al., 2018	access1-0,access1-3,bcc-csm1-1,csm1-1-m,cesm1-cam5,cnrm-cm5,csiro-mk3-6-0,gfdl-cm3,gfdl-esm2g,gfdl-esm2m,giss-e2-r,hadgem2-cc,hadgem2-es,inmcm4,ipsl-cm5a-lr,ipsl-cm5a-mr,miroc-esm,miroc-esm-chem,miroc5,mri-cgcm3	N/A	2100	Table 1
Freshwater stress	Cabo Verde	FSI (freshwater stress index) = PCI (population change index) × ACI (aridity change index)	1986–2005 (climatology), 2010 (population)	SSP1–5	0,6	20GCM, CMIP5, 2030, RCP85, SSP2	T	Y	N/A	1,2	N/A	N/A	1,2	2	1,4	0,5	Million people (2010)	Karnauskas et al., 2018	access1-0,access1-3,bcc-csm1-1,csm1-1-m,cesm1-cam5,cnrm-cm5,csiro-mk3-6-0,gfdl-cm3,gfdl-esm2g,gfdl-esm2m,giss-e2-r,hadgem2-cc,hadgem2-es,inmcm4,ipsl-cm5a-lr,ipsl-cm5a-mr,miroc-esm,miroc-esm-chem,miroc5,mri-cgcm3	N/A	2100	Table 1
Freshwater stress	Comoros	FSI (freshwater stress index) = PCI (population change index) × ACI (aridity change index)	1986–2005 (climatology), 2010 (population)	SSP1–5	0,6	20GCM, CMIP5, 2030, RCP85, SSP2	T	Y	1,43	N/A	N/A	N/A	1,43	1,5	0,9	0,73	Million people (2010)	Karnauskas et al., 2018	access1-0,access1-3,bcc-csm1-1,csm1-1-m,cesm1-cam5,cnrm-cm5,csiro-mk3-6-0,gfdl-cm3,gfdl-esm2g,gfdl-esm2m,giss-e2-r,hadgem2-cc,hadgem2-es,inmcm4,ipsl-cm5a-lr,ipsl-cm5a-mr,miroc-esm,miroc-esm-chem,miroc5,mri-cgcm3	N/A	2100	Table 1
Freshwater stress	Comoros	FSI (freshwater stress index) = PCI (population change index) × ACI (aridity change index)	1986–2005 (climatology), 2010 (population)	SSP1–5	0,6	20GCM, CMIP5, 2030, RCP85, SSP2	T	Y	N/A	1,44	N/A	N/A	1,44	2	1,4	0,73	Million people (2010)	Karnauskas et al., 2018	access1-0,access1-3,bcc-csm1-1,csm1-1-m,cesm1-cam5,cnrm-cm5,csiro-mk3-6-0,gfdl-cm3,gfdl-esm2g,gfdl-esm2m,giss-e2-r,hadgem2-cc,hadgem2-es,inmcm4,ipsl-cm5a-lr,ipsl-cm5a-mr,miroc-esm,miroc-esm-chem,miroc5,mri-cgcm3	N/A	2100	Table 1
Freshwater stress	Cuba	FSI (freshwater stress index) = PCI (population change index) × ACI (aridity change index)	1986–2005 (climatology), 2010 (population)	SSP1–5	0,6	20GCM, CMIP5, 2030, RCP85, SSP2	T	Y	0,98	N/A	N/A	N/A	0,98	1,5	0,9	11,26	Million people (2010)	Karnauskas et al., 2018	access1-0,access1-3,bcc-csm1-1,csm1-1-m,cesm1-cam5,cnrm-cm5,csiro-mk3-6-0,gfdl-cm3,gfdl-esm2g,gfdl-esm2m,giss-e2-r,hadgem2-cc,hadgem2-es,inmcm4,ipsl-cm5a-lr,ipsl-cm5a-mr,miroc-esm,miroc-esm-chem,miroc5,mri-cgcm3	N/A	2100	Table 1
Freshwater stress	Cuba	FSI (freshwater stress index) = PCI (population change index) × ACI (aridity change index)	1986–2005 (climatology), 2010 (population)	SSP1–5	0,6	20GCM, CMIP5, 2030, RCP85, SSP2	T	Y	N/A	0,99	N/A	N/A	0,99	2	1,4	11,26	Million people (2010)	Karnauskas et al., 2018	access1-0,access1-3,bcc-csm1-1,csm1-1-m,cesm1-cam5,cnrm-cm5,csiro-mk3-6-0,gfdl-cm3,gfdl-esm2g,gfdl-esm2m,giss-e2-r,hadgem2-cc,hadgem2-es,inmcm4,ipsl-cm5a-lr,ipsl-cm5a-mr,miroc-esm,miroc-esm-chem,miroc5,mri-cgcm3	N/A	2100	Table 1

Risk	Region	Metric (Unit)	Baseline Time Period against Which Change Measured	Socio-economic Scenario and Date	Baseline Global T above Pre-industrial	Climate Scenario Used	Transient (T) or Equilibrium (E)	Dynamic Model?	Projected Impact at 1.5°C above Pre-Industrial	2°C	3°C	4°C	Projected Impact at Delta T(°C)	Delta T Relative to Pre-Industrial	Delta T Relative to Baseline Temperature	Projected Impact (Reference Value)	Projected Impact (Unit)	Reference	GCM (e.g., MIROC5)	RCM	Future Period	Cited Part
Freshwater stress	Dominican Republic	FSI (freshwater stress index) = PCI (population change index) × ACI (aridity change index)	1986–2005 (climatology), 2010 (population)	SSP1–5	0,6	20GCM, CMIP5, 2030, RCP8.5, SSP2	T	Y	1,28	N/A	N/A	N/A	1,28	1,5	0,9	9,93	Million people (2010)	Karnauskas et al., 2018	access1-0,access1-3,bcc-csm1-1,csm1-1-m,cesm1-cam5,cnrm-cm5,csiro-mk3-6-0,gfdl-cm3,gfdl-esm2g,gfdl-esm2m,giss-e2-r,hadgem2-cc,hadgem2-es,inmcm4,ipsl-cm5a-lr,ipsl-cm5a-mr,miroc-esm,miroc-esm-chem,miroc5,mri-cgcm3	N/A	2100	Table 1
Freshwater stress	Dominican Republic	FSI (freshwater stress index) = PCI (population change index) × ACI (aridity change index)	1986–2005 (climatology), 2010 (population)	SSP1–5	0,6	20GCM, CMIP5, 2030, RCP8.5, SSP2	T	Y	N/A	1,36	N/A	N/A	1,36	2	1,4	9,93	Million people (2010)	Karnauskas et al., 2018	access1-0,access1-3,bcc-csm1-1,csm1-1-m,cesm1-cam5,cnrm-cm5,csiro-mk3-6-0,gfdl-cm3,gfdl-esm2g,gfdl-esm2m,giss-e2-r,hadgem2-cc,hadgem2-es,inmcm4,ipsl-cm5a-lr,ipsl-cm5a-mr,miroc-esm,miroc-esm-chem,miroc5,mri-cgcm3	N/A	2100	Table 1
Freshwater stress	Fiji	FSI (freshwater stress index) = PCI (population change index) × ACI (aridity change index)	1986–2005 (climatology), 2010 (population)	SSP1–5	0,6	20GCM, CMIP5, 2030, RCP8.5, SSP2	T	Y	1,13	N/A	N/A	N/A	1,13	1,5	0,9	0,86	Million people (2010)	Karnauskas et al., 2018	access1-0,access1-3,bcc-csm1-1,csm1-1-m,cesm1-cam5,cnrm-cm5,csiro-mk3-6-0,gfdl-cm3,gfdl-esm2g,gfdl-esm2m,giss-e2-r,hadgem2-cc,hadgem2-es,inmcm4,ipsl-cm5a-lr,ipsl-cm5a-mr,miroc-esm,miroc-esm-chem,miroc5,mri-cgcm3	N/A	2100	Table 1
Freshwater stress	Fiji	FSI (freshwater stress index) = PCI (population change index) × ACI (aridity change index)	1986–2005 (climatology), 2010 (population)	SSP1–5	0,6	20GCM, CMIP5, 2030, RCP8.5, SSP2	T	Y	N/A	1,16	N/A	N/A	1,16	2	1,4	0,86	Million people (2010)	Karnauskas et al., 2018	access1-0,access1-3,bcc-csm1-1,csm1-1-m,cesm1-cam5,cnrm-cm5,csiro-mk3-6-0,gfdl-cm3,gfdl-esm2g,gfdl-esm2m,giss-e2-r,hadgem2-cc,hadgem2-es,inmcm4,ipsl-cm5a-lr,ipsl-cm5a-mr,miroc-esm,miroc-esm-chem,miroc5,mri-cgcm3	N/A	2100	Table 1
Freshwater stress	Grenada	FSI (freshwater stress index) = PCI (population change index) × ACI (aridity change index)	1986–2005 (climatology), 2010 (population)	SSP1–5	0,6	20GCM, CMIP5, 2030, RCP8.5, SSP2	T	Y	1,16	N/A	N/A	N/A	1,16	1,5	0,9	0,1	Million people (2010)	Karnauskas et al., 2018	access1-0,access1-3,bcc-csm1-1,csm1-1-m,cesm1-cam5,cnrm-cm5,csiro-mk3-6-0,gfdl-cm3,gfdl-esm2g,gfdl-esm2m,giss-e2-r,hadgem2-cc,hadgem2-es,inmcm4,ipsl-cm5a-lr,ipsl-cm5a-mr,miroc-esm,miroc-esm-chem,miroc5,mri-cgcm3	N/A	2100	Table 1
Freshwater stress	Grenada	FSI (freshwater stress index) = PCI (population change index) × ACI (aridity change index)	1986–2005 (climatology), 2010 (population)	SSP1–5	0,6	20GCM, CMIP5, 2030, RCP8.5, SSP2	T	Y	N/A	1,21	N/A	N/A	1,21	2	1,4	0,1	Million people (2010)	Karnauskas et al., 2018	access1-0,access1-3,bcc-csm1-1,csm1-1-m,cesm1-cam5,cnrm-cm5,csiro-mk3-6-0,gfdl-cm3,gfdl-esm2g,gfdl-esm2m,giss-e2-r,hadgem2-cc,hadgem2-es,inmcm4,ipsl-cm5a-lr,ipsl-cm5a-mr,miroc-esm,miroc-esm-chem,miroc5,mri-cgcm3	N/A	2100	Table 1
Freshwater stress	Guinea-Bissau	FSI (freshwater stress index) = PCI (population change index) × ACI (aridity change index)	1986–2005 (climatology), 2010 (population)	SSP1–5	0,6	20GCM, CMIP5, 2030, RCP8.5, SSP2	T	Y	1,51	N/A	N/A	N/A	1,51	1,5	0,9	1,52	Million people (2010)	Karnauskas et al., 2018	access1-0,access1-3,bcc-csm1-1,csm1-1-m,cesm1-cam5,cnrm-cm5,csiro-mk3-6-0,gfdl-cm3,gfdl-esm2g,gfdl-esm2m,giss-e2-r,hadgem2-cc,hadgem2-es,inmcm4,ipsl-cm5a-lr,ipsl-cm5a-mr,miroc-esm,miroc-esm-chem,miroc5,mri-cgcm3	N/A	2100	Table 1
Freshwater stress	Guinea-Bissau	FSI (freshwater stress index) = PCI (population change index) × ACI (aridity change index)	1986–2005 (climatology), 2010 (population)	SSP1–5	0,6	20GCM, CMIP5, 2030, RCP8.5, SSP2	T	Y	N/A	1,5	N/A	N/A	1,5	2	1,4	1,52	Million people (2010)	Karnauskas et al., 2018	access1-0,access1-3,bcc-csm1-1,csm1-1-m,cesm1-cam5,cnrm-cm5,csiro-mk3-6-0,gfdl-cm3,gfdl-esm2g,gfdl-esm2m,giss-e2-r,hadgem2-cc,hadgem2-es,inmcm4,ipsl-cm5a-lr,ipsl-cm5a-mr,miroc-esm,miroc-esm-chem,miroc5,mri-cgcm3	N/A	2100	Table 1

Risk	Region	Metric (Unit)	Baseline Time Period against Which Change Measured	Socio-economic Scenario and Date	Baseline Global T above Pre-industrial	Climate Scenario Used	Transient (T) or Equilibrium (E)	Dynamic Model?	Projected Impact at 1.5°C above Pre-Industrial	2°C	3°C	4°C	Projected Impact at Delta T(°C)	Delta T Relative to Pre-Industrial	Delta T Relative to Baseline Temperature	Projected Impact (Reference Value)	Projected Impact (Unit)	Reference	GCM (e.g., MIROC5)	RCM	Future Period	Cited Part
Freshwater stress	Guyana	FSI (freshwater stress index) = PCI (population change index) × ACI (aridity change index)	1986–2005 (climatology), 2010 (population)	SSP1–5	0,6	20GCM, CMIP5, 2030, RCP85, SSP2	T	Y	1,11	N/A	N/A	N/A	1,11	1,5	0,9	0,75	Million people (2010)	Karnauskas et al., 2018	access1-0,access1-3,bcc-csm1-1,csm1-1-m,cesm1-cam5,cnrm-cm5,csiro-mk3-6-0,gfdl-cm3,gfdl-esm2g,gfdl-esm2m,giss-e2-r,hadgem2-cc,hadgem2-es,inmcm4,ipsl-cm5a-lr,ipsl-cm5a-mr,miroc-esm,miroc-esm-chem,miroc5,mri-cgcm3	N/A	2100	Table 1
Freshwater stress	Guyana	FSI (freshwater stress index) = PCI (population change index) × ACI (aridity change index)	1986–2005 (climatology), 2010 (population)	SSP1–5	0,6	20GCM, CMIP5, 2030, RCP85, SSP2	T	Y	N/A	1,12	N/A	N/A	1,12	2	1,4	0,75	Million people (2010)	Karnauskas et al., 2018	access1-0,access1-3,bcc-csm1-1,csm1-1-m,cesm1-cam5,cnrm-cm5,csiro-mk3-6-0,gfdl-cm3,gfdl-esm2g,gfdl-esm2m,giss-e2-r,hadgem2-cc,hadgem2-es,inmcm4,ipsl-cm5a-lr,ipsl-cm5a-mr,miroc-esm,miroc-esm-chem,miroc5,mri-cgcm3	N/A	2100	Table 1
Freshwater stress	Haiti	FSI (freshwater stress index) = PCI (population change index) × ACI (aridity change index)	1986–2005 (climatology), 2010 (population)	SSP1–5	0,6	20GCM, CMIP5, 2030, RCP85, SSP2	T	Y	1,25	N/A	N/A	N/A	1,25	1,5	0,9	9,99	Million people (2010)	Karnauskas et al., 2018	access1-0,access1-3,bcc-csm1-1,csm1-1-m,cesm1-cam5,cnrm-cm5,csiro-mk3-6-0,gfdl-cm3,gfdl-esm2g,gfdl-esm2m,giss-e2-r,hadgem2-cc,hadgem2-es,inmcm4,ipsl-cm5a-lr,ipsl-cm5a-mr,miroc-esm,miroc-esm-chem,miroc5,mri-cgcm3	N/A	2100	Table 1
Freshwater stress	Haiti	FSI (freshwater stress index) = PCI (population change index) × ACI (aridity change index)	1986–2005 (climatology), 2010 (population)	SSP1–5	0,6	20GCM, CMIP5, 2030, RCP85, SSP2	T	Y	N/A	1,31	N/A	N/A	1,31	2	1,4	9,99	Million people (2010)	Karnauskas et al., 2018	access1-0,access1-3,bcc-csm1-1,csm1-1-m,cesm1-cam5,cnrm-cm5,csiro-mk3-6-0,gfdl-cm3,gfdl-esm2g,gfdl-esm2m,giss-e2-r,hadgem2-cc,hadgem2-es,inmcm4,ipsl-cm5a-lr,ipsl-cm5a-mr,miroc-esm,miroc-esm-chem,miroc5,mri-cgcm3	N/A	2100	Table 1
Freshwater stress	Jamaica	FSI (freshwater stress index) = PCI (population change index) × ACI (aridity change index)	1986–2005 (climatology), 2010 (population)	SSP1–5	0,6	20GCM, CMIP5, 2030, RCP85, SSP2	T	Y	1,09	N/A	N/A	N/A	1,09	1,5	0,9	2,74	Million people (2010)	Karnauskas et al., 2018	access1-0,access1-3,bcc-csm1-1,csm1-1-m,cesm1-cam5,cnrm-cm5,csiro-mk3-6-0,gfdl-cm3,gfdl-esm2g,gfdl-esm2m,giss-e2-r,hadgem2-cc,hadgem2-es,inmcm4,ipsl-cm5a-lr,ipsl-cm5a-mr,miroc-esm,miroc-esm-chem,miroc5,mri-cgcm3	N/A	2100	Table 1
Freshwater stress	Jamaica	FSI (freshwater stress index) = PCI (population change index) × ACI (aridity change index)	1986–2005 (climatology), 2010 (population)	SSP1–5	0,6	20GCM, CMIP5, 2030, RCP85, SSP2	T	Y	N/A	1,13	N/A	N/A	1,13	2	1,4	2,74	Million people (2010)	Karnauskas et al., 2018	access1-0,access1-3,bcc-csm1-1,csm1-1-m,cesm1-cam5,cnrm-cm5,csiro-mk3-6-0,gfdl-cm3,gfdl-esm2g,gfdl-esm2m,giss-e2-r,hadgem2-cc,hadgem2-es,inmcm4,ipsl-cm5a-lr,ipsl-cm5a-mr,miroc-esm,miroc-esm-chem,miroc5,mri-cgcm3	N/A	2100	Table 1
Freshwater stress	Maldives	FSI (freshwater stress index) = PCI (population change index) × ACI (aridity change index)	1986–2005 (climatology), 2010 (population)	SSP1–5	0,6	20GCM, CMIP5, 2030, RCP85, SSP2	T	Y	1,25	N/A	N/A	N/A	1,25	1,5	0,9	0,32	Million people (2010)	Karnauskas et al., 2018	access1-0,access1-3,bcc-csm1-1,csm1-1-m,cesm1-cam5,cnrm-cm5,csiro-mk3-6-0,gfdl-cm3,gfdl-esm2g,gfdl-esm2m,giss-e2-r,hadgem2-cc,hadgem2-es,inmcm4,ipsl-cm5a-lr,ipsl-cm5a-mr,miroc-esm,miroc-esm-chem,miroc5,mri-cgcm3	N/A	2100	Table 1
Freshwater stress	Maldives	FSI (freshwater stress index) = PCI (population change index) × ACI (aridity change index)	1986–2005 (climatology), 2010 (population)	SSP1–5	0,6	20GCM, CMIP5, 2030, RCP85, SSP2	T	Y	N/A	1,22	N/A	N/A	1,22	2	1,4	0,32	Million people (2010)	Karnauskas et al., 2018	access1-0,access1-3,bcc-csm1-1,csm1-1-m,cesm1-cam5,cnrm-cm5,csiro-mk3-6-0,gfdl-cm3,gfdl-esm2g,gfdl-esm2m,giss-e2-r,hadgem2-cc,hadgem2-es,inmcm4,ipsl-cm5a-lr,ipsl-cm5a-mr,miroc-esm,miroc-esm-chem,miroc5,mri-cgcm3	N/A	2100	Table 1

Risk	Region	Metric (Unit)	Baseline Time Period against Which Change Measured	Socio-economic Scenario and Date	Baseline Global T above Pre-industrial	Climate Scenario Used	Transient (T) or Equilibrium (E)	Dynamic Model?	Projected Impact at 1.5°C above Pre-Industrial	2°C	3°C	4°C	Projected Impact at Delta T(°C)	Delta T Relative to Pre-Industrial	Delta T Relative to Baseline Temperature	Projected Impact (Reference Value)	Projected Impact (Unit)	Reference	GCM (e.g., MIROC5)	RCM	Future Period	Cited Part
Freshwater stress	Mauritius	FSI (freshwater stress index) = PCI (population change index) × ACI (aridity change index)	1986–2005 (climatology), 2010 (population)	SSP1–5	0,6	20GCM, CMIP5, 2030, RCP85, SSP2	T	Y	1,13	N/A	N/A	N/A	1,13	1,5	0,9	1,3	Million people (2010)	Karnauskas et al., 2018	access1-0,access1-3,bcc-csm1-1,csm1-1-m,cesm1-cam5,cnrm-cm5,csiro-mk3-6-0,gfdl-cm3,gfdl-esm2g,gfdl-esm2m,giss-e2-r,hadgem2-cc,hadgem2-es,inmcm4,ipsl-cm5a-lr,ipsl-cm5a-mr,miroc-esm,miroc-esm-chem,miroc5,mri-cgcm3	N/A	2100	Table 1
Freshwater stress	Mauritius	FSI (freshwater stress index) = PCI (population change index) × ACI (aridity change index)	1986–2005 (climatology), 2010 (population)	SSP1–5	0,6	20GCM, CMIP5, 2030, RCP85, SSP2	T	Y	N/A	1,17	N/A	N/A	1,17	2	1,4	1,3	Million people (2010)	Karnauskas et al., 2018	access1-0,access1-3,bcc-csm1-1,csm1-1-m,cesm1-cam5,cnrm-cm5,csiro-mk3-6-0,gfdl-cm3,gfdl-esm2g,gfdl-esm2m,giss-e2-r,hadgem2-cc,hadgem2-es,inmcm4,ipsl-cm5a-lr,ipsl-cm5a-mr,miroc-esm,miroc-esm-chem,miroc5,mri-cgcm3	N/A	2100	Table 1
Freshwater stress	Micronesia	FSI (freshwater stress index) = PCI (population change index) × ACI (aridity change index)	1986–2005 (climatology), 2010 (population)	SSP1–5	0,6	20GCM, CMIP5, 2030, RCP85, SSP2	T	Y	1,03	N/A	N/A	N/A	1,03	1,5	0,9	0,11	Million people (2010)	Karnauskas et al., 2018	access1-0,access1-3,bcc-csm1-1,csm1-1-m,cesm1-cam5,cnrm-cm5,csiro-mk3-6-0,gfdl-cm3,gfdl-esm2g,gfdl-esm2m,giss-e2-r,hadgem2-cc,hadgem2-es,inmcm4,ipsl-cm5a-lr,ipsl-cm5a-mr,miroc-esm,miroc-esm-chem,miroc5,mri-cgcm3	N/A	2100	Table 1
Freshwater stress	Micronesia	FSI (freshwater stress index) = PCI (population change index) × ACI (aridity change index)	1986–2005 (climatology), 2010 (population)	SSP1–5	0,6	20GCM, CMIP5, 2030, RCP85, SSP2	T	Y	N/A	1,03	N/A	N/A	1,03	2	1,4	0,11	Million people (2010)	Karnauskas et al., 2018	access1-0,access1-3,bcc-csm1-1,csm1-1-m,cesm1-cam5,cnrm-cm5,csiro-mk3-6-0,gfdl-cm3,gfdl-esm2g,gfdl-esm2m,giss-e2-r,hadgem2-cc,hadgem2-es,inmcm4,ipsl-cm5a-lr,ipsl-cm5a-mr,miroc-esm,miroc-esm-chem,miroc5,mri-cgcm3	N/A	2100	Table 1
Freshwater stress	Papua New Guinea	FSI (freshwater stress index) = PCI (population change index) × ACI (aridity change index)	1986–2005 (climatology), 2010 (population)	SSP1–5	0,6	20GCM, CMIP5, 2030, RCP85, SSP2	T	Y	1,37	N/A	N/A	N/A	1,37	1,5	0,9	6,86	Million people (2010)	Karnauskas et al., 2018	access1-0,access1-3,bcc-csm1-1,csm1-1-m,cesm1-cam5,cnrm-cm5,csiro-mk3-6-0,gfdl-cm3,gfdl-esm2g,gfdl-esm2m,giss-e2-r,hadgem2-cc,hadgem2-es,inmcm4,ipsl-cm5a-lr,ipsl-cm5a-mr,miroc-esm,miroc-esm-chem,miroc5,mri-cgcm3	N/A	2100	Table 1
Freshwater stress	Papua New Guinea	FSI (freshwater stress index) = PCI (population change index) × ACI (aridity change index)	1986–2005 (climatology), 2010 (population)	SSP1–5	0,6	20GCM, CMIP5, 2030, RCP85, SSP2	T	Y	N/A	1,37	N/A	N/A	1,37	2	1,4	6,86	Million people (2010)	Karnauskas et al., 2018	access1-0,access1-3,bcc-csm1-1,csm1-1-m,cesm1-cam5,cnrm-cm5,csiro-mk3-6-0,gfdl-cm3,gfdl-esm2g,gfdl-esm2m,giss-e2-r,hadgem2-cc,hadgem2-es,inmcm4,ipsl-cm5a-lr,ipsl-cm5a-mr,miroc-esm,miroc-esm-chem,miroc5,mri-cgcm3	N/A	2100	Table 1
Freshwater stress	St. Lucia	FSI (freshwater stress index) = PCI (population change index) × ACI (aridity change index)	1986–2005 (climatology), 2010 (population)	SSP1–5	0,6	20GCM, CMIP5, 2030, RCP85, SSP2	T	Y	1,23	N/A	N/A	N/A	1,23	1,5	0,9	0,17	Million people (2010)	Karnauskas et al., 2018	access1-0,access1-3,bcc-csm1-1,csm1-1-m,cesm1-cam5,cnrm-cm5,csiro-mk3-6-0,gfdl-cm3,gfdl-esm2g,gfdl-esm2m,giss-e2-r,hadgem2-cc,hadgem2-es,inmcm4,ipsl-cm5a-lr,ipsl-cm5a-mr,miroc-esm,miroc-esm-chem,miroc5,mri-cgcm3	N/A	2100	Table 1
Freshwater stress	St. Lucia	FSI (freshwater stress index) = PCI (population change index) × ACI (aridity change index)	1986–2005 (climatology), 2010 (population)	SSP1–5	0,6	20GCM, CMIP5, 2030, RCP85, SSP2	T	Y	N/A	1,27	N/A	N/A	1,27	2	1,4	0,17	Million people (2010)	Karnauskas et al., 2018	access1-0,access1-3,bcc-csm1-1,csm1-1-m,cesm1-cam5,cnrm-cm5,csiro-mk3-6-0,gfdl-cm3,gfdl-esm2g,gfdl-esm2m,giss-e2-r,hadgem2-cc,hadgem2-es,inmcm4,ipsl-cm5a-lr,ipsl-cm5a-mr,miroc-esm,miroc-esm-chem,miroc5,mri-cgcm3	N/A	2100	Table 1

Risk	Region	Metric (Unit)	Baseline Time Period against Which Change Measured	Socio-economic Scenario and Date	Baseline Global T above Pre-industrial	Climate Scenario Used	Transient (T) or Equilibrium (E)	Dynamic Model?	Projected Impact at 1.5°C above Pre-Industrial	2°C	3°C	4°C	Projected Impact at Delta T(°C)	Delta T Relative to Pre-Industrial	Delta T Relative to Baseline Temperature	Projected Impact (Reference Value)	Projected Impact (Unit)	Reference	GCM (e.g., MIROC5)	RCM	Future Period	Cited Part
Freshwater stress	St. Vincent & Grenadines	FSI (freshwater stress index) = PCI (population change index) × ACI (aridity change index)	1986–2005 (climatology), 2010 (population)	SSP1–5	0,6	20GCM, CMIP5, 2030, RCP85, SSP2	T	Y	1,06	N/A	N/A	N/A	1,06	1,5	0,9	0,11	Million people (2010)	Karnauskas et al., 2018	access1-0,access1-3,bcc-csm1-1,csm1-1-m,cesm1-cam5,cnrm-cm5,csiro-mk3-6-0,gfdl-cm3,gfdl-esm2g,gfdl-esm2m,giss-e2-r,hadgem2-cc,hadgem2-es,inmcm4,ipsl-cm5a-lr,ipsl-cm5a-mr,miroc-esm,miroc-esm-chem,miroc5,mri-cgcm3	N/A	2100	Table 1
Freshwater stress	St. Vincent & Grenadines	FSI (freshwater stress index) = PCI (population change index) × ACI (aridity change index)	1986–2005 (climatology), 2010 (population)	SSP1–5	0,6	20GCM, CMIP5, 2030, RCP85, SSP2	T	Y	N/A	1,11	N/A	N/A	1,11	2	1,4	0,11	Million people (2010)	Karnauskas et al., 2018	access1-0,access1-3,bcc-csm1-1,csm1-1-m,cesm1-cam5,cnrm-cm5,csiro-mk3-6-0,gfdl-cm3,gfdl-esm2g,gfdl-esm2m,giss-e2-r,hadgem2-cc,hadgem2-es,inmcm4,ipsl-cm5a-lr,ipsl-cm5a-mr,miroc-esm,miroc-esm-chem,miroc5,mri-cgcm3	N/A	2100	Table 1
Freshwater stress	Samoa	FSI (freshwater stress index) = PCI (population change index) × ACI (aridity change index)	1986–2005 (climatology), 2010 (population)	SSP1–5	0,6	20GCM, CMIP5, 2030, RCP85, SSP2	T	Y	1,02	N/A	N/A	N/A	1,02	1,5	0,9	0,18	Million people (2010)	Karnauskas et al., 2018	access1-0,access1-3,bcc-csm1-1,csm1-1-m,cesm1-cam5,cnrm-cm5,csiro-mk3-6-0,gfdl-cm3,gfdl-esm2g,gfdl-esm2m,giss-e2-r,hadgem2-cc,hadgem2-es,inmcm4,ipsl-cm5a-lr,ipsl-cm5a-mr,miroc-esm,miroc-esm-chem,miroc5,mri-cgcm3	N/A	2100	Table 1
Freshwater stress	Samoa	FSI (freshwater stress index) = PCI (population change index) × ACI (aridity change index)	1986–2005 (climatology), 2010 (population)	SSP1–5	0,6	20GCM, CMIP5, 2030, RCP85, SSP2	T	Y	N/A	1,06	N/A	N/A	1,06	2	1,4	0,18	Million people (2010)	Karnauskas et al., 2018	access1-0,access1-3,bcc-csm1-1,csm1-1-m,cesm1-cam5,cnrm-cm5,csiro-mk3-6-0,gfdl-cm3,gfdl-esm2g,gfdl-esm2m,giss-e2-r,hadgem2-cc,hadgem2-es,inmcm4,ipsl-cm5a-lr,ipsl-cm5a-mr,miroc-esm,miroc-esm-chem,miroc5,mri-cgcm3	N/A	2100	Table 1
Freshwater stress	Sao Tome & Principe	FSI (freshwater stress index) = PCI (population change index) × ACI (aridity change index)	1986–2005 (climatology), 2010 (population)	SSP1–5	0,6	20GCM, CMIP5, 2030, RCP85, SSP2	T	Y	1,17	N/A	N/A	N/A	1,17	1,5	0,9	0,17	Million people (2010)	Karnauskas et al., 2018	access1-0,access1-3,bcc-csm1-1,csm1-1-m,cesm1-cam5,cnrm-cm5,csiro-mk3-6-0,gfdl-cm3,gfdl-esm2g,gfdl-esm2m,giss-e2-r,hadgem2-cc,hadgem2-es,inmcm4,ipsl-cm5a-lr,ipsl-cm5a-mr,miroc-esm,miroc-esm-chem,miroc5,mri-cgcm3	N/A	2100	Table 1
Freshwater stress	Sao Tome & Principe	FSI (freshwater stress index) = PCI (population change index) × ACI (aridity change index)	1986–2005 (climatology), 2010 (population)	SSP1–5	0,6	20GCM, CMIP5, 2030, RCP85, SSP2	T	Y	N/A	1,17	N/A	N/A	1,17	2	1,4	0,17	Million people (2010)	Karnauskas et al., 2018	access1-0,access1-3,bcc-csm1-1,csm1-1-m,cesm1-cam5,cnrm-cm5,csiro-mk3-6-0,gfdl-cm3,gfdl-esm2g,gfdl-esm2m,giss-e2-r,hadgem2-cc,hadgem2-es,inmcm4,ipsl-cm5a-lr,ipsl-cm5a-mr,miroc-esm,miroc-esm-chem,miroc5,mri-cgcm3	N/A	2100	Table 1
Freshwater stress	Singapore	FSI (freshwater stress index) = PCI (population change index) × ACI (aridity change index)	1986–2005 (climatology), 2010 (population)	SSP1–5	0,6	20GCM, CMIP5, 2030, RCP85, SSP2	T	Y	1,25	N/A	N/A	N/A	1,25	1,5	0,9	5,09	Million people (2010)	Karnauskas et al., 2018	access1-0,access1-3,bcc-csm1-1,csm1-1-m,cesm1-cam5,cnrm-cm5,csiro-mk3-6-0,gfdl-cm3,gfdl-esm2g,gfdl-esm2m,giss-e2-r,hadgem2-cc,hadgem2-es,inmcm4,ipsl-cm5a-lr,ipsl-cm5a-mr,miroc-esm,miroc-esm-chem,miroc5,mri-cgcm3	N/A	2100	Table 1
Freshwater stress	Singapore	FSI (freshwater stress index) = PCI (population change index) × ACI (aridity change index)	1986–2005 (climatology), 2010 (population)	SSP1–5	0,6	20GCM, CMIP5, 2030, RCP85, SSP2	T	Y	N/A	1,26	N/A	N/A	1,26	2	1,4	5,09	Million people (2010)	Karnauskas et al., 2018	access1-0,access1-3,bcc-csm1-1,csm1-1-m,cesm1-cam5,cnrm-cm5,csiro-mk3-6-0,gfdl-cm3,gfdl-esm2g,gfdl-esm2m,giss-e2-r,hadgem2-cc,hadgem2-es,inmcm4,ipsl-cm5a-lr,ipsl-cm5a-mr,miroc-esm,miroc-esm-chem,miroc5,mri-cgcm3	N/A	2100	Table 1

Risk	Region	Metric (Unit)	Baseline Time Period against Which Change Measured	Socio-economic Scenario and Date	Baseline Global T above Pre-industrial	Climate Scenario Used	Transient (T) or Equilibrium (E)	Dynamic Model?	Projected Impact at 1.5°C above Pre-Industrial	2°C	3°C	4°C	Projected Impact at Delta T(°C)	Delta T Relative to Pre-Industrial	Delta T Relative to Baseline Temperature	Projected Impact (Reference Value)	Projected Impact (Unit)	Reference	GCM (e.g., MIROC5)	RCM	Future Period	Cited Part
Freshwater stress	Solomon Islands	FSI (freshwater stress index) = PCI (population change index) × ACI (aridity change index)	1986–2005 (climatology), 2010 (population)	SSP1–5	0,6	20GCM, CMIP5, 2030, RCP85, SSP2	T	Y	1,45	N/A	N/A	N/A	1,45	1,5	0,9	0,54	Million people (2010)	Karnauskas et al., 2018	access1-0,access1-3,bcc-csm1-1,csm1-1-m,cesm1-cam5,cnrm-cm5,csiro-mk3-6-0,gfdl-cm3,gfdl-esm2g,gfdl-esm2m,giss-e2-r,hadgem2-cc,hadgem2-es,inmcm4,ipsl-cm5a-lr,ipsl-cm5a-mr,miroc-esm,miroc-esm-chem,miroc5,mri-cgcm3	N/A	2100	Table 1
Freshwater stress	Solomon Islands	FSI (freshwater stress index) = PCI (population change index) × ACI (aridity change index)	1986–2005 (climatology), 2010 (population)	SSP1–5	0.6	20GCM, CMIP5, 2030, RCP85, SSP2	T	Y	N/A	1,47	N/A	N/A	1,47	2	1,4	0,54	Million people (2010)	Karnauskas et al., 2018	access1-0,access1-3,bcc-csm1-1,csm1-1-m,cesm1-cam5,cnrm-cm5,csiro-mk3-6-0,gfdl-cm3,gfdl-esm2g,gfdl-esm2m,giss-e2-r,hadgem2-cc,hadgem2-es,inmcm4,ipsl-cm5a-lr,ipsl-cm5a-mr,miroc-esm,miroc-esm-chem,miroc5,mri-cgcm3	N/A	2100	Table 1
Freshwater stress	Suriname	FSI (freshwater stress index) = PCI (population change index) × ACI (aridity change index)	1986–2005 (climatology), 2010 (population)	SSP1–5	0,6	20GCM, CMIP5, 2030, RCP85, SSP2	T	Y	1,25	N/A	N/A	N/A	1,25	1,5	0,9	0,52	Million people (2010)	Karnauskas et al., 2018	access1-0,access1-3,bcc-csm1-1,csm1-1-m,cesm1-cam5,cnrm-cm5,csiro-mk3-6-0,gfdl-cm3,gfdl-esm2g,gfdl-esm2m,giss-e2-r,hadgem2-cc,hadgem2-es,inmcm4,ipsl-cm5a-lr,ipsl-cm5a-mr,miroc-esm,miroc-esm-chem,miroc5,mri-cgcm3	N/A	2100	Table 1
Freshwater stress	Suriname	FSI (freshwater stress index) = PCI (population change index) × ACI (aridity change index)	1986–2005 (climatology), 2010 (population)	SSP1–5	0.6	20GCM, CMIP5, 2030, RCP85, SSP2	T	Y	N/A	1,25	N/A	N/A	1,25	2	1,4	0,52	Million people (2010)	Karnauskas et al., 2018	access1-0,access1-3,bcc-csm1-1,csm1-1-m,cesm1-cam5,cnrm-cm5,csiro-mk3-6-0,gfdl-cm3,gfdl-esm2g,gfdl-esm2m,giss-e2-r,hadgem2-cc,hadgem2-es,inmcm4,ipsl-cm5a-lr,ipsl-cm5a-mr,miroc-esm,miroc-esm-chem,miroc5,mri-cgcm3	N/A	2100	Table 1
Freshwater stress	Timor-Leste	FSI (freshwater stress index) = PCI (population change index) × ACI (aridity change index)	1986–2005 (climatology), 2010 (population)	SSP1–5	0,6	20GCM, CMIP5, 2030, RCP85, SSP2	T	Y	1,52	N/A	N/A	N/A	1,52	1,5	0,9	1,12	Million people (2010)	Karnauskas et al., 2018	access1-0,access1-3,bcc-csm1-1,csm1-1-m,cesm1-cam5,cnrm-cm5,csiro-mk3-6-0,gfdl-cm3,gfdl-esm2g,gfdl-esm2m,giss-e2-r,hadgem2-cc,hadgem2-es,inmcm4,ipsl-cm5a-lr,ipsl-cm5a-mr,miroc-esm,miroc-esm-chem,miroc5,mri-cgcm3	N/A	2100	Table 1
Freshwater stress	Timor-Leste	FSI (freshwater stress index) = PCI (population change index) × ACI (aridity change index)	1986–2005 (climatology), 2010 (population)	SSP1–5	0.6	20GCM, CMIP5, 2030, RCP85, SSP2	T	Y	N/A	1,54	N/A	N/A	1,54	2	1,4	1,12	Million people (2010)	Karnauskas et al., 2018	access1-0,access1-3,bcc-csm1-1,csm1-1-m,cesm1-cam5,cnrm-cm5,csiro-mk3-6-0,gfdl-cm3,gfdl-esm2g,gfdl-esm2m,giss-e2-r,hadgem2-cc,hadgem2-es,inmcm4,ipsl-cm5a-lr,ipsl-cm5a-mr,miroc-esm,miroc-esm-chem,miroc5,mri-cgcm3	N/A	2100	Table 1
Freshwater stress	Tonga	FSI (freshwater stress index) = PCI (population change index) × ACI (aridity change index)	1986–2005 (climatology), 2010 (population)	SSP1–5	0,6	20GCM, CMIP5, 2030, RCP85, SSP2	T	Y	1,07	N/A	N/A	N/A	1,07	1,5	0,9	0,1	Million people (2010)	Karnauskas et al., 2018	access1-0,access1-3,bcc-csm1-1,csm1-1-m,cesm1-cam5,cnrm-cm5,csiro-mk3-6-0,gfdl-cm3,gfdl-esm2g,gfdl-esm2m,giss-e2-r,hadgem2-cc,hadgem2-es,inmcm4,ipsl-cm5a-lr,ipsl-cm5a-mr,miroc-esm,miroc-esm-chem,miroc5,mri-cgcm3	N/A	2100	Table 1
Freshwater stress	Tonga	FSI (freshwater stress index) = PCI (population change index) × ACI (aridity change index)	1986–2005 (climatology), 2010 (population)	SSP1–5	0.6	20GCM, CMIP5, 2030, RCP85, SSP2	T	Y	N/A	1,07	N/A	N/A	1,07	2	1,4	0,1	Million people (2010)	Karnauskas et al., 2018	access1-0,access1-3,bcc-csm1-1,csm1-1-m,cesm1-cam5,cnrm-cm5,csiro-mk3-6-0,gfdl-cm3,gfdl-esm2g,gfdl-esm2m,giss-e2-r,hadgem2-cc,hadgem2-es,inmcm4,ipsl-cm5a-lr,ipsl-cm5a-mr,miroc-esm,miroc-esm-chem,miroc5,mri-cgcm3	N/A	2100	Table 1

Risk	Region	Metric (Unit)	Baseline Time Period against Which Change Measured	Socio-economic Scenario and Date	Baseline Global T above Pre-industrial	Climate Scenario Used	Transient (T) or Equilibrium (E)	Dynamic Model?	Projected Impact at 1.5°C above Pre-Industrial	2°C	3°C	4°C	Projected Impact at Delta T(°C)	Delta T Relative to Pre-Industrial	Delta T Relative to Baseline Temperature	Projected Impact (Reference Value)	Projected Impact (Unit)	Reference	GCM (e.g., MIROC5)	RCM	Future Period	Cited Part
Freshwater stress	Trinidad & Tobago	FSI (freshwater stress index) = PCI (population change index) × ACI (aridity change index)	1986–2005 (climatology), 2010 (population)	SSP1–5	0.6	20GCM, CMIP5, 2030, RCP8.5, SSP2	T	Y	1.1	N/A	N/A	N/A	1.1	1.5	0.9	1.34	Million people (2010)	Karnauskas et al., 2018	access1-0,access1-3,bcc-csm1-1,csm1-1-m,cesm1-cam5,cnrm-cm5,csiro-mk3-6-0,gfdl-cm3,gfdl-esm2g,gfdl-esm2m,giss-e2-r,hadgem2-cc,hadgem2-es,inmcm4,ipsl-cm5a-lr,ipsl-cm5a-mr,miroc-esm,miroc-esm-chem,miroc5,mri-cgcm3	N/A	2100	Table 1
Freshwater stress	Trinidad & Tobago	FSI (freshwater stress index) = PCI (population change index) × ACI (aridity change index)	1986–2005 (climatology), 2010 (population)	SSP1–5	0.6	20GCM, CMIP5, 2030, RCP8.5, SSP2	T	Y	N/A	1.14	N/A	N/A	1.14	2	1.4	1.34	Million people (2010)	Karnauskas et al., 2018	access1-0,access1-3,bcc-csm1-1,csm1-1-m,cesm1-cam5,cnrm-cm5,csiro-mk3-6-0,gfdl-cm3,gfdl-esm2g,gfdl-esm2m,giss-e2-r,hadgem2-cc,hadgem2-es,inmcm4,ipsl-cm5a-lr,ipsl-cm5a-mr,miroc-esm,miroc-esm-chem,miroc5,mri-cgcm3	N/A	2100	Table 1
Freshwater stress	Vanuatu	FSI (freshwater stress index) = PCI (population change index) × ACI (aridity change index)	1986–2005 (climatology), 2010 (population)	SSP1–5	0.6	20GCM, CMIP5, 2030, RCP8.5, SSP2	T	Y	1.5	N/A	N/A	N/A	1.5	1.5	0.9	0.24	Million people (2010)	Karnauskas et al., 2018	access1-0,access1-3,bcc-csm1-1,csm1-1-m,cesm1-cam5,cnrm-cm5,csiro-mk3-6-0,gfdl-cm3,gfdl-esm2g,gfdl-esm2m,giss-e2-r,hadgem2-cc,hadgem2-es,inmcm4,ipsl-cm5a-lr,ipsl-cm5a-mr,miroc-esm,miroc-esm-chem,miroc5,mri-cgcm3	N/A	2100	Table 1
Freshwater stress	Vanuatu	FSI (freshwater stress index) = PCI (population change index) × ACI (aridity change index)	1986–2005 (climatology), 2010 (population)	SSP1–5	0.6	20GCM, CMIP5, 2030, RCP8.5, SSP2	T	Y	N/A	1.52	N/A	N/A	1.52	2	1.4	0.24	Million people (2010)	Karnauskas et al., 2018	access1-0,access1-3,bcc-csm1-1,csm1-1-m,cesm1-cam5,cnrm-cm5,csiro-mk3-6-0,gfdl-cm3,gfdl-esm2g,gfdl-esm2m,giss-e2-r,hadgem2-cc,hadgem2-es,inmcm4,ipsl-cm5a-lr,ipsl-cm5a-mr,miroc-esm,miroc-esm-chem,miroc5,mri-cgcm3	N/A	2100	Table 1
Water scarcity, water withdrawal	Global	%	1971–2000	SSP1–5	0.4	RCP2.6, 2011–2040, MIROC-ESM-CHEM, H08	T	Y	N/A	1.4	N/A	N/A	1.4	2.1	1.7	3214	$km^3 yr^{-1}$	Hanasaki et al., 2013	MIROC-ESM-CHEM	N/A	2011–2040	Table 6, Table 9
Water scarcity, water withdrawal	Global	%	1971–2000	SSP1–5	0.4	RCP2.6, 2041–2070, MIROC-ESM-CHEM, H08	E	Y	N/A	N/A	N/A	N/A	0.8	2.8	2.4	3214	$km^3 yr^{-1}$	Hanasaki et al., 2013	MIROC-ESM-CHEM	N/A	2041–2070	Table 6, Table 9
Water scarcity, water withdrawal	Global	%	1971–2000	SSP1–5	0.4	RCP2.6, 2071–2100, MIROC-ESM-CHEM, H08	E	Y	N/A	N/A	N/A	N/A	1.6	2.8	2.4	3214	$km^3 yr^{-1}$	Hanasaki et al., 2013	MIROC-ESM-CHEM	N/A	2071–2100	Table 6, Table 9
Water scarcity, water withdrawal	Global	%	1971–2000	SSP1–5	0.4	RCP2.6, 2011–2040, HadGEM2-ES, H08	T	Y	N/A	N/A	N/A	N/A	0.9	2.2	1.8	3214	$km^3 yr^{-1}$	Hanasaki et al., 2013	HadGEM2-ES	N/A	2011–2040	Table 6, Table 9
Water scarcity, water withdrawal	Global	%	1971–2000	SSP1–5	0.4	RCP2.6, 2041–2070, HadGEM2-ES, H08	E	Y	N/A	N/A	N/A	N/A	-0.0	2.8	2.4	3214	$km^3 yr^{-1}$	Hanasaki et al., 2013	HadGEM2-ES	N/A	2041–2070	Table 6, Table 9
Water scarcity, water withdrawal	Global	%	1971–2000	SSP1–5	0.4	RCP2.6, 2071–2100, HadGEM2-ES, H08	E	Y	N/A	N/A	N/A	N/A	-0.2	2.7	2.3	3214	$km^3 yr^{-1}$	Hanasaki et al., 2013	HadGEM2-ES	N/A	2071–2100	Table 6, Table 9
Water scarcity, water withdrawal	Global	%	1971–2000	SSP1–5	0.4	RCP2.6, 2011–2040, GFDL-ESM2M, H08	T	Y	1.8	N/A	N/A	N/A	1.8	1.5	1.1	3214	$km^3 yr^{-1}$	Hanasaki et al., 2013	GFDL-ESM2M	N/A	2011–2040	Table 6, Table 9
Water scarcity, water withdrawal	Global	%	1971–2000	SSP1–5	0.4	RCP2.6, 2041–2070, GFDL-ESM2M, H08	E	Y	N/A	N/A	N/A	N/A	2	1.7	1.3	3214	$km^3 yr^{-1}$	Hanasaki et al., 2013	GFDL-ESM2M	N/A	2041–2070	Table 6, Table 9
Water scarcity, water withdrawal	Global	%	1971–2000	SSP1–5	0.4	RCP2.6, 2071–2100, GFDL-ESM2M, H08	E	Y	1.1	N/A	N/A	N/A	1.1	1.6	1.2	3214	$km^3 yr^{-1}$	Hanasaki et al., 2013	GFDL-ESM2M	N/A	2071–2100	Table 6, Table 9
Water scarcity, water withdrawal	Global	%	1971–2000	SSP1–5	0.4	RCP4.5, 2011–2040, MIROC-ESM-CHEM, H08	T	Y	N/A	1.4	N/A	N/A	1.4	1.9	1.5	3214	$km^3 yr^{-1}$	Hanasaki et al., 2013	MIROC-ESM-CHEM	N/A	2011–2040	Table 6, Table 9
Water scarcity, water withdrawal	Global	%	1971–2000	SSP1–5	0.4	RCP4.5, 2041–2070, MIROC-ESM-CHEM, H08	T	Y	N/A	N/A	N/A	N/A	2.4	3.3	2.9	3214	$km^3 yr^{-1}$	Hanasaki et al., 2013	MIROC-ESM-CHEM	N/A	2041–2070	Table 6, Table 9
Water scarcity, water withdrawal	Global	%	1971–2000	SSP1–5	0.4	RCP4.5, 2071–2100, MIROC-ESM-CHEM, H08	T	Y	N/A	N/A	N/A	2.8	2.8	4	3.6	3214	$km^3 yr^{-1}$	Hanasaki et al., 2013	MIROC-ESM-CHEM	N/A	2071–2100	Table 6, Table 9
Water scarcity, water withdrawal	Global	%	1971–2000	SSP1–5	0.4	RCP4.5, 2011–2040, HadGEM2-ES, H08	T	Y	N/A	0.6	N/A	N/A	0.6	2.1	1.7	3214	$km^3 yr^{-1}$	Hanasaki et al., 2013	HadGEM2-ES	N/A	2011–2040	Table 6, Table 9
Water scarcity, water withdrawal	Global	%	1971–2000	SSP1–5	0.4	RCP4.5, 2041–2070, HadGEM2-ES, H08	T	Y	N/A	N/A	N/A	N/A	1.7	3.5	3.1	3214	$km^3 yr^{-1}$	Hanasaki et al., 2013	HadGEM2-ES	N/A	2041–2070	Table 6, Table 9
Water scarcity, water withdrawal	Global	%	1971–2000	SSP1–5	0.4	RCP4.5, 2071–2100, HadGEM2-ES, H08	T	Y	N/A	N/A	N/A	N/A	1.9	4.3	3.9	3214	$km^3 yr^{-1}$	Hanasaki et al., 2013	HadGEM2-ES	N/A	2071–2100	Table 6, Table 9
Water scarcity, water withdrawal	Global	%	1971–2000	SSP1–5	0.4	RCP4.5, 2011–2040, GFDL-ESM2M, H08	T	Y	2.3	N/A	N/A	N/A	2.3	1.6	1.2	3214	$km^3 yr^{-1}$	Hanasaki et al., 2013	GFDL-ESM2M	N/A	2011–2040	Table 6, Table 9
Water scarcity, water withdrawal	Global	%	1971–2000	SSP1–5	0.4	RCP4.5, 2041–2070, GFDL-ESM2M, H08	T	Y	N/A	N/A	N/A	N/A	2.3	2.2	1.8	3214	$km^3 yr^{-1}$	Hanasaki et al., 2013	GFDL-ESM2M	N/A	2041–2070	Table 6, Table 9
Water scarcity, water withdrawal	Global	%	1971–2000	SSP1–5	0.4	RCP4.5, 2071–2100, GFDL-ESM2M, H08	T	Y	N/A	N/A	N/A	N/A	2.4	2.4	2	3214	$km^3 yr^{-1}$	Hanasaki et al., 2013	GFDL-ESM2M	N/A	2071–2100	Table 6, Table 9
Water scarcity, water withdrawal	Global	%	1971–2000	SSP1–5	0.4	RCP8.5, 2011–2040, MIROC-ESM-CHEM, H08	T	Y	N/A	2	N/A	N/A	2	2.1	1.7	3214	$km^3 yr^{-1}$	Hanasaki et al., 2013	MIROC-ESM-CHEM	N/A	2011–2040	Table 6, Table 9
Water scarcity, water withdrawal	Global	%	1971–2000	SSP1–5	0.4	RCP8.5, 2041–2070, MIROC-ESM-CHEM, H08	T	Y	N/A	N/A	N/A	N/A	4.8	4.2	3.8	3214	$km^3 yr^{-1}$	Hanasaki et al., 2013	MIROC-ESM-CHEM	N/A	2041–2070	Table 6, Table 9
Water scarcity, water withdrawal	Global	%	1971–2000	SSP1–5	0.4	RCP8.5, 2071–2100, MIROC-ESM-CHEM, H08	T	Y	N/A	N/A	N/A	N/A	10	6.7	6.3	3214	$km^3 yr^{-1}$	Hanasaki et al., 2013	MIROC-ESM-CHEM	N/A	2071–2100	Table 6, Table 9
Water scarcity, water withdrawal	Global	%	1971–2000	SSP1–5	0.4	RCP8.5, 2011–2040, HadGEM2-ES, H08	T	Y	N/A	N/A	N/A	N/A	0.9	2.3	1.9	3214	$km^3 yr^{-1}$	Hanasaki et al., 2013	HadGEM2-ES	N/A	2011–2040	Table 6, Table 9
Water scarcity, water withdrawal	Global	%	1971–2000	SSP1–5	0.4	RCP8.5, 2041–2070, HadGEM2-ES, H08	T	Y	N/A	N/A	N/A	N/A	2.9	4.4	4	3214	$km^3 yr^{-1}$	Hanasaki et al., 2013	HadGEM2-ES	N/A	2041–2070	Table 6, Table 9
Water scarcity, water withdrawal	Global	%	1971–2000	SSP1–5	0.4	RCP8.5, 2071–2100, HadGEM2-ES, H08	T	Y	N/A	N/A	N/A	N/A	6.7	6.8	6.4	3214	$km^3 yr^{-1}$	Hanasaki et al., 2013	HadGEM2-ES	N/A	2071–2100	Table 6, Table 9
Water scarcity, water withdrawal	Global	%	1971–2000	SSP1–5	0.4	RCP8.5, 2011–2040, GFDL-ESM2M, H08	T	Y	1.7	N/A	N/A	N/A	1.7	1.6	1.2	3214	$km^3 yr^{-1}$	Hanasaki et al., 2013	GFDL-ESM2M	N/A	2011–2040	Table 6, Table 9

Risk	Region	Metric (Unit)	Baseline Time Period against Which Change Measured	Socio-economic Scenario and Date	Baseline Global T above Pre-industrial	Climate Scenario Used	Transient (T) or Equilibrium (E)	Dynamic Model?	Projected Impact at 1.5°C above Pre-Industrial	2°C	3°C	4°C	Projected Impact at Delta T(°C)	Delta T Relative to Pre-Industrial	Delta T Relative to Baseline Temperature	Projected Impact (Reference Value)	Projected Impact (Unit)	Reference	GCM (e.g., MIROC5)	RCM	Future Period	Cited Part
Water scarcity, water withdrawal	Global	%	1971–2000	SSP1–S	0,4	RCP8S, 2041–2070, GFDL-ESM2M, H08	T	Y	N/A	N/A	N/A	N/A	3,8	2,8	2,4	3214	$km^3 yr^{-1}$	Hanasaki et al., 2013	GFDL-ESM2M	N/A	2041–2070	Table 6, Table 9
Water scarcity, water withdrawal	Global	%	1971–2000	SSP1–S	0,4	RCP8S, 2071–2100, GFDL-ESM2M, H08	T	Y	N/A	N/A	N/A	N/A	7,1	4,2	3,8	3214	$km^3 yr^{-1}$	Hanasaki et al., 2013	GFDL-ESM2M	N/A	2071–2100	Table 6, Table 9
Impacts on hydropower production	Greece, Portugal, Spain	% (power change)	1971–2000	N/A	N/A	3 GCMs and 3 RCMs, RCP4.5, 8.5, 2004–2043	N/A	N/A	Decrease 5% or less	N/A	N/A	N/A	Decrease 5% or less	1,5	N/A	N/A	N/A	Tobin et al., 2018	MPI-ESM-LR-r1, HadGEM2-ES-r1, EC-EARTH(r1,-r12)	CSC-REMO, SMHI-RCA4, KNMI-RACMO22E	N/A	p5, Fig.1c
Impacts on hydropower production	Greece, Portugal, Spain	% (power change)	1971–2000	N/A	N/A	3 GCMs and 3 RCMs, RCP4.5, 8.5, 2016–2059	N/A	N/A	N/A	Decrease below 10%	N/A	N/A	Decrease below 10%	2	N/A	N/A	N/A	Tobin et al., 2018	MPI-ESM-LR-r1, HadGEM2-ES-r1, EC-EARTH(r1,-r12)	CSC-REMO, SMHI-RCA4, KNMI-RACMO22E	N/A	p5, Fig.1c
Impacts on hydropower production	Greece, Portugal, Spain	% (power change)	1971–2000	N/A	N/A	3 GCMs and 3 RCMs, RCP4.5, 8.5, 2037–2084	N/A	N/A	N/A	N/A	Decrease between 15–20%	N/A	Decrease between 15–20%	3	N/A	N/A	N/A	Tobin et al., 2018	MPI-ESM-LR-r1, HadGEM2-ES-r1, EC-EARTH(r1,-r12)	CSC-REMO, SMHI-RCA4, KNMI-RACMO22E	N/A	p5, Fig.1c
Impacts on thermoelectric power production	Europe	% (power change)	1971–2000	N/A	N/A	3 GCMs and 3 RCMs, RCP4.5, 8.5, 2004–2043	N/A	N/A	Decrease about 5%	N/A	N/A	N/A	Decrease about 5%	1,5	N/A	N/A	N/A	Tobin et al., 2018	MPI-ESM-LR-r1, HadGEM2-ES-r1, EC-EARTH(r1,-r12)	CSC-REMO, SMHI-RCA4, KNMI-RACMO22E	N/A	p5, Fig. 1d
Impacts on thermoelectric power production	Europe	% (power change)	1971–2000	N/A	N/A	3 GCMs and 3 RCMs, RCP4.5, 8.5, 2016–2059	N/A	N/A	N/A	Decrease about 10%	N/A	N/A	Decrease about 10%	2	N/A	N/A	N/A	Tobin et al., 2018	MPI-ESM-LR-r1, HadGEM2-ES-r1, EC-EARTH(r1,-r12)	CSC-REMO, SMHI-RCA4, KNMI-RACMO22E	N/A	p5, Fig. 1d
Impacts on thermoelectric power production	Europe	% (power change)	1971–2000	N/A	N/A	3 GCMs and 3 RCMs, RCP4.5, 8.5, 2037–2084	N/A	N/A	N/A	N/A	Decrease about 15% (Bulgaria, Greece, Spain; 15–20% decrease)	N/A	Decrease about 15% (Bulgaria, Greece, Spain; 15–20% decrease)	3	N/A	N/A	N/A	Tobin et al., 2018	MPI-ESM-LR-r1, HadGEM2-ES-r1, EC-EARTH(r1,-r12)	CSC-REMO, SMHI-RCA4, KNMI-RACMO22E	N/A	p5, Fig. 1d
Increased flooding, population affected	Global	%	1976–2005	N/A	N/A	Transition, 7 GCMs, EC-EARTH3-HR v3.1, RCP8.5	T	N/A	100	N/A	N/A	N/A	100	1.5	N/A	N/A	N/A	Alfieri et al., 2017	IPSL-CM5A-LR, GFDL-ESM2M, HadGEM2-ES, EC-EARTH, GISS-E2-H, IPSL-CM5A-MR, HadCM3LC	N/A	2100	p 176-179 Fig4-Fig6
Increased flooding, population affected	Global	%	1976–2005	N/A	N/A	Transition, 7 GCMs, EC-EARTH3-HR v3.1, RCP8.5	T	N/A	N/A	170	N/A	N/A	170	2	N/A	N/A	N/A	Alfieri et al., 2017	IPSL-CM5A-LR, GFDL-ESM2M, HadGEM2-ES, EC-EARTH, GISS-E2-H, IPSL-CM5A-MR, HadCM3LC	N/A	2100	p 176-179 Fig4-Fig6
Increased flooding, population affected	Global	%	1976–2005	N/A	N/A	Transition, 7 GCMs, EC-EARTH3-HR v3.1, RCP8.5	T	N/A	N/A	N/A	N/A	580	580	4	N/A	N/A	N/A	Alfieri et al., 2017	IPSL-CM5A-LR, GFDL-ESM2M, HadGEM2-ES, EC-EARTH, GISS-E2-H, IPSL-CM5A-MR, HadCM3LC	N/A	2100	p 176-179 Fig4-Fig6
River flood risk	28 European countries	Population affected (1000pp/year)	1976–2005	N/A	N/A	7 JRC-EU, 5 ISIMIP, 7 JRC-GL, RCP8.5, SWLs (specific warming levels)	N/A	N/A	650	N/A	N/A	N/A	650	1,5	N/A	350	Population affected (1000pp/year)	Alfieri et al., 2018	3 JRC-EU(EC-EARTH,HadGEM2-ES,MPI-ESM-LR),5 ISIMIP(GFDL-ESM2M,HadGEM2-ES,IPSL-CM5A-LR,MIROC-ESM-CHEM,NorESM1-M),7 JRC-GL(IPSL-CM5A-LR,GFDL-ESM2M,HadGEM2-ES,EC-EARTH,GISS-E2-H,IPSL-CM5A-MR,HadCM3LC)	4 JRC-EU(RACMO22E,REMO2009,CCLM4-8-17,RCA4),JRC-GL(EC-EARTH3-HR)	N/A	Table 3
River flood risk	28 European countries	Population affected (1000pp/year)	1976–2005	N/A	N/A	7 JRC-EU, 5 ISIMIP, 7 JRC-GL, RCP8.5, SWLs (specific warming levels)	N/A	N/A	N/A	674	N/A	N/A	674	2	N/A	350	Population affected (1000pp/year)	Alfieri et al., 2018	3 JRC-EU(EC-EARTH,HadGEM2-ES,MPI-ESM-LR),5 ISIMIP(GFDL-ESM2M,HadGEM2-ES,IPSL-CM5A-LR,MIROC-ESM-CHEM,NorESM1-M),7 JRC-GL(IPSL-CM5A-LR,GFDL-ESM2M,HadGEM2-ES,EC-EARTH,GISS-E2-H,IPSL-CM5A-MR,HadCM3LC)	4 JRC-EU(RACMO22E,REMO2009,CCLM4-8-17,RCA4),JRC-GL(EC-EARTH3-HR)	N/A	Table 3
River flood risk	28 European countries	Population affected (1000pp/year)	1976–2005	N/A	N/A	7 JRC-EU, 5 ISIMIP, 7 JRC-GL, RCP8.5, SWLs (specific warming levels)	N/A	N/A	N/A	N/A	781	N/A	781	3	N/A	350	Population affected (1000pp/year)	Alfieri et al., 2018	3 JRC-EU(EC-EARTH,HadGEM2-ES,MPI-ESM-LR),5 ISIMIP(GFDL-ESM2M,HadGEM2-ES,IPSL-CM5A-LR,MIROC-ESM-CHEM,NorESM1-M),7 JRC-GL(IPSL-CM5A-LR,GFDL-ESM2M,HadGEM2-ES,EC-EARTH,GISS-E2-H,IPSL-CM5A-MR,HadCM3LC)	4 JRC-EU(RACMO22E,REMO2009,CCLM4-8-17,RCA4),JRC-GL(EC-EARTH3-HR)	N/A	Table 3
River flood risk	28 European countries	Population affected, relative change (%)	1976–2005	N/A	N/A	7 JRC-EU, 5 ISIMIP, 7 JRC-GL, RCP8.5, SWLs (specific warming levels)	N/A	N/A	86	N/A	N/A	N/A	86	1,5	N/A	350	Population affected (1000pp/year)	Alfieri et al., 2018	3 JRC-EU(EC-EARTH,HadGEM2-ES,MPI-ESM-LR),5 ISIMIP(GFDL-ESM2M,HadGEM2-ES,IPSL-CM5A-LR,MIROC-ESM-CHEM,NorESM1-M),7 JRC-GL(IPSL-CM5A-LR,GFDL-ESM2M,HadGEM2-ES,EC-EARTH,GISS-E2-H,IPSL-CM5A-MR,HadCM3LC)	4 JRC-EU(RACMO22E,REMO2009,CCLM4-8-17,RCA4),JRC-GL(EC-EARTH3-HR)	N/A	Table 3
River flood risk	28 European countries	Population affected, relative change (%)	1976–2005	N/A	N/A	7 JRC-EU, 5 ISIMIP, 7 JRC-GL, RCP8.5, SWLs (specific warming levels)	N/A	N/A	N/A	93	N/A	N/A	93	2	N/A	350	Population affected (1000pp/year)	Alfieri et al., 2018	3 JRC-EU(EC-EARTH,HadGEM2-ES,MPI-ESM-LR),5 ISIMIP(GFDL-ESM2M,HadGEM2-ES,IPSL-CM5A-LR,MIROC-ESM-CHEM,NorESM1-M),7 JRC-GL(IPSL-CM5A-LR,GFDL-ESM2M,HadGEM2-ES,EC-EARTH,GISS-E2-H,IPSL-CM5A-MR,HadCM3LC)	4 JRC-EU(RACMO22E,REMO2009,CCLM4-8-17,RCA4),JRC-GL(EC-EARTH3-HR)	N/A	Table 3

Risk	Region	Metric (Unit)	Baseline Time Period against Which Change Measured	Socio-economic Scenario and Date	Baseline Global T above Pre-industrial	Climate Scenario Used	Transient (T) or Equilibrium (E)	Dynamic Model?	Projected Impact at 1.5°C above Pre-Industrial	2°C	3°C	4°C	Projected Impact at Delta T(°C)	Delta T Relative to Pre-Industrial	Delta T Relative to Baseline Temperature	Projected Impact (Reference Value)	Projected Impact (Unit)	Reference	GCM (e.g., MIROC5)	RCM	Future Period	Cited Part
River flood risk	38 European countries	Population affected, relative change (%)	1976–2005	N/A	N/A	7 JRC-EU, 5 ISIMIP, 7 JRC-GL, RCP8.5, SWLs (specific warming levels)	N/A	N/A	N/A	N/A	123	N/A	123	3	N/A	350	Population affected (1000 pp/year)	Alfieri et al., 2018	3 JRC-EU(EC-EARTH,HadGEM2-ES,MPI-ESM-LR),5 ISIMIP(GFDL-ESM2M,HadGEM2-ES,IPSL-CM5A-LR,MIROC-ESM-CHEM,NorESM1-M),7 JRC-GL(IPSL-CM5A-LR,GFDL-ESM2M,HadGEM2-ES,EC-EARTH,GISS-E2-H,IPSL-CM5A-MR,HadCM3LC)	4 JRC-EU(RACMO22E,REMO2009,CCLM4-8-17,RCA4),JRC-GL(EC-EARTH3-HR)	N/A	Table 3
Increased flooding, Increased river flood frequency	Global	Million people (>1000m3capita-1yr-1)	1961–1990	SSP1	0,3	Transition of RCP2.6 in 2050s, 19 CMIP5 GCMs	T	N/A	253	N/A	N/A	N/A	253 (83-473)	Around 1.6	Around 1.3	Population in 2050, total 8411, flood prone 847	Million people	Arnell and Lloyd-Hughes, 2014	CSIRO-Mk3-6-0, FIO-ESM, GFDL-CM3, GFDL-ESM2G, GFDL-ESM2M, GISS-E2-H, GISS-E2-R, HadGEM2-AO, HadGEM2-ES, IPSL-CM5A-LR, IPSL-CM5A-MR, MIROC-ESM, MIROC-ESM-CHEM, MIROC5, MRI-CGCM3, NorESM1-M, NorESM1-ME, bcc-csm1-1, bcc-csm1-1-m	N/A	2070–2099	Table 2 Table 3 c) Fig.1
Increased flooding, Increased river flood frequency	Global	Million people (>1000m3capita-1yr-1)	1961–1990	SSP1	0,3	Transition of RCP4.5 in 2050s, 19 CMIP5 GCMs	T	N/A	N/A	279	N/A	N/A	279 (77-478)	Around 2	Around 1.7	Population in 2050, total 8411, flood prone 847	Million people	Arnell and Lloyd-Hughes, 2014	CSIRO-Mk3-6-0, FIO-ESM, GFDL-CM3, GFDL-ESM2G, GFDL-ESM2M, GISS-E2-H, GISS-E2-R, HadGEM2-AO, HadGEM2-ES, IPSL-CM5A-LR, IPSL-CM5A-MR, MIROC-ESM, MIROC-ESM-CHEM, MIROC5, MRI-CGCM3, NorESM1-M, NorESM1-ME, bcc-csm1-1, bcc-csm1-1-m	N/A	2070–2099	Table 2 Table 3 c) Fig.1
Increased flooding, Increased river flood frequency	Global	Million people (>1000m3capita-1yr-1)	1961–1990	SSP2	0,3	Transition of RCP2.6 in 2050s, 19 CMIP5 GCMs	T	N/A	280	N/A	N/A	N/A	280 (93-525)	Around 1.6	Around 1.3	Population in 2050, total 9245, flood prone 931	Million people	Arnell and Lloyd-Hughes, 2014	CSIRO-Mk3-6-0, FIO-ESM, GFDL-CM3, GFDL-ESM2G, GFDL-ESM2M, GISS-E2-H, GISS-E2-R, HadGEM2-AO, HadGEM2-ES, IPSL-CM5A-LR, IPSL-CM5A-MR, MIROC-ESM, MIROC-ESM-CHEM, MIROC5, MRI-CGCM3, NorESM1-M, NorESM1-ME, bcc-csm1-1, bcc-csm1-1-m	N/A	2070–2099	Table 2 Table 3 c) Fig.1
Increased flooding, Increased river flood frequency	Global	Million people (>1000m³capita⁻¹yr⁻¹)	1961–1990	SSP2	0,3	Transition of RCP4.5 in 2050s, 19 CMIP5 GCMs	T	N/A	N/A	309	N/A	N/A	309 (84-530)	Around 2	Around 1.7	Population in 2050, total 9245, flood prone 931	Million people	Arnell and Lloyd-Hughes, 2014	CSIRO-Mk3-6-0, FIO-ESM, GFDL-CM3, GFDL-ESM2G, GFDL-ESM2M, GISS-E2-H, GISS-E2-R, HadGEM2-AO, HadGEM2-ES, IPSL-CM5A-LR, IPSL-CM5A-MR, MIROC-ESM, MIROC-ESM-CHEM, MIROC5, MRI-CGCM3, NorESM1-M, NorESM1-ME, bcc-csm1-1, bcc-csm1-1-m	N/A	2070–2099	Table 2 Table 3 c) Fig.1
Increased flooding, Increased river flood frequency	Global	Million people (>1000m3capita-1yr-1	1961–1990	SSP3	0,3	Transition of RCP2.6 in 2050s, 19 CMIP5 GCMs	T	N/A	317	N/A	N/A	N/A	317 (105-596)	Around 1.6	Around 1.3	Population in 2050, total 10233, flood prone 1041	Million people	Arnell and Lloyd-Hughes, 2014	CSIRO-Mk3-6-0, FIO-ESM, GFDL-CM3, GFDL-ESM2G, GFDL-ESM2M, GISS-E2-H, GISS-E2-R, HadGEM2-AO, HadGEM2-ES, IPSL-CM5A-LR, IPSL-CM5A-MR, MIROC-ESM, MIROC-ESM-CHEM, MIROC5, MRI-CGCM3, NorESM1-M, NorESM1-ME, bcc-csm1-1, bcc-csm1-1-m	N/A	2070–2099	Table 2 Table 3 c) Fig.1
Increased flooding, Increased river flood frequency	Global	Million people (>1000m3capita-1yr-1)	1961–1990	SSP3	0,3	Transition of RCP4.5 in 2050s, 19 CMIP5 GCMs	T	N/A	N/A	351	N/A	N/A	351 (93-602)	Around 2	Around 1.7	Population in 2050, total 10233, flood prone 1041	Million people	Arnell and Lloyd-Hughes, 2014	CSIRO-Mk3-6-0, FIO-ESM, GFDL-CM3, GFDL-ESM2G, GFDL-ESM2M, GISS-E2-H, GISS-E2-R, HadGEM2-AO, HadGEM2-ES, IPSL-CM5A-LR, IPSL-CM5A-MR, MIROC-ESM, MIROC-ESM-CHEM, MIROC5, MRI-CGCM3, NorESM1-M, NorESM1-ME, bcc-csm1-1, bcc-csm1-1-m	N/A	2070–2099	Table 2 Table 3 c) Fig.1

Risk	Region	Metric (Unit)	Baseline Time Period against Which Change Measured	Socio-economic Scenario and Date	Baseline Global T above Pre-industrial	Climate Scenario Used	Transient (T) or Equilibrium (E)	Dynamic Model?	Projected Impact at 1.5°C above Pre-Industrial	2°C	3°C	4°C	Projected Impact at Delta T(°C)	Delta T Relative to Pre-Industrial	Delta T Relative to Baseline Temperature	Projected Impact (Reference Value)	Projected Impact (Unit)	Reference	GCM (e.g., MIROC5)	RCM	Future Period	Cited Part
Increased flooding, increased river flood frequency	Global	Million people (>1000m3a-1yr-1)	1961–1990	SSP4	0,3	Transition of RCP2.6 in 2050s, 19 CMIP5 GCMs	T	N/A	268	N/A	N/A	N/A	268 (90-503)	Around 1.6	Around 1.3	Population in 2050, total 9366 flood prone 907	Million people	Arnell and Lloyd-Hughes, 2014	CSIRO-Mk3-6-0,FIO-ESM,GFDL-CM3,GFDL-ESM2G,GFDL-ESM2M,GISS-E2-H,GISS-E2-R,HadGEM2-AO,HadGEM2-ES,IPSL-CM5A-LR,IPSL-CM5A-MR,MIROC-ESM,MIROC-ESM-CEM,MIROC5,MRI-CGCM3,NorESM1-M,NorESM1-ME,bcc-csm1-1,bcc-csm1-1-m	N/A	2070–2099	Table 2 Table 3 c) Fig.1
Increased flooding, increased river flood frequency	Global	Million people (>1000m3a-1yr-1)	1961–1990	SSP4	0,3	Transition of RCP4.5 in 2050s, 19 CMIP5 GCMs	T	N/A	N/A	297	N/A	N/A	297 (81-507)	Around 2	Around 1.7	Population in 2050, total 9366 flood prone 907	Million people	Arnell and Lloyd-Hughes, 2014	CSIRO-Mk3-6-0,FIO-ESM,GFDL-CM3,GFDL-ESM2G,GFDL-ESM2M,GISS-E2-H,GISS-E2-R,HadGEM2-AO,HadGEM2-ES,IPSL-CM5A-LR,IPSL-CM5A-MR,MIROC-ESM,MIROC-ESM-CEM,MIROC5,MRI-CGCM3,NorESM1-M,NorESM1-ME,bcc-csm1-1,bcc-csm1-1-m	N/A	2070–2099	Table 2 Table 3 c) Fig.1
Increased flooding, increased river flood frequency	Global	Million people (>1000m3a-1yr-1)	1961–1990	SSP5	0,3	Transition of RCP2.6 in 2050s, 19 CMIP5 GCMs	T	N/A	250	N/A	N/A	N/A	250 (83-468)	Around 1.6	Around 1.3	Population in 2050, total 8508 flood prone 846	Million people	Arnell and Lloyd-Hughes, 2014	CSIRO-Mk3-6-0,FIO-ESM,GFDL-CM3,GFDL-ESM2G,GFDL-ESM2M,GISS-E2-H,GISS-E2-R,HadGEM2-AO,HadGEM2-ES,IPSL-CM5A-LR,IPSL-CM5A-MR,MIROC-ESM,MIROC-ESM-CEM,MIROC5,MRI-CGCM3,NorESM1-M,NorESM1-ME,bcc-csm1-1,bcc-csm1-1-m	N/A	2070–2099	Table 2 Table 3 c) Fig.1
Increased flooding, increased river flood frequency	Global	Million people (>1000m3a-1yr-1)	1961–1990	SSP5	0,3	Transition of RCP4.5 in 2050s, 19 CMIP5 GCMs	T	N/A	N/A	276	N/A	N/A	276 (77-473)	Around 2	Around 1.7	Population in 2050, total 8508 flood prone 846	Million people	Arnell and Lloyd-Hughes, 2014	CSIRO-Mk3-6-0,FIO-ESM,GFDL-CM3,GFDL-ESM2G,GFDL-ESM2M,GISS-E2-H,GISS-E2-R,HadGEM2-AO,HadGEM2-ES,IPSL-CM5A-LR,IPSL-CM5A-MR,MIROC-ESM,MIROC-ESM-CEM,MIROC5,MRI-CGCM3,NorESM1-M,NorESM1-ME,bcc-csm1-1,bcc-csm1-1-m	N/A	2070–2099	Table 2 Table 3 c) Fig.1
Monthly population exposed to extreme drought	Global	Million people	1955–2005	N/A	N/A	SPEI, 16 CMIP5, RCP8.5, 2021–2040	N/A	Y	114,3	N/A	N/A	N/A	114,3	Around 1.5	N/A	N/A	N/A	Smirnov et al., 2016	ACCESS1-0, BCC-CSM1.1, BNU-ESM, CCSM4, CESM1-CAM5, CMCC-CM, CSIRO-Mk3-6-0, EC-EARTH, FGOALS-g2, GFDL-CM3, IPSL-CM5A-MR, MIROC5, MPI-ESM-MR, MRI-CGCM3, NorESM1-M	N/A	2018–2100	Table 1
Monthly population exposed to extreme drought	Global	Million people	1955–2005	N/A	N/A	SPEI, 16 CMIP5, RCP8.5, 2041–2060	N/A	Y	N/A	190,4	N/A	N/A	190,4	Around 2	N/A	N/A	N/A	Smirnov et al., 2016	ACCESS1-0, BCC-CSM1.1, BNU-ESM, CCSM4, CESM1-CAM5, CMCC-CM, CSIRO-Mk3-6-0, EC-EARTH, FGOALS-g2, GFDL-CM3, IPSL-CM5A-MR, MIROC5, MPI-ESM-MR, MRI-CGCM3, NorESM1-M	N/A	2018–2100	Table 1
Drought	Globally	Affected total population (million)	1986–2005 (GMT), 2000 (population)	SSP1	0,6	11CMIP5, RCP4.5 (2027–2038), RCP8.5 (2029–2047), SSP1	T	Y	+132.5±216.2	N/A	N/A	N/A	+132.5± 216.2	1.3-1.7	N/A	N/A	N/A	Liu et al., 2018	ACCESS1.0,BCC_CSM1.1,BNU-ESM,CanESM2.3,CNRM-CM5,CSIRO Mk3.6.0,GFDL CM3,INM-CM4.0,IPSL-CM5B-LR,MRI-CGCM3,MIROC-ESM	N/A	2010–2100	p274
Drought	Globally	Affected total population (million)	1986–2005 (GMT), 2000 (population)	SSP1	0,6	11CMIP5, RCP4.5 (2053–2081), RCP8.5 (2042–2053), SSP1	T	Y	N/A	+194.5±276.5	N/A	N/A	+194.5± 276.5	1.8-2.2	N/A	N/A	N/A	Liu et al., 2018	ACCESS1.0,BCC_CSM1.1,BNU-ESM,CanESM2.3,CNRM-CM5,CSIRO Mk3.6.0,GFDL CM3,INM-CM4.0,IPSL-CM5B-LR,MRI-CGCM3,MIROC-ESM	N/A	2010–2100	p274

Risk	Region	Metric (Unit)	Baseline Time Period against Which Change Measured	Socio-economic Scenario and Date	Baseline Global T above Pre-industrial	Climate Scenario Used	Transient (T) or Equilibrium (E)	Dynamic Model?	Projected Impact at 1.5°C above Pre-Industrial	2°C	3°C	4°C	Projected Impact at Delta T(°C)	Delta T Relative to Pre-Industrial	Delta T Relative to Baseline Temperature	Projected Impact (Reference Value)	Projected Impact (Unit)	Reference	GCM (e.g., MIROC5)	RCM	Future Period	Cited Part
Drought	Globally	Affected urban population (million)	1986–2005 (GMT), 2000 (population)	SSP1	0,6	11CMIP5, RCP4.5 (2027–2039), RCP8.5 (2029–2047), SSP1	T	Y	+350.2±158.8	N/A	N/A	N/A	+350.2± 158.8	1.3-1.7	N/A	N/A	N/A	Liu et al., 2018	ACCESS1.0, BCC_CSM1.1, BNU-ESM, CanESM2.3, CNRM-CM5, CSIRO Mk3.6.0, GFDL CM3, INM-CM4.0, IPSL-CM5B-LR, MRI-CGCM3, MIROC-ESM	N/A	2010–2100	p274
Drought	Globally	Affected total population (million)	1986–2005 (GMT), 2000 (population)	SSP1	0,6	11CMIP5, RCP4.5 (2053–2091), RCP8.5 (2042–2053), SSP1	T	Y	N/A	+410.7±213.5	N/A	N/A	+410.7± 213.5	1.8-2.2	N/A	N/A	N/A	Liu et al., 2018	ACCESS1.0, BCC_CSM1.1, BNU-ESM, CanESM2.3, CNRM-CM5, CSIRO Mk3.6.0, GFDL CM3, INM-CM4.0, IPSL-CM5B-LR, MRI-CGCM3, MIROC-ESM	N/A	2010–2100	p274
Drought	Globally	Affected rural population (million)	1986–2005 (GMT), 2000 (population)	SSP1	0,6	11CMIP5, RCP4.5 (2027–2039), RCP8.5 (2029–2047), SSP1	T	Y	-217.7±79.2	N/A	N/A	N/A	-217.7±79.2	1.3-1.7	N/A	N/A	N/A	Liu et al., 2018	ACCESS1.0, BCC_CSM1.1, BNU-ESM, CanESM2.3, CNRM-CM5, CSIRO Mk3.6.0, GFDL CM3, INM-CM4.0, IPSL-CM5B-LR, MRI-CGCM3, MIROC-ESM	N/A	2100	p274
Drought	Globally	Affected rural population (million)	1986–2005 (GMT), 2000 (population)	SSP1	0,6	11CMIP5, RCP4.5 (2053-2091), RCP8.5 (2042-2053), SSP1	T	Y	N/A	-216.2±82.4	N/A	N/A	-216.2±82.4	1.8-2.2	N/A	N/A	N/A	Liu et al., 2018	ACCESS1.0, BCC_CSM1.1, BNU-ESM, CanESM2.3, CNRM-CM5, CSIRO Mk3.6.0, GFDL CM3, INM-CM4.0, IPSL-CM5B-LR, MRI-CGCM3, MIROC-ESM	N/A	2100	p274
Drought	China, the Haihe River Basin (HRB)	Population exposed to drought (million)	1986–2005 (GMT), 2010 (population)	N/A	0,61	COSMO-CLM (CCLM) model, RCP2.6 (2020–2039)	N/A	N/A	236,4	N/A	N/A	N/A	236,4	1,5	N/A	339,65	Population exposure (million)	Sun et al., 2017	N/A	COSMO-CLM(CCLM)model	N/A	p79
Drought	China, the Haihe River Basin (HRB)	Population exposed to drought (million)	1986–2005 (GMT), 2010 (population)	N/A	0,61	COSMO-CLM (CCLM) model, RCP4.5 (2040–2059)	N/A	N/A	N/A	593,6	N/A	N/A	593,6	2	N/A	339,65	Population exposure (million)	Sun et al., 2017	N/A	COSMO-CLM(CCLM)model	N/A	p79
River flood risk	28 European countries	Expected damage (B€/year)	1976–2005	N/A	N/A	7 JRC-EU, RCP8.5, SWLs (specific warming levels)	N/A	N/A	11	N/A	N/A	N/A	11	1,5	N/A	5	Expected damage (B€/year)	Alfieri et al., 2018	3 JRC-EU(EC-EARTH, HadGEM2-ES, MPI-ESM-LR)	4 JRC-EU(RACMO22E, REMO2009, CCLM4-8-17, RCA4)	N/A	Table 2
River flood risk	28 European countries	Expected damage (B€/year)	1976–2005	N/A	N/A	7 JRC-EU, RCP8.5, SWLs (specific warming levels)	N/A	N/A	N/A	13	N/A	N/A	13	2	N/A	5	Expected damage (B€/year)	Alfieri et al., 2018	3 JRC-EU(EC-EARTH, HadGEM2-ES, MPI-ESM-LR)	4 JRC-EU(RACMO22E, REMO2009, CCLM4-8-17, RCA4)	N/A	Table 2
River flood risk	28 European countries	Expected damage (B€/year)	1976–2005	N/A	N/A	7 JRC-EU, RCP8.5, SWLs (specific warming levels)	N/A	N/A	N/A	N/A	14	N/A	14	3	N/A	5	Expected damage (B€/year)	Alfieri et al., 2018	3 JRC-EU(EC-EARTH, HadGEM2-ES, MPI-ESM-LR)	4 JRC-EU(RACMO22E, REMO2009, CCLM4-8-17, RCA4)	N/A	Table 2
River flood risk	28 European countries	Expected damage, relative change (%)	1976–2005	N/A	N/A	7 JRC-EU, RCP8.5, SWLs (specific warming levels)	N/A	N/A	116	N/A	N/A	N/A	116	1,5	N/A	5	Expected damage (B€/year)	Alfieri et al., 2018	3 JRC-EU(EC-EARTH, HadGEM2-ES, MPI-ESM-LR)	4 JRC-EU(RACMO22E, REMO2009, CCLM4-8-17, RCA4)	N/A	Table 2
River flood risk	28 European countries	Expected damage, relative change (%)	1976–2005	N/A	N/A	7 JRC-EU, RCP8.5, SWLs (specific warming levels)	N/A	N/A	N/A	137	N/A	N/A	137	2	N/A	5	Expected damage (B€/year)	Alfieri et al., 2018	3 JRC-EU(EC-EARTH, HadGEM2-ES, MPI-ESM-LR)	4 JRC-EU(RACMO22E, REMO2009, CCLM4-8-17, RCA4)	N/A	Table 2
River flood risk	28 European countries	Expected damage, relative change (%)	1976–2005	N/A	N/A	7 JRC-EU, RCP8.5, SWLs (specific warming levels)	N/A	N/A	N/A	N/A	173	N/A	173	3	N/A	5	Expected damage (B€/year)	Alfieri et al., 2018	3 JRC-EU(EC-EARTH, HadGEM2-ES, MPI-ESM-LR)	4 JRC-EU(RACMO22E, REMO2009, CCLM4-8-17, RCA4)	N/A	Table 2
Groundwater resources	Global	%	1971–2000	N/A	0,4	5 GCMs, RCP8.5, 2070–2099	T	N/A	N/A	2 (1.1-2.6)	N/A	N/A	2 (1.1-2.6)	2	N/A	N/A	N/A	Portmann et al., 2013	HadGEM2-ES, IPSL-CM5A-LR, MIROC-ESM-CHEM, GFDL-ESM2M, NorESM1-M	N/A	2070–2099	Fig.5a, p7
Groundwater resources	Global	%	1971–2000	N/A	0,4	5 GCMs, RCP8.5, 2070–2099	T	N/A	N/A	N/A	3 (1.5-5.3)	N/A	3 (1.5-5.3)	3	N/A	N/A	N/A	Portmann et al., 2013	HadGEM2-ES, IPSL-CM5A-LR, MIROC-ESM-CHEM, GFDL-ESM2M, NorESM1-M	N/A	2070–2099	Fig.5a, p7
Groundwater resources	Global	%	1971–2000	N/A	0,4	3 GCMs, RCP8.5, 2070–2099	T	N/A	N/A	N/A	N/A	3.4 (1.9-4.8)	3.4 (1.9-4.8)	4	N/A	N/A	N/A	Portmann et al., 2013	HadGEM2-ES, IPSL-CM5A-LR, MIROC-ESM-CHEM,	N/A	2070–2099	Fig.5a, p7
Groundwater level	Northwest Bangladesh	m	1991–2009	N/A	N/A	MLR	N/A	Y	N/A	N/A	N/A	N/A	-0,15	N/A	1	N/A	N/A	Salem et al., 2017	N/A	N/A	N/A	Fig.5, p89
Groundwater level	Northwest Bangladesh	m	1991–2009	N/A	N/A	MLR	N/A	Y	N/A	N/A	N/A	N/A	-2,01	N/A	5	N/A	N/A	Salem et al., 2017	N/A	N/A	N/A	Fig.5, p89
Chloride concentration	Lake IJsselmeer, the Netherlands	mg/l	1997–2007 (climate change scenarios); 2007–2000 (reference scenarios); 1990 (temperature)	N/A	N/A	KNMI scenario G, 2010	N/A	Y	N/A	N/A	N/A	N/A	103 (73;177)	N/A	+1 (since1990)	103 (81;136)	mg/l	Bonte and Zwolsman, 2010	N/A	N/A	2050	Table 4, p4416
Chloride concentration	Lake IJsselmeer, the Netherlands	mg/l	1997–2007 (climate change scenarios); 2007–2000 (reference scenarios); 1990 (temperature)	N/A	N/A	KNMI scenario W+, 2010	N/A	Y	N/A	N/A	N/A	N/A	121 (77;267)	N/A	+2 (since1990)	103 (81;136)	mg/l	Bonte and Zwolsman, 2010	N/A	N/A	2050	Table 4, p4416
The daily probability of exceeding the chloride standard for drinking water	Lake IJsselmeer, the Netherlands	%	1997–2007 (climate change scenarios); 2007–2000 (reference scenarios); 1990 (temperature)	N/A	N/A	KNMI scenario G, 2010	N/A	Y	N/A	N/A	N/A	N/A	3,1	N/A	+1 (since1990)	2,5	%	Bonte and Zwolsman, 2010	N/A	N/A	2050	Table 5, p4422

Risk	Region	Metric (Unit)	Baseline Time Period against Which Change Measured	Socio-economic Scenario and Date	Baseline Global T above Pre-industrial	Climate Scenario Used	Transient (T) or Equilibrium (E)	Dynamic Model?	Projected Impact at 1.5°C above Pre-Industrial	2°C	3°C	4°C	Projected Impact at Delta T(°C)	Delta T Relative to Pre-Industrial	Delta T Relative to Baseline Temperature	Projected Impact (Reference Value)	Projected Impact (Unit)	Reference	GCM (e.g., MIROC5)	RCM	Future Period	Cited Part
The daily probability of exceeding the chloride standard for drinking water	Lake IJsselmeer, the Netherlands	%	1997–2007 (climate change scenarios), 2007–2008 (reference scenarios), 1980 (temperature)	N/A	N/A	KNMI scenario W+, 2050	N/A	Y	N/A	N/A	N/A	N/A	14,3	N/A	+2 (since1990)	2,5	%	Bonte and Zwolsman, 2010	N/A	N/A	2050	Table 5, p4422
The maximum duration of the exceedance	Lake IJsselmeer, the Netherlands	Days	1997–2007 (climate change scenarios), 2007–2008 (reference scenarios), 1980 (temperature)	N/A	N/A	KNMI scenario G, 2050	N/A	Y	N/A	N/A	N/A	N/A	124	N/A	+1 (since1990)	103	Days	Bonte and Zwolsman, 2010	N/A	N/A	2050	Table 5, p4422
The maximum duration of the exceedance	Lake IJsselmeer, the Netherlands	Days	1997–2007 (climate change scenarios), 2007–2008 (reference scenarios), 1980 (temperature)	N/A	N/A	KNMI scenario W+, 2050	N/A	Y	N/A	N/A	N/A	N/A	178	N/A	+2 (since1990)	103	Days	Bonte and Zwolsman, 2010	N/A	N/A	2050	Table 5, p4422
Water quality (nutrient yield)	Southeast Asia (Cambodia, Laos, Vietnam) 3S River Basin (Sekong, Srepok, Sesan)	Change in nitrogen (N) yield (%), annual	1981–2008 (air temperatures), 2004–2008 (water quality)	N/A	N/A	5 GCM, RCP4.5, 2015–2039 (2030s), SWAT	N/A	N/A	7,3	N/A	N/A	N/A	7,3	Around 1.5	0,89	1 249 564	Tons	Trang et al., 2017	HadGEM2-AO, CanESM2, IPSL-CM5A-LR, CNRM-CM5, and MPI-ESM-MR	N/A	2030s (2015–2039), 2060s (2045–2069), 2090s (2075–2099)	Table 11
Water quality (nutrient yield)	Southeast Asia (Cambodia, Laos, Vietnam) 3S River Basin (Sekong, Srepok, Sesan)	Change in nitrogen (N) yield (%), annual	1981–2008 (air temperatures), 2004–2008 (water quality)	N/A	N/A	5 GCM, RCP8.5, 2015–2039 (2030s), SWAT	N/A	N/A	N/A	-6,6	N/A	N/A	-6,6	Around 2	1,05	1 249 564	Tons	Trang et al., 2017	HadGEM2-AO, CanESM2, IPSL-CM5A-LR, CNRM-CM5, and MPI-ESM-MR	N/A	2030s (2015–2039), 2060s (2045–2069), 2090s (2075–2099)	Table 11
Water quality (nutrient yield)	Southeast Asia (Cambodia, Laos, Vietnam) 3S River Basin (Sekong, Srepok, Sesan)	Change in nitrogen (N) yield (%), annual	1981–2008 (air temperatures), 2004–2008 (water quality)	N/A	N/A	5 GCM, RCP4.5, 2015–2039 (2030s), SWAT, FG1	N/A	N/A	5,2	N/A	N/A	N/A	5,2	Around 1.5	0,89	1 249 564	Tons	Trang et al., 2017	HadGEM2-AO, CanESM2, IPSL-CM5A-LR, CNRM-CM5, and MPI-ESM-MR	N/A	2030s (2015–2039), 2060s (2045–2069), 2090s (2075–2099)	Table 11
Water quality (nutrient yield)	Southeast Asia (Cambodia, Laos, Vietnam) 3S River Basin (Sekong, Srepok, Sesan)	Change in nitrogen (N) yield (%), annual	1981–2008 (air temperatures), 2004–2008 (water quality)	N/A	N/A	5 GCM, RCP8.5, 2015–2039 (2030s), SWAT, FG1	N/A	N/A	N/A	8,8	N/A	N/A	8,8	Around 2	1,05	1 249 564	Tons	Trang et al., 2017	HadGEM2-AO, CanESM2, IPSL-CM5A-LR, CNRM-CM5, and MPI-ESM-MR	N/A	2030s (2015–2039), 2060s (2045–2069), 2090s (2075–2099)	Table 11
Water quality (nutrient yield)	Southeast Asia (Cambodia, Laos, Vietnam) 3S River Basin (Sekong, Srepok, Sesan)	Change in nitrogen (N) yield (%), annual	1981–2008 (air temperatures), 2004–2008 (water quality)	N/A	N/A	5 GCM, RCP4.5, 2015–2039 (2030s), SWAT, FA1	N/A	N/A	7,5	N/A	N/A	N/A	7,5	Around 1.5	0,89	1 249 564	Tons	Trang et al., 2017	HadGEM2-AO, CanESM2, IPSL-CM5A-LR, CNRM-CM5, and MPI-ESM-MR	N/A	2030s (2015–2039), 2060s (2045–2069), 2090s (2075–2099)	Table 11
Water quality (nutrient yield)	Southeast Asia (Cambodia, Laos, Vietnam) 3S River Basin (Sekong, Srepok, Sesan)	Change in nitrogen (N) yield (%), annual	1981–2008 (air temperatures), 2004–2008 (water quality)	N/A	N/A	5 GCM, RCP8.5, 2015–2039 (2030s), SWAT, FA1	N/A	N/A	N/A	3,7	N/A	N/A	3,7	Around 2	1,05	1 249 564	Tons	Trang et al., 2017	HadGEM2-AO, CanESM2, IPSL-CM5A-LR, CNRM-CM5, and MPI-ESM-MR	N/A	2030s (2015–2039), 2060s (2045–2069), 2090s (2075–2099)	Table 11
Water quality (nutrient yield)	Southeast Asia (Cambodia, Laos, Vietnam) 3S River Basin (Sekong, Srepok, Sesan)	Change in phosphorus (P) yield (%), annual	1981–2008 (air temperatures), 2004–2008 (water quality)	N/A	N/A	5 GCM, RCP4.5, 2015–2039 (2030s), SWAT	N/A	N/A	5,1	N/A	N/A	N/A	5,1	Around 1.5	0,89	459 134	Tons	Trang et al., 2017	HadGEM2-AO, CanESM2, IPSL-CM5A-LR, CNRM-CM5, and MPI-ESM-MR	N/A	2030s (2015–2039), 2060s (2045–2069), 2090s (2075–2099)	Table 12
Water quality (nutrient yield)	Southeast Asia (Cambodia, Laos, Vietnam) 3S River Basin (Sekong, Srepok, Sesan)	Change in phosphorus (P) yield (%), annual	1981–2008 (air temperatures), 2004–2008 (water quality)	N/A	N/A	5 GCM, RCP8.5, 2015–2039 (2030s), SWAT	N/A	N/A	N/A	-3,6	N/A	N/A	-3,6	Around 2	1,05	459 134	Tons	Trang et al., 2017	HadGEM2-AO, CanESM2, IPSL-CM5A-LR, CNRM-CM5, and MPI-ESM-MR	N/A	2030s (2015–2039), 2060s (2045–2069), 2090s (2075–2099)	Table 12
Water quality (nutrient yield)	Southeast Asia (Cambodia, Laos, Vietnam) 3S River Basin (Sekong, Srepok, Sesan)	Change in phosphorus (P) yield (%), annual	1981–2008 (air temperatures), 2004–2008 (water quality)	N/A	N/A	5 GCM, RCP4.5, 2015–2039 (2030s), SWAT, FG1	N/A	N/A	12,6	N/A	N/A	N/A	12,6	Around 1.5	0,89	459 134	Tons	Trang et al., 2017	HadGEM2-AO, CanESM2, IPSL-CM5A-LR, CNRM-CM5, and MPI-ESM-MR	N/A	2030s (2015–2039), 2060s (2045–2069), 2090s (2075–2099)	Table 12

Risk	Region	Metric (Unit)	Baseline Time Period against Which Change Measured	Socio-economic Scenario and Date	Baseline Global T above Pre-industrial	Climate Scenario Used	Transient (T) or Equilibrium (E)	Dynamic Model?	Projected Impact at 1.5°C above Pre-Industrial	2°C	3°C	4°C	Projected Impact at Delta T(°C)	Delta T Relative to Pre-Industrial	Delta T Relative to Baseline Temperature	Projected Impact (Reference Value)	Projected Impact (Unit)	Reference	GCM (e.g., MIROC5)	RCM	Future Period	Cited Part
Water quality (nutrient yield)	Southeast Asia (Cambodia, Laos, Vietnam) 3S River Basin (Sekong, Srepok, Sesan)	Change in phosphorus (P) yield (%), annual	1981–2008 (air temperatures), 2004–2008 (water quality)	N/A	N/A	5 GCM, RCP8.5, 2015–2039 (2030s), SWAT, FG1	N/A	N/A	N/A	11,7	N/A	N/A	11,7	Around 2	1,05	459 134	Tons	Trang et al., 2017	HadGEM2-AO, CanESM2, IPSL-CM5A-LR, CNRM-CM5, and MPI ESM-MR	N/A	2030s (2015–2039), 2060s (2045–2069), 2090s (2075–2099)	Table 12
Water quality (nutrient yield)	Southeast Asia (Cambodia, Laos, Vietnam) 3S River Basin (Sekong, Srepok, Sesan)	Change in phosphorus (P) yield (%), annual	1981–2008 (air temperatures), 2004–2008 (water quality)	N/A	N/A	5 GCM, RCP4.5, 2015–2039 (2030s), SWAT, FA1	N/A	N/A	14,9	N/A	N/A	N/A	14,9	Around 1.5	0,89	459 134	Tons	Trang et al., 2017	HadGEM2-AO, CanESM2, IPSL-CM5A-LR, CNRM-CM5, and MPI ESM-MR	N/A	2030s (2015–2039), 2060s (2045–2069), 2090s (2075–2099)	Table 12
Water quality (nutrient yield)	Southeast Asia (Cambodia, Laos, Vietnam) 3S River Basin (Sekong, Srepok, Sesan)	Change in phosphorus (P) yield (%), annual	1981–2008 (air temperatures), 2004–2008 (water quality)	N/A	N/A	5 GCM, RCP8.5, 2015–2039 (2030s), SWAT, FA1	N/A	N/A	N/A	8,8	N/A	N/A	8,8	Around 2	1,05	459 134	Tons	Trang et al., 2017	HadGEM2-AO, CanESM2, IPSL-CM5A-LR, CNRM-CM5, and MPI ESM-MR	N/A	2030s (2015–2039), 2060s (2045–2069), 2090s (2075–2099)	Table 12

Table 3.SM.2: 3.4.3 Terrestrial and wetland ecosystems

Risk	Region	Metric (Unit)	Baseline Time Period against Which Change Measured	Socio-Economic Scenario and Date	Baseline Global T	Climate Scenario	Transient (T) or Equilibrium (E)	Overshoot Scenario?	Dynamic Model?	Projected Impact at 1.5°C above Pre-Industrial	Projected Impact at 2°C above Pre-Industrial	Projected Impact at Delta T(°C)	Level of Risk after Adaptation at 1.5°C	Level of Risk after Adaptation at 2°C	Type of Adaptation Modelled	Reference
Biome shift to north and to higher elevation	Global	%	1980–2010	Present day population	0.7°C	4 RCP	T	No	Y	1°C above baseline: 3 to 8 %	2°C above baseline: 5 to 19%	4°C above baseline: 35%	N/A	N/A	N/A	Warszawski et al. (2013)
Biomass loss (tropical forest to savanna/grassland)	Central America	kg m^{-2}	1961–1990	0.5°C	1°C	HadGEM2-ES, RCP4.5, 2071-2100	T	No	Y	For 2050, biomass decrease to 6.5 kg/m2	N/A	Local warming of 2 to 4°C (NDC): -4 kg m^{-2} (from 7 to 3 kg m^{-2})	N/A	N/A	N/A	Lyra et al. (2017)
Phenological shifts for primary producers (PP), primary consumers (PC), secondary consumers (SC)	UK	Days	1961–1990	N/A	-	UKCP09 projections in 2050	T	-	Y	(Low emission scenario) PP: -2.2 (-1 to -3) / PC: -5 (-2.5 to -7.5) / SC: -2 (-1 to -3)	(Medium emission scenario) PP: -2.3(-1.2 to -4) / PC: -6 (-3.5 to -8.5) / SC: -2.1 (-	-	N/A	N/A	N/A	Thackeray et al. (2016)
Loss of 50% or more of their climate range	Globe	%	2100 (A1B), no mitigation	-	Pre-industrial	SRES all scenarioos are +2°C or more	T	-	Y		-60% losses if emissions peak in 2016, -40% if peak in 2030	-	N/A	N/A	N/A	Warren et al. (2013)
Loss of 50% or more of their climate range for insects	Globe	%	Not provided	N/A	Pre-industrial	21 CMIP5 models	T	No	N	9% (4–24%)	25% (10–44%)	-	6% (1–18%)	18% (6–35%)	Dispersal	Warren et al. 2018a
Loss of 50% or more of their climate range for vertebrates	Globe	%	Not provided	N/A	Pre-industrial	21 CMIP5 models	T	No	N	5% (3–11%)	10% (6–24%)		4% (2–9%)	8% (4–16%)	Dispersal	Warren et al. 2018a
Loss of 50% or more of their climate range for plants	Globe	%	Not provided	N/A	Pre-industrial	21 CMIP5 models	T	No	N	8% (4–15%)	16% (9–28%)	-	8% (4–15%)	16% (9–28%)	Dispersal	Warren et al. 2018a
% of globe identified as climatic refugia for the different taxa (plants/animals)	Global	%	-	-	-	7 CMIP5 models, AVOID2 scenario	T	Y	Y	An additional 4–15% acts as a refugium	-	-	N/A	N/A	N/A	Smith et al. (2018)
Loss of 50% or more of their climate range for plants	Global	%	-	-	-	21 CMIP5 models	-	-	-	Significant reduction	-	-	N/A	N/A	N/A	Smith et al. (2018)
Increase of potental habitat of bamboo	Japan	%	pre-industrial	N/A	Pre-industrial	MRI AGCM CMIP5RCP8.5 at 2027 and 2041	T	No	Y	+11–13%	+16–19%	2°C–1.5°C = 6%	N/A	N/A	N/A	Takano et al. (2017)
Carbon storage in vegetation (GPP) and soil	Europe	%	pre-industrial	-	1881–1910	Euro-Cordex with RCP4.5, 2034-2063	T	No	Y	N/A	+5% in soil and +20% in GPP		N/A	N/A	N/A	Sakalli et al. (2017)
Area of cryogenic land surface processes (nivation, cryoturbation, gelifluction, permafrost)	Northern Europe	%	1981–2010	-	-	CMIP5 ensemble RCP2.6, RCP4.5, RCP8.5	T	-	Y	RCP2.6, 2040–69: -19% (maximum of the 4 processes)	RCP2.6 2070–99: -19% (max)	0%	-	-	-	Aalto et al. (2017)
Spring events in temperate forests (oak)	UK	Days	1961–1990	-	0.5°C	SRES (A1F1) near term (2010–2039) and medium term (2040–2069)	T	-	Y	-14.3 days	-24.6 days	2°C–1.5°C = 10.3 days	-	-	-	Roberts et al. (2015)
Starting date of growing season	Northern China	Days	1961–1990	-	0.5°C	HadGEM3- RA: RCP4.5 and 8.5 (2050)		-	-	-6.5 days (s.d.=4.8 days)	-7.4 days (s.d.=4.8 days)	2°C–1.5°C = 0.9 days	-	-	-	Luo et al. (2014)
Ecosystem NPP and GPP	Europe	%	1971–2000	N/A	0.46°C	Euro-Cordex / IMPACT2C / 3 RCP	T	No	Y	N/A	N/A	2°C–1.5°C: -6 to 10% according to regions	N/A	N/A	N/A	Jacob et al. (2018)
Permafrost area	Globe	km^2	1960–1990	-	0.5°C	CMIP5	T	No	Y	11 millions km^2 (present = 15	9 millions km2 (present = 15	2 millions km^2 (1.55 to 2.5)	N/A	N/A	N/A	Chadburn et al. (2017)
	-	-	-	-	-	CMIP3 SRES A2	-	-	-	-	-	-	-	-	-	Meehl et al. (2007)
Forest biomass	Central America	%	1961–1990	-	-	Eta-HadGEM2	T	-	Y	-20%	-30%	10%	-	-	-	Lyra et al. (2017)
Fynbos biome area	South Africa	%	1961–1990	-	0.5°C above pre-industrial	Regional CCAM os 6 GCM, SRES A2	T	-	Y	-20%	-32% (average between 1°C and 2°C)	12%	-	-	-	Engelbrecht and Engelbrecht (2016)

Table 3.SM.3: 3.4.4 Ocean Systems

Risk	Region	Metric (Unit)	Baseline Time Period against Which Change Measured	Baseline Global T	Climate Scenario	Transient (T) or Equilibrium (E)	Overshoot Scenario?	Dynamic Model?	Projected Impact at 1.5°C above Pre-Industrial	Projected Impact at 2°C above Pre-Industrial	Projected Impact at Delta T(°C)	Level of Risk after Adaptation at 1.5°C	Level of Risk after Adaptation at 2°C	Reference
SST/distributions of pelagic fish species	Northeast Pacific shelf seas	km/decade migrated	2000–2050	0.5°C	(SRES) A2	T	N	Y	30.1 ± 2.34 (SRES A2 is around 1.5°C at 2050, average across 28 species)	Likely to increase further	-	-	-	Cheung et al. (2015) (NW Pacific paper)
SST/distributions of pelagic fish species	West coast USA	Local exitinction rate	2000–2050	0.5°C	(SRES) A2	T	N	Y	Increased	Likely to increase further	-	-	-	Cheung et al. (2015) (NW Pacific paper)
SST/distributions of pelagic fish species	Northeast Pacific shelf seas	Species invasion rate	2000–2050	0.5°C	(SRES) A2	T	N	Y	Increased	Likely to increase further	-	-	-	Cheung et al. (2015) (NW Pacific paper)
Increased SST (surface), reduced O2, decreased NPP	Global	Species turnover	1950–1969	Pre-industrial	19 CMIP5 models: RCP8.5 (3.5°C at end of century)	T	N	Y	-	-	21.6 ± 0.33%	-	-	Cheung et al. (2016)
Increased SST (surface), reduced O2, decreased NPP	Global	Species turnover	1950–1969	Pre-industrial	19 CMIP5 models: RCP2.6	E	N	Y	8.3 ± 0.05%	Likely to increase further	-	-	-	Cheung et al. (2016)
Increased SST (surface), reduced O2, decreased NPP	Indo-Pacific	Species turnover	1950–2100	1950 and 1969	19 CMIP5 models: RCP8.5	E	N	Y	-	-	36.4 ± 2.1%	-	-	Cheung et al. (2016)
Increased SST (surface), reduced O2, decreased NPP (species turnover)	Indo-Pacific	Species turnover	1950–2100	1950 and 1969	19 CMIP5 models: RCP2.6	E	N	Y	9.2 ± 0.8%	12.1 ± 0.8%	-	-	-	Cheung et al. (2016)
Increased SST (surface), reduced O2, decreased NPP (maximum catch potential)	Indo-Pacific	10^6 metric tons	1950–2100	Average of the top 10-year global annual catches since 1950	19 CMIP5 models: RCP8.5	E	N	Y	-	Linear with change in increased SST, O2, NPP decrease, etc.)	−46.8 ± 1.2%	-	-	Cheung et al. (2016)
Increased SST (surface), reduced O2, decreased NPP (maximum catch potential)	Indo-Pacific	10^6 metric tons	1950–2100	Average of the top 10-year global annual catches since 1950	19 CMIP5 models: RCP8.5	E	N	Y	-	-	−46.8 ± 1.2%	-	-	Cheung et al. (2016)
Increased SST (surface), reduced O2, decreased NPP (maximum catch potential)	Global	10^6 metric tons	1950–2100	Average of the top 10-year global annual catches since 1950	19 CMIP5 models: RCP2.6	E	N	Y	-11.5 ± 0.6%	-20.2 ± 0.6%	-	-	-	Cheung et al. (2016)
Increased SST (surface), reduced O2, decreased NPP (maximum catch potential)	Arctic/temperate regions	%	1950–2100	Pre-industrial	19 CMIP5 models: RCP8.5	E	N	Y	50	Likely to increase further	400	-	-	Cheung et al. (2016)
Increased SST (surface), reduced O2, decreased NPP (maximum catch potential)	Equator	%	1950-2100	Pre-industrial	19 CMIP5 models: RCP8.5	E	N	Y	-70	Likely to increase further	-30	-	-	Cheung et al. (2016)
Increased SST (surface), reduced O2, decreased NPP (species turnover)	Arctic/temperate regions	%	1950–2100	Prei-ndustrial	19 CMIP5 models: RCP8.5	E	N	Y	3	Likely to increase further	20	-	-	Cheung et al. (2016)
Increased SST (surface), reduced O2, decreased NPP (species turnover)	Equator	%	1950–2100	Pre-industrial	19 CMIP5 models: RCP2.6	E	N	Y	5	Likely to increase further	35	-	-	Cheung et al. (2016)
Increased SST/coral bleaching and mortality	Tropics/subtropics	% loss of today's corals.	2000	0.5°C	"Commit", A1b, A1F1, B1, A2 (B1 is closest to 1.5°C)	T	N	N	80	95	100	Close to zero if corals can increase their tolerance by +1.5°C (no evidence but discussed)	No change	Donner et al. (2009)
Increased SST/coral bleaching and mortality	Tropics/subtropics	% loss of today's corals	1982–2005	-	RCP2.6	E	N	N	95	Even in the pathway with most pronounced emission reductions (RCP2.6), where CO2 equivalent concentrations peak at 455 ppm (Supplementary Fig. S1), 95% of reef locations experience annual bleaching conditions by the end of the century	100	No change	No change	Hooidonk et al. (2013)
Increased SST/coral bleaching and mortality	Tropics/subtropics	Median year at which annual bleaching occurs	1983–2005	Pre-industrial	RCP8.5	T	N	N	2045		2055	No change	No change	Hooidonk et al. (2016)
Increased SST/coral bleaching and mortality	Australia	Likelihood of extreme events like 2015–2016 occurring, that cause coral bleaching	1861–2005 under both natural and anthropogenic forcings (historical), 1861–2005 under natural forcings only, and 2006–2100 under 4 RCP scenarios (RCP2.6, RCP4.5, RCP6.0 and RCP8.5) were analysed	1901–2005	16 models CMIP5	T,E	N	-	64% (53–76%)	87% (79–93%)	Even more likely	No change	No change	King et al. (2017)

Table 3.SM.4: 3.4.5 Coastal and low-lying areas

Risk	Region	Metric (Unit)	Baseline Time Period against Which Change Measured	Socio-Economic Scenario and Date	Baseline Global T	Climate Scenario	Transient (T) or Equilibrium (E)	Is it an Overshoot Scenario? How Long is it above 1.5°C and What is the Maximum Temperature and When?	Dynamic Model?	Projected Impact at 1.5°C above Pre-Industrial	Projected Impact at 2°C above Pre-Industrial	Projected Impact at Delta T for Defined Year (°C)	Delta T Relative to Pre-Industrial in Defined Year; Delta T(°C)	Level of Risk after Adaptation at 1.5°C	Level of Risk after Adaptation at 2°C	Type of Adaptation Modeled	Reference
Area situated below the 1-in-100-year flood plain	Global	(th km^2)	1995	N/A	1850–1900	AMP1.5 (50th percentile). Stabilization at approx. 1.5°C	N/A	Yes. Overshoots after 2035 to 2150	No	562	N/A	N/A	N/A	Increasing (no adaptation assumed)	N/A	None	Brown et al. (2018a)
Area situated below the 1-in-100-year flood plain	Global	(th km^2)	1995	N/A	1850–1900	AMP1.5 (95th percentile). Stabilization at approx. 1.5°C	N/A	Yes. Overshoots after 2045. Does not return to 1.5°C	No	575	590	N/A	N/A	Increasing (no adaptation assumed)	Increasing (no adaptation assumed)	None	Brown et al. (2018a)
Population situated below the 1-in-100-year flood plain	Global	(millions)	1995	SSP1–5	1850–1900	AMP1.5 (50th percentile). Stabilization at approx. 1.5°C	N/A	Yes. Overshoots after 2035 to 2150	No	128–137	N/A	N/A	N/A	Increasing (no adaptation assumed)	N/A	None	Brown et al. (2018a)
Population situated below the 1-in-100-year flood plain	Global	(millions)	1995	SSP1–5	1850–1900	AMP1.5 (95th percentile). Stabilization at approx. 1.5°C	N/A	Yes. Overshoots after 2045. Does not return to 1.5°C	No	134–143	136–144	N/A	N/A	Increasing (no adaptation assumed)	Increasing (no adaptation assumed)	None	Brown et al. (2018a)
Area situated below the 1-in-100-year flood plain	Global	(th km^2)	1995	N/A	1850–1900	AMP2.0 (50th percentile). Stabilization at approx. 2.0°C	N/A	Yes. Overshoots after 2035. Does not return to 1.5°C	No	561	613	N/A	N/A	Increasing (no adaptation assumed)	Increasing (no adaptation assumed)	None	Brown et al. (2018a)
Area situated below the 1-in-100-year flood plain	Global	(th km^2)	1995	N/A	1850–1900	AMP2.0 (95th percentile). Stabilization at approx. 2.0°C	N/A	Yes. Overshoots after 2025. Does not return to 1.5°C	No	562	590	N/A	N/A	Increasing (no adaptation assumed)	Increasing (no adaptation assumed)	None	Brown et al. (2018a)
Area situated below the 1-in-100-year flood plain	Global	(th km^2)	1995	N/A	1850–1900	AMP2.0 (5th percentile). Stabilization at approx. 2.0°C	N/A	Yes. Overshoots after 2050. Does not return to 1.5°C	No	557	N/A	N/A	N/A	Increasing (no adaptation assumed)	N/A	None	Brown et al. (2018a)
Population situated below the 1-in-100-year flood plain	Global	(millions)	1995	SSP1–5	1850–1900	AMP2.0 (50th percentile). Stabilization at approx. 2.0°C	N/A	Yes. Overshoots after 2035. Does not return to 1.5°C	No	127–132	114–151	N/A	N/A	Increasing (no adaptation assumed)	Increasing (no adaptation assumed)	None	Brown et al. (2018a)
Population situated below the 1-in-100-year flood plain	Global	(millions)	1995	SSP1–5	1850–1900	AMP2.0 (95th percentile). Stabilization at approx. 2.0°C	N/A	Yes. Overshoots after 2025. Does not return to 1.5°C	No	126–129	134–143	N/A	N/A	Increasing (no adaptation assumed)	Increasing (no adaptation assumed)	None	Brown et al. (2018a)
Population situated below the 1-in-100-year flood plain	Global	(millions)	1995	SSP1–5	1850–1900	AMP2.0 (5th percentile). Stabilization at approx. 2.0°C	N/A	Yes. Overshoots after 2050. Does not return to 1.5°C	No	124–134	N/A	N/A	N/A	Increasing (no adaptation assumed)	N/A	None	Brown et al. (2018a)
Area situated below the 1-in-100-year flood plain	Global	(th km^2)	1995	N/A	1850–1900	AMP2.5 (50th percentile). Stabilization at approx. 2.5°C	N/A	Yes. Overshoots after 2035. Does not return to 1.5°C	No	561	598	N/A	N/A	Increasing (no adaptation assumed)	Increasing (no adaptation assumed)	None	Brown et al. (2018a)
Area situated below the 1-in-100-year flood plain	Global	(th km^2)	1995	N/A	1850–1900	AMP2.5 (95th percentile). Stabilization at approx. 2.5°C	N/A	Yes. Overshoots after 2030. Does not return to 1.5°C	No	569	591	N/A	N/A	Increasing (no adaptation assumed)	Increasing (no adaptation assumed)	None	Brown et al. (2018a)
Area situated below the 1-in-100-year flood plain	Global	(th km^2)	1995	N/A	1850–1900	AMP2.5 (5th percentile). Stabilization at approx. 2.5°C	N/A	Yes. Overshoots after 2050. Does not return to 1.5°C	No	561	N/A	N/A	N/A	Increasing (no adaptation assumed)	N/A	None	Brown et al. (2018a)
Population situated below the 1-in-100-year flood plain	Global	(millions)	1995	SSP1–5	1850–1900	AMP2.5 (50th percentile). Stabilization at approx. 2.5°C	N/A	Yes. Overshoots after 2035. Does not return to 1.5°C	No	127–132	122–146	N/A	N/A	Increasing (no adaptation assumed)	Increasing (no adaptation assumed)	None	Brown et al. (2018a)
Population situated below the 1-in-100-year flood plain	Global	(millions)	1995	SSP1–5	1850–1900	AMP2.5 (95th percentile). Stabilization at approx. 2.5°C	N/A	Yes. Overshoots after 2030. Does not return to 1.5°C	No	128–132	134–143	N/A	N/A	Increasing (no adaptation assumed)	Increasing (no adaptation assumed)	None	Brown et al. (2018a)
Population situated below the 1-in-100-year flood plain	Global	(millions)	1995	SSP1–5	1850–1900	AMP2.5 (5th percentile). Stabilization at approx. 2.5°C	N/A	Yes. Overshoots after 2050. Does not return to 1.5°C	No	124–134	N/A	N/A	N/A	Increasing (no adaptation assumed)	N/A	None	Brown et al. (2018a)
Area situated below the 1-in-100-year flood plain	Global	(th km^2)	1995	N/A	1850–1900	AMP3.0 (50th percentile). Stabilization at approx. 3.0°C	N/A	Yes. Overshoots after 2035. Does not return to 1.5°C	No	561	598	N/A	N/A	Increasing (no adaptation assumed)	Increasing (no adaptation assumed)	None	Brown et al. (2018a)
Area situated below the 1-in-100-year flood plain	Global	(th km^2)	1995	N/A	1850–1900	AMP3.0 (95th percentile). Stabilization at approx. 3.0°C	N/A	Yes. Overshoots after 2025. Does not return to 1.5°C	No	562	591	N/A	N/A	Increasing (no adaptation assumed)	Increasing (no adaptation assumed)	None	Brown et al. (2018a)
Area situated below the 1-in-100-year flood plain	Global	(th km^2)	1995	N/A	1850–1900	AMP3.0 (5th percentile). Stabilization at approx. 3.0°C	N/A	Yes. Overshoots after 2050. Does not return to 1.5°C	No	599	N/A	N/A	N/A	Increasing (no adaptation assumed)	N/A	None	Brown et al. (2018a)
Population situated below the 1-in-100-year flood plain	Global	(millions)	1995	SSP1–5	1850–1900	AMP3.0 (50th percentile). Stabilization at approx. 3.0°C	N/A	Yes. Overshoots after 2035. Does not return to 1.5°C	No	127–132	122–136	N/A	N/A	Increasing (no adaptation assumed)	Increasing (no adaptation assumed)	None	Brown et al. (2018a)
Population situated below the 1-in-100-year flood plain	Global	(millions)	1995	SSP1–5	1850–1900	AMP3.0 (95th percentile). Stabilization at approx. 3.0°C	N/A	Yes. Overshoots after 2025. Does not return to 1.5°C	No	126–128	134–143	N/A	N/A	Increasing (no adaptation assumed)	Increasing (no adaptation assumed)	None	Brown et al. (2018a)
Population situated below the 1-in-100-year flood plain	Global	(millions)	1995	SSP1–5	1850–1900	AMP3.0 (5th percentile). Stabilization at approx. 3.0°C	N/A	Yes. Overshoots after 2050. Does not return to 1.5°C	No	124–134	N/A	N/A	N/A	Increasing (no adaptation assumed)	N/A	None	Brown et al. (2018a)
Area situated below the 1-in-100-year flood plain	Global	(th km^2)	1995	N/A	1850–1900	AMP4.5 (50th percentile). Stabilization at approx. 4.5°C	N/A	Yes. Overshoots after 2035. Does not return to 1.5°C	No	561	593	N/A	N/A	Increasing (no adaptation assumed)	Increasing (no adaptation assumed)	None	Brown et al. (2018a)
Area situated below the 1-in-100-year flood plain	Global	(th km^2)	1995	N/A	1850–1900	AMP4.5 (95th percentile). Stabilization at approx. 4.5°C	N/A	Yes. Overshoots after 2030. Does not return to 1.5°C	No	568	591	N/A	N/A	Increasing (no adaptation assumed)	Increasing (no adaptation assumed)	None	Brown et al. (2018a)

Risk	Region	Metric (Unit)	Baseline Time Period against Which Change Measured	Socio-Economic Scenario and Date	Baseline Global T	Climate Scenario	Transient (T) or Equilibrium (E)	Is it an Overshoot Scenario? How Long is it above 1.5°C and What is the Maximum Temperature and When?	Dynamic Model?	Projected Impact at 1.5°C above Pre-Industrial	Projected Impact at 2°C above Pre-Industrial	Projected Impact at Delta T for Defined Year (°C)	Delta T Relative to Pre-Industrial in Defined Year; Delta T(°C)	Level of Risk after Adaptation at 1.5°C	Level of Risk after Adaptation at 2°C	Type of Adaptation Modeled	Reference
Area situated below the 1-in-100-year flood plain	Global	(th km^2)	1995	N/A	1850–1900	AMP4.5 (5th percentile). Stabilization at approx. 4.5°C	N/A	Yes. Overshoots after 2050. Does not return to 1.5°C	No	560	590	N/A	N/A	Increasing (no adaptation assumed)	Increasing (no adaptation assumed)	None	Brown et al. (2018a)
Population situated below the 1-in-100-year flood plain	Global	(millions)	1995	SSP1–5	1850–1900	AMP4.5 (50th percentile). Stabilization at approx. 4.5°C	N/A	Yes. Overshoots after 2035. Does not return to 1.5°C	No	127–131	125–137	N/A	N/A	Increasing (no adaptation assumed)	Increasing (no adaptation assumed)	None	Brown et al. (2018a)
Population situated below the 1-in-100-year flood plain	Global	(millions)	1995	SSP1–5	1850–1900	AMP4.5 (95th percentile). Stabilization at approx. 4.5°C	N/A	Yes. Overshoots after 2030. Does not return to 1.5°C	No	128–133	134–143	N/A	N/A	Increasing (no adaptation assumed)	Increasing (no adaptation assumed)	None	Brown et al. (2018a)
Population situated below the 1-in-100-year flood plain	Global	(millions)	1995	SSP1–5	1850–1900	AMP4.5 (5th percentile). Stabilization at approx. 4.5°C	N/A	Yes. Overshoots after 2050. Does not return to 1.5°C	No	124–134	101–144	N/A	N/A	Increasing (no adaptation assumed)	Increasing (no adaptation assumed)	None	Brown et al. (2018a)
Area situated below the 1-in-100-year flood plain	Global	(th km^2)	1995	N/A	1850–1900	RCP8.5 (50th percentile)	N/A	Yes. Overshoots after 2035. Does not return to 1.5°C	No	563	576	N/A	N/A	Increasing (no adaptation assumed)	Increasing (no adaptation assumed)	None	Brown et al. (2018a)
Area situated below the 1-in-100-year flood plain	Global	(th km^2)	1995	N/A	1850–1900	RCP8.5 (95th percentile)	N/A	Yes. Overshoots after 2030. Does not return to 1.5°C	No	569	585	N/A	N/A	Increasing (no adaptation assumed)	Increasing (no adaptation assumed)	None	Brown et al. (2018a)
Area situated below the 1-in-100-year flood plain	Global	(th km^2)	1995	N/A	1850–1900	RCP8.5 (5th percentile)	N/A	Yes. Overshoots after 2040. Does not return to 1.5°C	No	557	567	N/A	N/A	Increasing (no adaptation assumed)	Increasing (no adaptation assumed)	None	Brown et al. (2018a)
Population situated below the 1-in-100-year flood plain	Global	(millions)	1995	SSP1–5	1850–1900	RCP8.5 (50th percentile)	N/A	Yes. Overshoots after 2045. Does not return to 1.5°C	No	127–133	130–139	N/A	N/A	Increasing (no adaptation assumed)	Increasing (no adaptation assumed)	None	Brown et al. (2018a)
Population situated below the 1-in-100-year flood plain	Global	(millions)	1995	SSP1–5	1850–1900	RCP8.5 (95th percentile)	N/A	Yes. Overshoots after 2040. Does not return to 1.5°C	No	128–132	133–141	N/A	N/A	Increasing (no adaptation assumed)	Increasing (no adaptation assumed)	None	Brown et al. (2018a)
Population situated below the 1-in-100-year flood plain	Global	(millions)	1995	SSP1–5	1850–1900	RCP8.5 (5th percentile)	N/A	Yes. Overshoots after 2050. Does not return to 1.5°C	No	125–132	125–136	N/A	N/A	Increasing (no adaptation assumed)	Increasing (no adaptation assumed)	None	Brown et al. (2018a)
Area situated below the 1-in-100-year flood plain	Global	(th km^2)	1995	N/A	1850–1900	AMP1.5 (5th percentile). Stabilization at approx. 1.5°C	N/A	N/A	No	N/A	N/A	575	1.26°C in 2100	N/A	N/A	N/A	Brown et al. (2018a)
Area situated below the 1-in-100-year flood plain	Global	(th km^2)	1995	N/A	1850–1900	AMP1.5 (5th percentile). Stabilization at approx. 1.5°C	N/A	N/A	No	N/A	N/A	592	1.15°C in 2200	N/A	N/A	N/A	Brown et al. (2018a)
Area situated below the 1-in-100-year flood plain	Global	(th km^2)	1995	N/A	1850–1900	AMP1.5 (5th percentile). Stabilization at approx. 1.5°C	N/A	N/A	No	N/A	N/A	606	1.12°C in 2300	N/A	N/A	N/A	Brown et al. (2018a)
Area situated below the 1-in-100-year flood plain	Global	(th km^2)	1995	N/A	1850–1900	AMP1.5 (95th percentile). Stabilization at approx. 1.5°C	N/A	Yes. Overshoots after 2045. Does not return to 1.5°C	No	575	590	669	2.33°C in 2100	Increasing (no adaptation assumed)	Increasing (no adaptation assumed)	None	Brown et al. (2018a)
Area situated below the 1-in-100-year flood plain	Global	(th km^2)	1995	N/A	1850–1900	AMP1.5 (95th percentile). Stabilization at approx. 1.5°C	N/A	Yes. Overshoots after 2045. Does not return to 1.5°C	No	575	590	827	2.18°C in 2200	Increasing (no adaptation assumed)	Increasing (no adaptation assumed)	None	Brown et al. (2018a)
Area situated below the 1-in-100-year flood plain	Global	(th km^2)	1995	N/A	1850–1900	AMP1.5 (95th percentile). Stabilization at approx. 1.5°C	N/A	Yes. Overshoots after 2045. Does not return to 1.5°C	No	575	590	843	1.82°C in 2300	Increasing (no adaptation assumed)	Increasing (no adaptation assumed)	None	Brown et al. (2018a)
Area situated below the 1-in-100-year flood plain	Global	(th km^2)	1995	N/A	1850–1900	AMP1.5 (50th percentile). Stabilization at approx. 1.5°C	N/A	Yes. Overshoots after 2035 to 2150	No	562	N/A	620	1.58°C in 2100	Increasing (no adaptation assumed)	N/A	None	Brown et al. (2018a)
Area situated below the 1-in-100-year flood plain	Global	(th km^2)	1995	N/A	1850–1900	AMP1.5 (50th percentile). Stabilization at approx. 1.5°C	N/A	Yes. Overshoots after 2035 to 2150	No	562	N/A	666	1.41°C in 2200	Increasing (no adaptation assumed)	N/A	None	Brown et al. (2018a)
Area situated below the 1-in-100-year flood plain	Global	(th km^2)	1995	N/A	1850–1900	AMP1.5 (50th percentile). Stabilization at approx. 1.5°C	N/A	Yes. Overshoots after 2035 to 2150	No	562	N/A	702	1.33°C in 2300	Increasing (no adaptation assumed)	N/A	None	Brown et al. (2018a)
Area situated below the 1-in-100-year flood plain	Global	(th km^2)	1995	N/A	1850–1900	AMP2.0 (5th percentile). Stabilization at approx. 2.0°C	N/A	Yes. Overshoots after 2050. Does not return to 1.5°C	No	557	N/A	585	1.72°C in 2100	Increasing (no adaptation assumed)	N/A	None	Brown et al. (2018a)
Area situated below the 1-in-100-year flood plain	Global	(th km^2)	1995	N/A	1850–1900	AMP2.0 (5th percentile). Stabilization at approx. 2.0°C	N/A	Yes. Overshoots after 2050. Does not return to 1.5°C	No	557	N/A	618	1.66°C in 2200	Increasing (no adaptation assumed)	N/A	None	Brown et al. (2018a)
Area situated below the 1-in-100-year flood plain	Global	(th km^2)	1995	N/A	1850–1900	AMP2.0 (5th percentile). Stabilization at approx. 2.0°C	N/A	Yes. Overshoots after 2050. Does not return to 1.5°C	No	557	N/A	642	1.60°C in 2300	Increasing (no adaptation assumed)	N/A	None	Brown et al. (2018a)
Area situated below the 1-in-100-year flood plain	Global	(th km^2)	1995	N/A	1850–1900	AMP2.0 (95th percentile). Stabilization at approx. 2.0°C	N/A	Yes. Overshoots after 2025. Does not return to 1.5°C	No	562	590	686	2.64°C in 2100	Increasing (no adaptation assumed)	Increasing (no adaptation assumed)	None	Brown et al. (2018a)
Area situated below the 1-in-100-year flood plain	Global	(th km^2)	1995	N/A	1850–1900	AMP2.0 (95th percentile). Stabilization at approx. 2.0°C	N/A	Yes. Overshoots after 2025. Does not return to 1.5°C	No	562	590	827	2.57°C in 2200	Increasing (no adaptation assumed)	Increasing (no adaptation assumed)	None	Brown et al. (2018a)

Risk	Region	Metric (Unit)	Baseline Time Period against Which Change Measured	Socio-Economic Scenario and Date	Baseline Global T	Climate Scenario	Transient (T) or Equilibrium (E)	Is it an Overshoot Scenario? How Long is it above 1.5°C and What is the Maximum Temperature and When?	Dynamic Model?	Projected Impact at 1.5°C above Pre-Industrial	Projected Impact at 2°C above Pre-Industrial	Projected Impact at Delta T for Defined Year (°C)	Delta T Relative to Pre-Industrial in Defined Year; Delta T(°C)	Level of Risk after Adaptation at 1.5°C	Level of Risk after Adaptation at 2°C	Type of Adaptation Modeled	Reference
Area situated below the 1-in-100-year flood plain	Global	(th km^2)	1995	N/A	1850–1900	AMP2.0 (95th percentile). Stabilization at approx. 2.0°C	N/A	Yes. Overshoots after 2025. Does not return to 1.5°C	No	562	590	937	2.23°C in 2300	Increasing (no adaptation assumed)	Increasing (no adaptation assumed)	None	Brown et al. (2018a)
Area situated below the 1-in-100-year flood plain	Global	(th km^2)	1995	N/A	1850–1900	AMP2.0 (50th percentile). Stabilization at approx. 2.0°C	N/A	Yes. Overshoots after 2035. Does not return to 1.5°C	No	561	613	637	1.90°C in 2100	Increasing (no adaptation assumed)	Increasing (no adaptation assumed)	None	Brown et al. (2018a)
Area situated below the 1-in-100-year flood plain	Global	(th km^2)	1995	N/A	1850–1900	AMP2.0 (50th percentile). Stabilization at approx. 2.0°C	N/A	Yes. Overshoots after 2035. Does not return to 1.5°C	No	561	613	705	2.03°C in 2200	Increasing (no adaptation assumed)	Increasing (no adaptation assumed)	None	Brown et al. (2018a)
Area situated below the 1-in-100-year flood plain	Global	(th km2)	1995	N/A	1850–1900	AMP2.0 (50th percentile). Stabilization at approx. 2.0°C	N/A	Yes. Overshoots after 2035. Does not return to 1.5°C	No	561	613	767	1.81°C in 2300	Increasing (no adaptation assumed)	Increasing (no adaptation assumed)	None	Brown et al. (2018a)
Area situated below the 1-in-100-year flood plain	Global	(th km^2)	1995	N/A	1850–1900	AMP2.5 (5th percentile). Stabilization at approx. 2.5°C	N/A	Yes. Overshoots after 2050. Does not return to 1.5°C	No	561	N/A	589	1.89°C in 2100	Increasing (no adaptation assumed)	N/A	None	Brown et al. (2018a)
Area situated below the 1-in-100-year flood plain	Global	(th km^2)	1995	N/A	1850–1900	AMP2.5 (5th percentile). Stabilization at approx. 2.5°C	N/A	Yes. Overshoots after 2050. Does not return to 1.5°C	No	561	N/A	639	2.12°C in 2200	Increasing (no adaptation assumed)	N/A	None	Brown et al. (2018a)
Area situated below the 1-in-100-year flood plain	Global	(th km^2)	1995	N/A	1850–1900	AMP2.5 (5th percentile). Stabilization at approx. 2.5°C	N/A	Yes. Overshoots after 2050. Does not return to 1.5°C	No	561	N/A	677	2.05°C in 2300	Increasing (no adaptation assumed)	N/A	None	Brown et al. (2018a)
Area situated below the 1-in-100-year flood plain	Global	(th km^2)	1995	N/A	1850–1900	AMP2.5 (95th percentile). Stabilization at approx. 2.5°C	N/A	Yes. Overshoots after 2030. Does not return to 1.5°C	No	569	591	693	2.95°C in 2100	Increasing (no adaptation assumed)	Increasing (no adaptation assumed)	None	Brown et al. (2018a)
Area situated below the 1-in-100-year flood plain	Global	(th km^2)	1995	N/A	1850–1900	AMP2.5 (95th percentile). Stabilization at approx. 2.5°C	N/A	Yes. Overshoots after 2030. Does not return to 1.5°C	No	569	591	875	3.02°C in 2200	Increasing (no adaptation assumed)	Increasing (no adaptation assumed)	None	Brown et al. (2018a)
Area situated below the 1-in-100-year flood plain	Global	(th km^2)	1995	N/A	1850–1900	AMP2.5 (95th percentile). Stabilization at approx. 2.5°C	N/A	Yes. Overshoots after 2030. Does not return to 1.5°C	No	569	591	1030	3.71°C in 2300	Increasing (no adaptation assumed)	Increasing (no adaptation assumed)	None	Brown et al. (2018a)
Area situated below the 1-in-100-year flood plain	Global	(th km^2)	1995	N/A	1850–1900	AMP2.5 (50th percentile). Stabilization at approx. 2.5°C	N/A	Yes. Overshoots after 2035. Does not return to 1.5°C	No	561	598	633	2.30°C in 2100	Increasing (no adaptation assumed)	Increasing (no adaptation assumed)	None	Brown et al. (2018a)
Area situated below the 1-in-100-year flood plain	Global	(th km^2)	1995	N/A	1850–1900	AMP2.5 (50th percentile). Stabilization at approx. 2.5°C	N/A	Yes. Overshoots after 2035. Does not return to 1.5°C	No	561	598	737	2.40°C in 2200	Increasing (no adaptation assumed)	Increasing (no adaptation assumed)	None	Brown et al. (2018a)
Area situated below the 1-in-100-year flood plain	Global	(th km^2)	1995	N/A	1850–1900	AMP2.5 (50th percentile). Stabilization at approx. 2.5°C	N/A	Yes. Overshoots after 2035. Does not return to 1.5°C	No	561	598	825	2.29°C in 2300	Increasing (no adaptation assumed)	Increasing (no adaptation assumed)	None	Brown et al. (2018a)
Area situated below the 1-in-100-year flood plain	Global	(th km^2)	1995	N/A	1850–1900	AMP3.0 (5th percentile). Stabilization at approx. 3.0°C	N/A	Yes. Overshoots after 2050. Does not return to 1.5°C	No	599	N/A	592	1.97°C in 2100	Increasing (no adaptation assumed)	N/A	None	Brown et al. (2018a)
Area situated below the 1-in-100-year flood plain	Global	(th km^2)	1995	N/A	1850–1900	AMP3.0 (5th percentile). Stabilization at approx. 3.0°C	N/A	Yes. Overshoots after 2050. Does not return to 1.5°C	No	599	N/A	654	2.41°C in 2200	Increasing (no adaptation assumed)	N/A	None	Brown et al. (2018a)
Area situated below the 1-in-100-year flood plain	Global	(th km^2)	1995	N/A	1850–1900	AMP3.0 (5th percentile). Stabilization at approx. 3.0°C	N/A	Yes. Overshoots after 2050. Does not return to 1.5°C	No	599	N/A	707	2.45°C in 2300	Increasing (no adaptation assumed)	N/A	None	Brown et al. (2018a)
Area situated below the 1-in-100-year flood plain	Global	(th km^2)	1995	N/A	1850–1900	AMP3.0 (95th percentile). Stabilization at approx. 3.0°C	N/A	Yes. Overshoots after 2025. Does not return to 1.5°C	No	562	591	696	3.21°C in 2100	Increasing (no adaptation assumed)	Increasing (no adaptation assumed)	None	Brown et al. (2018a)
Area situated below the 1-in-100-year flood plain	Global	(th km^2)	1995	N/A	1850–1900	AMP3.0 (95th percentile). Stabilization at approx. 3.0°C	N/A	Yes. Overshoots after 2025. Does not return to 1.5°C	No	562	591	911	3.49°C in 2200	Increasing (no adaptation assumed)	Increasing (no adaptation assumed)	None	Brown et al. (2018a)
Area situated below the 1-in-100-year flood plain	Global	(th km^2)	1995	N/A	1850–1900	AMP3.0 (95th percentile). Stabilization at approx. 3.0°C	N/A	Yes. Overshoots after 2025. Does not return to 1.5°C	No	562	591	1130	3.15°C in 2300	Increasing (no adaptation assumed)	Increasing (no adaptation assumed)	None	Brown et al. (2018a)
Area situated below the 1-in-100-year flood plain	Global	(th km^2)	1995	N/A	1850–1900	AMP3.0 (50th percentile). Stabilization at approx. 3.0°C	N/A	Yes. Overshoots after 2035. Does not return to 1.5°C	No	561	598	635	2.40°C in 2100	Increasing (no adaptation assumed)	Increasing (no adaptation assumed)	None	Brown et al. (2018a)
Area situated below the 1-in-100-year flood plain	Global	(th km^2)	1995	N/A	1850–1900	AMP3.0 (50th percentile). Stabilization at approx. 3.0°C	N/A	Yes. Overshoots after 2035. Does not return to 1.5°C	No	561	598	759	2.85°C in 2200	Increasing (no adaptation assumed)	Increasing (no adaptation assumed)	None	Brown et al. (2018a)
Area situated below the 1-in-100-year flood plain	Global	(th km^2)	1995	N/A	1850–1900	AMP3.0 (50th percentile). Stabilization at approx. 3.0°C	N/A	Yes. Overshoots after 2035. Does not return to 1.5°C	No	561	598	872	2.76°C in 2300	Increasing (no adaptation assumed)	Increasing (no adaptation assumed)	None	Brown et al. (2018a)
Area situated below the 1-in-100-year flood plain	Global	(th km^2)	1995	N/A	1850–1900	AMP4.5 (5th percentile). Stabilization at approx. 4.5°C	N/A	Yes. Overshoots after 2050. Does not return to 1.5°C	No	560	590	593	2.05°C in 2100	Increasing (no adaptation assumed)	Increasing (no adaptation assumed)	None	Brown et al. (2018a)
Area situated below the 1-in-100-year flood plain	Global	(th km^2)	1995	N/A	1850–1900	AMP4.5 (5th percentile). Stabilization at approx. 4.5°C	N/A	Yes. Overshoots after 2050. Does not return to 1.5°C	No	560	590	672	2.75°C in 2200	Increasing (no adaptation assumed)	Increasing (no adaptation assumed)	None	Brown et al. (2018a)

Risk	Region	Metric (Unit)	Baseline Time Period against Which Change Measured	Socio-Economic Scenario and Date	Baseline Global T	Climate Scenario	Transient (T) or Equilibrium (E)	Is it an Overshoot Scenario? How Long is it above 1.5°C and What is the Maximum Temperature and When?	Dynamic Model?	Projected Impact at 1.5°C above Pre-Industrial	Projected Impact at 2°C above Pre-Industrial	Projected Impact at Delta T for Defined Year (°C)	Delta T Relative to Pre-Industrial in Defined Year; Delta T(°C)	Level of Risk after Adaptation at 1.5°C	Level of Risk after Adaptation at 2°C	Type of Adaptation Modeled	Reference
Area situated below the 1-in-100-year flood plain	Global	(th km^2)	1995	N/A	1850–1900	AMP4.5 (5th percentile). Stabilization at approx. 4.5°C	N/A	Yes. Overshoots after 2050. Does not return to 1.5°C	No	560	590	760	3.17°C in 2300	Increasing (no adaptation assumed)	Increasing (no adaptation assumed)	None	Brown et al. (2018a)
Area situated below the 1-in-100-year flood plain	Global	(th km^2)	1995	N/A	1850–1900	AMP4.5 (95th percentile). Stabilization at approx. 4.5°C	N/A	Yes. Overshoots after 2030. Does not return to 1.5°C	No	568	591	700	3.28°C in 2100	Increasing (no adaptation assumed)	Increasing (no adaptation assumed)	None	Brown et al. (2018a)
Area situated below the 1-in-100-year flood plain	Global	(th km^2)	1995	N/A	1850–1900	AMP4.5 (95th percentile). Stabilization at approx. 4.5°C	N/A	Yes. Overshoots after 2030. Does not return to 1.5°C	No	568	591	961	4.66°C in 2200	Increasing (no adaptation assumed)	Increasing (no adaptation assumed)	None	Brown et al. (2018a)
Area situated below the 1-in-100-year flood plain	Global	(th km^2)	1995	N/A	1850–1900	AMP4.5 (95th percentile). Stabilization at approx. 4.5°C	N/A	Yes. Overshoots after 2030. Does not return to 1.5°C	No	568	591	1290	4.75°C in 2300	Increasing (no adaptation assumed)	Increasing (no adaptation assumed)	None	Brown et al. (2018a)
Area situated below the 1-in-100-year flood plain	Global	(th km^2)	1995	N/A	1850–1900	AMP4.5 (50th percentile). Stabilization at approx. 4.5°C	N/A	Yes. Overshoots after 2035. Does not return to 1.5°C	No	561	593	638	2.50°C in 2100	Increasing (no adaptation assumed)	Increasing (no adaptation assumed)	None	Brown et al. (2018a)
Area situated below the 1-in-100-year flood plain	Global	(th km^2)	1995	N/A	1850–1900	AMP4.5 (50th percentile). Stabilization at approx. 4.5°C	N/A	Yes. Overshoots after 2035. Does not return to 1.5°C	No	561	593	786	3.4°C in 2200	Increasing (no adaptation assumed)	Increasing (no adaptation assumed)	None	Brown et al. (2018a)
Area situated below the 1-in-100-year flood plain	Global	(th km^2)	1995	N/A	1850–1900	AMP4.5 (50th percentile). Stabilization at approx. 4.5°C	N/A	Yes. Overshoots after 2035. Does not return to 1.5°C	No	561	593	960	3.85°C in 2300	Increasing (no adaptation assumed)	Increasing (no adaptation assumed)	None	Brown et al. (2018a)
Area situated below the 1-in-100-year flood plain	Global	(th km^2)	1995	N/A	1850–1900	RCP8.5 (5th percentile)	N/A	Yes. Overshoots after 2040. Does not return to 1.5°C	No	557	567	646	4.35°C in 2100	Increasing (no adaptation assumed)	Increasing (no adaptation assumed)	None	Brown et al. (2018a)
Area situated below the 1-in-100-year flood plain	Global	(th km^2)	1995	N/A	1850–1900	RCP8.5 (5th percentile)	N/A	Yes. Overshoots after 2040. Does not return to 1.5°C	No	557	567	887	7.02°C in 2200	Increasing (no adaptation assumed)	Increasing (no adaptation assumed)	None	Brown et al. (2018a)
Area situated below the 1-in-100-year flood plain	Global	(th km^2)	1995	N/A	1850–1900	RCP8.5 (5th percentile)	N/A	Yes. Overshoots after 2040. Does not return to 1.5°C	No	557	567	1190	7.52°C in 2300	Increasing (no adaptation assumed)	Increasing (no adaptation assumed)	None	Brown et al. (2018a)
Area situated below the 1-in-100-year flood plain	Global	(th km^2)	1995	N/A	1850–1900	RCP8.5 (95th percentile)	N/A	Yes. Overshoots after 2030. Does not return to 1.5°C	No	569	585	792	5.83°C in 2100	Increasing (no adaptation assumed)	Increasing (no adaptation assumed)	None	Brown et al. (2018a)
Area situated below the 1-in-100-year flood plain	Global	(th km^2)	1995	N/A	1850–1900	RCP8.5 (95th percentile)	N/A	Yes. Overshoots after 2030. Does not return to 1.5°C	No	569	585	1490	11.23°C in 2200	Increasing (no adaptation assumed)	Increasing (no adaptation assumed)	None	Brown et al. (2018a)
Area situated below the 1-in-100-year flood plain	Global	(th km^2)	1995	N/A	1850–1900	RCP8.5 (95th percentile)	N/A	Yes. Overshoots after 2030. Does not return to 1.5°C	No	569	585	2220	13.14°C in 2300	Increasing (no adaptation assumed)	Increasing (no adaptation assumed)	None	Brown et al. (2018a)
Area situated below the 1-in-100-year flood plain	Global	(th km^2)	1995	N/A	1850–1900	RCP8.5 (50th percentile)	N/A	Yes. Overshoots after 2035. Does not return to 1.5°C	No	563	576	708	4.93°C in 2100	Increasing (no adaptation assumed)	Increasing (no adaptation assumed)	None	Brown et al. (2018a)
Area situated below the 1-in-100-year flood plain	Global	(th km^2)	1995	N/A	1850–1900	RCP8.5 (50th percentile)	N/A	Yes. Overshoots after 2035. Does not return to 1.5°C	No	563	576	1140	8.55°C in 2200	Increasing (no adaptation assumed)	Increasing (no adaptation assumed)	None	Brown et al. (2018a)
Area situated below the 1-in-100-year flood plain	Global	(th km^2)	1995	N/A	1850–1900	RCP8.5 (50th percentile)	N/A	Yes. Overshoots after 2035. Does not return to 1.5°C	No	563	576	1630	9.54°C in 2300	Increasing (no adaptation assumed)	Increasing (no adaptation assumed)	None	Brown et al. (2018a)
Population situated below the 1-in-100-year flood plain	Global	(millions)	1995	SSP1–5 until 2100, then no change to 2300	1850–1900	AMP1.5 (5th percentile). Stabilization at approx. 1.5°C	N/A	N/A	No	N/A	N/A	95–141	1.26°C in 2100	N/A	N/A	None	Brown et al. (2018a)
Population situated below the 1-in-100-year flood plain	Global	(millions)	1995	SSP1–5 until 2100, then no change to 2300	1850–1900	AMP1.5 (5th percentile). Stabilization at approx. 1.5°C	N/A	N/A	No	N/A	N/A	112–170	1.12°C in 2300	N/A	N/A	None	Brown et al. (2018a)
Population situated below the 1-in-100-year flood plain	Global	(millions)	1995	SSP1–5 until 2100, then no change to 2300	1850–1900	AMP1.5 (95th percentile). Stabilization at approx. 1.5°C	N/A	Yes. Overshoots after 2045. Does not return to 1.5°C	No	134–143	136–144	114–173	2.33°C in 2100	Increasing (no adaptation assumed)	Increasing (no adaptation assumed)	None	Brown et al. (2018a)
Population situated below the 1-in-100-year flood plain	Global	(millions)	1995	SSP1–5 until 2100, then no change to 2300	1850–1900	AMP1.5 (95th percentile). Stabilization at approx. 1.5°C	N/A	Yes. Overshoots after 2045. Does not return to 1.5°C	No	134–143	136–144	165–263	1.82°C in 2300	Increasing (no adaptation assumed)	Increasing (no adaptation assumed)	None	Brown et al. (2018a)
Population situated below the 1-in-100-year flood plain	Global	(millions)	1995	SSP1–5 until 2100, then no change to 2300	1850–1900	AMP1.5 (50th percentile). Stabilization at approx. 1.5°C	N/A	Yes. Overshoots after 2035 to 2150	No	128–137	N/A	103–154	1.58°C in 2100	Increasing (no adaptation assumed)	N/A	None	Brown et al. (2018a)
Population situated below the 1-in-100-year flood plain	Global	(millions)	1995	SSP1–5 until 2100, then no change to 2300	1850–1900	AMP1.5 (50th percentile). Stabilization at approx. 1.5°C	N/A	Yes. Overshoots after 2035 to 2150	No	128–137	N/A	133–207	1.33°C in 2300	Increasing (no adaptation assumed)	N/A	None	Brown et al. (2018a)
Population situated below the 1-in-100-year flood plain	Global	(millions)	1995	SSP1–5 until 2100, then no change to 2300	1850–1900	AMP2.0 (5th percentile). Stabilization at approx. 2.0°C	N/A	Yes. Overshoots after 2050. Does not return to 1.5°C	No	124–133	N/A	97–144	1.72°C in 2100	Increasing (no adaptation assumed)	N/A	None	Brown et al. (2018a)
Population situated below the 1-in-100-year flood plain	Global	(millions)	1995	SSP1–5 until 2100, then no change to 2300	1850–1900	AMP2.0 (5th percentile). Stabilization at approx. 2.0°C	N/A	Yes. Overshoots after 2050. Does not return to 1.5°C	No	124–133	N/A	120–183	1.60°C in 2300	Increasing (no adaptation assumed)	N/A	None	Brown et al. (2018a)

Risk	Region	Metric (Unit)	Baseline Time Period against Which Change Measured	Socio-Economic Scenario and Date	Baseline Global T	Climate Scenario	Transient (T) or Equilibrium (E)	Is it an Overshoot Scenario? How Long is it above 1.5°C and What is the Maximum Temperature and When?	Dynamic Model?	Projected Impact at 1.5°C above Pre-Industrial	Projected Impact at 2°C above Pre-Industrial	Projected Impact at Delta T for Defined Year (°C)	Delta T Relative to Pre-Industrial in Defined Year; Delta T(°C)	Level of Risk after Adaptation at 1.5°C	Level of Risk after Adaptation at 2°C	Type of Adaptation Modeled	Reference
Population situated below the 1-in-100-year flood plain	Global	(millions)	1995	SSP1–5 until 2100, then no change to 2300	1850–1900	AMP2.0 (95th percentile). Stabilization at approx. 2.0°C	N/A	Yes. Overshoots after 2025. Does not return to 1.5°C	No	126–127	134–143	118–179	2.64°C in 2100	Increasing (no adaptation assumed)	Increasing (no adaptation assumed)	None	Brown et al. (2018a)
Population situated below the 1-in-100-year flood plain	Global	(millions)	1995	SSP1–5 until 2100, then no change to 2300	1850–1900	AMP2.0 (95th percentile). Stabilization at approx. 2.0°C	N/A	Yes. Overshoots after 2025. Does not return to 1.5°C	No	126–127	134–143	192.9–301.8	2.23°C in 2300	Increasing (no adaptation assumed)	Increasing (no adaptation assumed)	None	Brown et al. (2018a)
Population situated below the 1-in-100-year flood plain	Global	(millions)	1995	SSP1–5 until 2100, then no change to 2300	1850–1900	AMP2.0 (50th percentile). Stabilization at approx. 2.0°C	N/A	Yes. Overshoots after 2035. Does not return to 1.5°C	No	127–132	114–151	106–158	2.03°C in 2100	Increasing (no adaptation assumed)	Increasing (no adaptation assumed)	None	Brown et al. (2018a)
Population situated below the 1-in-100-year flood plain	Global	(millions)	1995	SSP1–5 until 2100, then no change to 2300	1850–1900	AMP2.0 (50th percentile). Stabilization at approx. 2.0°C	N/A	Yes. Overshoots after 2035. Does not return to 1.5°C	No	127–132	114–151	147–232	1.81°C in 2300	Increasing (no adaptation assumed)	Increasing (no adaptation assumed)	None	Brown et al. (2018a)
Population situated below the 1-in-100-year flood plain	Global	(millions)	1995	SSP1–5 until 2100, then no change to 2300	1850–1900	AMP2.5 (5th percentile). Stabilization at approx. 2.5°C	N/A	Yes. Overshoots after 2050. Does not return to 1.5°C	No	124–134	N/A	98–146	1.89°C in 2100	Increasing (no adaptation assumed)	N/A	None	Brown et al. (2018a)
Population situated below the 1-in-100-year flood plain	Global	(millions)	1995	SSP1–5 until 2100, then no change to 2300	1850–1900	AMP2.5 (5th percentile). Stabilization at approx. 2.5°C	N/A	Yes. Overshoots after 2050. Does not return to 1.5°C	No	124–134	N/A	128–197	2.05°C in 2300	Increasing (no adaptation assumed)	N/A	None	Brown et al. (2018a)
Population situated below the 1-in-100-year flood plain	Global	(millions)	1995	SSP1–5 until 2100, then no change to 2300	1850–1900	AMP2.5 (95th percentile). Stabilization at approx. 2.5°C	N/A	Yes. Overshoots after 2030. Does not return to 1.5°C	No	128-132	134–143	119–182	2.95°C in 2100	Increasing (no adaptation assumed)	N/A	None	Brown et al. (2018a)
Population situated below the 1-in-100-year flood plain	Global	(millions)	1995	SSP1–5 until 2100, then no change to 2300	1850–1900	AMP2.5 (95th percentile). Stabilization at approx. 2.5°C	N/A	Yes. Overshoots after 2030. Does not return to 1.5°C	No	128-132	134–143	208–342	2.71°C in 2300	Increasing (no adaptation assumed)	N/A	None	Brown et al. (2018a)
Population situated below the 1-in-100-year flood plain	Global	(millions)	1995	SSP1–5 until 2100, then no change to 2300	1850–1900	AMP2.5 (50th percentile). Stabilization at approx. 2.5°C	N/A	Yes. Overshoots after 2035. Does not return to 1.5°C	No	127-132	122–146	107–160	2.30°C in 2100	Increasing (no adaptation assumed)	Increasing (no adaptation assumed)	None	Brown et al. (2018a)
Population situated below the 1-in-100-year flood plain	Global	(millions)	1995	SSP1–5 until 2100, then no change to 2300	1850–1900	AMP2.5 (50th percentile). Stabilization at approx. 2.5°C	N/A	Yes. Overshoots after 2035. Does not return to 1.5°C	No	127-132	122–146	162–257	2.29°C in 2300	Increasing (no adaptation assumed)	Increasing (no adaptation assumed)	None	Brown et al. (2018a)
Population situated below the 1-in-100-year flood plain	Global	(millions)	1995	SSP1–5 until 2100, then no change to 2300	1850–1900	AMP3.0 (5th percentile). Stabilization at approx. 3.0°C	N/A	Yes. Overshoots after 2050. Does not return to 1.5°C	No	134-146	N/A	98–146	1.97°C in 2100	Increasing (no adaptation assumed)	Increasing (no adaptation assumed)	None	Brown et al. (2018a)
Population situated below the 1-in-100-year flood plain	Global	(millions)	1995	SSP1–5 until 2100, then no change to 2300	1850–1900	AMP3.0 (5th percentile). Stabilization at approx. 3.0°C	N/A	Yes. Overshoots after 2050. Does not return to 1.5°C	No	134-146	N/A	134–207	2.45°C in 2300	Increasing (no adaptation assumed)	Increasing (no adaptation assumed)	None	Brown et al. (2018a)
Population situated below the 1-in-100-year flood plain	Global	(millions)	1995	SSP1–5 until 2100, then no change to 2300	1850–1900	AMP3.0 (95th percentile). Stabilization at approx. 3.0°C	N/A	Yes. Overshoots after 2025. Does not return to 1.5°C	No	125–128	134–143	120–183	3.21°C in 2100	Increasing (no adaptation assumed)	Increasing (no adaptation assumed)	None	Brown et al. (2018a)
Population situated below the 1-in-100-year flood plain	Global	(millions)	1995	SSP1–5 until 2100, then no change to 2300	1850–1900	AMP3.0 (95th percentile). Stabilization at approx. 3.0°C	N/A	Yes. Overshoots after 2025. Does not return to 1.5°C	No	125-128	134–143	227–376	3.15°C in 2300	Increasing (no adaptation assumed)	Increasing (no adaptation assumed)	None	Brown et al. (2018a)
Population situated below the 1-in-100-year flood plain	Global	(millions)	1995	SSP1–5 until 2100, then no change to 2300	1850–1900	AMP3.0 (50th percentile). Stabilization at approx. 3.0°C	N/A	Yes. Overshoots after 2035. Does not return to 1.5°C	No	127–132	122–136	107–161	2.40°C in 2100	Increasing (no adaptation assumed)	Increasing (no adaptation assumed)	None	Brown et al. (2018a)
Population situated below the 1-in-100-year flood plain	Global	(millions)	1995	SSP1–5 until 2100, then no change to 2300	1850–1900	AMP3.0 (50th percentile). Stabilization at approx. 3.0°C	N/A	Yes. Overshoots after 2035. Does not return to 1.5°C	No	127-132	122–136	172–276	2.76°C in 2300	Increasing (no adaptation assumed)	Increasing (no adaptation assumed)	None	Brown et al. (2018a)
Population situated below the 1-in-100-year flood plain	Global	(millions)	1995	SSP1–5 until 2100, then no change to 2300	1850–1900	AMP4.5 (5th percentile). Stabilization at approx. 4.5°C	N/A	Yes. Overshoots after 2050. Does not return to 1.5°C	No	124–134	101–144	99–147	2.05°C in 2100	Increasing (no adaptation assumed)	Increasing (no adaptation assumed)	None	Brown et al. (2018a)
Population situated below the 1-in-100-year flood plain	Global	(millions)	1995	SSP1–5 until 2100, then no change to 2300	1850–1900	AMP4.5 (5th percentile). Stabilization at approx. 4.5°C	N/A	Yes. Overshoots after 2050. Does not return to 1.5°C	No	124–134	101–144	146–228	3.17°C in 2300	Increasing (no adaptation assumed)	Increasing (no adaptation assumed)	None	Brown et al. (2018a)
Population situated below the 1-in-100-year flood plain	Global	(millions)	1995	SSP1–5 until 2100, then no change to 2300	1850–1900	AMP4.5 (95th percentile). Stabilization at approx. 4.5°C	N/A	Yes. Overshoots after 2030. Does not return to 1.5°C	No	128–133	134–143	120–184	3.28°C in 2100	Increasing (no adaptation assumed)	Increasing (no adaptation assumed)	None	Brown et al. (2018a)
Population situated below the 1-in-100-year flood plain	Global	(millions)	1995	SSP1–5 until 2100, then no change to 2300	1850–1900	AMP4.5 (95th percentile). Stabilization at approx. 4.5°C	N/A	Yes. Overshoots after 2030. Does not return to 1.5°C	No	128–133	134–143	262–441	4.75°C in 2300	Increasing (no adaptation assumed)	Increasing (no adaptation assumed)	None	Brown et al. (2018a)
Population situated below the 1-in-100-year flood plain	Global	(millions)	1995	SSP1–5 until 2100, then no change to 2300	1850–1900	AMP4.5 (50th percentile). Stabilization at approx. 4.5°C	N/A	Yes. Overshoots after 2035. Does not return to 1.5°C	No	127–131	125–137	108–162	2.50°C in 2100	Increasing (no adaptation assumed)	Increasing (no adaptation assumed)	None	Brown et al. (2018a)
Population situated below the 1-in-100-year flood plain	Global	(millions)	1995	SSP1–5 until 2100, then no change to 2300	1850–1900	AMP4.5 (50th percentile). Stabilization at approx. 4.5°C	N/A	Yes. Overshoots after 2035. Does not return to 1.5°C	No	127–131	125–137	193–313	3.85°C in 2300	Increasing (no adaptation assumed)	Increasing (no adaptation assumed)	None	Brown et al. (2018a)
Population situated below the 1-in-100-year flood plain	Global	(millions)	1995	SSP1–5 until 2100, then no change to 2300	1850–1900	RCP8.5 (5th percentile)	N/A	Yes. Overshoots after 2050. Does not return to 1.5°C	No	125–132	125–136	110–166	4.35°C in 2100	Increasing (no adaptation assumed)	Increasing (no adaptation assumed)	None	Brown et al. (2018a)
Population situated below the 1-in-100-year flood plain	Global	(millions)	1995	SSP1–5 until 2100, then no change to 2300	1850–1900	RCP8.5 (5th percentile)	N/A	Yes. Overshoots after 2050. Does not return to 1.5°C	No	125–132	125–136	243–407	7.52°C in 2300	Increasing (no adaptation assumed)	Increasing (no adaptation assumed)	None	Brown et al. (2018a)

Risk	Region	Metric (Unit)	Baseline Time Period against Which Change Measured	Socio-Economic Scenario and Date	Baseline Global T	Climate Scenario	Transient (T) or Equilibrium (E)	Is it an Overshoot Scenario? How Long is it above 1.5°C and What is the Maximum Temperature and When?	Dynamic Model?	Projected Impact at 1.5°C above Pre-Industrial	Projected Impact at 2°C above Pre-Industrial	Projected Impact at Delta T for Defined Year (°C)	Delta T Relative to Pre-Industrial in Defined Year; Delta T(°C)	Level of Risk after Adaptation at 1.5°C	Level of Risk after Adaptation at 2°C	Type of Adaptation Modeled	Reference
Population situated below the 1-in-100-year flood plain	Global	(millions)	1995	SSP1–5 until 2100, then no change to 2300	1850–1900	RCP8.5 (95th percentile)	N/A	Yes. Overshoots after 2040. Does not return to 1.5°C	No	128–132	133–141	142–221	5.83°C in 2100	Increasing (no adaptation assumed)	Increasing (no adaptation assumed)	None	Brown et al. (2018a)
Population situated below the 1-in-100-year flood plain	Global	(millions)	1995	SSP1–5 until 2100, then no change to 2300	1850–1900	RCP8.5 (95th percentile)	N/A	Yes. Overshoots after 2040. Does not return to 1.5°C	No	128–132	133–141	504–879	13.14°C in 2300	Increasing (no adaptation assumed)	Increasing (no adaptation assumed)	None	Brown et al. (2018a)
Population situated below the 1-in-100-year flood plain	Global	(millions)	1995	SSP1–5 until 2100, then no change to 2300	1850–1900	RCP8.5 (50th percentile)	N/A	Yes. Overshoots after 2045. Does not return to 1.5°C	No	127–133	130–139	123–189	4.93°C in 2100	Increasing (no adaptation assumed)	Increasing (no adaptation assumed)	None	Brown et al. (2018a)
Population situated below the 1-in-100-year flood plain	Global	(millions)	1995	SSP1–5 until 2100, then no change to 2300	1850–1900	RCP8.5 (50th percentile)	N/A	Yes. Overshoots after 2045. Does not return to 1.5°C	No	127–133	130–139	361–620	9.54°C in 2300	Increasing (no adaptation assumed)	Increasing (no adaptation assumed)	None	Brown et al. (2018a)
People at risk from flooding	Global	(millions yr^{-1})	1995	Average of SSP1–5	1850–1900	1.5°C scenario (50th percentile)	N/A	No	Yes	27,8	N/A	N/A	N/A	Increasing (assuming no upgrade to adaptation)	Increasing (assuming no upgrade to adaptation)	Dikes in base year, then no upgrade to adaptation	Nicholls et al. (2018)
People at risk from flooding	Global	(millions yr^{-1})	1995	Average of SSP1–5	1850–1900	1.5°C scenario (95th percentile)	N/A	No	Yes	2,3	N/A	N/A	N/A	Increasing (assuming no upgrade to adaptation)	Increasing (assuming no upgrade to adaptation)	Dikes in base year, then no upgrade to adaptation	Nicholls et al. (2018)
People at risk from flooding	Global	(millions yr^{-1})	1995	Average of SSP1–5	1850–1900	2.0°C scenario (50th percentile)	N/A	Yes. Overshoots in 2040. Does not return to 1.5°C	Yes	19,5	52,3	N/A	N/A	Increasing (assuming no upgrade to adaptation)	Increasing (assuming no upgrade to adaptation)	Dikes in base year, then no upgrade to adaptation	Nicholls et al. (2018)
People at risk from flooding	Global	(millions yr^{-1})	1995	Average of SSP1–5	1850–1900	2.0°C scenario (95th percentile)	N/A	Yes. Overshoots in 2005. Does not return to 1.5°C	Yes	2,3	14,9	N/A	N/A	Increasing (assuming no upgrade to adaptation)	Increasing (assuming no upgrade to adaptation)	Dikes in base year, then no upgrade to adaptation	Nicholls et al. (2018)
People at risk from flooding	Global	(millions yr^{-1})	1995	Average of SSP1–5	1850–1900	2.0°C scenario (5th percentile)	N/A	Yes. Overshoots in 2060. Does not return to 1.5°C	Yes	25,8	N/A	N/A	N/A	Increasing (assuming no upgrade to adaptation)	Increasing (assuming no upgrade to adaptation)	Dikes in base year, then no upgrade to adaptation	Nicholls et al. (2018)
People at risk from flooding	Global	(millions yr^{-1})	1995	Average of SSP1–5	1850–1900	RCP8.5 (50th percentile)	N/A	Yes. Overshoots in 2035. Does not return to 1.5°C	Yes	30	36,4	N/A	N/A	Increasing (assuming no upgrade to adaptation)	Increasing (assuming no upgrade to adaptation)	Dikes in base year, then no upgrade to adaptation	Nicholls et al. (2018)
People at risk from flooding	Global	(millions yr^{-1})	1995	Average of SSP1–5	1850–1900	RCP8.5 (95th percemtile)	N/A	Yes. Overshoots in 2005. Does not return to 1.5°C	Yes	2,3	14,8	N/A	N/A	Increasing (assuming no upgrade to adaptation)	Increasing (assuming no upgrade to adaptation)	Dikes in base year, then no upgrade to adaptation	Nicholls et al. (2018)
People at risk from flooding	Global	(millions yr^{-1})	1995	Average of SSP1–5	1850–1900	RCP8.5 (5th percentile)	N/A	Yes. Overshoots in 2045. Does not return to 1.5°C	Yes	21,2	25	N/A	N/A	Increasing (assuming no upgrade to adaptation)	Increasing (assuming no upgrade to adaptation)	Dikes in base year, then no upgrade to adaptation	Nicholls et al. (2018)
People at risk from flooding	Global	(millions yr^{-1})	1995	Average of SSP1–5	1850–1900	1.5°C scenario (50th percentile)	N/A	No	Yes	N/A	N/A	62,7	1.48°C in 2100	Increasing (assuming no upgrade to adaptation)	Increasing (assuming no upgrade to adaptation)	Dikes in base year, then no upgrade to adaptation	Nicholls et al. (2018)
People at risk from flooding	Global	(millions yr^{-1})	1995	Average of SSP1–5	1850–1900	1.5°C scenario (95th percentile)	N/A	No	Yes	N/A	N/A	116,8	1.55°C in 2100	Increasing (assuming no upgrade to adaptation)	Increasing (assuming no upgrade to adaptation)	Dikes in base year, then no upgrade to adaptation	Nicholls et al. (2018)
People at risk from flooding	Global	(millions yr^{-1})	1995	Average of SSP1–5	1850–1900	1.5°C scenario (5th percentile)	N/A	No	Yes	N/A	N/A	33,4	1.25°C in 2100	Increasing (assuming no upgrade to adaptation)	Increasing (assuming no upgrade to adaptation)	Dikes in base year, then no upgrade to adaptation	Nicholls et al. (2018)
People at risk from flooding	Global	(millions yr^{-1})	1995	Average of SSP1–5	1850–1900	2.0°C scenario (50th percentile)	N/A	Yes. Overshoots in 2040. Does not return to 1.5°C	Yes	N/A	N/A	75	2.03°C in 2100	Increasing (assuming no upgrade to adaptation)	Increasing (assuming no upgrade to adaptation)	Dikes in base year, then no upgrade to adaptation	Nicholls et al. (2018)
People at risk from flooding	Global	(millions yr^{-1})	1995	Average of SSP1–5	1850–1900	2.0°C scenario (95th percentile)	N/A	Yes. Overshoots in 2005. Does not return to 1.5°C	Yes	N/A	N/A	131,9	2.32°C in 2100	Increasing (assuming no upgrade to adaptation)	Increasing (assuming no upgrade to adaptation)	Dikes in base year, then no upgrade to adaptation	Nicholls et al. (2018)
People at risk from flooding	Global	(millions yr^{-1})	1995	Average of SSP1–5	1850–1900	2.0°C scenario (5th percentile)	N/A	Yes. Overshoots in 2060. Does not return to 1.5°C	Yes	N/A	N/A	41,7	1.77°C in 2100	Increasing (assuming no upgrade to adaptation)	Increasing (assuming no upgrade to adaptation)	Dikes in base year, then no upgrade to adaptation	Nicholls et al. (2018)
People at risk from flooding	Global	(millions yr^{-1})	1995	Average of SSP1–5	1850–1900	RCP8.5 (50th percentile)	N/A	Yes. Overshoots in 2035. Does not return to 1.5°C	Yes	N/A	N/A	103	3.81°C in 2100	Increasing (assuming no upgrade to adaptation)	Increasing (assuming no upgrade to adaptation)	Dikes in base year, then no upgrade to adaptation	Nicholls et al. (2018)
People at risk from flooding	Global	(millions yr^{-1})	1995	Average of SSP1–5	1850–1900	RCP8.5 (95th percemtile)	N/A	Yes. Overshoots in 2005. Does not return to 1.5°C	Yes	N/A	N/A	166,3	6.29°C in 2100	Increasing (assuming no upgrade to adaptation)	Increasing (assuming no upgrade to adaptation)	Dikes in base year, then no upgrade to adaptation	Nicholls et al. (2018)

Risk	Region	Metric (Unit)	Baseline Time Period against Which Change Measured	Socio-Economic Scenario and Date	Baseline Global T	Climate Scenario	Transient (T) or Equilibrium (E)	Is it an Overshoot Scenario? How Long is it above 1.5°C and What is the Maximum Temperature and When?	Dynamic Model?	Projected Impact at 1.5°C above Pre-Industrial	Projected Impact at 2°C above Pre-Industrial	Projected Impact at Delta T for Defined Year (°C)	Delta T Relative to Pre-Industrial in Defined Year; Delta T(°C)	Level of Risk after Adaptation at 1.5°C	Level of Risk after Adaptation at 2°C	Type of Adaptation Modeled	Reference
People at risk from flooding	Global	(millions yr^{-1})	1995	Average of SSP1–5	1850–1900	RCP8.5 (5th percentile)	N/A	Yes. Overshoots in 2045. Does not return to 1.5°C	Yes	N/A	N/A	69	3.04°C in 2100	Increasing (assuming no upgrade to adaptation)	Increasing (assuming no upgrade to adaptation)	Dikes in base year, then no upgrade to adaptation	Nicholls et al. (2018)
People at risk from flooding	Global	(millions yr^{-1})	1995	Average of SSP1–5	1850–1900	1.5°C scenario (50th percentile)	N/A	No	Yes	N/A	N/A	103,5	1.46°C in 2200	Increasing (assuming no upgrade to adaptation)	Increasing (assuming no upgrade to adaptation)	Dikes in base year, then no upgrade to adaptation	Nicholls et al. (2018)
People at risk from flooding	Global	(millions yr^{-1})	1995	Average of SSP1–5	1850–1900	1.5°C scenario (95th percentile)	N/A	No	Yes	N/A	N/A	180,4	1.55°C in 2200	Increasing (assuming no upgrade to adaptation)	Increasing (assuming no upgrade to adaptation)	Dikes in base year, then no upgrade to adaptation	Nicholls et al. (2018)
People at risk from flooding	Global	(millions yr^{-1})	1995	Average of SSP1–5	1850–1900	1.5°C scenario (5th percentile)	N/A	No	Yes	N/A	N/A	60	1.45°C in 2200	Increasing (assuming no upgrade to adaptation)	Increasing (assuming no upgrade to adaptation)	Dikes in base year, then no upgrade to adaptation	Nicholls et al. (2018)
People at risk from flooding	Global	(millions yr^{-1})	1995	Average of SSP1–5	1850–1900	2.0°C scenario (50th percentile)	N/A	Yes. Overshoots in 2040. Does not return to 1.5°C	Yes	N/A	N/A	124	1.98°C in 2200	Increasing (assuming no upgrade to adaptation)	Increasing (assuming no upgrade to adaptation)	Dikes in base year, then no upgrade to adaptation	Nicholls et al. (2018)
People at risk from flooding	Global	(millions yr^{-1})	1995	Average of SSP1–5	1850–1900	2.0°C scenario (95th percentile)	N/A	Yes. Overshoots in 2005. Does not return to 1.5°C	Yes	N/A	N/A	210,5	2.05C in 2200	Increasing (assuming no upgrade to adaptation)	Increasing (assuming no upgrade to adaptation)	Dikes in base year, then no upgrade to adaptation	Nicholls et al. (2018)
People at risk from flooding	Global	(millions yr^{-1})	1995	Average of SSP1–5	1850–1900	2.0°C scenario (5th percentile)	N/A	Yes. Overshoots in 2060. Does not return to 1.5°C	Yes	N/A	N/A	75	1.94°C in 2200	Increasing (assuming no upgrade to adaptation)	Increasing (assuming no upgrade to adaptation)	Dikes in base year, then no upgrade to adaptation	Nicholls et al. (2018)
People at risk from flooding	Global	(millions yr^{-1})	1995	Average of SSP1–5	1850–1900	RCP8.5 (50th percentile)	N/A	Yes. Overshoots in 2035. Does not return to 1.5°C	Yes	N/A	N/A	238,3	6.87°C in 2200	Increasing (assuming no upgrade to adaptation)	Increasing (assuming no upgrade to adaptation)	Dikes in base year, then no upgrade to adaptation	Nicholls et al. (2018)
People at risk from flooding	Global	(millions yr^{-1})	1995	Average of SSP1–5	1850–1900	RCP8.5 (95th percemtile)	N/A	Yes. Overshoots in 2005. Does not return to 1.5°C	Yes	N/A	N/A	402,4	12.01°C in 2200	Increasing (assuming no upgrade to adaptation)	Increasing (assuming no upgrade to adaptation)	Dikes in base year, then no upgrade to adaptation	Nicholls et al. (2018)
People at risk from flooding	Global	(millions yr^{-1})	1995	Average of SSP1–5	1850–1900	RCP8.5 (5th percentile)	N/A	Yes. Overshoots in 2045. Does not return to 1.5°C	Yes	N/A	N/A	152,3	4.97°C in 2200	Increasing (assuming no upgrade to adaptation)	Increasing (assuming no upgrade to adaptation)	Dikes in base year, then no upgrade to adaptation	Nicholls et al. (2018)
People at risk from flooding	Global	(millions yr^{-1})	1995	Average of SSP1–5	1850–1900	1.5°C scenario (50th percentile)	N/A	No	Yes	N/A	N/A	137,6	1.46°C in 2300	Increasing (assuming no upgrade to adaptation)	Increasing (assuming no upgrade to adaptation)	Dikes in base year, then no upgrade to adaptation	Nicholls et al. (2018)
People at risk from flooding	Global	(millions yr^{-1})	1995	Average of SSP1–5	1850–1900	1.5°C scenario (95th percentile)	N/A	No	Yes	N/A	N/A	233,2	1.54°C in 2300	Increasing (assuming no upgrade to adaptation)	Increasing (assuming no upgrade to adaptation)	Dikes in base year, then no upgrade to adaptation	Nicholls et al. (2018)
People at risk from flooding	Global	(millions yr^{-1})	1995	Average of SSP1–5	1850–1900	1.5°C scenario (5th percentile)	N/A	No	Yes	N/A	N/A	83,6	1.45°C in 2300	Increasing (assuming no upgrade to adaptation)	Increasing (assuming no upgrade to adaptation)	Dikes in base year, then no upgrade to adaptation	Nicholls et al. (2018)
People at risk from flooding	Global	(millions yr^{-1})	1995	Average of SSP1–5	1850–1900	2.0°C scenario (50th percentile)	N/A	Yes. Overshoots in 2040. Does not return to 1.5°C	Yes	N/A	N/A	164	1.96°C in 2300	Increasing (assuming no upgrade to adaptation)	Increasing (assuming no upgrade to adaptation)	Dikes in base year, then no upgrade to adaptation	Nicholls et al. (2018)
People at risk from flooding	Global	(millions yr^{-1})	1995	Average of SSP1–5	1850–1900	2.0°C scenario (95th percentile)	N/A	Yes. Overshoots in 2005. Does not return to 1.5°C	Yes	N/A	N/A	276,5	2.04°C in 2300	Increasing (assuming no upgrade to adaptation)	Increasing (assuming no upgrade to adaptation)	Dikes in base year, then no upgrade to adaptation	Nicholls et al. (2018)
People at risk from flooding	Global	(millions yr^{-1})	1995	Average of SSP1–5	1850–1900	2.0°C scenario (5th percentile)	N/A	Yes. Overshoots in 2060. Does not return to 1.5°C	Yes	N/A	N/A	100,1	1.95°C in 2300	Increasing (assuming no upgrade to adaptation)	Increasing (assuming no upgrade to adaptation)	Dikes in base year, then no upgrade to adaptation	Nicholls et al. (2018)
People at risk from flooding	Global	(millions yr^{-1})	1995	Average of SSP1–5	1850–1900	RCP8.5 (50th percentile)	N/A	Yes. Overshoots in 2035. Does not return to 1.5°C	Yes	N/A	N/A	385,7	7.95°C in 2300	Increasing (assuming no upgrade to adaptation)	Increasing (assuming no upgrade to adaptation)	Dikes in base year, then no upgrade to adaptation	Nicholls et al. (2018)
People at risk from flooding	Global	(millions yr^{-1})	1995	Average of SSP1–5	1850–1900	RCP8.5 (95th percemtile)	N/A	Yes. Overshoots in 2005. Does not return to 1.5°C	Yes	N/A	N/A	703,3	14.77°C in 2300	Increasing (assuming no upgrade to adaptation)	Increasing (assuming no upgrade to adaptation)	Dikes in base year, then no upgrade to adaptation	Nicholls et al. (2018)
People at risk from flooding	Global	(millions yr^{-1})	1995	Average of SSP1–5	1850–1900	RCP8.5 (5th percentile)	N/A	Yes. Overshoots in 2045. Does not return to 1.5°C	Yes	N/A	N/A	228,4	5.46°C in 2300	Increasing (assuming no upgrade to adaptation)	Increasing (assuming no upgrade to adaptation)	Dikes in base year, then no upgrade to adaptation	Nicholls et al. (2018)

Risk	Region	Metric (Unit)	Baseline Time Period against Which Change Measured	Socio-Economic Scenario and Date	Baseline Global T	Climate Scenario	Transient (T) or Equilibrium (E)	Is it an Overshoot Scenario? How Long is it above 1.5°C and What is the Maximum Temperature and When?	Dynamic Model?	Projected Impact at 1.5°C above Pre-Industrial	Projected Impact at 2°C above Pre-Industrial	Projected Impact at Delta T for Defined Year (°C)	Delta T Relative to Pre-Industrial in Defined Year; Delta T(°C)	Level of Risk after Adaptation at 1.5°C	Level of Risk after Adaptation at 2°C	Type of Adaptation Modeled	Reference
People at risk from flooding	Global	(millions yr^{-1})	1995	SSP1–5	Not defined	RCP2.6. HadGEM2-ES. Medium	N/A	Yes. Overshoots in 2020. Does not return to 1.5°C by 2100	Yes	1.3–1.4	0.6–1.0	N/A	N/A	Risk increases, but decreases with adaptation	Risk increases, but decreases with adaptation	Dikes are upgraded as sea levels and socio-economic conditions change	Hinkel et al. (2014)
People at risk from flooding	Global	(millions yr^{-1})	1995	SSP1–5	Not defined	RCP2.6. HadGEM2-ES. High	N/A	Yes. Overshoots in 2020. Does not return to 1.5°C by 2100	Yes	1.4–1.5	0.6–1.1	N/A	N/A	Risk increases, but decreases with adaptation	Risk increases, but decreases with adaptation	Dikes are upgraded as sea levels and socio-economic conditions change	Hinkel et al. (2014)
People at risk from flooding	Global	(millions yr^{-1})	1995	SSP1–5	Not defined	RCP2.6. HadGEM2-ES. Low	N/A	Yes. Overshoots in 2020. Does not return to 1.5°C by 2100	Yes	1.3–1.4	0.6–1.0	N/A	N/A	Risk increases, but decreases with adaptation	Risk increases, but decreases with adaptation	Dikes are upgraded as sea levels and socio-economic conditions change	Hinkel et al. (2014)
People at risk from flooding	Global	(millions yr^{-1})	1995	SSP1–5	Not defined	RCP2.6. HadGEM2-ES. Medium	N/A	Yes. Overshoots in 2020. Does not return to 1.5°C by 2100	Yes	0.6–0.7	11.9–13.5	N/A	N/A	Increasing (assuming no upgrade to adaptation)	Increasing (assuming no upgrade to adaptation)	Dikes in base year, then no upgrade to adaptation	Hinkel et al. (2014)
People at risk from flooding	Global	(millions yr^{-1})	1995	SSP1–5	Not defined	RCP2.6. HadGEM2-ES. High	N/A	Yes. Overshoots in 2020. Does not return to 1.5°C by 2100	Yes	0.8–0.8	19.0–21.6	N/A	N/A	Increasing (assuming no upgrade to adaptation)	Increasing (assuming no upgrade to adaptation)	Dikes in base year, then no upgrade to adaptation	Hinkel et al. (2014)
People at risk from flooding	Global	(millions yr^{-1})	1995	SSP1–5	Not defined	RCP2.6. HadGEM2-ES. Low	N/A	Yes. Overshoots in 2020. Does not return to 1.5°C by 2100	Yes	0.6–0.7	10.4–11.1	N/A	N/A	Increasing (assuming no upgrade to adaptation)	Increasing (assuming no upgrade to adaptation)	Dikes in base year, then no upgrade to adaptation	Hinkel et al. (2014)
People at risk from flooding	Global	(millions yr^{-1})	1995	SSP1–5	Not defined	RCP4.5. HadGEM2-ES. Medium	N/A	Yes. Overshoots in 2020. Does not return to 1.5°C by 2100	Yes	1.4–1.5	0.5–1.0	N/A	N/A	Risk increases, but decreases with adaptation	Risk increases, but decreases with adaptation	Dikes are upgraded as sea levels and socio-economic conditions change	Hinkel et al. (2014)
People at risk from flooding	Global	(millions yr^{-1})	1995	SSP1–5	Not defined	RCP4.5. HadGEM2-ES. High	N/A	Yes. Overshoots in 2020. Does not return to 1.5°C by 2100	Yes	1.5–1.6	0.5–1.1	N/A	N/A	Risk increases, but decreases with adaptation	Risk increases, but decreases with adaptation	Dikes are upgraded as sea levels and socio-economic conditions change	Hinkel et al. (2014)
People at risk from flooding	Global	(millions yr^{-1})	1995	SSP1–5	Not defined	RCP4.5. HadGEM2-ES. Low	N/A	Yes. Overshoots in 2020. Does not return to 1.5°C by 2100	Yes	1.4–1.5	0.5–1.0	N/A	N/A	Risk increases, but decreases with adaptation	Risk increases, but decreases with adaptation	Dikes are upgraded as sea levels and socio-economic conditions change	Hinkel et al. (2014)
People at risk from flooding	Global	(millions yr^{-1})	1995	SSP1–5	Not defined	RCP4.5. HadGEM2-ES. Medium	N/A	Yes. Overshoots in 2020. Does not return to 1.5°C by 2100	Yes	0.7–0.7	15.9–18.6	N/A	N/A	Increasing (assuming no upgrade to adaptation)	Increasing (assuming no upgrade to adaptation)	Dikes in base year, then no upgrade to adaptation	Hinkel et al. (2014)
People at risk from flooding	Global	(millions yr^{-1})	1995	SSP1–5	Not defined	RCP4.5. HadGEM2-ES. High	N/A	Yes. Overshoots in 2020. Does not return to 1.5°C by 2100	Yes	0.8–0.8	27.1–31.8	N/A	N/A	Increasing (assuming no upgrade to adaptation)	Increasing (assuming no upgrade to adaptation)	Dikes in base year, then no upgrade to adaptation	Hinkel et al. (2014)
People at risk from flooding	Global	(millions yr^{-1})	1995	SSP1–5	Not defined	RCP4.5. HadGEM2-ES. Low	N/A	Yes. Overshoots in 2020. Does not return to 1.5°C by 2100	Yes	6.3–6.6	13.6–15.9	N/A	N/A	Increasing (assuming no upgrade to adaptation)	Increasing (assuming no upgrade to adaptation)	Dikes in base year, then no upgrade to adaptation	Hinkel et al. (2014)
People at risk from flooding	Global	(millions yr^{-1})	1995	SSP1–5	Not defined	RCP8.5. HadGEM2-ES. Medium	N/A	Yes. Overshoots in 2020. Does not return to 1.5°C by 2100	Yes	1.4–1.5	0.7–1.2	N/A	N/A	Risk increases, but decreases with adaptation	Risk increases, but decreases with adaptation	Dikes are upgraded as sea levels and socio-economic conditions change	Hinkel et al. (2014)
People at risk from flooding	Global	(millions yr^{-1})	1995	SSP1–5	Not defined	RCP8.5. HadGEM2-ES. High	N/A	Yes. Overshoots in 2020. Does not return to 1.5°C by 2100	Yes	1.5–1.6	0.7–1.3	N/A	N/A	Risk increases, but decreases with adaptation	Risk increases, but decreases with adaptation	Dikes are upgraded as sea levels and socio-economic conditions change	Hinkel et al. (2014)
People at risk from flooding	Global	(millions yr^{-1})	1995	SSP1–5	Not defined	RCP8.5. HadGEM2-ES. Low	N/A	Yes. Overshoots in 2020. Does not return to 1.5°C by 2100	Yes	1.3–1.4	0.7–1.2	N/A	N/A	Risk increases, but decreases with adaptation	Risk increases, but decreases with adaptation	Dikes are upgraded as sea levels and socio-economic conditions change	Hinkel et al. (2014)
People at risk from flooding	Global	(millions yr^{-1})	1995	SSP1–5	Not defined	RCP8.5. HadGEM2-ES. Medium	N/A	Yes. Overshoots in 2020. Does not return to 1.5°C by 2100	Yes	6.9–7.2	14.4–16.5	N/A	N/A	Increasing (assuming no upgrade to adaptation)	Increasing (assuming no upgrade to adaptation)	Dikes in base year, then no upgrade to adaptation	Hinkel et al. (2014)
People at risk from flooding	Global	(millions yr^{-1})	1995	SSP1–5	Not defined	RCP8.5. HadGEM2-ES. High	N/A	Yes. Overshoots in 2020. Does not return to 1.5°C by 2100	Yes	8.4–8.6	23.7–27.0	N/A	N/A	Increasing (assuming no upgrade to adaptation)	Increasing (assuming no upgrade to adaptation)	Dikes in base year, then no upgrade to adaptation	Hinkel et al. (2014)
People at risk from flooding	Global	(millions yr^{-1})	1995	SSP1–5	Not defined	RCP8.5. HadGEM2-ES. Low	N/A	Yes. Overshoots in 2020. Does not return to 1.5°C by 2100	Yes	6.6–6.9	12.6–14.3	N/A	N/A	Increasing (assuming no upgrade to adaptation)	Increasing (assuming no upgrade to adaptation)	Dikes in base year, then no upgrade to adaptation	Hinkel et al. (2014)
Annual sea flood costs	Global	(billions USD yr^{-1})	1995	SSP1–5	Not defined	RCP2.6. HadGEM2-ES. Medium	N/A	Yes. Overshoots in 2020. Does not return to 1.5°C by 2100	Yes	9.8–10.3	10.4–11.3	N/A	N/A	Risk increases, but decreases with adaptation	Risk increases, but decreases with adaptation	Dikes are upgraded as sea levels and socio-economic conditions change	Hinkel et al. (2014)
Annual sea flood costs	Global	(billions USD yr^{-1})	1995	SSP1–5	Not defined	RCP2.6. HadGEM2-ES. High	N/A	Yes. Overshoots in 2020. Does not return to 1.5°C by 2100	Yes	10.4–11.4	11.5–12.4	N/A	N/A	Risk increases, but decreases with adaptation	Risk increases, but decreases with adaptation	Dikes are upgraded as sea levels and socio-economic conditions change	Hinkel et al. (2014)

Risk	Region	Metric (Unit)	Baseline Time Period against Which Change Measured	Socio-Economic Scenario and Date	Baseline Global T	Climate Scenario	Transient (T) or Equilibrium (E)	Is it an Overshoot Scenario? How Long is it above 1.5°C and What is the Maximum Temperature and When?	Dynamic Model?	Projected Impact at 1.5°C above Pre-Industrial	Projected Impact at 2°C above Pre-Industrial	Projected Impact at Delta T for Defined Year (°C)	Delta T Relative to Pre-Industrial in Defined Year; Delta T(°C)	Level of Risk after Adaptation at 1.5°C	Level of Risk after Adaptation at 2°C	Type of Adaptation Modeled	Reference
Annual sea flood costs	Global	(billions USD yr^{-1})	1995	SSP1–5	Not defined	RCP2.6. HadGEM2-ES. Low	N/A	Yes. Overshoots in 2020. Does not return to 1.5°C by 2100	Yes	9.6–10.6	10.1–11.0	N/A	N/A	Risk increases, but decreases with adaptation	Risk increases, but decreases with adaptation	Dikes are upgraded as sea levels and socio-economic conditions change	Hinkel et al. (2014)
Annual sea flood costs	Global	(billions USD yr^{-1})	1995	SSP1–5	Not defined	RCP2.6. HadGEM2-ES. Medium	N/A	Yes. Overshoots in 2020. Does not return to 1.5°C by 2100	Yes	47.4–53.6	152.7–2678.5	N/A	N/A	Increasing (assuming no upgrade to adaptation)	Increasing (assuming no upgrade to adaptation)	Dikes in base year, then no upgrade to adaptation	Hinkel et al. (2014)
Annual sea flood costs	Global	(billions USD yr^{-1})	1995	SSP1–5	Not defined	RCP2.6. HadGEM2-ES. High	N/A	Yes. Overshoots in 2020. Does not return to 1.5°C by 2100	Yes	57.6–65.0	259.2–452.8	N/A	N/A	Increasing (assuming no upgrade to adaptation)	Increasing (assuming no upgrade to adaptation)	Dikes in base year, then no upgrade to adaptation	Hinkel et al. (2014)
Annual sea flood costs	Global	(billions USD yr^{-1})	1995	SSP1–5	Not defined	RCP2.6. HadGEM2-ES. Low	N/A	Yes. Overshoots in 2020. Does not return to 1.5°C by 2100	Yes	543.3–51.1	132.8–23.6	N/A	N/A	Increasing (assuming no upgrade to adaptation)	Increasing (assuming no upgrade to adaptation)	Dikes in base year, then no upgrade to adaptation	Hinkel et al. (2014)
Annual sea flood costs	Global	(billions USD yr^{-1})	1995	SSP1–5	Not defined	RCP4.5. HadGEM2-ES. Medium	N/A	Yes. Overshoots in 2020. Does not return to 1.5°C by 2100	Yes	10.8–11.9	10.8–11.5	N/A	N/A	Risk increases, but decreases with adaptation	Risk increases, but decreases with adaptation	Dikes are upgraded as sea levels and socio-economic conditions change	Hinkel et al. (2014)
Annual sea flood costs	Global	(billions USD yr^{-1})	1995	SSP1–5	Not defined	RCP4.5. HadGEM2-ES. High	N/A	Yes. Overshoots in 2020. Does not return to 1.5°C by 2100	Yes	11.6–12.7	12.2–12.9	N/A	N/A	Risk increases, but decreases with adaptation	Risk increases, but decreases with adaptation	Dikes are upgraded as sea levels and socio-economic conditions change	Hinkel et al. (2014)
Annual sea flood costs	Global	(billions USD yr^{-1})	1995	SSP1–5	Not defined	RCP4.5. HadGEM2-ES. Low	N/A	Yes. Overshoots in 2020. Does not return to 1.5°C by 2100	Yes	10.7–11.7	10.4–11.1	N/A	N/A	Risk increases, but decreases with adaptation	Risk increases, but decreases with adaptation	Dikes are upgraded as sea levels and socio-economic conditions change	Hinkel et al. (2014)
Annual sea flood costs	Global	(billions USD yr^{-1})	1995	SSP1–5	Not defined	RCP4.5. HadGEM2-ES. Medium	N/A	Yes. Overshoots in 2020. Does not return to 1.5°C by 2100	Yes	52.2–59.3	214.2–410.5	N/A	N/A	Increasing (assuming no upgrade to adaptation)	Increasing (assuming no upgrade to adaptation)	Dikes in base year, then no upgrade to adaptation	Hinkel et al. (2014)
Annual sea flood costs	Global	(billions USD yr^{-1})	1995	SSP1–5	Not defined	RCP4.5. HadGEM2-ES. High	N/A	Yes. Overshoots in 2020. Does not return to 1.5°C by 2100	Yes	64.8–73.6	396.1–752.3	N/A	N/A	Increasing (assuming no upgrade to adaptation)	Increasing (assuming no upgrade to adaptation)	Dikes in base year, then no upgrade to adaptation	Hinkel et al. (2014)
Annual sea flood costs	Global	(billions USD yr^{-1})	1995	SSP1–5	Not defined	RCP4.5. HadGEM2-ES. Low	N/A	Yes. Overshoots in 2020. Does not return to 1.5°C by 2100	Yes	49.4–56.0	180.0–345.2	N/A	N/A	Increasing (assuming no upgrade to adaptation)	Increasing (assuming no upgrade to adaptation)	Dikes in base year, then no upgrade to adaptation	Hinkel et al. (2014)
Annual sea flood costs	Global	(billions USD yr^{-1})	1995	SSP1–5	Not defined	RCP8.5. HadGEM2-ES. Medium	N/A	Yes. Overshoots in 2020. Does not return to 1.5°C by 2100	Yes	10.1–11.1	10.9–11.8	N/A	N/A	Risk increases, but decreases with adaptation	Risk increases, but decreases with adaptation	Dikes are upgraded as sea levels and socio-economic conditions change	Hinkel et al. (2014)
Annual sea flood costs	Global	(billions USD yr^{-1})	1995	SSP1–5	Not defined	RCP8.5. HadGEM2-ES. High	N/A	Yes. Overshoots in 2020. Does not return to 1.5°C by 2100	Yes	10.8–11.9	12.2–13.1	N/A	N/A	Risk increases, but decreases with adaptation	Risk increases, but decreases with adaptation	Dikes are upgraded as sea levels and socio-economic conditions change	Hinkel et al. (2014)
Annual sea flood costs	Global	(billions USD yr^{-1})	1995	SSP1–5	Not defined	RCP8.5. HadGEM2-ES. Low	N/A	Yes. Overshoots in 2020. Does not return to 1.5°C by 2100	Yes	9.9–10.8	10.6–11.5	N/A	N/A	Risk increases, but decreases with adaptation	Risk increases, but decreases with adaptation	Dikes are upgraded as sea levels and socio-economic conditions change	Hinkel et al. (2014)
Annual sea flood costs	Global	(billions USD yr^{-1})	1995	SSP1–5	Not defined	RCP8.5. HadGEM2-ES. Medium	N/A	Yes. Overshoots in 2020. Does not return to 1.5°C by 2100	Yes	50.6–57.2	170.0–594.8	N/A	N/A	Increasing (assuming no upgrade to adaptation)	Increasing (assuming no upgrade to adaptation)	Dikes in base year, then no upgrade to adaptation	Hinkel et al. (2014)
Annual sea flood costs	Global	(billions USD yr^{-1})	1995	SSP1–5	Not defined	RCP8.5. HadGEM2-ES. High	N/A	Yes. Overshoots in 2020. Does not return to 1.5°C by 2100	Yes	62.5–70.6	296.5–512.0	N/A	N/A	Increasing (assuming no upgrade to adaptation)	Increasing (assuming no upgrade to adaptation)	Dikes in base year, then no upgrade to adaptation	Hinkel et al. (2014)
Annual sea flood costs	Global	(billions USD yr^{-1})	1995	SSP1–5	Not defined	RCP8.5. HadGEM2-ES. Low	N/A	Yes. Overshoots in 2020. Does not return to 1.5°C by 2100	Yes	48.0–54.2	145.7–252.9	N/A	N/A	Increasing (assuming no upgrade to adaptation)	Increasing (assuming no upgrade to adaptation)	Dikes in base year, then no upgrade to adaptation	Hinkel et al. (2014)
Long-term degradation of coral reefs	Global	N/A	1850–1900	N/A	N/A	Emulates the sea-level response of GCMs	N/A	The illustrative 1.5°C scenario used here does not allow for a GMT overshoot, but stays below 1.5°C over the course of the 21st century	N/A	89% [48% and 99% indicating the 66% range] and more of all global reef grid cells will be at risk of long-term degradation for a 1.5°C scenario in 2050	98% [86% and 100% indicating the 66% range] and more of all global reef grid cells will be at risk of long-term degradation for a 2.0°C scenario in 2050	N/A	N/A	N/A	N/A	Constant adaptive capacity	Schleussner et al. (2016)

Risk	Region	Metric (Unit)	Baseline Time Period against Which Change Measured	Socio-Economic Scenario and Date	Baseline Global T	Climate Scenario	Transient (T) or Equilibrium (E)	Is it an Overshoot Scenario? How Long is it above 1.5°C and What is the Maximum Temperature and When?	Dynamic Model?	Projected Impact at 1.5°C above Pre-Industrial	Projected Impact at 2°C above Pre-Industrial	Projected Impact at Delta T for Defined Year (°C)	Delta T Relative to Pre-Industrial in Defined Year; Delta T(°C)	Level of Risk after Adaptation at 1.5°C	Level of Risk after Adaptation at 2°C	Type of Adaptation Modeled	Reference
Long-term degradation of coral reefs	Global	N/A	1850–1900	N/A	N/A	Emulates the sea-level response of GCMs	N/A	The illustrative 1.5°C scenario used here does not allow for a GMT overshoot, but stays below 1.5°C over the course of the 21st century	N/A	69% [14% and 98% indicating the 66% range] and more of all global reef cells will be at risk of long-term degradation for a 1.5°C scenario in 2100	99% [85% and 100% indicating the 66% range] and more of all global reef grid cells will be at risk of long-term degradation for a 2.0°C scenario in 2050	N/A	N/A	N/A	N/A	Constant adaptive capacity	Schleussner et al. (2016)
Long-term degradation of coral reefs	Global	N/A	1850–1900	N/A	N/A	Emulates the sea-level response of GCMs	N/A	The illustrative 1.5°C scenario used here does not allow for a GMT overshoot, but stays below 1.5°C over the course of the 21st century	N/A	94% [60% and 100% indicating the 66% range] and more of all global reef grid cells will be at risk of long-term degradation for a 1.5°C scenario in 2050	100% [95% and 100% indicating the 66% range] and more of all global reef grid cells will be at risk of long-term degradation for a 2.0°C scenario in 2050	N/A	N/A	N/A	N/A	Saturation adaptive capacity	Schleussner et al. (2016)
Long-term degradation of coral reefs	Global	N/A	1850–1900	N/A	N/A	Emulates the sea-level response of GCMs	N/A	The illustrative 1.5°C scenario used here does not allow for a GMT overshoot, but stays below 1.5°C over the course of the 21st century	N/A	69% [14% and 98% indicating the 66% range] and more of all global reef cells will be at risk of long-term degradation for a 1.5°C scenario in 2100	6% [1% and 50% indicating the 66% range] and more of all global reef cells will be at risk of long-term degradation for a 2.0°C scenario in 2100	N/A	N/A	N/A	N/A	Saturation adaptive capacity	Schleussner et al. (2016)
Long-term degradation of coral reefs	Global	N/A	1850–1900	N/A	N/A	Emulates the sea-level response of GCMs	N/A	The illustrative 1.5°C scenario used here does not allow for a GMT overshoot, but stays below 1.5°C over the course of the 21st century	N/A	9% [2% and 49% indicating the 66% range] and more of all global reef grid cells will be at risk of long-term degradation for a 1.5°C scenario in 2050	39% [8% and 81% indicating the 66% range] and more of all global reef grid cells will be at risk of long-term degradation for a 2.0°C scenario in 2050	N/A	N/A	N/A	N/A	Adaptation adaptive capacity	Schleussner et al. (2016)

Risk	Region	Metric (Unit)	Baseline Time Period against Which Change Measured	Socio-Economic Scenario and Date	Baseline Global T	Climate Scenario	Transient (T) or Equilibrium (E)	Is it an Overshoot Scenario? How Long is it above 1.5°C and What is the Maximum Temperature and When?	Dynamic Model?	Projected Impact at 1.5°C above Pre-Industrial	Projected Impact at 2°C above Pre-Industrial	Projected Impact at Delta T for Defined Year (°C)	Delta T Relative to Pre-Industrial in Defined Year; Delta T(°C)	Level of Risk after Adaptation at 1.5°C	Level of Risk after Adaptation at 2°C	Type of Adaptation Modeled	Reference
Long-term degradation of coral reefs	Global	N/A	1850–1900	N/A	N/A	Emulates the sea-level response of GCMs	N/A	The illustrative 1.5°C scenario used here does not allow for a GMT overshoot, but stays below 1.5°C over the course of the 21st century	N/A	1% [0% and 2% indicating the 66% range] and more of all global reef cells will be at risk of long-term degradation for a 1.5°C scenario in 2100	1% [0% and 2% indicating the 66% range] and more of all global reef cells will be at risk of long-term degradation for a 2.0°C scenario in 2100	N/A	N/A	N/A	N/A	Adaptation adaptive capacity	Schleussner et al. (2016)
Human population exposure	Global	millions people	1875–1900	2010 population levels	N/A	Not available	T - 19-yr running average relative to 2000	1.5°C ± 0.25°C in 2100 (50th)	N/A	46.12 in 2100	N/A	N/A	N/A	N/A	N/A	None	Rasmussen et al. (2018)
Human population exposure	Global	millions people	1875–1900	2010 population levels	N/A	Not available	T - 19-yr running average relative to 2000	1.5°C ± 0.25°C in 2100 (95th)	N/A	69.23 in 2100	N/A	N/A	N/A	N/A	N/A	None	Rasmussen et al. (2018)
Human population exposure	Global	millions people	1875–1900	2010 population levels	N/A	Not available	T - 19-yr running average relative to 2000	1.5°C ± 0.25°C in 2100 (5th)	N/A	31.92 in 2100	N/A	N/A	N/A	N/A	N/A	None	Rasmussen et al. (2018)
Human population exposure	Global	millions people	1875–1900	2010 population levels	N/A	Not available	T - 19-yr running average relative to 2000	2.0°C ± 0.25°C in 2100 (50th)	N/A	N/A	48.76 in 2100	N/A	N/A	N/A	N/A	None	Rasmussen et al. (2018)
Human population exposure	Global	millions people	1875–1900	2010 population levels	N/A	Not available	T - 19-yr running average relative to 2000	2.0°C ± 0.25°C in 2100 (95th)	N/A	N/A	79.65 in 2100	N/A	N/A	N/A	N/A	None	Rasmussen et al. (2018)
Human population exposure	Global	millions people	1875–1900	2010 population levels	N/A	Not available	T - 19-yr running average relative to 2000	2.0°C ± 0.25°C in 2100 (5th)	N/A	N/A	32.01 in 2100	N/A	N/A	N/A	N/A	None	Rasmussen et al. (2018)
Human population exposure	Global	millions people	1875–1900	2010 population levels	N/A	Not available	T - 19-yr running average relative to 2000	2.5°C ± 0.25°C in 2100 (50th)	N/A	N/A	N/A	50.35 in 2100	N/A	N/A	N/A	None	Rasmussen et al. (2018)
Human population exposure	Global	millions people	1875–1900	2010 population levels	N/A	Not available	T - 19-yr running average relative to 2000	2.5°C ± 0.25°C in 2100 (95th)	N/A	N/A	N/A	77.38 in 2100	N/A	N/A	N/A	None	Rasmussen et al. (2018)
Human population exposure	Global	millions people	1875–1900	2010 population levels	N/A	Not available	T - 19-yr running average relative to 2000	2.5°C ± 0.25°C in 2100 (5th)	N/A	N/A	N/A	33.33 in 2100	N/A	N/A	N/A	None	Rasmussen et al. (2018)
Human population exposure	Global	millions people	1875–1900	2010 population levels	N/A	Not available	T - 19-yr running average relative to 2000	1.5°C ± 0.25°C in 2150 (50th)	N/A	56.05 in 2150	N/A	N/A	N/A	N/A	N/A	None	Rasmussen et al. (2018)
Human population exposure	Global	millions people	1875–1900	2010 population levels	N/A	Not available	T - 19-yr running average relative to 2000	1.5°C ± 0.25°C in 2150 (95th)	N/A	112.97 in 2150	N/A	N/A	N/A	N/A	N/A	None	Rasmussen et al. (2018)
Human population exposure	Global	millions people	1875–1900	2010 population levels	N/A	Not available	T - 19-yr running average relative to 2000	1.5°C ± 0.25°C in 2150 (5th)	N/A	32.54 in 2150	N/A	N/A	N/A	N/A	N/A	None	Rasmussen et al. (2018)

Risk	Region	Metric (Unit)	Baseline Time Period against Which Change Measured	Socio-Economic Scenario and Date	Baseline Global T	Climate Scenario	Transient (T) or Equilibrium (E)	Is it an Overshoot Scenario? How Long is it above 1.5°C and What is the Maximum Temperature and When?	Dynamic Model?	Projected Impact at 1.5°C above Pre-Industrial	Projected Impact at 2°C above Pre-Industrial	Projected Impact at Delta T for Defined Year (°C)	Delta T Relative to Pre-Industrial in Defined Year; Delta T(°C)	Level of Risk after Adaptation at 1.5°C	Level of Risk after Adaptation at 2°C	Type of Adaptation Modeled	Reference
Human population exposure	Global	millions people	1875–1900	2010 population levels	N/A	Not available	T - 19-yr running average relative to 2000	2.0°C ± 0.25°C in 2150 (50th)	N/A	N/A	61.84 in 2150	N/A	N/A	N/A	N/A	None	Rasmussen et al. (2018)
Human population exposure	Global	millions people	1875–1900	2010 population levels	N/A	Not available	T - 19-yr running average relative to 2000	2.0°C ± 0.25°C in 2150 (95th)	N/A	N/A	138.63 in 2150	N/A	N/A	N/A	N/A	None	Rasmussen et al. (2018)
Human population exposure	Global	millions people	1875–1900	2010 population levels	N/A	Not available	T - 19-yr running average relative to 2000	2.0°C ± 0.25°C in 2150 (5th)	N/A	N/A	32.89 in 2150	N/A	N/A	N/A	N/A	None	Rasmussen et al. (2018)
Human population exposure	Global	millions people	1875–1900	2010 population levels	N/A	Not available	T - 19-yr running average relative to 2000	2.5°C ± 0.25°C in 2150 (50th)	N/A	N/A	N/A	62.27 in 2150	N/A	N/A	N/A	None	Rasmussen et al. (2018)
Human population exposure	Global	millions people	1875–1900	2010 population levels	N/A	Not available	T - 19-yr running average relative to 2000	2.5°C ± 0.25°C in 2150 (95th)	N/A	N/A	N/A	126.9 in 2150	N/A	N/A	N/A	None	Rasmussen et al. (2018)
Human population exposure	Global	millions people	1875–1900	2010 population levels	N/A	Not available	T - 19-yr running average relative to 2000	2.5°C ± 0.25°C in 2150 (5th)	N/A	N/A	N/A	34.08 in 2150	N/A	N/A	N/A	None	Rasmussen et al. (2018)
Potentially inundated areas from SLR (exposure)	Global	th km^2	2006	N/A	1850–1990	MIROC-ESM RCP2.6	T	1.5°C occurs between 2010 and 2020 and temperature continues to increase	N/A	67.7–74.2	80.4–83.4	N/A	N/A	Increasing (no adaptation assumed)	Increasing (no adaptation assumed)	None	Yotsukuri et al. (2017) (in Japanese)
Potentially inundated areas from SLR (exposure)	Global	th km^2	2006	N/A	1850–1990	MIROC-ESM RCP4.5	T	1.5°C occurs between 2010 and 2020 and temperature continues to increase	N/A	69.9–74.0	81.4–84.7	N/A	N/A	Increasing (no adaptation assumed)	Increasing (no adaptation assumed)	None	Yotsukuri et al. (2017) (in Japanese)
Potentially inundated areas from SLR (exposure)	Global	th km^2	2006	N/A	1850–1990	MIROC-ESM RCP8.5	T	1.5°C occurs between 2010 and 2020 and temperature continues to increase	N/A	69.3–73.9	73.9–81.9	N/A	N/A	Increasing (no adaptation assumed)	Increasing (no adaptation assumed)	None	Yotsukuri et al. (2017) (in Japanese)
Potentially inundated areas from SLR and astronomical high tides (exposure)	Global	th km^2	2006	N/A	1850–1990	MIROC-ESM RCP2.6	T	1.5°C occurs between 2010 and 2020 and temperature continues to increase	N/A	283.0–291.9	308.2–313.3	N/A	N/A	Increasing (no adaptation assumed)	Increasing (no adaptation assumed)	None	Yotsukuri et al. (2017) (in Japanese)
Potentially inundated areas from SLR and astronomical high tides (exposure)	Global	th km^2	2006	N/A	1850–1990	MIROC-ESM RCP4.5	T	1.5°C occurs between 2010 and 2020 and temperature continues to increase	N/A	283.9–291.1	303.2–314.5	N/A	N/A	Increasing (no adaptation assumed)	Increasing (no adaptation assumed)	None	Yotsukuri et al. (2017) (in Japanese)
Potentially inundated areas from SLR and astronomical high tides (exposure)	Global	th km^2	2006	N/A	1850–1990	MIROC-ESM RCP8.5	T	1.5°C occurs between 2010 and 2020 and temperature continues to increase	N/A	285.0–291.1	303.2–322.2	N/A	N/A	Increasing (no adaptation assumed)	Increasing (no adaptation assumed)	None	Yotsukuri et al. (2017) (in Japanese)
Exposed population from SLR and astronomical high tides	Global	millions people	2006	SSP1,2,3	1850–1990	MIROC-ESM RCP2.6	T	1.5°C occurs between 2010 and 2020 and temperature continues to increase	N/A	48.6–65.9	72.8–77.9	N/A	N/A	Increasing (no adaptation assumed)	Increasing (no adaptation assumed)	None	Yotsukuri et al. (2017) (in Japanese)
Exposed population from SLR and astronomical high tides	Global	millions people	2006	SSP1,2,3	1850–1990	MIROC-ESM RCP4.5	T	1.5°C occurs between 2010 and 2020 and temperature continues to increase	N/A	48.9–65.4	72.7–77.7	N/A	N/A	Increasing (no adaptation assumed)	Increasing (no adaptation assumed)	None	Yotsukuri et al. (2017) (in Japanese)
Exposed population from SLR and astronomical high tides	Global	millions people	2006	SSP1,2,3	1850–1990	MIROC-ESM RCP8.5	T	1.5°C occurs between 2010 and 2020 and temperature continues to increase	N/A	58.9–65.8	65.3–73.6	N/A	N/A	Increasing (no adaptation assumed)	Increasing (no adaptation assumed)	None	Yotsukuri et al. (2017) (in Japanese)
Economic damage due to SLR and astronomical high tides (Three damage function)	Global	billions USD (2005)	2006	SSP1,2,3	1850–1990	MIROC-ESM RCP2.6	T	1.5°C occurs between 2010 and 2020 and temperature continues to increase	N/A	32–54	75–133	N/A	N/A	Increasing (no adaptation assumed)	Increasing (no adaptation assumed)	None	Yotsukuri et al. (2017) (in Japanese)

Risk	Region	Metric (Unit)	Baseline Time Period against Which Change Measured	Socio-Economic Scenario and Date	Baseline Global T	Climate Scenario	Transient (T) or Equilibrium (E)	Is it an Overshoot Scenario? How Long is it above 1.5°C and What is the Maximum Temperature and When?	Dynamic Model?	Projected Impact at 1.5°C above Pre-Industrial	Projected Impact at 2°C above Pre-Industrial	Projected Impact at Delta T for Defined Year (°C)	Delta T Relative to Pre-Industrial in Defined Year; Delta T(°C)	Level of Risk after Adaptation at 1.5°C	Level of Risk after Adaptation at 2°C	Type of Adaptation Modeled	Reference
Economic damage due to SLR and astronomical high tides (Three damage function)	Global	billions USD (2005)	2006	SSP1,2,3	1850–1990	MIROC-ESM RCP4.5	T	1.5°C occurs between 2010 and 2020 and temperature continues to increase	N/A	32–53	75–134	N/A	N/A	Increasing (no adaptation assumed)	Increasing (no adaptation assumed)	None	Yotsukuri et al. (2017) (in Japanese)
Economic damage due to SLR and astronomical high tides (Three damage function)	Global	billions USD (2005)	2006	SSP1,2,3	1850–1990	MIROC-ESM RCP8.5	T	1.5°C occurs between 2010 and 2020 and temperature continues to increase	N/A	33–54	53–91	N/A	N/A	Increasing (no adaptation assumed)	Increasing (no adaptation assumed)	None	Yotsukuri et al. (2017) (in Japanese)

Table 3.SM.5: 3.4.6 Food security and food production systems

Risk	Region	Metric (Unit)	Baseline Time Period Against Which Change Measured	Socio-Economic Scenario and Date	Baseline Global T	Climate Scenario	Transient (T) or Equilibrium (E)	Overshoot Scenario?	Dynamic Model?	Projected Impact at 1.5°C above Pre-Industrial	Projected Impact at 2°C above Pre-Industrial	Projected Impact at Delta T (°C)	Delta T Relative to Pre-Industrial	Level of Risk After Adaptation at 1.5°C	Level of Risk After Adaptation at 2°C	Type of Adaptation Modelled	Reference
Water scarcity	Mediterranean	%	1986–2005	Not available	0,6	RCP8.5, ISIMIP	N/A	N/A	Y	-9	-17	Not available	Not available	N/A	N/A	Not available	Schleussner et al. (2017)
Crop yield – wheat	Tropical regions	%	1986–2005	Not available	0,6	RCP8.5, ISIMIP	N/A	N/A	Y	-9	-16	Not available	Not available	N/A	N/A	Not available	
Crop yield – maize	Tropical regions	%	1986–2005	Not available	0,6	RCP8.5, ISIMIP	N/A	N/A	Y	-3	-6	Not available	Not available	N/A	N/A	Not available	
Crop yield – soy	Tropical regions	%	1986–2005	Not available	0,6	RCP8.5, ISIMIP	N/A	N/A	Y	6	7	Not available	Not available	N/A	N/A	Not available	
Crop yield – rice	Tropical regions	%	1986–2005	Not available	0,6	RCP8.5, ISIMIP	N/A	N/A	Y	6	6	Not available	Not available	N/A	N/A	Not available	
Crop yield – wheat	Global	%	1986–2005	Not available	0,6	RCP8.5, ISIMIP	N/A	N/A	Y	2	0	Not available	Not available	N/A	N/A	Not available	
Crop yield – maize	Global	%	1986–2005	Not available	0,6	RCP8.5, ISIMIP	N/A	N/A	Y	-1,5	-6	Not available	Not available	N/A	N/A	Not available	
Crop yield – soy	Global	%	1986–2005	Not available	0,6	RCP8.5, ISIMIP	N/A	N/A	Y	7	1	Not available	Not available	N/A	N/A	Not available	
Crop yield – rice	Global	%	1986–2005	Not available	0,6	RCP8.5, ISIMIP	N/A	N/A	Y	7	7	Not available	Not available	N/A	N/A	Not available	
Crop yield	France	%	1980–2009	Not available	Mean seasonal T (°C) 1980–2009 (17°C)	Temperature (-3, 0, 3, 6, 9°C) and CO_2 concentration (360, 450, 540, 630, 720 ppm) factor levels	N/A	N/A	N	-6,75	-9	Not available	Not available	N/A	N/A	Not available	Bassu et al. (2015)
Crop yield	USA	%	1980–2009	Not available	Mean seasonal T (°C) 1980–2009 (21°C)	Temperature (-3, 0, 3, 6, 9°C) and CO_2 concentration (360, 450, 540, 630, 720 ppm) factor levels	N/A	N/A	N	-9	-12	Not available	Not available	N/A	N/A	Not available	
Crop yield	Brazil	%	1980–2009	Not available	Mean seasonal T (°C) 1980–2009 (25°C)	Temperature (-3, 0, 3, 6, 9°C) and CO_2 concentration (360, 450, 540, 630, 720 ppm) factor levels	N/A	N/A	N	-11,7	-13,6	Not available	Not available	N/A	N/A	Not available	
Crop yield	Tanzania	%	1980–2009	Not available	Mean seasonal T (°C) 1980–2009 (27°C)	Temperature (-3, 0, 3, 6, 9°C) and CO_2 concentration (360, 450, 540, 630, 720 ppm) factor levels	N/A	N/A	N	-10,6	-14,2	Not available	Not available	N/A	N/A	Not available	
Crop yield – maize	Drylands	%	1971–1981	SSP2	Not available	RCP8.5, 2006–2100	N/A	N/A	Not available	-0,9	~ -1.1	Not available	Not available	N/A	N/A	Not available	Huang et al. (2017)
Crop yield – maize	Humid lands	%	1971–1981	SSP2	Not available	RCP8.5, 2006–2100	N/A	N/A	Not available	3,2	~ 3.3	Not available	Not available	N/A	N/A	Not available	
Crop yield – maize	Global	%	1971–1981	SSP2	Not available	RCP8.5, 2006–2100	N/A	N/A	Not available	2,6	~ 2.8	Not available	Not available	N/A	N/A	Not available	
Crop yield – wheat	Global	%	1981–2010	Not available	Not available	Temperature (12, 14°C) factor levels	N/A	N/A	N	-9	-12	Not available	Not available	N/A	N/A	Not available	Asseng et al. (2015)
Crop yield – maize	Brazil	%	1982–2012	Not available	Precipitation: -30 to -20%	Temperature (10.5, 11, 11.5, 12, 12.5, 13°C) and precipitation (-30, -20, -10, 0, 110, 120, 130%) factor levels	N/A	N/A	N	-10/ -15	~ -15/ -20	Not available	Not available	N/A	N/A	Not available	Lana et al. (2017)
Crop yield – maize	Brazil	%	1982–2012	Not available	Precipitation: -20 to -10%	Temperature (10.5, 11, 11.5, 12, 12.5, 13°C) and precipitation (-30, -20, -10, 0, 110, 120, 130%) factor levels	N/A	N/A	N	-5/ -10	~ -10/ -15	Not available	Not available	N/A	N/A	Not available	
Crop yield – maize	Brazil	%	1982–2012	Not available	Precipitation: -10 to 0%	Temperature (10.5, 11, 11.5, 12, 12.5, 13°C) and precipitation (-30, -20, -10, 0, 110, 120, 130%) factor levels	N/A	N/A	N	0/ -5	~ -5/ -10	Not available	Not available	N/A	N/A	Not available	
Crop yield – maize	Brazil	%	1982–2012	Not available	Precipitation: 0 to 130%	Temperature (10.5, 11, 11.5, 12, 12.5, 13°C) and precipitation (-30, -20, -10, 0, 110, 120, 130%) factor levels	N/A	N/A	N	0/ 15	0/ -5	Not available	Not available	N/A	N/A	Not available	
Crop yield – wheat	Global	%	1980–2012	SSP1,2,5	Not available	RCP2.6 (11.8°C), 4.5 (12.7°C), 6.0 (13.2°C), 8.5 (14.5°C), 2000–2100	N/A	N/A	Not available	38	39	Not available	Not available	N/A	N/A	Not available	Iizumi et al. (2017)
Crop yield – maize	Global	%	1980–2012	SSP1,2,5	Not available	RCP2.6 (11.8°C), 4.5 (12.7°C), 6.0 (13.2°C), 8.5 (14.5°C), 2000–2100	N/A	N/A	Not available	28	25	Not available	Not available	N/A	N/A	Not available	
Crop yield – soy	Global	%	1980–2012	SSP1,2,5	Not available	RCP2.6 (11.8°C), 4.5 (12.7°C), 6.0 (13.2°C), 8.5 (14.5°C), 2000–2100	N/A	N/A	Not available	35	47	Not available	Not available	N/A	N/A	Not available	
Crop yield – rice	Global	%	1980–2012	SSP1,2,5	Not available	RCP2.6 (11.8°C), 4.5 (12.7°C), 6.0 (13.2°C), 8.5 (14.5°C), 2000–2100	N/A	N/A	Not available	36	41	Not available	Not available	N/A	N/A	Not available	
Crop yield – onions	Netherlands	Fraction	1992–2008	Not available	Not available	Temperature (11 and 12) factor levels, 2042–2058	N/A	N/A	Not available	-0,235	~ -0.57	Not available	Not available	N/A	N/A	Chemical protection, UV-light protection	Mandryk et al. (2017)
Crop yield – potatoes	Netherlands	Fraction	1992–2008	Not available	Not available	Temperature (11 and 12) factor levels, 2042–2058	N/A	N/A	Not available	-0,08	~ -0.82	Not available	Not available	N/A	N/A	Plant in wider range, drip irrigation, crop cover, air conditioning, chemical protection, UV-light protection	
Crop yield – maize	Southeast United States	%	1950–1999	Not available	0,5	RCP4.5 (2006–2055), RCP8.5 (2006–2055)	N/A	N/A	Not available	-6,9	-9,2	-4.6 (1.1°C)	1.5°C	N/A	N/A	Not available	Cammarano and Tian (2018)
Crop yield – wheat	Southeast United States	%	1950–1999	Not available	0,5	RCP4.5 (2006–2055), RCP8.5 (2006–2055)	N/A	N/A	Not available	-3,7	-7,6	-5.8 (1.1°C)	1.5°C	N/A	N/A	Not available	
Crop yield – maize	Southeast United States	%	1979–2008	Not available	Not available	SRES A2 (2041–2070)	N/A	N/A	Not available	Not available	156/ 185	-3,-15 (12.5°C)	Not available	N/A	-3,6	Biochar	Lychuk et al. (2017)
Crop yield – maize	Southeast United States	%	1979–2008	Not available	Not available	SRES A2 (2041–2070)	N/A	N/A	Not available	Not available	156/ 185	-3,-15 (12.5°C)	Not available	N/A	10	Irrigation	
Crop yield – soy	Southeast United States	%	1979–2008	Not available	Not available	SRES A2 (2041–2070)	N/A	N/A	Not available	Not available	-1/ -15	Not available	Not available	N/A	N/A	Biochar	
Crop yield – soy	Southeast United States	%	1979–2008	Not available	Not available	SRES A2 (2041–2070)	N/A	N/A	Not available	Not available	-1/ -15	Not available	Not available	N/A	N/A	Irrigation	
Crop – C3 aggregated (soybean, alfalfa, winter wheat)	Southeast United States	%	1979–2008	Not available	Not available	SRES A2 (2041–2070)	N/A	N/A	Not available	Not available	-10/ -22	Not available	Not available	N/A	-3, -7	Biochar	
Crop – C3 aggregated (soybean, alfalfa, winter wheat)	Southeast United States	%	1979–2008	Not available	Not available	SRES A2 (2041–2070)	N/A	N/A	Not available	Not available	-10/ -22	Not available	Not available	N/A	0	Irrigation	
Crop – C4 aggregated (corn, sorghum, pearl millet)	Southeast United States	%	1979–2008	Not available	Not available	SRES A2 (2041–2070)	N/A	N/A	Not available	Not available	-6/ -10	Not available	Not available	N/A	-3, -5	Biochar	
Crop – C4 aggregated (corn, sorghum, pearl millet)	Southeast United States	%	1979–2008	Not available	Not available	SRES A2 (2041–2070)	N/A	N/A	Not available	Not available	-6/ -10	Not available	Not available	N/A	N/A	Irrigation	
Crop shift – olive tree	Mediterranean	%	1950–1999	Not available	Not available	SRES A1B (2031–2060)	N/A	N/A	Not available	Not available	14	Not available	Not available	N/A	N/A	Not available	Moriondo et al. (2013)
Crop shift – olive tree	Mediterranean	%	1950–1999	Not available	Not available	SRES A1B (2061–2090)	N/A	N/A	Not available	Not available	18	Not available	Not available	N/A	N/A	Not available	
Loss of area in global biodiversity	Global	%	1500–2005	Not available	Not available	RCP4.5 (model ensemble)	N/A	N/A	Not available	Not available	~ -25	Not available	Not available	N/A	N/A	Not available	Jantz et al. (2015)
Wildfire – dead fuel moisture	Western USA	%	1950–2005	Not available	Not available	RCP8.5 (CMIP5 models)	N/A	N/A	Not available	0/ -5	-10/ -15	Not available	Not available	N/A	N/A	Not available	Gergel et al. (2017)
Wildfire – increase in number of days per fire season with conditions conducive to fire growth	Canada (East)	%	1971–2000	Not available	Not available	RCP8.5 (model ensemble)	N/A	N/A	Not available	112/ 145	Not available	Not available	Not available	N/A	N/A	Not available	Wotton et al. (2017)
Wildfire – increase in number of days per fire season with conditions conducive to fire growth	Canada (West)	%	1971–2000	Not available	Not available	RCP8.5 (model ensemble)	N/A	N/A	Not available	12/ 115	Not available	Not available	Not available	N/A	N/A	Not available	
Wildfire – annual probability of fire	USA (Alaska)	Ratio	1950–2009	Not available	Not available	RCP6.0 (model ensemble)	N/A	N/A	N	~ 1125	~ 1144	Not available	Not available	N/A	N/A	Not available	Young et al. (2016)
Wildfire – fire weather index	Mediterranean	%	1961–1990	Not available	Not available	SRES B2	N/A	N/A	N	Not available	19,8	Not available	Not available	N/A	N/A	Not available	Moriondo et al. (2006)
Wildfire – fire weather index	France	%	1961–1990	Not available	Not available	SRES B2	N/A	N/A	N	Not available	21	Not available	Not available	N/A	N/A	Not available	
Wildfire – fire weather index	Portugal	%	1961–1990	Not available	Not available	SRES B2	N/A	N/A	N	Not available	11	Not available	Not available	N/A	N/A	Not available	
Wildfire – fire weather index	Spain	%	1961–1990	Not available	Not available	SRES B2	N/A	N/A	N	Not available	18	Not available	Not available	N/A	N/A	Not available	
Wildfire – increased annual area burned	Canada	%	1961–1990	Not available	Not available	SRES A2 (2041–2070)	N/A	N/A	N	Not available	~ 1157	Not available	Not available	N/A	N/A	Not available	Boulanger et al. (2014)
Wildfire – fire occurrence	Canada	%	1961–1990	Not available	Not available	SRES A2 (2041–2070)	N/A	N/A	N	Not available	~ 1182	Not available	Not available	N/A	N/A	Not available	
Wildfire – fire occurrence density	Northeast China	%	1965–2009	Not available	Not available	SRES B1 (2081–2100 – 550 CO2)	N/A	N/A	N	Not available	~ 130	Not available	Not available	N/A	N/A	Not available	Liu et al. (2012)

3.SM.3.1 Supplementary information to Section 3.4.2

3.SM.3.1.1 Freshwater Resources (Quantity and Quality)

In this section, Arnell and Lloyd-Hughes (2014) assess water scarcity based on the simple indicator of average annual runoff per capita called “water resources stress”, and define that watershed as exposed to such stress if watershed average annual runoff is less than 1000 m^3 cap^{-1} yr^{-1}. The same condition is applied to identify chronic supply-side water scarcity within a given spatial unit in the study by Gerten et al. (2013) that refers to Falkenmark and Widstrand (1992), whose index is called Withdrawal to Water Resouces (WWR) ratio. With WWR, Hanasaki et al. (2013) indicate a chronic water shortage if water withdrawal exceeds 40% of the water resources in a region. A quantitative metric of freshwater stress is defined in terms of future projections of population and aridity, where freshwater stress index is calculated as a population change index multiplied by an aridity change index (Karnauskas et al. 2018). Schewe et al. (2014) apply two water scarcity classes: annual blue water availability below 500 m^3 per capita, namely absolute water scarcity, and below 1000 m^3 per capita that is referred to as chronic water scarcity.

3.SM.3.1.1.2 Extreme hydrological events (floods and droughts)

Alfieri et al. (2017) assume and estimate potential population affected for any positive flood depth by overlaying population density and flood hazard maps. Arnell et al. (2018) define exposure to river flooding by the average annual number of people living in major floodplains affected by floods greater than the baseline 30-year flood. Arnell and Lloyd-Hughes (2014) use an indicator in which the number of flood-prone people living in areas where the frequency of the baseline (1960–1990) 20-year flood either doubles (occurs more frequently than one in 10 years) or halves (occurs more rarely than one in 40 years), although these thresholds are arbitrary. Kinoshita et al. (2018) estimate fatalities due to flooding by multiplying exposure (population prone to flooding, defined in the study as gridded population) by vulnerability, and numerically calculate flood hazard as the extent and depth of flood, while estimating potential affected exposure by superimposing the modelled hazard on the population data. In the study, Kinoshita et al. (2018) consider exposure as gridded population whereas historical vulnerability is defined as a ratio of the observed flood consequences and potentially affected exposure at a national level in equations.

In the study by Arnell et al. (2018), drought is presented by the standardized runoff index called SRI, which is calculated from monthly runoff simulated with the MacPDM.09 global hydrological model described in Gosling and Arnell (2011) . The occurrence of a drought is defined as when the SRI is less than –1.5; and as for drought frequency for a given time series of monthly runoff, it is determined by counting the number of months with SRI less than –1.5. Liu et al. (2018) quantify the changes in drought characteristics, adopting Palmer Drought Severity Index (PDSI) that describes the balance between water supply (precipitation) and atmospheric evaporative demand required by the precipitation estimated under climatically appropriate for existing conditions, which is described by Zhang et al. (2016), Wells et al. (2004) and Zhang et al. (2016). Liu et al.’s (2018) study suggests that PDSI is commonly applicable as an indication of meteorological drought and a hydrological drought for a multi-year time series. Liu et al. (2018) assume a severe drought event when the monthly PDSI is < –3, and identify a severe drought year if a severe drought occurs for at least a month in a year, while multiplying population by annual frequency of severe drought to quantify the population affected by severe drought per grid-cell.

3.SM.3.1.1.3 Groundwater

Portmann et al. (2013) assess groundwater with groundwater recharge (GWR), which is assumed to be curbed by a maximum groundwater recharge rate per day. GWR occurs if daily precipitation exceeds 12.5 mm d^{-1} in case of medium to coarse grained soils (Portmann et al., 2013). In some regions, groundwater is often intensively used to supplement the excess demand, often leading to groundwater depletion; besides climate change, this adds further pressure on water resources and exaggerates human water demands due to increasing temperatures over agricultural lands (Wada et al. 2017).

3.SM.3.1.1.4 Water quality

Water temperature directly affects water quality, and most chemical and bacteriological processes are accelerated according to the temperature rise (Watts et al. 2015). Hosseini et al. (2017) summarize that the main impact on water quality due to climate change is attributed to changing air temperature and hydrology; and particularly ambient air temperature directly affects water temperature, that is projected to increase due to global warming. Watts et al. (2015) describe water quality as affected by many factors, including water temperature, hydrological regime, nutrient status and mobilization of toxic substances, as well as point source, diffuse discharge and acidification potential, referring to Whitehead et al. (2009). Patiño et al. (2014) reveal that changes in water quality can influence the spread of harmful aquatic species, referring to the fact that toxic algae are lethal to some aquatic animals and has posed considerable ecological and economic impacts on freshwater and marine ecosystems. Bonte and Zwolsman (2010) state that salinization due to rising sea levels as well as poor land management and excessive groundwater extractions is putting a strain on freshwater resources availability around the world. Attributing changes in river water quality to specific factors is difficult since multiple factors act at different temporal and spatial scales, and it often requires examining a long-term series of continuous data (Aguilera et al. 2015).

References

Aguilera, R., R. Marcé, and S. Sabater, 2015: Detection and attribution of global change effects on river nutrient dynamics in a large Mediterranean basin. Biogeosciences, 12, 4085–4098, doi:10.5194/bg-12-4085-2015.

Alfieri, L., B. Bisselink, F. Dottori, G. Naumann, A. de Roo, P. Salamon, K. Wyser, and L. Feyen, 2017: Global projections of river flood risk in a warmer world. Earth's Futur., 5, 171–182, doi:10.1002/2016EF000485. http://doi.wiley.com/10.1002/2016EF000485 (Accessed March 26, 2017).

Arnell, N. W., and B. Lloyd-Hughes, 2014: The global-scale impacts of climate change on water resources and flooding under new climate and socio-economic scenarios. Clim. Change, 122, 127–140, doi:10.1007/s10584-013-0948-4. http://link.springer.com/10.1007/s10584-013-0948-4 (Accessed April 5, 2017).

Arnell, N. W., J. A. Lowe, B. Lloyd-Hughes, and T. J. Osborn, 2018: The impacts avoided with a 1.5°C climate target: a global and regional assessment. Clim. Change, 147, 61–76, doi:10.1007/s10584-017-2115-9. https://doi.org/10.1007/s10584-017-2115-9.

Bonte, M., and J. J. G. Zwolsman, 2010: Climate change induced salinisation of artificial lakes in the Netherlands and consequences for drinking water production. Water Res., 44, 4411–4424, doi:10.1016/j.watres.2010.06.004. http://www.sciencedirect.com/science/article/pii/S0043135410003799 (Accessed April 7, 2017).

Falkenmark, M., and C. Widstrand, 1992: Population and water resources: a delicate balance. Popul. Bull., 47, 1–36. http://www.ncbi.nlm.nih.gov/pubmed/12344702 (Accessed September 15, 2018).

Gerten, D., and Coauthors, 2013: Asynchronous exposure to global warming: freshwater resources and terrestrial ecosystems. Environ. Res. Lett., 8, 034032, doi:10.1088/1748-9326/8/3/034032. http://stacks.iop.org/1748-9326/8/i=3/a=034032?key=crossref.8f60cb76b3324084849e22201ba879bf (Accessed April 7, 2017).

Gosling, S. N., and N. W. Arnell, 2011: Simulating current global river runoff with a global hydrological model: model revisions, validation, and sensitivity analysis. Hydrol. Process., 25, 1129–1145, doi:10.1002/hyp.7727. https://onlinelibrary.wiley.com/doi/abs/10.1002/hyp.7727.

Hanasaki, N., and Coauthors, 2013: A global water scarcity assessment under Shared Socio-economic Pathways - Part 2: Water availability and scarcity. Hydrol. Earth Syst. Sci., 17, 2393–2413, doi:10.5194/hess-17-2393-2013. http://www.hydrol-earth-syst-sci.net/17/2393/2013/ (Accessed April 7, 2017).

Hosseini, N., J. Johnston, and K.-E. Lindenschmidt, 2017: Impacts of Climate Change on the Water Quality of a Regulated Prairie River. Water, 9, 199, doi:10.3390/w9030199. http://www.mdpi.com/2073-4441/9/3/199 (Accessed July 15, 2017).

Karnauskas, K. B., C.-F. Schleussner, J. P. Donnelly, K. J. Anchukaitis, K. Archukaitis, and K. J. Anchukaitis, 2018: Freshwater Stress on Small Island Developing States: Population Projections and Aridity Changes at 1.5°C and 2°C. Reg. Environ. Chang., 1–10, doi:10.1007/s10113-018-1331-9.

Kinoshita, Y., M. Tanoue, S. Watanabe, and Y. Hirabayashi, 2018: Quantifying the effect of autonomous adaptation to global river flood projections: Application to future flood risk assessments. Environ. Res. Lett., 13, 014006, doi:10.1088/1748-9326/aa9401. http://iopscience.iop.org/article/10.1088/1748-9326/aa9401.

Liu, W., F. Sun, W. H. Lim, J. Zhang, H. Wang, H. Shiogama, and Y. Zhang, 2018: Global drought and severe drought-affected populations in 1.5 and 2 °C warmer worlds. Earth Syst. Dyn., 9, 267–283, doi:10.5194/esd-9-267-2018.

Patiño, R., D. Dawson, and M. M. Vanlandeghem, 2014: Retrospective Analysis of Associations between Water Quality and Toxic Blooms of Golden Alga (Prymnesium parvum) in Texas Reservoirs: Implications for Understanding Dispersal Mechanisms and Impacts of Climate Change. Harmful Algae, 33, 1–11, doi:10.1016/j.hal.2013.12.006.

Portmann, F. T., P. Döll, S. Eisner, and M. Flörke, 2013: Impact of climate change on renewable groundwater resources: assessing the benefits of avoided greenhouse gas emissions using selected CMIP5 climate projections. Environ. Res. Lett., 8, 024023, doi:10.1088/1748-9326/8/2/024023. http://stacks.iop.org/1748-9326/8/i=2/a=024023?key=crossref.b0a543a479eeff6c76b319c99956a993 (Accessed April 7, 2017).

Schewe, J., and Coauthors, 2014: Multimodel assessment of water scarcity under climate change. Proc. Natl. Acad. Sci., 111, 3245–3250, doi:10.1073/pnas.1222460110. http://www.pnas.org/content/111/9/3245.full.pdf (Accessed April 6, 2017).

Wada, Y., and Coauthors, 2017: Human–water interface in hydrological modelling: current status and future directions. Earth Syst. Sci, 215194, 4169–4193, doi:10.5194/hess-21-4169-2017.

Watts, G., and Coauthors, 2015: Climate change and water in the UK – past changes and future prospects. Prog. Phys. Geogr., 39, 6–28, doi:10.1177/0309133314542957.

Wells, N., S. Goddard, and M. J. Hayes, 2004: A Self-Calibrating Palmer Drought Severity Index. J. Clim., 17, 2335–2351, doi:10.1175/1520-0442(2004)017<2335:ASPDSI>2.0.CO;2. https://doi.org/10.1175/1520-0442(2004)017%3C2335:ASPDSI%3E2.0.CO.

Whitehead, P. G., R. L. Wilby, R. W. Battarbee, M. Kernan, and A. J. Wade, 2009: A review of the potential impacts of climate change on surface water quality. Hydrol. Sci. J., 54, 101–123, doi:10.1623/hysj.54.1.101. https://doi.org/10.1623/hysj.54.1.101.

Zhang, F., J. Tong, B. Su, J. Huang, and X. Zhu, 2016: Simulation and projection of climate change in the south Asian River basin by CMIP5 multi-model ensembles. J. Trop. Meteorol., 32, 734–742.

3.SM.3.2 Supplementary Information to Section 3.4.4

Update of Expert Assessment by Gattuso et al. (2015)

J.-P. Gattuso, A. Magnan, R. Billé, W. W. L. Cheung, E. L. Howes, F. Joos, D. Allemand, L. Bopp, S. R. Cooley, C. M. Eakin, O. Hoegh-Guldberg, R. P. Kelly, H.-O. Pörtner, A. D. Rogers, J. M. Baxter, D. Laffoley, D. Osborn, A. Rankovic, J. Rochette, U. R. Sumaila, S. Treyer, C. Turley

Published 3 July 2015, Science 349, aac4722 (2015)

DOI: 10.1126/science.aac4722

Risk assessment update: November 18, 2017 (by lead authors and contributing authors of Chapter 3, other chapters of the Special Report on Global Warming of 1.5˚C, and relevant external experts).

This Section 3.SM.3.2 includes:

Supplementary Text

Table 3.SM.6

Full Reference List

Background Information and Rationale of Expert Judgement on the Risk of Impact Due to CO_2 Levels by 2100

This supplementary material provides the background information and rationale for the construction of the burning embers diagrams used in Figure 3.18 to represent the increase in risk as well as the limits to adaptation from rising CO_2 levels for keystone marine and coastal organisms and ecosystem services.

This is the expert judgement by the group on the overall risk – balancing negative, neutral and positive impacts across species and regions using current literature.

Table 3.SM.6: The temperature at which transitions in the level of risk occur in response to climate change, from expert judgement by Gattuso et al. (2015) and updated in March 2018 for the following three years of scientific literature. [White: No detectable risks from climate change; Yellow: Moderate levels of risk; Red: High level of risk; and Purple: Very high level of risk]
Note: These data were used to build the burning embers for representative marine organisms, ecosystems and sectors. Note: Red numbers are where the update has resulted in slightly different conclusions to those of Gattuso et al. (2015).

		Average Global Sea Surface Temperature (SST, ˚C)		
Component	**Colour transition**		**2015**	**2018**
Seagrasses (mid-latitude)	White to Yellow	Begin	0.5	0.5
		End	0.8	0.8
	Yellow to Red	Begin	1.5	1.5
		End	1.8	1.8

		Average Global Sea Surface Temperature (SST, ˚C)		
Component	**Colour transition**		**2015**	**2018**
	Red to Purple	Begin	2.2	2.2
		End	3	3
Mangroves	White to Yellow	Begin	1.8	1.3
		End	3	1.5 (2.5)*
	Yellow to Red	Begin	3	2.5
		End	3.2	2.7
	Red to Purple	Begin	N/A	NA
		End	N/A	NA
Warm-water corals	White to Yellow	Begin	0.3	0.2
		End	0.4	0.4
	Yellow to Red	Begin	0.5	0.4
		End	0.8	0.6
	Red to Purple	Begin	0.8	0.6
		End	1.5	1.2
Pteropods (high latitude)	White to Yellow	Begin	0.7	0.7
		End	0.8	0.8
	Yellow to Red	Begin	0.8	0.8
		End	1.5	1.5
	Red to Purple	Begin	1.5	1.5
		End	2	2
Bivalves (mid-latitude)	White to Yellow	Begin	0.4	0.4
		End	0.6	0.6
	Yellow to Red	Begin	0.9	0.9
		End	1.1	1.1
	Red to Purple	Begin	1.3	1.3
		End	1.5	1.5
Krill (high latitude)	White to Yellow	Begin	0.7	0.7
		End	0.9	0.9
	Yellow to Red	Begin	1	1
		End	1.6	1.6
	Red to Purple	Begin	1.8	1.8
		End	3.2	3.2
Fin fish	White to Yellow	Begin	0.5	0.5

		Average Global Sea Surface Temperature (SST, ˚C)		
Component	**Colour transition**		**2015**	**2018**
		End	0.7	0.7
	Yellow to Red	Begin	1.1	1.1
		End	1.3	1.3
	Red to Purple	Begin	1.4	1.4
		End	1.6	1.6
Open-ocean carbon uptake	White to Yellow	Begin	1	1
		End	1.5	1.5
	Yellow to Red	Begin	2	2
		End	3.2	3.2
	Red to Purple	Begin	N/A	N/A
		End	N/A	N/A
Coastal protection	White to Yellow	Begin	0.5	0.5
		End	0.8	0.8
	Yellow to Red	Begin	1.5	1.5
		End	1.8	1.8
	Red to Purple	Begin	2.2	2.2
		End	3.2	3.2
Recreational services from coral reefs	White to Yellow	Begin	0.6	0.6
		End	0.8	0.8
	Yellow to Red	Begin	1	1
		End	1.5	1.5
	Red to Purple	Begin	2	2
		End	3.2	3.2
Bivalve fisheries and aquaculture (mid-latitude)	White to Yellow	Begin	1.1	1.1
		End	1.3	1.3
	Yellow to Red	Begin	1.7	1.7
		End	1.9	1.9
	Red to Purple	Begin	2.8	2.8
		End	3.2	3.2
Fin-fish (small scale) fisheries (low latitude)	White to Yellow	Begin	0.7	0.5
		End	0.9	0.7
	Yellow to Red	Begin	1	0.9
		End	1.2	1.1

		Average Global Sea Surface Temperature (SST, ˚C)		
Component	**Colour transition**		**2015**	**2018**
	Red to Purple	Begin	2	2
		End	2.5	2.5
Fin-fish fisheries (mid- and high latitude)	White to Yellow	Begin	0.7	0.7
		End	0.9	0.9
	Yellow to Red	Begin	2.2	2.2
		End	3.2	3.2
	Red to Purple	Begin	N/A	N/A
		End	N/A	N/A

Note: *Mangrove value differs from table value but is consistent with main text and general expert consensus.

Expert assessment: Original assessment by Gattuso et al. (2015) using the IPCC Fifth Assessment Report (AR5) and literature published up to 2014. This current assessment updated the original assessment using literature from 2015 to early 2018. References for the current and past assessments are listed at the end of this document. This is online supplementary material for the special report on the implications of 1.5ºC warming.

3.SM.3.2.1 Seagrasses (Mid-Latitude)

Update: Recent literature supports the consensus reached by Gattuso et al. (2015), with increasing ocean temperatures being a major threat and projections of the potential loss of key species such as *Posidonia oceanica* in the Mediterranean by mid-century (Jordà et al., 2012). Recent work has shown that increasing temperatures is a major threat to the shoot density (Guerrero-Meseguer et al., 2017) and quality of the seagrass *Zostera marina* (Repolho et al., 2017). Other studies on related systems reveal subchronic changes to the quality of seagrass shoots and leaves (Unsworth et al., 2014) and have speculated on the impact that these changes might have on coastal food webs (York et al. 2016). Several studies have speculated on the impact of rising seas, storms and flooding on seagrass productivity (Ondiviela et al., 2014; Rasheed et al., 2014; Pergent et al., 2015; Telesca et al., 2015). The consensus of the literature for the last two years, examined since AR5, suggests that the current risk levels for seagrasses proposed by Gattuso et al. (2015) are appropriate.

Therefore, seagrasses are already showing responses to climate change; hence the expert consensus that the transition from undetectable to moderate risk occurs between 0.5°C and 0.8°C. Given the clear sensitivity of seagrass communities to rising sea temperatures, and other aspects of climate change such as sea level rise, storms and flooding, these risks transition from moderate to high from 1.5°C to 1.8°C, and from high to very high risk over the interval from 2.2°C to 3°C.

Expert assessment by Gattuso et al. (2015; SOM):

Seagrasses, important habitats in coastal waters around the world, will be affected by climate change through a number of routes, including: direct effects of temperature on growth rates (Nejrup and Pedersen, 2008; Höffle et al., 2011), occurrence of disease (Burge et al., 2013), mortality and physiology, changes in light levels arising from sea level changes, changes in exposure to wave action (Short and Neckles, 1999), sometimes mediated through effects on adjacent ecosystems (Saunders et al., 2014), and also by changes in the frequency and magnitude of extreme weather events. There will be changes in the distribution of seagrass communities locally and regionally. Here we take the example of temperate seagrasses, including *Posidonia oceanica* from the Mediterranean and *Zostera* spp from the USA, Europe and Australia, because the information on the effects of ocean warming and acidification for these species from several field studies is robust. Results indicate that temperate seagrass meadows have already been negatively impacted by rising sea surface temperatures (SSTs) (Marbà and Duarte, 2010). Models based on observations of natural populations indicate that at temperature increases of 1.5°C – 3°C mortality of shoots of seagrasses will be such that populations will be unsustainable and meadows will decline to the point where their ecological functions as a habitat will cease (reduction to 10% of present density of a healthy meadow; Marbà and Duarte 2010; Jordà et al. 2012; Carr et al. 2012; York et al. 2013).

The confidence level is *very high* under Representative Concentration Pathway (RCP)2.6 because of strong agreement in the literature. Confidence declines to *high* under RCP8.5 due to some uncertainty surrounding regional differences. For example, it has been suggested that the balance of effects on seagrass populations in the northeast Atlantic could tip to positive due to the hypothetical opening of ecological niches with the decline of more sensitive species, and potential reduction of carbon limitation by elevated CO_2 which may help to ameliorate negative effects of other environmental drivers, such as warming, known to impact seagrass growth and survival (Brodie et al., 2014).

3.SM.3.2.2 Mangroves

Update: Recent literature is consistent with previous conclusions regarding the complex changes facing mangroves, together with increasing concern regarding the interaction between climate change (e.g., elevated air and water temperatures, drought and sea level rise) and local factors (deforestation, damming of catchments and reduced sediment and freshwater) as outlined below (Alongi, 2015; Feller et al., 2017). Decreases in the supply of sediments to deltas and coastal areas is impeding the ability of most mangroves (69% of sites) to keep pace with sea level rise through shoreward migration (Lovelock et al., 2015). At the same time, recent extremes associated with El Niño have also had large-scale impacts (e.g., extreme low sea level events; Duke et al., 2017; Lovelock et al., 2017). Shoreward migration is also challenged by the increasing amounts of coastal infrastructure preventing the relocation of mangroves (Di Nitto et al., 2014; Saunders et al., 2014). In some areas, mangroves are increasing in distribution (Godoy and De Lacerda, 2015). The total losses projected for mangrove loss (10–15%) under a 0.6 m sea level rise continue to be dwarfed by the loss of mangroves to deforestation (1–2% per annum).

However, given the scale of the dieback of mangroves in Australia's Gulf of Carpentaria (in 2015–2016), as well as evidence that similar conditions to those of 2015–2016 (extreme heat and low tides) and the projection of greater El Niño-Southern Oscillation (ENSO) variability, (Widlansky et al., 2015; Risser and Wehner, 2017), the risks from climate change for mangroves were judged to be higher than assessed by AR5, and subsequently by Gattuso et al. (2015), leading to the transitions having greater risk of occurring (Figure 3.18). Formal attribution of recent extreme events on mangroves to climate change, however, is at an early stage (*medium agreement*, *limited data*, *hence low-medium confidence*).

Expert assessment by Gattuso et al. (2015; SOM):

Mangroves are critically important coastal habitats for numerous species. Mangrove responses to increasing atmospheric CO_2 are complex, with some species thriving while others decline or exhibit little or no change (Alongi, 2015). Temperature increase alone is likely to result in faster growth, reproduction, photosynthesis and respiration, and changes in community composition, diversity and an expansion of latitudinal limits up to a certain point (Tittensor et al., 2010). Mangroves have already been observed to retreat with sea level rise (McKee et al., 2012). In many areas, mangroves can adapt to sea level rise by landward migration, but these shifts threaten other coastal habitats, such as salt marshes, which have other important biogeochemical and ecological roles. It is in areas with steep coastal inclines or coastal human infrastructure limiting landward migration that mangroves are most at risk. Climate change may lead to a maximum global loss of 10–15% of mangrove forest for a sea level rise of 0.6 m (high end of IPCC projections in AR4), but must be considered of secondary importance compared with current annual rates of deforestation of 1–2% (Alongi, 2008). A large reservoir of below-ground nutrients, rapid rates of nutrient flux microbial decomposition, complex and highly efficient biotic controls, self-design and redundancy of keystone species, and numerous feedbacks, all contribute to mangrove resilience to various types of disturbance.

Mangrove response is species-specific and interacts with temperature, salinity, nutrient availability and patterns of precipitation. Many of these parameters are also subject to regional and local variation, as well as to human-induced pressures, with changes over the coming decades being difficult to assess. Thus, the confidence level decreases from *high* under RCP2.6 to *low* under RCP8.5.

3.SM.3.2.3 Warm-Water Corals

Update: The exceptionally warm conditions of 2015–2017 drove an unprecedented global mass coral bleaching and mortality event which affected coral reefs in a large number of countries (information still being gathered at time of writing; Normile, 2016). In the case of Australia, 50% of shallow-water reef-building corals across the Great Barrier Reef died in unprecedented back-to-back bleaching events (Hughes et al., 2017). Elevated sea temperatures and record mortalities were recorded from the central to the far northern sectors of the Great Barrier Reef. Similar effects occurred in a range of regions, including the Indian Ocean, the western Pacific, Hawaii and the Caribbean Sea (Normile, 2016). The set of events has increased risk with current conditions being of high risk, and even low levels of future climate change having series implications for coral reefs. There continues to be a *high* to *very high* level of confidence as to where the transitions between risk levels due to climate change are located.

The unprecedented thermal stress along many tropical coastlines over the past three years (2015–2017) has led to extraordinary changes to coral reefs across the planet (as described above). The advent of back-to-back bleaching events, which were projected to occur around mid-century, appear to have already begun to occur as demonstrated by impacts on warm-water corals and hence coral reefs. While corals were already stressed from climate change, and are in decline in many parts of the world, the scale and impact of recent events suggests that risk levels for the transitions between risk categories need to be adjusted to represent the current status of corals and coral reefs. For this reason, expert consultation since 2015 concluded that the transition from undetectable to moderate risk has already occurred (0.2°C to 0.4°C). Similarly, the transition from moderate to high levels of risks for warm-water corals occurred approximately from 0.4°C to 0.6°C. In line with these changes, the transition from high to very high levels of risk are associated with increases in GMST from 0.6°C to 1.2°C above the pre-industrial period.

Expert assessment by Gattuso et al. (2015; SOM):

Warm-water corals form reefs that harbour great biodiversity and protect the coasts of low-lying land masses. There are *very high* levels of confidence that impacts were undetectable up until the early 1980s, when coral reefs in the Caribbean and eastern Pacific exhibited mass coral bleaching, as well as temperature-related disease outbreaks in the Caribbean Sea (Glynn, 1984). Given a conservative lag time of 10 years between the atmospheric concentration of CO_2 and changes in SST, the atmospheric CO_2 level of 325 ppm reached in the early 1970s was sufficient to initiate widespread coral bleaching and decline of coral health worldwide (Veron et al., 2009). During the 1980s, visible impacts of increasing were seen in a widening number of areas, with the first global event in 1997–1998 and the loss of 16% of coral reefs (*high confidence*; C. R. Wilkinson 2000). Further increases in atmospheric carbon dioxide and SST have increased the risk to corals (*high confidence*), with multiple widespread bleaching events, including loss of a large fraction of living corals in the Caribbean in 2005 (Eakin et al., 2010) and a subsequent global bleaching in 2010 (e.g., Moore et al. 2012), and current conditions suggesting the development of a third global event in 2015–2016 (C.M. Eakin, unpublished observation). If CO_2 levels continue to increase, there is a very high risk that coral reefs would be negatively affected by doubled pre-industrial CO_2 through impacts of both warming-induced bleaching and ocean acidification (high confidence), supported by a wide array of modelling (e.g., Hoegh-Guldberg et al. 2014, Logan et al. 2014, Hoegh-Guldberg 1999, Donner et al. 2005, van Hooidonk et al. 2014), experimental (e.g., Dove et al. 2013) and field studies (Silverman et al. 2014, De'ath et al. 2012). This leads to a *very high* level of confidence under RCP2.6 and a *high* level of confidence under RCP8.5.

3.SM.3.2.4 Pteropods (High Latitude)

Update: Literature from the last two years is largely consistent with the expert assessment by Gattuso et al. (2015). There is increasing evidence of declining aragonite saturation in the open ocean with the detection of impacts that are most pronounced closest to the surface, and with the severe biological impacts occurring within inshore regions. In this regard, pteropod shell dissolution has increased by 19–26% in both nearshore and offshore waters since the pre-industrial period (Feely et al., 2016). Impacts of ocean acidification are also cumulative with other stresses, such as elevated sea temperature and hypoxia (Bednaršek et al., 2016). These changes are consistent with observations of large portions of the shelf waters associated with the Washington–Oregon–California coast being strongly corrosive, with 53% of onshore and 24% of offshore pteropod individuals showing severe damage from dissolution (Bednaršek et al., 2014). Several researchers propose that the pteropod condition be used as a biological indicator, which they argue will become increasingly important as society attempts to understand the characteristics and rate of change in ocean acidification impacts on marine organisms and ecosystems (Bednaršek et al., 2017; Manno et al., 2017). The last two years of research has increased confidence in our understanding of the impact of ocean acidification on pteropods under field conditions. The question of the genetic adaptation of pteropods to increasing ocean acidification remains unresolved, although the observation of increasing damage to pteropods from field measurements argues against this being a significant factor in the future.

As described here and by Gattuso et al. (2015), multiple lines of evidence conclude that pteropods are being impacted by climate change and ocean acidification, especially in polar regions. Therefore, the transition from undetectable to moderate levels of stress has been judged to occur between 0.7°C and 0.8°C. The transition from moderate to high levels of risk of impact on these important organisms was judged to occur from 0.8°C to 1.5°C, with the transition from high to very high occurring from 1.5°C to 2°C.

Expert assessment by Gattuso et al. (2015; SOM):

Pteropods are key links in ocean food webs between microscopic and larger organisms, including fish, birds and whales. Ocean acidification at levels anticipated under RCP8.5 leads to a decrease in pteropod shell production (Comeau et al., 2009, 2010; Lischka et al., 2011), an increase in shell degradation (Comeau et al., 2012; Lischka and Riebesell, 2012), a decrease in swimming activity when ocean acidification is combined with freshening (Mannoa et al., 2012), and an increase in mortality that is enhanced at temperature changes smaller than those projected for RCP8.5 (Lischka et al., 2011; Lischka and Riebesell, 2012). Shell dissolution has already been observed in high latitude populations (Bednaršek et al., 2012). Aragonite saturation (Ωa) levels below 1.4 results in shell dissolution, with severe shell dissolution between 0.8 and 1 (Bednaršek and Ohman, 2015). Despite high agreement amongst published findings, uncertainty remains surrounding the potential to adapt to environmental drivers because long-term laboratory experiments with pteropods are notoriously difficult. Hence the confidence level is *medium* under RCP2.6. However, confidence increases to *very high* under RCP8.5 because it is almost certain that genetic adaptation to such large and rapid changes in pH and temperature will not be possible.

3.SM.3.2.5 Bivalves (Mid-Latitude)

Update: Literature has rapidly expanded since 2015, with a large number of studies showing impacts of ocean warming and acidification on a wide range of life history stages of bivalve molluscs (e.g., Asplund et al., 2014; Castillo et al., 2017; Lemasson et al., 2017; Mackenzie et al., 2014; Ong et al., 2017; Rodrigues et al., 2015; Shi et al., 2016; Velez et al., 2016; Waldbusser et al., 2014; Wang et al., 2016; Zhao et al., 2017; Zittier et al., 2015). Impacts on adult bivalves include decreased growth, increased respiration and reduced calcification, with larval stages tending to have an increase in developmental abnormalities and elevated mortality after exposure (Wang et al., 2016; Lemasson et al., 2017; Ong et al., 2017; Zhao et al., 2017). Many recent studies have also identified interactions between factors such as increased temperature and ocean acidification, with salinity perturbations as well as decreases in oxygen concentrations (Velez et al., 2016; Lemasson et al., 2017; Parker et al., 2017). Changes in metabolism with increasing ocean acidification has been detected in a number of transcriptome studies, suggesting a complex and wide-ranging response by bivalves to increasing CO_2

and temperature (Li et al., 2016a, 2016b). Observations of reduced immunity may have implications for disease management (Castillo et al., 2017). These changes are likely to impact the ecology of oysters, and may be important when it comes to the maintenance of oyster reefs, which provide important ecological structure for other species. Bivalves, for example, are more susceptible to the impacts of temperature and salinity if they have been exposed to high levels of CO_2, leading to the suggestion that there will be a narrowing of the physiological range and hence distribution of oyster species such as *Saccostrea glomerata* (Parker et al., 2017). The confidence level is adjusted to *high* given the convergence of recent literature. These studies continue to report growing impacts as opposed to a reduction under rapid genetic adaptation by bivalve molluscs. The overall levels of risk are retained – reflecting the moderate risk that already exists, and the potential for transformation into high or very high levels of risk with relatively small amounts of further climate change.

Recent literature reinforces the conclusions of Gattuso et al. (2015) and confirms the transition of risk from low to moderate for the bivalves associated with mid-latitude environments is occurring between 0.4°C and 0.6°C. The transition for these organisms from moderate to high levels of risk occurs at 0.9°C and 1.1°C. Subsequent transition from high to very high was judged to occur between 1.3°C and 1.5°C.

Expert assessment by Gattuso et al. (2015; SOM):

Both cultured and wild bivalves are an important food source worldwide. Temperate bivalve shellfish, such as oysters, clams, mussels and scallops, have already been negatively impacted by ocean acidification. In the northwest United States, Pacific oyster larval mortality has been associated with upwelling of natural CO_2-rich waters acidified by additional fossil fuel CO_2 (*high confidence*; Barton et al. 2012). Ocean acidification acts synergistically with deoxygenation (Gobler et al., 2014) and warming (Kroeker et al., 2013; Mackenzie et al., 2014a) to heighten physiological stress (Wittmann and Pörtner, 2013) on bivalve shellfish (*high confidence*), suggesting that future ocean conditions that include warming, deoxygenation and acidification will be particularly difficult for members of this taxon. Archaeological/geological and modelling studies show range shifts of bivalves in response to prior and projected warming (Raybaud et al., 2015) and acidification (Lam et al., 2014). Model projections also anticipate decreases in mollusc body size under continued harvesting as conditions change farther from the present (Cooley et al., 2015). Impacts are expected to be high to very high when CO_2 concentrations exceed those expected for 2100 in the RCP2.6 and 4.5 levels (*medium confidence*; Lam et al., 2014; Cooley et al., 2015). The confidence level is medium both under RCP2.6 and RCP8.5 primarily due to the possibility of bivalves adapting over generations (Pespeni et al., 2013), or for specific species to outcompete other wild species in future conditions (e.g., Miller et al., 2009).

3.SM.3.2.6 Krill (High Latitude)

Update: Summer sea ice continues to retreat at high rates in polar oceans with both the Artic and Antarctica being among the fastest warming regions on the planet (Notz and Stroeve, 2016; Turner et al., 2017). In Antarctic waters, a decrease in sea ice represents a loss of critical habitat for krill (David et al., 2017). Projected changes of this habitat through increasing temperature and acidification could have major impacts on food, reproduction and development, and hence the abundance of this key organism for Antarctic food webs. Differences appear to be a consequence of regional dynamics in factors such as regional variation in ice, productivity and predation rates, and an array of other factors (Steinberg et al., 2015). Other factors such as interactions with factors such as ocean acidification and the shoaling of the aragonite saturation horizon are likely to play key roles. (Kawaguchi et al., 2013; Piñones and Fedorov, 2016). While factors such as ocean acidification and the loss of sea ice (due to increasing temperatures) are unambiguous in their effects, there continues to be considerable uncertainty around the details of how krill populations are likely to respond to factors such as changing productivity, storms and food web structure.

While there are considerable gaps in our knowledge about the impacts of climate change on krill, there is consensus that direct climate impacts are beginning to be detected at average global SST of around

0.7°C to 0.9ºC. With a *low* level of confidence and hence much uncertainty, expert consensus concludes that transition from moderate to high levels of risk is expected to occur between 1.0°C and 1.6°C. Subsequent transitions from high to very high levels of risk are projected to lie somewhere between 1.8°C and 3.2°C, although levels of confidence are *low* at this time.

Expert assessment by Gattuso et al. (2015; SOM):

Krill (euphausid crustaceans) is a critical link in the food web at higher latitudes, supporting mammals and birds among many other species. Distributional changes and decreases in krill abundance have already been observed associated with temperature increase (Atkinson et al., 2004). The effect of changes in the extent of sea ice is considered to be an indirect effect of temperature. Temperature effects are predicted to be regional (Hill et al., 2013). If the extent of sea ice is maintained, populations in cooler waters may experience positive effects in response to small increases in temperature. In contrast, populations in warmer areas may experience some negative temperature effects by 2100 under RCP2.6. Since all life stages are associated with sea ice, decreases in krill stocks are projected to occur concurrently with the loss of sea ice habitat, potentially outweighing possible positive impacts (Flores et al., 2012). Increases in SST of 1°C–2°C have significant impacts on krill. From Figure 4 in Flores et al. (2012) severe disruptions of the life cycle are expected at a level of 2°C SST rise and 500 µatm pCO_2. Therefore, high impact on populations would be reached approximately at the CO_2 level projected for 2100 by RCP4.5. Conditions in 2100 under the RCP2.6 scenario would be around the upper limit of the high-risk range. Negative effects of ocean acidification on reproduction, larval and early life stages have been observed above 1250 µatm pCO_2, a value that is likely to be reached in parts of the Southern Ocean by 2100 under RCP8.5 (Kawaguchi et al., 2013). Figure 1 in Flores et al. (2012) shows that the area with strongest sea ice decline partly overlaps with areas of high krill density (from the peninsula to the South Orkneys). There is also a significant warming trend in this area which may force populations southwards into less productive regions. Substantial decline in the viability of major krill populations in the Southern Ocean may occur within the next 100 years (Kawaguchi et al., 2013), which could have catastrophic consequences for dependent marine mammals and birds. The genetic homogeneity of krill suggests that rapid adaptation through natural selection of more tolerant genotypes is unlikely (Bortolotto et al., 2011).

3.SM.3.2.7 Fin Fish

Update: Impacts and responses identified in 2015 regarding the relative risk of climate change to fin fish have strengthened. In this regard, there are a growing number of studies indicating that different stages of development may also be made more complex by fish having different stages of the life-cycle in different habitats, which may each be influenced by climate change in different ways and to different extents, as well as evidence of differing sensitivities to change between different stages (Ong et al., 2015, 2017; Esbaugh, 2017). Increasing numbers of fish species have been identified as relocating to higher latitudes, with tropical species being found increasingly in temperate zones (‘tropicalization’, Horta E Costa et al., 2014; Verges et al., 2014; Vergés et al., 2016) and temperate species being found in some polar regions (‘borealization’, Fossheim et al., 2015). Concern has been raised that greater numbers of extinctions will occur in the tropics as species are pushed out of low-latitude areas as conditions become warmer and increasingly unsuitable (Burrows et al., 2014; García Molinos et al., 2015; Poloczanska et al., 2016). Changing conditions in polar regions are particularly risky due to the rapid rates of warming (Notz and Stroeve, 2016; Turner et al., 2017). One of the consequences of this is that an increasing number of fish species are expanding their distributional ranges into the Arctic, being followed by large, migratory fish predators. The borealization of fish communities in the Arctic is leading to a reorganization of species and ecological processes which is not well understood (Fossheim et al., 2015).There is considerable evidence that changes in the distribution of fin fish are, and have been, occurring over the last few decades. Evidence of the movement of tropical species to higher latitudes is unambiguous, as is the shift in many pelagic species of fin fish. Consequently, the distribution and abundance of fin fish is already occurring, and based on the updated expert consensus of Gattuso et al. (2015), appears to have transitioned from undetectable to moderate levels of risk at average global SSTs of 0.5°C and 0.7°C. There is little evidence that these changes are slowing, and therefore risks are estimated as transitioning from moderate to high levels of risk at 1.1°C to 1.3°C, and from high to very high levels of risk at 1.4°C to 1.6°C.

Expert assessment by Gattuso et al. (2015; SOM):

Marine fishes are important predators and prey in ocean ecosystems, contributing substantially to coastal economies, food security and livelihood. Warming-induced shifts in the abundance, geographic distribution, migration patterns and phenology of marine species, including fishes, were reported and projected with *very high confidence* in the IPCC AR5 (Pörtner et al., 2014).

Empirical and theoretical evidence of range shifts in response to temperature gradients are reported across various taxa and many geographical locations (Couce et al., 2013; Poloczanska et al., 2013; Bates et al., 2014), with observations suggesting that range shifts correspond with the rate and directionality of climate shifts or 'climate velocity' across landscapes (Pinsky et al., 2013). Observed range shifts associated with ocean warming may result in hybridization between native and invasive species through overlapping ranges, leading to reduced fitness and thus potentially increasing the risks of genetic extinction and reducing the adaptability to environmental changes (Muhlfeld et al., 2014; Potts et al., 2014). Some taxa are incapable of keeping pace with climate velocities, as observed with benthic invertebrates in the North Sea (Hiddink et al., 2015). The tropicalization of temperate marine ecosystems through poleward range shifts of tropical fish grazers increases the grazing rate of temperate macroalgae as seen in Japan and the Mediterranean (Verges et al., 2014). Such trophic impacts resulting from climate-induced range shifts are expected to affect ecosystem structure and dynamic in temperate reefs (Verges et al., 2014).

Projected future changes in temperature and other physical and chemical oceanographic factors are expected to affect the distribution and abundance of marine fishes, as elaborated by species distribution models with rate of shift at present day rate under the RCP8.5 scenario (Cheung et al., 2009). Limiting emissions to RCP2.6 is projected to reduce the average rate of range shift by 65% by mid-21st century (Jones and Cheung, 2015). Shifts in distribution of some species may be limited by the bathymetry or geographic boundaries, potentially resulting in a high risk of local extinction, particularly under high CO_2 emissions scenarios (Ben Rais Lasram et al., 2010).

While evidence suggests that adult fishes can survive high levels of CO_2, behavioural studies have found significant changes in species' responses under levels of CO_2 elevated above those of the present day level (Munday et al., 2014). Long-term persistence of these phenomena remains unknown. Based on the above, fishes already experience moderate risk of impacts at present day (*high confidence*). Risk increases from moderate to high by the end of the 21st century, when emissions change from RCP2.6 to RCP4.5 and become very high under RCP8.5, highlighting the potential non-reversibility of the potential impacts. Some evidence for direct and indirect impacts of ocean acidification on fin fish is available but varies substantially between species. Also, understanding about the scope of evolutionary adaptation for marine fishes to climate change and ocean acidification is limited, although it is unlikely that the majority of the species can fully adapt to expected changes in ocean properties without any impacts on their biology and ecology. Overall, we have robust evidence and high agreement (thus *high confidence*) from experimental data, field observations and mathematical modelling in detecting and attributing impacts for fin fish in the present day and under RCP2.6. The uncertainty about the sensitivity to ocean acidification and scope for evolutionary adaptation leads to *medium* confidence levels for their risk under high emissions scenarios.

3.SM.3.2.8 Open-Ocean Carbon Uptake

Update: Several recent studies have shown a decreasing CO_2 flux into the Pacific and Atlantic Oceans, Southern Ocean, and oceans in general (Iida et al., 2015). Concern over changes to the circulation of the ocean (e.g., Atlantic Meridional Overturning Circulation; AMOC) has grown since 2015, with the observation of cooling surface areas of the Atlantic (Rahmstorf et al., 2015).

Recent literature is consistent with the expert assessment of Gattuso et al. (2015) with risks of impact from changing ocean carbon uptake being barely detectable today but transitioning to moderate risk between 1°C and 1.5°C. Risks transition from moderate to high levels of risk between 2°C and 3.2°C. Higher levels of risk such as a rapid change in the circulation of the MOC are speculative at this point.

Expert assessment by Gattuso et al. (2015; SOM):

The uptake of anthropogenic carbon by the ocean in the industrial period and in the future is a service that is predominantly provided by physico-chemical processes (Prentice and J. T. Houghton et al., 2001). The sensitivity of ocean carbon uptake to increasing cumulative CO_2 emissions, including effects of changing ocean chemistry, temperature, circulation and biology, is assessed along the following lines of quantitative evidence: (i) the fraction of total cumulative anthropogenic emissions taken up by the ocean over the industrial period and the 21st century in CMIP5 Earth System Model projections for the four RCPs (Jones et al., 2013) (ii) the fraction of additional (marginal) emissions remaining airborne or taken up by the ocean for background atmospheric CO_2 following the four RCPs (Joos et al., 2013). In addition, the risk of large-scale reorganization of ocean circulation, such as a collapse of the North Atlantic overturning circulation and associated reductions in allowable carbon emissions towards CO_2 stabilization, is increasing with the magnitude and rate of CO_2 emissions, in particular beyond the year 2100. Confidence level is *high* for both RCP2.6 and RCP8.5 because the underlying physical and chemical processes are well known.

3.SM.3.2.9 Coastal Protection

Update: Sea level rise and intensifying storms are placing increasing stress on coastal environments and communities. Coastal protection by ecosystems as well as man-made infrastructure are important in terms of mitigating risks ranging from the physical destruction of ecosystems and human infrastructure to the salinization of coastal water supplies and direct impacts on human safety (Bosello and De Cian, 2014). Risks are particularly high for low-lying areas, such as carbonate atoll islands in the tropical Pacific where land for food, dwelling and water are limited, and effects of a rising sea plus intensifying storms create circumstances that may make many of these island systems uninhabitable within decades (Storlazzi et al., 2015). Even in advantaged countries such as the United States, these factors place millions at serious risk from even modest changes in inundation, with over four million US-based people at serious risk in response to a 90 cm sea level rise by 2100 (Hauer et al., 2016).

Both natural and human coastal protection have the potential to reduce the impacts (Fu and Song, 2017). Coral reefs, for example, provide effective protection by dissipating around 97% of wave energy, with 86% of the energy being dissipated by reef crests alone (Ferrario et al., 2014). Natural ecosystems, when healthy, also have the ability to repair themselves after being damaged, which sets them apart from coastal hardening and other human responses that require constant maintenance (Barbier, 2015; Elliff and Silva, 2017). Recognising and restoring coastal ecosystems such as coral reefs, mangroves and coastal vegetation in general may be more cost-effective than human remedies in terms of seawalls and coastal hardening, where costs of creating and maintaining structures may not always be cost-effective (Temmerman et al., 2013).

The last two years have seen an increase in the number of studies identifying the importance of coastal ecosystems as important to the protection of people and property along coastlines against sea level rise and storms. Analysis of the role of natural habitats for the protection people and infrastructure in Florida, New York and California, for example, has delivered a key insight into the significance of the problems and opportunities for the United States (Arkema et al., 2013). Some ecosystems which are important to coastal protection can keep pace with sea level rise, but only if other factors such as harvesting (e.g., of oysters; Rodriguez et al., 2014) or sediment supply (i.e., to mangroves, Lovelock et al., 2015) are managed. Several studies have pointed to the opportunity to reduce risks by promoting more holistic approaches to mitigating damage from sea level rise and storms by developing integrated coastal plans that ensure that human infrastructure enables the shoreward relocation of coastal vegetation, such as mangroves and salt marsh; the latter enhances coastal protection as well as having other important ecological functions, such as habitat for fish and the sources of a range of other resources (Di Nitto et al., 2014; Lovelock et al., 2015; Mills et al., 2016).

Recent studies have increasingly stressed that coastal protection needs to be considered in the context of new ways of managing coastal land, including protecting and managing coastal ecosystems as they also undergo shifts in their distribution and abundance (Saunders et al., 2014; André et al., 2016). These shifts in thinking require new tools in terms of legal and financial instruments, as well as integrated planning that involves not only human communities and infrastructure but also ecosystem responses. In this regard, the interactions between climate change, sea level rise and coastal disasters are being increasingly informed by models (Bosello and De Cian, 2014), with a widening appreciation of the role of natural ecosystems as an alternative to hardened coastal structures (Cooper et al., 2016).

Increased evidence of a rapid decay in ecosystems such as coral reefs and mangroves has increased the confidence around the conclusion that risks in coastal areas are increasing. Escalation of coastal impacts arising from Super Storm Sandy and Typhoon Haiyan (Long et al., 2016; Villamayor et al., 2016) have improved understanding of the future of coastal areas in terms of impacts, response and mitigation (Rosenzweig and Solecki, 2014; Shults and Galea, 2017).

Recent assessments of the last couple of years of literature confirm the expert judgement of Gattuso et al. (2015), although are emphasised by growing evidence that heat stress, ocean acidification and intensifying storms are increasing the breakdown of natural coastal barriers that otherwise provide important protection for coastal communities, ecosystems and infrastructure. While there is growing evidence of changes in the frequency and intensity of climate change, levels of risk remain similar to Gattuso et al. (2015) . Risk of impacts with respect to coastal protection transition from undetectable to moderate at 0.5°C and 0.8°C, with the transition from moderate to high levels of risk occurring from 1.5°C to 1.8°C. Further transition of impact risks from the loss of coastal protection has been judged to occur between 2.2°C and 3.2°C.

Expert assessment by Gattuso et al. (2015; SOM):

Estimating the sensitivity of natural coastal protection to climate change requires combining sensitivity across different ecosystems, especially coral reefs, mangrove forests and seagrass beds. Other ecosystems provide coastal protection, including salt marshes, macroalgae, oyster and mussel beds, and also beaches, dunes and barrier islands (stabilized by organisms; Spalding et al. 2014; Defeo et al. 2009), but there is less understanding of the level of protection conferred by these other organisms and habitats (Spalding et al., 2014). Although studies indicate some of these systems are already impacted by the effects of rising CO_2, or suggest they will be in the near future, levels of sensitivity are not well established, are highly variable, and in some cases their overall influence on coastal protection may be uncertain (i.e., species are replaced by functional equivalents in this context; K. B. Gedan 2009).

We reason that some coastal protection has already been lost – a result of impacts on coral reefs, seagrasses and other ecosystems from sea temperature rise. In the case of corals, this began in the late 1970s. Recent papers demonstrate collapse in the three-dimensional structure of reefs in the Caribbean (Alvarez-Filip et al., 2009) and the Seychelles (Sheppard et al., 2005), the second phase of which appears to be climate-related. Other studies show that some areas have not recovered from the 1997–1998 and 2010 bleaching events and that some reefs have collapsed there (e.g., parts of the Seychelles). There is thus little doubt that the coastal protection function of some reefs has already been reduced. A decreasing protection may also be the case for seagrasses, although such effects have not been measured. It should also be noted that other human impacts have already largely destroyed, or are progressively destroying, some of these ecosystems through direct action (e.g., 85% oyster reefs lost globally and 1–2% of mangrove forests cut down per annum; Beck et al. 2011). It therefore appears that some impact on coastal protection has already occurred, but there is a lack of data to extrapolate globally, hence the confidence level in the present day is *low*.

Confidence in the loss of coastal protection decreases with increasing CO_2 emissions because coastal protection is conferred by a range of habitats and the co-dependency or interactions between them make projections difficult. For example, protection to seagrass beds conferred by coral reefs or the replacement of salt marsh with mangrove forest (Saunders et al., 2014; Alongi, 2015). Additionally, human-driven pressure on these ecosystems is inherently difficult to forecast decades from now due to the possible implementation of new policies. Interacting effects of different symptoms of climate change such as increased temperature, decreasing pH, salinity, nutrient availability, patterns of precipitation and occurrence of pathogens will all influence the physiological response of individual species and ecosystems, and thus further reduce the predictability of responses at higher emissions.

3.SM.3.2.10 Recreational Services from Coral Reefs

Update: Tourism is one of the largest industries globally. A significant part of the global tourist industry is associated with tropical coastal regions and islands (Spalding et al., 2017). Coastal tourism can be a dominant money earner in terms of foreign exchange for many countries, particularly small island developing states (SIDS; Weatherdon et al., 2016). The direct relationship between increased global temperatures, elevated thermal stress and the loss of coral reefs (Section 3.4.4.10; Box 3.4) has raised concern about the risk that climate change poses for local economies and industries based on coral reefs and related ecosystems (e.g., mangroves seagrass beds).

Risks to the recreational services of coral reefs from climate change are considered here. The recent heavy loss of coral reefs from tourist locations worldwide has prompted interest in the relationship between increasing sea temperatures, declining coral reef ecosystems and tourist revenue (Normile, 2016). About 30% of the world's corals support tourism, which generates close to 36 billion USD on an annual basis (Spalding et al., 2017). Tourist expenditure, in this case, represents economic activity which supports jobs, revenue for business and taxes. Climate change in turn can influence the quality of the tourist experience through such aspects, because of changing weather patterns, physical impacts such as storms, and coastal erosion, as well as the effects of extremes on biodiversity within a region. Recent impacts in the Caribbean in 2017 highlight the impacts of climate change related risks associated with coastal tourism, with the prospect that many businesses will take years to recover from impacts such as hurricanes Harvey, Irma and Maria (Gewin, 2017; Shults and Galea, 2017).

A number of projects have attempted to estimate the impact (via economic valuation) of losing key coral reef ecosystems such as the Great Barrier Reef (Oxford Economics, 2009; Spalding et al., 2017). A recent study by O'Mahony et al.(2017) revealed that the Great Barrier Reef contributed 6.4 billion AUD and 64,000 jobs annually to the Australian economy in 2015–16. In terms of its social, economic and iconic value to Australia, the Great Barrier Reef is worth 56 billion AUD. The extreme temperatures of 2015–2017 removed 50% of the reef-building corals on the Great Barrier Reef (Hughes et al., 2017); there is considerable concern about the growing risk of climate change to the Great Barrier Reef, not only for its value biologically but also as part of a series of economic risks at local, state and national levels.

Our understanding of the potential impacts of climate change on tourism within small island and low-lying coastal areas in tropical and subtropical is made less certain by the flexibility and creativity of people. For example, the downturn of coral reefs in countries that are dependent on coral reef tourism does not necessarily mean a decline in gross domestic product (GDP), given that many countries may have other options for attracting international revenue. In addition, our understanding of future tourist expectations and desires are uncertain at this point.

Additional literature over the past couple of years confirms the risk from climate change to the recreational services that are derived from coral reefs, and which are important for a large number of coastal communities throughout the tropics. A transition in the risk of impacts to recreational services from coral reefs occurs between 0.6°C and 0.8°C, with a further transition from moderate to high levels of risk between 1.0°C and 1.5°C. Very high levels of risk occur between 2.0°C and higher as the frequency and intensity of extreme events (i.e. storm events, coastal inundation, and/or droughts, depending on the region) become increasingly difficult to manage for coastal tourism such as that associated with coral reefs. Note, the risks to corals are higher than those to the recreational services that corals provide to coastal communities. This highlights the fact that many communities today have lost coral but still are able to operate using recreational services from other sources. This difference disappears as one goes to higher levels of climate change and hence risk – particularly as the options for supporting recreational activities from the remnants of coral reefs are seriously reduced.

Expert assessment by Gattuso et al. (2015; SOM):

The impacts of CO_2 and SST on the condition of coral reefs ultimately affect the flow of ecosystem goods and services to human communities and businesses. There is an interesting lag between the degradation of corals and coral reefs and a detectable effect on human users. For this reason, the risk of impacts on human recreation and tourism begins significantly later than ecosystem changes are detected by marine scientists. As of 2015, atmospheric CO_2 concentration is 400 ppm and average SST is 0.8°C above that of the pre-industrial period. Mass bleaching and mortality events have degraded coral populations, and this has negatively impacted the recreational choices of a few, but not most, clients (*high confidence*; Hoegh-Guldberg et al. 2007). This impact on tourists' choice is expected to reach moderate to high levels as CO_2 approaches 450 ppm, at which point reefs begin net erosion and sea level, coral cover, storms and other environmental risks become significant considerations in destination attractiveness (*medium confidence*). By 600 ppm, the breakdown of the structure of most reefs becomes obvious, other changes such as reduced coral cover and increased sea level and storm damage mean that significant coastal recreation and tourism becomes difficult in most circumstances and many operations may be discarded (Hoegh-Guldberg et al., 2007). This will have a very high impact on recreational services (*medium confidence*). Confidence levels under RCP2.6 and RCP8.5 are *medium* because predicting tourists' expectations several decades from now remains relatively uncertain.

3.SM.3.2.11 Bivalve Fisheries and Aquaculture (Mid Latitude)

Update: Aquaculture is one of the fastest growing food sectors and is becoming increasingly essential for meeting the demand for protein for the global population (FAO, 2016). Studies published over the period 2015–2017 showed a steady increase in the risks associated with bivalve fisheries and aquaculture at mid-latitude locations coincident with increases in temperature, ocean acidification, introduced species, disease and other associated risks (Lacoue-Labarthe et al., 2016; Clements and Chopin, 2017; Clements et al., 2017; Parker et al., 2017). These have been met with a range of adaptation responses by bivalve fishing and aquaculture industries (Callaway et al., 2012; Weatherdon et al., 2016).

Risks are also likely to increase as a result of sea level rise and intensifying storms which pose a risk to hatcheries and other infrastructure (Callaway et al., 2012; Weatherdon et al., 2016). Some of the least predictable yet potentially most important risks are associated with the invasion of diseases, parasites and pathogens, which may be mitigated to a certain extent by active intervention by humans. Many of these have reduced the risks from these factors although costs have increased in at least some industries.

The risk of impact from ocean warming and acidification to bivalve aquaculture and fisheries is increasing – although not enough to warrant redefinition of the size and transition of risks from climate change. Therefore, literature since 2015 is consistent with the conclusion of how the risk of impact changes with greater levels of climate change. Risk to these important industries increases from nondetectable to moderate at 1.1°C and 1.3°C, with the transition from moderate to high levels of risk occurring from 1.7°C to 1.9°C. The transition from high to very high levels of risk is projected to between 2.8°C and 3.2°C.

Expert assessment by Gattuso et al. (2015; SOM):

Ecosystem services provided by temperate bivalves include marine harvests (both from capture fisheries and aquaculture), water quality maintenance and coastal stabilization. Of these, marine harvests are easiest to quantify and have been the subject of several assessments. Confidence is high that ocean acidification has already jeopardized marine harvest revenues in the northwest United States (Washington State Blue Ribbon Panel on Ocean Acidification, 2012). Although the affected hatcheries have taken steps to enhance monitoring, alter hatchery water intake and treatment, and diversify hatchery locations (Barton et al., 2015), these adaptations will only delay the onset of ocean acidification-related problems (high confidence). Wild harvest populations are fully exposed to ocean acidification and warming, and societal adaptations such as these are not applicable. Services provided by bivalves will continue even if populations migrate, decrease in size, or individuals become smaller, so effects are somewhat more delayed than those on shellfish themselves. In 2100, impacts are expected to be moderate under RCP2.6 and very high under RCP8.5. The level of confidence declines as a function of increasing CO_2 emissions due to the uncertainty about the extent of local adaptation, medium under RCP2.6 and low under RCP8.5.

3.SM.3.2.12 Small-Scale Fin-Fish Fisheries at Low Latitude

Update: Small-scale fin-fish fisheries (low latitude) provide food for millions of people along tropical coastlines and hence play an important role in the food security of a large number of countries (McClanahan et al., 2015; Pauly and Charles, 2015). In many cases, populations are heavily dependent on these sources of protein given the lack of alternatives (Cinner et al., 2012, 2016; Pendleton et al., 2016). The climate-related stresses affecting fin fish (see Section 'Fin fish' above), however, are producing a number of challenges for small-scale fisheries based on these species (e.g., (Kittinger, 2013; Pauly and Charles, 2015; Bell et al., 2017). Recent literature (2015–2017) has continued to outline growing threats from the rapid shifts in the biogeography of key species (Poloczanska et al., 2013, 2016; Burrows et al., 2014; García Molinos et al., 2015) and the ongoing rapid degradation of key habitats such as coral reefs, seagrass and mangroves (see Sections above on 'Seagrasses (mid-latitude)', 'Mangroves' and 'Pteropods', as well as Chapter 3, Box 3.4). As these changes have accelerated, so have the risks to the food and livelihoods associated with small-scale fisheries (Cheung et al., 2010). These risks have compounded with non-climate-related stresses (e.g., pollution, overfishing, unsustainable coastal development) to drive many small-scale fisheries well below the sustainable harvesting levels required to keep these resources functioning as a source of food (McClanahan et al., 2009, 2015; Pendleton et al., 2016). As a result, projections of climate change and the growth in human populations increasingly predict shortages of fish protein for many regions (e.g., Pacific, e.g., Bell et al., 2013, 2017; Indian Ocean, e.g., McClanahan et al., 2015). Mitigation of these risks involved marine spatial planning, fisheries repair, sustainable aquaculture and the development of alternative livelihoods (Kittinger, 2013; McClanahan et al., 2015; Song and Chuenpagdee, 2015; Weatherdon et al., 2016). Threats to small-scale fisheries have also come from the increasing incidence of alien (nuisance) species as well as an increasing incidence of disease, although the literature on these threats is at a low level of development and understanding (Kittinger et al., 2013; Weatherdon et al., 2016).

As assessed by Gattuso et al. (2015), risks of impacts on small-scale fisheries are moderate today, but are expected to reach very high levels under scenarios extending beyond RCP2.6. The research literature plus the growing evidence that many countries will have trouble adapting to these changes place confidence at a high level as to the risks of climate change on low latitude in fisheries. These effects are more sensitive, hence the higher risks at lower levels of temperature change.

Small-scale fisheries are highly dependent on healthy coastal ecosystems. With the growing evidence of impacts described above, the loss of habitat for small-scale fisheries is intensifying the risks of impact from climate change. For this reason, expert consensus has judged that risks have become greater since the assessment of Gattuso et al. (2015). Therefore, the transition from undetectable to moderate levels of risk is projected to occur between 0.5°C and 0.7°C, with the transition from moderate to high levels of risk occurring between 0.9°C and 1.1°C. The transition from high to very high levels of risk of impact is being judged to occur between 2.0°C and 2.5°C.

Expert assessment by Gattuso et al. (2015; SOM):

Evidence of climate change altering species composition of tropical marine fisheries is already apparent globally (Cheung et al., 2013). Simulations suggest that, as a result of range shifts and decrease in abundance of fish stocks, fisheries catch is likely to decline in tropical regions (Barange et al. 2014, Cheung et al. 2010). Projections also suggest that marine taxa in tropical regions are likely to lose critical habitat (e.g., coral reefs), leading to a decrease in fisheries productivity (Bell et al., 2013). Because of the magnitude of impacts, capacity for the fisheries to reduce such risks by protection, repair or adaptation is expected to be low (Pörtner et al., 2014). Thus, these impacts increase with increasing CO_2 emissions. Risk of impacts is close to moderate level in present day, and increases to high and very high when CO_2 concentration reaches the levels expected in 2100 under RCP4.5 and RCP8.5, respectively.

The scope of adaptation for low latitude fin-fish fisheries is narrow because of the high level of impacts on ecosystems and fisheries resources, lack of new fishing opportunities from species range shifts to compensate for the impacts, and relatively lower social-economic capacity of many countries to adapt to changes. Thus, the confidence level is *high* on projected impacts on low latitude fin-fish fisheries.

3.SM.3.2.13 Fin-Fish Fisheries (Mid- and High Latitude)

Update: While risks and reality of decline are high for low latitude fin fisheries, projections for mid- to high latitude fisheries include increases in fishery productivity in many cases (Cheung et al., 2013; Hollowed et al., 2013; Lam et al., 2014; FAO, 2016). These changes are associated with the biogeographical shift of species towards higher latitudes ('borealization', Fossheim et al., 2015) which brings benefits as well as challenges (e.g., increased risk of disease and invasive species). Factors underpinning the expansion of fisheries production to high latitude locations include warming and increase light and mixing due to retreating sea ice (Cheung et al., 2009). As a result of this, fisheries in the cold temperate regions of the north Pacific and north Atlantic are undergoing a major increase of primary productivity, and consequently in the increased harvest of fish from cod and pollock fisheries (Hollowed and Sundby, 2014). At more temperate locations, intensification of some upwelling systems is also boosting primary production and fisheries catch (Sydeman et al., 2014; Shepherd et al., 2017), although there are increasing threats from deoxygenation as excess biomass falls into the deep ocean, fueling higher metabolic rates and oxygen drawdown (Sydeman et al., 2014; Bakun et al., 2015).

Similar to the assessment by Gattuso et al. (2015), our confidence in understanding risks at higher levels of climate change and longer periods diminishes over time. The ability of fishing industries to adapt to changes is considerable, although the economic costs of adapting can be high. Complex changes in fin fisheries at high latitudes has a number of climate-related risks associated with it (as described above and by Gattuso et al. (2015). In this case, risks of climate impacts on fin fisheries at high latitudes is projected to transition from undetectable to moderate levels of risk at 0.7°C to 0.9°C. The shift from moderate to high levels of risk is projected by the expert consensus to occur between 2.2°C and 3.2°C.

Expert assessment by Gattuso et al. (2015; SOM):

Evidence that climate change effects altering species composition in mid- and high latitude fisheries can already be observed globally, with increasing dominance of warmer-water species since the 1970s (Cheung et al., 2013). Global-scale projections suggest substantial increases in potential fisheries catch in high latitude regions (Cheung et al., 2010; Barange et al., 2014) under RCP8.5 by mid- to end-21st century. However, ocean acidification increases uncertainty surrounding the potential fisheries gain, because the Arctic is a hotspot of ocean acidification (Lam et al., 2014). Risks of impacts of warming, ocean acidification and deoxygenation on mid-latitude regions are variable (Cheung et al., 2013; Barange et al., 2014). Overall, existing fish stocks are expected to decrease in catch, while new opportunities for fisheries may emerge from range expansion of warmer-water. Declines in catch have been projected for fisheries in the northeast Pacific (Ainsworth et al., 2011), northwest Atlantic (Guénette et al., 2014) and waters around the UK (Jones et al., 2014) by mid-21st century under SRES A1B and A2 scenarios (equivalent to RCP6.0 to 8.5). While it is uncertain whether small-scale fisheries will have the mobility to follow shifts in ranges of target species, those with access to multiple gears types may be able to adapt more easily to climate-related changes in stock composition. Societal adaptation to reduce the risk of impacts is expected to be relatively higher than tropical fisheries. Thus, moderate risk is assigned from the present day, and the risk increases to high when CO_2 concentration is beyond levels expected from RCP4.5.

Risk to fisheries at mid- and high latitudes depends on how the fishers, fishing industries and fisheries management bodies respond and adapt to changes in species composition and distribution. Prediction of the scope of such adaptive response is uncertain, particularly under greater changes in fisheries resources. Thus, the confidence level is *high* under RCP2.6 and *low* under RCP8.5.

References

Ainsworth, C. H., Samhouri, J. F., Busch, D. S., Cheung, W. W. L., Dunne, J., and Okey, T. A. (2011). Potential impacts of climate change on Northeast Pacific marine foodwebs and fisheries. ICES J. Mar. Sci. 68, 1217–1229. Available at: http://dx.doi.org/10.1093/icesjms/fsr043.

Alongi, D. M. (2008). Mangrove forests: Resilience, protection from tsunamis, and responses to global climate change. Estuar. Coast. Shelf Sci. 76, 1–13. doi:10.1016/j.ecss.2007.08.024.

Alongi, D. M. (2015). The Impact of Climate Change on Mangrove Forests. Curr. Clim. Chang. Reports 1, 30–39. doi:10.1007/s40641-015-0002-x.

Alvarez-Filip, L., Dulvy, N. K., Gill, J. A., Cote, I. M., and Watkinson, A. R. (2009). Flattening of Caribbean coral reefs: region-wide declines in architectural complexity. Proc. R. Soc. B Biol. Sci. 276, 3019–3025. doi:10.1098/rspb.2009.0339.

André, C., Boulet, D., Rey-Valette, H., and Rulleau, B. (2016). Protection by hard defence structures or relocation of assets exposed to coastal risks: Contributions and drawbacks of cost-benefit analysis for long-term adaptation choices to climate change. Ocean Coast. Manag. 134, 173–182. doi:10.1016/j.ocecoaman.2016.10.003.

Arkema, K. K., Guannel, G., Verutes, G., Wood, S. A., Guerry, A., Ruckelshaus, M., et al. (2013). Coastal habitats shield people and property from sea-level rise and storms. Nat. Clim. Chang. 3, 913–918. doi:10.1038/nclimate1944.

Asplund, M. E., Baden, S. P., Russ, S., Ellis, R. P., Gong, N., and Hernroth, B. E. (2014). Ocean acidification and host-pathogen interactions: Blue mussels, Mytilus edulis, encountering Vibrio tubiashii. Environ. Microbiol. 16, 1029–1039. doi:10.1111/1462-2920.12307.

Atkinson, A., Siegel, V., Pakhomov, E., and Rothery, P. (2004). Long-term decline in krill stock and increase in salps within the Southern Ocean. Nature 432, 100–103. doi:10.1038/nature02996.

Bakun, A., Black, B. A., Bograd, S. J., García-Reyes, M., Miller, A. J., Rykaczewski, R. R., et al. (2015). Anticipated Effects of Climate Change on Coastal Upwelling Ecosystems. Curr. Clim. Chang. Reports 1, 85–93. doi:10.1007/s40641-015-0008-4.

Barange, M., Merino, G., Blanchard, J. L., Scholtens, J., Harle, J., Allison, E. H., et al. (2014). Impacts of climate change on marine ecosystem production in societies dependent on fisheries. Nat. Clim. Chang. 4, 211–216. doi:10.1038/nclimate2119.

Barbier, E. B. (2015). Valuing the storm protection service of estuarine and coastal ecosystems. Ecosyst. Serv. 11, 32–38. doi:10.1016/j.ecoser.2014.06.010.

Barton, A., Hales, B., Waldbusser, G. G., Langdon, C., and Feely, R. A. (2012). The Pacific oyster, Crassostrea gigas, shows negative correlation to naturally elevated carbon dioxide levels: Implications for near-term ocean acidification effects. Limnol. Oceanogr. 57, 698–710. doi:10.4319/lo.2012.57.3.0698.

Barton, A., Waldbusser, G. G., Feely, R. A., Weisberg, S. B., Newton, J. A., Hales, B., et al. (2015). Impacts of coastal acidification on the Pacific Northwest shellfish industry and adaptation strategies implemented in response. Oceanography 28, 146–159. doi:10.5670/oceanog.2015.38.

Bates, A. E., Pecl, G. T., Frusher, S., Hobday, A. J., Wernberg, T., Smale, D. A., et al. (2014). Defining and observing stages of climate-mediated range shifts in marine systems. Glob. Environ. Chang. 26, 27–38. doi:10.1016/j.gloenvcha.2014.03.009.

Beck, M. W., Brumbaugh, R. D., Airoldi, L., Carranza, A., Coen, L. D., Crawford, C., et al. (2011). Oyster Reefs at Risk and Recommendations for Conservation, Restoration, and Management. Bioscience 61, 107–116. doi:10.1525/bio.2011.61.2.5.

Bednaršek, N., Feely, R. A., Reum, J. C. P., Peterson, B., Menkel, J., Alin, S. R., et al. (2014). Limacina helicina shell dissolution as an indicator of declining habitat suitability owing to ocean acidification in the California Current Ecosystem. Proc. R. Soc. B Biol. Sci. 281, 20140123–20140123. doi:10.1098/rspb.2014.0123.

Bednaršek, N., Harvey, C. J., Kaplan, I. C., Feely, R. A., and Možina, J. (2016). Pteropods on the edge: Cumulative effects of ocean acidification, warming, and deoxygenation. Prog. Oceanogr. 145, 1–24. doi:10.1016/j.pocean.2016.04.002.

Bednaršek, N., Klinger, T., Harvey, C. J., Weisberg, S., McCabe, R. M., Feely, R. A., et al. (2017). New ocean, new needs: Application of pteropod shell dissolution as a biological indicator for marine resource management. Ecol. Indic. 76, 240–244. doi:10.1016/j.ecolind.2017.01.025.
Bednaršek, N., and Ohman, M. D. (2015). Changes in pteropod distributions and shell dissolution across a frontal system in the California Current System. Mar. Ecol. Prog. Ser. 523, 93–103. doi:10.3354/meps11199.
Bednaršek, N., Tarling, G. A., Bakker, D. C. E., Fielding, S., Jones, E. M., Venables, H. J., et al. (2012). Extensive dissolution of live pteropods in the Southern Ocean. Nat. Geosci. 5, 881–885. doi:10.1038/ngeo1635.
Bell, J. D., Cisneros-Montemayor, A., Hanich, Q., Johnson, J. E., Lehodey, P., Moore, B. R., et al. (2017). Adaptations to maintain the contributions of small-scale fisheries to food security in the Pacific Islands. Mar. Policy. doi:10.1016/j.marpol.2017.05.019.
Bell, J. D., Ganachaud, A., Gehrke, P. C., Griffiths, S. P., Hobday, A. J., Hoegh-Guldberg, O., et al. (2013). Mixed responses of tropical Pacific fisheries and aquaculture to climate change. Nat. Clim. Chang. 3, 591–599. doi:10.1038/nclimate1838.
Ben Rais Lasram, F., Guilhaumon, F., Albouy, C., Somot, S., Thuiller, W., and Mouillot, D. (2010). The Mediterranean Sea as a ‘cul-de-sac’ for endemic fishes facing climate change. Glob. Chang. Biol. 16, 3233–3245. doi:10.1111/j.1365-2486.2010.02224.x.
Bortolotto, E., Bucklin, A., Mezzavilla, M., Zane, L., and Patarnello, T. (2011). Gone with the currents: lack of genetic differentiation at the circum-continental scale in the Antarctic krill Euphausia superba. BMC Genet. 12, 32. doi:10.1186/1471-2156-12-32.
Bosello, F., and De Cian, E. (2014). Climate change, sea level rise, and coastal disasters. A review of modeling practices. Energy Econ. 46, 593–605. doi:10.1016/j.eneco.2013.09.002.
Brodie, J., Williamson, C. J., Smale, D. A., Kamenos, N. A., Mieszkowska, N., Santos, R., et al. (2014). The future of the northeast Atlantic benthic flora in a high CO2 world. Ecol. Evol. 4, 2787–2798. doi:10.1002/ece3.1105.
Burge, C. A., Kim, C. J. S., Lyles, J. M., and Harvell, C. D. (2013). Special issue Oceans and Humans Health: The ecology of marine opportunists. Microb. Ecol. 65, 869–879. doi:10.1007/s00248-013-0190-7.
Burrows, M. T., Schoeman, D. S., Richardson, A. J., Molinos, J. G., Hoffmann, A., Buckley, L. B., et al. (2014). Geographical limits to species-range shifts are suggested by climate velocity. Nature 507, 492–495. doi:10.1038/nature12976.
C. R. Wilkinson (2000). Status of Coral Reefs of the World: 2000. Aust. Inst. Mar. Sci. Townsville, Aust., 363.
Callaway, R., Shinn, A. P., Grenfell, S. E., Bron, J. E., Burnell, G., Cook, E. J., et al. (2012). Review of climate change impacts on marine aquaculture in the UK and Ireland. Aquat. Conserv. Mar. Freshw. Ecosyst. 22, 389–421. doi:10.1002/aqc.2247.
Carr, J. A., D’Odorico, P., McGlathery, K. J., and P. L. Wiberg (2012). Modeling the effects of climate change on eelgrass stability and resilience: Future scenarios and leading indicators of collapse. Mar. Ecol. Prog. Ser. 448, 289–301.
Castillo, N., Saavedra, L. M., Vargas, C. A., Gallardo-Escárate, C., and Détrée, C. (2017). Ocean acidification and pathogen exposure modulate the immune response of the edible mussel Mytilus chilensis. Fish Shellfish Immunol. 70, 149–155. doi:10.1016/j.fsi.2017.08.047.
Cheung, W. W. L., Lam, V. W. Y., Sarmiento, J. L., Kearney, K., Watson, R., and Pauly, D. (2009). Projecting global marine biodiversity impacts under climate change scenarios. Fish Fish. 10, 235–251. doi:10.1111/j.1467-2979.2008.00315.x.
Cheung, W. W. L., Lam, V. W. Y., Sarmiento, J. L., Kearney, K., Watson, R., Zeller, D., et al. (2010). Large-scale redistribution of maximum fisheries catch potential in the global ocean under climate change. Glob. Chang. Biol. 16, 24–35. doi:10.1111/j.1365-2486.2009.01995.x.
Cheung, W. W. L., Watson, R., and Pauly, D. (2013). Signature of ocean warming in global fisheries catch. Nature 497, 365–368. doi:10.1038/nature12156.
Cinner, J. E., McClanahan, T. R., Graham, N. A. J., Daw, T. M., Maina, J., Stead, S. M., et al. (2012). Vulnerability of coastal communities to key impacts of climate change on coral reef fisheries. Glob. Environ. Chang. 22, 12–20. doi:10.1016/j.gloenvcha.2011.09.018.

Cinner, J. E., Pratchett, M. S., Graham, N. A. J., Messmer, V., Fuentes, M. M. P. B., Ainsworth, T., et al. (2016). A framework for understanding climate change impacts on coral reef social–ecological systems. Reg. Environ. Chang. 16, 1133–1146. doi:10.1007/s10113-015-0832-z.

Clements, J. C., Bourque, D., McLaughlin, J., Stephenson, M., and Comeau, L. A. (2017). Extreme ocean acidification reduces the susceptibility of eastern oyster shells to a polydorid parasite. J. Fish Dis. 40, 1573–1585. doi:10.1111/jfd.12626.

Clements, J. C., and Chopin, T. (2017). Ocean acidification and marine aquaculture in North America: Potential impacts and mitigation strategies. Rev. Aquac. 9, 326341. doi:10.1111/raq.12140.

Comeau, S., Alliouane, S., and Gattuso, J.-P. (2012). Effects of ocean acidification on overwintering juvenile Arctic pteropods Limacina helicina. Ecol. Prog. Ser. 456, 279–284. doi:10.3354/meps09696.

Comeau, S., Gorsky, G., Jeffree, R., Teyssié, J.-L., and Gattuso, J.-P. (2009). Impact of ocean acidification on a key Arctic pelagic mollusc (Limacina helicina). Biogeosciences 6, 1877–1882. doi:10.5194/bg-6-1877-2009.

Comeau, S., Jeffree, R., Teyssié, J.-L., and Gattuso, J.-P. (2010). Response of the Arctic pteropod Limacina helicina to projected future environmental conditions. PLoS One 5. doi:10.1371/journal.pone.0011362.

Cooley, S. R., Rheuban, J. E., Hart, D. R., Luu, V., Glover, D. M., Hare, J. A., et al. (2015). An Integrated Assessment Model for Helping the United States Sea Scallop (Placopecten magellanicus) Fishery Plan Ahead for Ocean Acidification and Warming. PLoS One 10, e0124145. doi:10.1371/journal.pone.0124145.

Cooper, J. A. G., O'Connor, M. C., and McIvor, S. (2016). Coastal defences versus coastal ecosystems: A regional appraisal. Mar. Policy. doi:10.1016/j.marpol.2016.02.021.

Couce, E., Ridgwell, A., and Hendy, E. J. (2013). Future habitat suitability for coral reef ecosystems under global warming and ocean acidification. Glob. Chang. Biol. 19, 3592–3606. doi:10.1111/gcb.12335.

David, C., Schaafsma, F. L., van Franeker, J. A., Lange, B., Brandt, A., and Flores, H. (2017). Community structure of under-ice fauna in relation to winter sea-ice habitat properties from the Weddell Sea. Polar Biol. 40, 247–261. doi:10.1007/s00300-016-1948-4.

De'ath, G., Fabricius, K. E., Sweatman, H., and Puotinen, M. (2012). The 27-year decline of coral cover on the Great Barrier Reef and its causes. Proc. Natl. Acad. Sci. U. S. A. 109, 17995–9. doi:10.1073/pnas.1208909109.

Defeo, O., McLachlan, A., Schoeman, D. S., Schlacher, T. A., Dugan, J., Jones, A., et al. (2009). Threats to sandy beach ecosystems: A review. Estuar. Coast. Shelf Sci. 81, 1–12. doi:10.1016/j.ecss.2008.09.022.

Di Nitto, D., Neukermans, G., Koedam, N., Defever, H., Pattyn, F., Kairo, J. G., et al. (2014). Mangroves facing climate change: Landward migration potential in response to projected scenarios of sea level rise. Biogeosciences 11, 857–871. doi:10.5194/bg-11-857-2014.

Donner, S. D., Skirving, W. J., Little, C. M., Oppenheimer, M., and Hoegh-Guldberg, O. (2005). Global assessment of coral bleaching and required rates of adaptation under climate change. Glob. Chang. Biol. 11, 2251–2265. doi:10.1111/j.1365-2486.2005.01073.x.

Dove, S. G., Kline, D. I., Pantos, O., Angly, F. E., Tyson, G. W., and Hoegh-Guldberg, O. (2013). Future reef decalcification under a business-as-usual CO2 emission scenario. Proc. Natl. Acad. Sci. U. S. A. 110, 15342–15347. doi:10.1073/pnas.1302701110.

Duke, N. C., Kovacs, J. M., Griffiths, A. D., Preece, L., Hill, D. J. E., Van Oosterzee, P., et al. (2017). Large-scale dieback of mangroves in Australia's Gulf of Carpentaria: A severe ecosystem response, coincidental with an unusually extreme weather event. Mar. Freshw. Res. 68, 1816–1829. doi:10.1071/MF16322.

Eakin, C. M., Morgan, J. A., Heron, S. F., Smith, T. B., Liu, G., Alvarez-Filip, L., et al. (2010). Caribbean corals in crisis: Record thermal stress, bleaching, and mortality in 2005. PLoS One 5, e13969. doi:10.1371/journal.pone.0013969.

Elliff, C. I., and Silva, I. R. (2017). Coral reefs as the first line of defense: Shoreline protection in face of climate change. Mar. Environ. Res. 127, 148–154. doi:10.1016/j.marenvres.2017.03.007.

Esbaugh, A. J. (2017). Physiological implications of ocean acidification for marine fish: emerging patterns and new insights. J. Comp. Physiol. B 188, 1–13. doi:10.1007/s00360-017-1105-6.

FAO (2016). The State of World Fisheries and Aquaculture 2016. Contributing to food security and nutrition for all. Rome, Italy: Food and Agriculture Organization of the United Nations (FAO).
Feely, R. A., Alin, S. R., Carter, B., Bednar??ek, N., Hales, B., Chan, F., et al. (2016). Chemical and biological impacts of ocean acidification along the west coast of North America. Estuar. Coast. Shelf Sci. 183, 260–270. doi:10.1016/j.ecss.2016.08.043.
Feller, I. C., Friess, D. A., Krauss, K. W., and Lewis, R. R. (2017). The state of the world's mangroves in the 21st century under climate change. Hydrobiologia 803, 1–12. doi:10.1007/s10750-017-3331-z.
Ferrario, F., Beck, M. W., Storlazzi, C. D., Micheli, F., Shepard, C. C., and Airoldi, L. (2014). The effectiveness of coral reefs for coastal hazard risk reduction and adaptation. Nat. Commun. 5, 3794. doi:10.1038/ncomms4794.
Flores, H., Atkinson, A., Kawaguchi, S., Krafft, B. A., Milinevsky, G., Nicol, S., et al. (2012). Impact of climate change on Antarctic krill. Mar. Ecol. Prog. Ser. 458, 1–19. doi:10.3354/meps09831.
Fossheim, M., Primicerio, R., Johannesen, E., Ingvaldsen, R. B., Aschan, M. M., and Dolgov, A. V. (2015). Recent warming leads to a rapid borealization of fish communities in the Arctic. Nat. Clim. Chang. 5, 673–677. doi:10.1038/nclimate2647.
Fu, X., and Song, J. (2017). Assessing the economic costs of sea level rise and benefits of coastal protection: A spatiotemporal approach. Sustainability 9. doi:10.3390/su9081495.
García Molinos, J., Halpern, B. S., Schoeman, D. S., Brown, C. J., Kiessling, W., Moore, P. J., et al. (2015). Climate velocity and the future global redistribution of marine biodiversity. Nat. Clim. Chang. 6, 83–88. doi:10.1038/nclimate2769.
Gattuso, J.-P., Magnan, A., Bille, R., Cheung, W. W. L., Howes, E. L., Joos, F., et al. (2015). Contrasting futures for ocean and society from different anthropogenic CO2 emissions scenarios. Science (80-.). 349, aac4722. doi:10.1126/science.aac4722.
Gedan, K. B., and Bertness, M. D. (2009). Experimental warming causes rapid loss of plant diversity in New England salt marshes. Ecol. Lett. 12, 842–848. doi:10.1111/j.1461-0248.2009.01337.x.
Gewin, V. (2017). Scientists hit hard by powerful hurricanes in 2017 share tips for weathering future disasters. Nature 551, 401–403.
Glynn, P. W. (1984). Widespread coral mortality and the 1982-83 El Niño warming event. Environ. Conserv. 11, 133–146. doi:10.1017/S0376892900013825.
Gobler, C. J., DePasquale, E. L., Griffith, A. W., and Baumann, H. (2014). Hypoxia and Acidification Have Additive and Synergistic Negative Effects on the Growth, Survival, and Metamorphosis of Early Life Stage Bivalves. PLoS One 9, e83648. doi:10.1371/journal.pone.0083648.
Godoy, M. D. P., and De Lacerda, L. D. (2015). Mangroves Response to Climate Change: A Review of Recent Findings on Mangrove Extension and Distribution. An Acad Bras CiencAnnals Brazilian Acad. Sci. 87, 651–667. doi:10.1590/0001-3765201520150055.
Guénette, S., Araújo, J. N., and Bundy, A. (2014). Exploring the potential effects of climate change on the Western Scotian Shelf ecosystem, Canada. J. Mar. Syst. 134, 89–100. doi:10.1016/j.jmarsys.2014.03.001.
Guerrero-Meseguer, L., Marín, A., and Sanz-Lázaro, C. (2017). Future heat waves due to climate change threaten the survival of P. oceanica seedlings. Environ. Pollut. 230, 40–45. doi:10.1016/j.envpol.2017.06.039.
Hauer, M. E., Evans, J. M., and Mishra, D. R. (2016). Millions projected to be at risk from sea-level rise in the continental United States. Nat. Clim. Chang. 6, 691–695. doi:10.1038/nclimate2961.
Hiddink, J. G., Burrows, M. T., and García Molinos, J. (2015). Temperature tracking by North Sea benthic invertebrates in response to climate change. Glob. Chang. Biol. 21, 117–129. doi:10.1111/gcb.12726.
Hill, S. L., Phillips, T., and Atkinson, A. (2013). Potential Climate Change Effects on the Habitat of Antarctic Krill in the Weddell Quadrant of the Southern Ocean. PLoS One 8. doi:10.1371/journal.pone.0072246.
Hoegh-Guldberg, O. (1999). Climate change, coral bleaching and the future of the world's coral reefs. Mar. Freshw. Res. 50, 839. doi:10.1071/MF99078.
Hoegh-Guldberg, O., Cai, R., Poloczanska, E. S., Brewer, P. G., Sundby, S., Hilmi, K., et al. (2014). "The Ocean," in Climate Change 2014: Impacts, Adaptation, and Vulnerability. Part B: Regional Aspects. Contribution of Working Group II to the Fifth Assessment Report of the

Intergovernmental Panel of Climate Change, eds. V. R. Barros, C. B. Field, D. J. Dokken, M. D. Mastrandrea, K. J. Mach, T. E. Bilir, et al. (Cambridge, United Kingdom and New York, NY, USA, United Kingdom and New York, NY, USA: Cambridge University Press), 1655–1731.

Hoegh-Guldberg, O., Mumby, P. J., Hooten, A. J., Steneck, R. S., Greenfield, P., Gomez, E., et al. (2007). Coral Reefs Under Rapid Climate Change and Ocean Acidification. Science (80-.). 318, 1737–1742. Available at: http://science.sciencemag.org/content/318/5857/1737 [Accessed April 12, 2017].

Höffle, H., Thomsen, M. S., and Holmer, M. (2011). High mortality of Zostera marina under high temperature regimes but minor effects of the invasive macroalgae Gracilaria vermiculophylla. doi: Estuar. Coast. Shelf Sci. 92, 35–46. doi:10.1016/j.ecss.2010.12.017e.

Hollowed, A. B., Barange, M., Beamish, R. J., Brander, K., Cochrane, K., Drinkwater, K., et al. (2013). Projected impacts of climate change on marine fish and fisheries. ICES J. Mar. Sci. 70, 1023–1037. doi:10.1093/icesjms/fst081.

Hollowed, A. B., and Sundby, S. (2014). Change is coming to the northern oceans. Science (80-.). 344, 1084–1085. doi:10.1126/science.1251166.

Horta E Costa, B., Assis, J., Franco, G., Erzini, K., Henriques, M., Gonçalves, E. J., et al. (2014). Tropicalization of fish assemblages in temperate biogeographic transition zones. Mar. Ecol. Prog. Ser. 504, 241–252. doi:10.3354/meps10749.

Hughes, T. P., Kerry, J. T., Álvarez-Noriega, M., Álvarez-Romero, J. G., Anderson, K. D., Baird, A. H., et al. (2017). Global warming and recurrent mass bleaching of corals. Nature 543, 373–377. doi:10.1038/nature21707.

Iida, Y., Kojima, A., Takatani, Y., Nakano, T., Sugimoto, H., Midorikawa, T., et al. (2015). Trends in pCO2 and sea–air CO2 flux over the global open oceans for the last two decades. J. Oceanogr. 71, 637–661. doi:10.1007/s10872-015-0306-4.

Jones, C., Robertson, E., Arora, V., Friedlingstein, P., Shevliakova, E., Bopp, L., et al. (2013). Twenty-First-Century Compatible CO2 Emissions and Airborne Fraction Simulated by CMIP5 Earth System Models under Four Representative Concentration Pathways. J. Clim. 26, 4398–4413. doi:10.1175/JCLI-D-12-00554.1.

Jones, M. C., and Cheung, W. W. L. (2015). Multi-model ensemble projections of climate change effects on global marine biodiversity. ICES J. Mar. Sci. 72, 741–752. doi:10.1093/icesjms/fsu172.

Jones, M. C., Dye, S. R., Pinnegar, J. K., Warren, R., and Cheung, W. W. (2014). Using scenarios to project the changing profitability of fisheries under climate change. Fish Fish. doi:10.1111/faf.12081.

Joos, F., Roth, R., Fuglestvedt, J. S., Peters, G. P., Enting, I. G., von Bloh, W., et al. (2013). Carbon dioxide and climate impulse response functions for the computation of greenhouse gas metrics: a multi-model analysis. Atmos. Chem. Phys. 13, 2793–2825. doi:10.5194/acp-13-2793-2013.

Jordà, G., Marbà, N., and Duarte, C. M. (2012). Mediterranean seagrass vulnerable to regional climate warming. Nat. Clim. Chang. 2, 821–824. doi:10.1038/nclimate1533.

Kawaguchi, S., Ishida, A., King, R., Raymond, B., Waller, N., Constable, A., et al. (2013). Risk maps for Antarctic krill under projected Southern Ocean acidification. Nat. Clim. Chang. 3, 843–847. doi:10.1038/nclimate1937.

Kittinger, J. N. (2013). Human Dimensions of Small-Scale and Traditional Fisheries in the Asia-Pacific Region. Pacific Sci. 67, 315–325. doi:10.2984/67.3.1.

Kittinger, J. N., Finkbeiner, E. M., Ban, N. C., Broad, K., Carr, M. H., Cinner, J. E., et al. (2013). Emerging frontiers in social-ecological systems research for sustainability of small-scale fisheries. Curr. Opin. Environ. Sustain. 5, 352–357. doi:10.1016/j.cosust.2013.06.008.

Kroeker, K. J., Kordas, R. L., Crim, R., Hendriks, I. E., Ramajo, L., Singh, G. S., et al. (2013). Impacts of ocean acidification on marine organisms: Quantifying sensitivities and interaction with warming. Glob. Chang. Biol. 19, 1884–1896. doi:10.1111/gcb.12179.

Lacoue-Labarthe, T., Nunes, P. A. L. D., Ziveri, P., Cinar, M., Gazeau, F., Hall-Spencer, J. M., et al. (2016). Impacts of ocean acidification in a warming Mediterranean Sea: An overview. Reg. Stud. Mar. Sci. 5, 1–11. doi:10.1016/j.rsma.2015.12.005.

Lam, V. W. Y., Cheung, W. W. L., and Sumaila, U. R. (2014). Marine capture fisheries in the Arctic: Winners or losers under climate change and ocean acidification? Fish Fish. 17, 335–357. doi:10.1111/faf.12106.

Lemasson, A. J., Fletcher, S., Hall-Spencer, J. M., and Knights, A. M. (2017). Linking the biological impacts of ocean acidification on oysters to changes in ecosystem services: A review. J. Exp. Mar. Bio. Ecol. 492, 49–62. doi:10.1016/j.jembe.2017.01.019.

Li, S., Huang, J., Liu, C., Liu, Y., Zheng, G., Xie, L., et al. (2016a). Interactive Effects of Seawater Acidification and Elevated Temperature on the Transcriptome and Biomineralization in the Pearl Oyster Pinctada fucata. Environ. Sci. Technol. 50, 1157–1165. doi:10.1021/acs.est.5b05107.

Li, S., Liu, C., Huang, J., Liu, Y., Zhang, S., Zheng, G., et al. (2016b). Transcriptome and biomineralization responses of the pearl oyster Pinctada fucata to elevated CO2 and temperature. Sci. Rep. 6, 18943. doi:10.1038/srep18943.

Lischka, S., Büdenbender, J., Boxhammer, T., and Riebesell, U. (2011). Impact of ocean acidification and elevated temperatures on early juveniles of the polar shelled pteropod Limacina helicina: mortality, shell degradation, and shell growth. Biogeosciences 8, 919–932. doi:10.5194/bg-8-919-2011.

Lischka, S., and Riebesell, U. (2012). Synergistic effects of ocean acidification and warming on overwintering pteropods in the Arctic. Glob. Chang. Biol. 18, 3517–3528. doi:10.1111/gcb.12020.

Logan, C. A., Dunne, J. P., Eakin, C. M., and Donner, S. D. (2014). Incorporating adaptive responses into future projections of coral bleaching. Glob. Chang. Biol. 20, 125–139. doi:10.1111/gcb.12390.

Long, J., Giri, C., Primavera, J., and Trivedi, M. (2016). Damage and recovery assessment of the Philippines’ mangroves following Super Typhoon Haiyan. Mar. Pollut. Bull. 109, 734–743. doi:10.1016/j.marpolbul.2016.06.080.

Lovelock, C. E., Cahoon, D. R., Friess, D. A., Guntenspergen, G. R., Krauss, K. W., Reef, R., et al. (2015). The vulnerability of Indo-Pacific mangrove forests to sea-level rise. Nature 526, 559–563. doi:10.1038/nature15538.

Lovelock, C. E., Feller, I. C., Reef, R., Hickey, S., and Ball, M. C. (2017). Mangrove dieback during fluctuating sea levels. Sci. Rep. 7, 1680. doi:10.1038/s41598-017-01927-6.

Mackenzie, C. L., Lynch, S. A., Culloty, S. C., and Malham, S. K. (2014a). Future oceanic warming and acidification alter immune response and disease status in a commercial shellfish species, Mytilus edulis L. PLoS One 9. doi:10.1371/journal.pone.0099712.

Mackenzie, C. L., Ormondroyd, G. A., Curling, S. F., Ball, R. J., Whiteley, N. M., and Malham, S. K. (2014b). Ocean warming, more than acidification, reduces shell strength in a commercial shellfish species during food limitation. PLoS One 9. doi:10.1371/journal.pone.0086764.

Manno, C., Bednaršek, N., Tarling, G. A., Peck, V. L., Comeau, S., Adhikari, D., et al. (2017). Shelled pteropods in peril: Assessing vulnerability in a high CO2 ocean. Earth-Science Rev. 169, 132–145. doi:10.1016/j.earscirev.2017.04.005.

Mannoa, C., Morataa, N., and Primiceriob, R. (2012). Limacina retroversa’s response to combined effects of ocean acidification and sea water freshening. Estuar. Coast. Shelf Sci. 113, 163–171. doi:10.1016/j.ecss.2012.07.019.

Marbà, N., and Duarte, C. M. (2010). Mediterranean warming triggers seagrass (Posidonia oceanica) shoot mortality. Glob. Chang. Biol. 16, 2366–2375. doi:10.1111/j.1365- 2486.2009.02130.x.

McClanahan, T. R., Allison, E. H., and Cinner, J. E. (2015). Managing fisheries for human and food security. Fish Fish. 16, 78–103. doi:10.1111/faf.12045.

McClanahan, T. R., Castilla, J. C., White, A. T., and Defeo, O. (2009). Healing small-scale fisheries by facilitating complex socio-ecological systems. Rev. Fish Biol. Fish. 19, 33–47. doi:10.1007/s11160-008-9088-8.

McKee, K., Rogers, K., and Saintilan, N. (2012). Response of salt marsh and mangrove wetlands to changes in atmospheric CO2, climate, and sea level. Glob. Chang. Funct. Distrib. Wetl., 63–96.

Miller, A. W., Reynolds, A. C., Sobrino, C., and Riedel, G. F. (2009). Shellfish face uncertain future in high CO2 world: Influence of acidification on oyster larvae calcification and growth in estuaries. PLoS One 4. doi:10.1371/journal.pone.0005661.

Mills, M., Leon, J. X., Saunders, M. I., Bell, J., Liu, Y., O'Mara, J., et al. (2016). Reconciling Development and Conservation under Coastal Squeeze from Rising Sea Level. Conserv. Lett. 9, 361–368. doi:10.1111/conl.12213.

Moore, J. A. Y., Bellchambers, L. M., Depczynski, M. R., Evans, R. D., Evans, S. N., Field, S. N., et al. (2012). Unprecedented mass bleaching and loss of coral across 12° of latitude in Western Australia in 2010-11. PLoS One 7. doi:10.1371/journal.pone.0051807.

Muhlfeld, C. C., Kovach, R. P., Jones, L. A., Al-Chokhachy, R., Boyer, M. C., Leary, R. F., et al. (2014). Invasive hybridization in a threatened species is accelerated by climate change. Nat. Clim. Chang. 4, 620–624. doi:10.1038/nclimate2252.

Munday, P. L., Cheal, A. J., Dixson, D. L., Rummer, J. L., and Fabricius, K. E. (2014). Behavioural impairment in reef fishes caused by ocean acidification at CO2 seeps. Nat. Clim. Chang. 4, 487–492. doi:10.1038/nclimate2195.

Nejrup, L. B., and Pedersen, M. F. (2008). Effects of salinity and water temperature on the ecological performance of the Zostera marina. Aquat. Bot. 88, 239–246. doi:10.1016/j.aquabot.2007.10.006.

Normile, D. (2016). El Niño's warmth devastating reefs worldwide. Science 352, 15–16. doi:10.1126/science.352.6281.15.

Notz, D., and Stroeve, J. (2016). Observed Arctic sea-ice loss directly follows anthropogenic CO 2 emission. Science (80-.). 354, 747–750. doi:10.1126/science.aag2345.

O'Mahony, J., Simes, R., Redhill, D., Heaton, K., Atkinson, C., Hayward, E., et al. (2017). At What Price? The Economic, Social and Icon Value of the Great Barrier Reef. Brisbane, Australia Available at: http://elibrary.gbrmpa.gov.au/jspui/bitstream/11017/3205/1/deloitte-au-economics-great-barrier-reef-230617.pdf.

Ondiviela, B., Losada, I. J., Lara, J. L., Maza, M., Galván, C., Bouma, T. J., et al. (2014). The role of seagrasses in coastal protection in a changing climate. Coast. Eng. 87, 158–168. doi:10.1016/j.coastaleng.2013.11.005.

Ong, E. Z., Briffa, M., Moens, T., and Van Colen, C. (2017). Physiological responses to ocean acidification and warming synergistically reduce condition of the common cockle Cerastoderma edule. Mar. Environ. Res. 130, 38–47. doi:10.1016/j.marenvres.2017.07.001.

Ong, J. J. L., Nicholas Rountrey, A., Jane Meeuwig, J., John Newman, S., Zinke, J., and Gregory Meekan, M. (2015). Contrasting environmental drivers of adult and juvenile growth in a marine fish: implications for the effects of climate change. Sci. Rep. 5, 10859. doi:10.1038/srep10859.

Oxford Economics (2009). Valuing the Effects of Great Barrier Reef Bleaching. Newstead, QLD, Australia: Great Barrier Reef Foundation.

Parker, L. M., Scanes, E., O'Connor, W. A., Coleman, R. A., Byrne, M., Pörtner, H. O., et al. (2017). Ocean acidification narrows the acute thermal and salinity tolerance of the Sydney rock oyster Saccostrea glomerata. Mar. Pollut. Bull. 122, 263–271. doi:10.1016/j.marpolbul.2017.06.052.

Pauly, D., and Charles, A. (2015). Counting on small-scale fisheries. Science (80-.). 347, 242–243. doi:10.1126/science.347.6219.242-b.

Pendleton, L., Comte, A., Langdon, C., Ekstrom, J. A., Cooley, S. R., Suatoni, L., et al. (2016). Coral reefs and people in a high-CO2 world: Where can science make a difference to people? PLoS One 11, 1–21. doi:10.1371/journal.pone.0164699.

Pergent, G., Pergent-Martini, C., Bein, A., Dedeken, M., Oberti, P., Orsini, A., et al. (2015). Dynamic of Posidonia oceanica seagrass meadows in the northwestern Mediterranean: Could climate change be to blame? Comptes Rendus - Biol. 338, 484–493. doi:10.1016/j.crvi.2015.04.011.

Pespeni, M. H., Sanford, E., Gaylord, B., Hill, T. M., Hosfelt, J. D., Jaris, H. K., et al. (2013). Evolutionary change during experimental ocean acidification. Proc. Natl. Acad. Sci. 110, 6937–6942. doi:10.1073/pnas.1220673110.

Piñones, A., and Fedorov, A. V. (2016). Projected changes of Antarctic krill habitat by the end of the 21st century. Geophys. Res. Lett. 43, 8580–8589. doi:10.1002/2016GL069656.

Pinsky, M. L., Worm, B., Fogarty, M. J., Sarmiento, J. L., and Levin, S. A. (2013). Marine Taxa Track Local Climate Velocities. Science (80-.). 341, 1239–1242. doi:10.1126/science.1239352.

Poloczanska, E. S., Brown, C. J., Sydeman, W. J., Kiessling, W., Schoeman, D. S., Moore, P. J., et al. (2013). Global imprint of climate change on marine life. Nat. Clim. Chang. 3, 919–925. doi:10.1038/nclimate1958.

Poloczanska, E. S., Burrows, M. T., Brown, C. J., García Molinos, J., Halpern, B. S., Hoegh-Guldberg, O., et al. (2016). Responses of Marine Organisms to Climate Change across Oceans. Front. Mar. Sci. 3, 62. doi:10.3389/fmars.2016.00062.

Pörtner, H. O., Karl, D. M., Boyd, P. W., Cheung, W. W. L., Lluch-Cota, S. E., Nojiri, Y., et al. (2014). "Ocean Systems," in Climate Change 2014: Impacts, Adaptation, and Vulnerability. Part A: Global and Sectoral Aspects. Contribution of Working Group II to the Fifth Assessment Report of the Intergovernmental Panel on Climate Change, eds. C. B. Field, V. R. Barros, D. J. Dokken, K. J. Mach, M. D. Mastrandrea, T. E. Bilir, et al. (Cambridge, United Kingdom and New York, NY, USA: Cambridge University Press), 411–484. Available at: https://www.ipcc.ch/pdf/assessment-report/ar5/wg2/WGIIAR5-Chap6_FINAL.pdf.

Potts, W. M., Henriques, R., Santos, C. V., Munnik, K., Ansorge, I., Dufois, F., et al. (2014). Ocean warming, a rapid distributional shift, and the hybridization of a coastal fish species. Glob. Chang. Biol. 20, 2765–2777. doi:10.1111/gcb.12612.

Prentice, C., and J. T. Houghton et al., E. (2001). "The carbon cycle and atmospheric carbon dioxide" in Climate Change 2001: the Scientific Basis. Contributions of Working Group I to the Third Assessment Report of the Intergovernmental Panel on Climate Change. Cambridge Univ. Press, 183–237.

Rahmstorf, S., Box, J. E., Feulner, G., Mann, M. E., Robinson, A., Rutherford, S., et al. (2015). Exceptional twentieth-century slowdown in Atlantic Ocean overturning circulation. Nat. Clim. Chang. 5, 475–480. doi:10.1038/nclimate2554.

Rasheed, M. A., McKenna, S. A., Carter, A. B., and Coles, R. G. (2014). Contrasting recovery of shallow and deep water seagrass communities following climate associated losses in tropical north Queensland, Australia. Mar. Pollut. Bull. 83, 491–499. doi:10.1016/j.marpolbul.2014.02.013.

Raybaud, V., Beaugrand, G., Dewarumez, J.-M., and Luczak, C. (2015). Climate-induced range shifts of the American jackknife clam Ensis directus in Europe. Biol. Invasions 17, 725–741. doi:10.1007/s10530-014-0764-4.

Repolho, T., Duarte, B., Dionísio, G., Paula, J. R., Lopes, A. R., Rosa, I. C., et al. (2017). Seagrass ecophysiological performance under ocean warming and acidification. Sci. Rep. 7, 41443. doi:10.1038/srep41443.

Risser, M. D., and Wehner, M. F. (2017). Attributable human-induced changes in the likelihood and magnitude of the observed extreme precipitation during Hurricane Harvey. Geophys. Res. Lett., n/a--n/a. doi:10.1002/2017GL075888.

Rodrigues, L. C., Bergh, J. C. J. M. Van Den, Massa, F., Theodorou, J. A., Ziveri, P., and Gazeau, F. (2015). Sensitivity of Mediterranean Bivalve Mollusc Aquaculture to Climate Change, Ocean Acidification, and Other Environmental Pressures: Findings from a Producer Survey. J. Shellfish Res. 34, 1161–1176. doi:10.2983/035.034.0341.

Rodriguez, A. B., Fodrie, F. J., Ridge, J. T., Lindquist, N. L., Theuerkauf, E. J., Coleman, S. E., et al. (2014). Oyster reefs can outpace sea-level rise. Nat. Clim. Chang. 4, 493–497. doi:10.1038/nclimate2216.

Rosenzweig, C., and Solecki, W. (2014). Hurricane Sandy and adaptation pathways in New York: Lessons from a first-responder city. Glob. Environ. Chang. 28, 395–408. doi:10.1016/j.gloenvcha.2014.05.003.

Saunders, M. I., Leon, J. X., Callaghan, D. P., Roelfsema, C. M., Hamylton, S., Brown, C. J., et al. (2014). Interdependency of tropical marine ecosystems in response to climate change. Nat. Clim. Chang. 4, 724–729. doi:10.1038/NCLIMATE2274.

Shepherd, J. G., Brewer, P. G., Oschlies, A., and Watson, A. J. (2017). Ocean ventilation and deoxygenation in a warming world: introduction and overview. Philos. Trans. R. Soc. A Math. Phys. Eng. Sci. 375, 20170240. doi:10.1098/rsta.2017.0240.

Sheppard, C., Dixon, D. J., Gourlay, M., Sheppard, A., and Payet, R. (2005). Coral mortality increases wave energy reaching shores protected by reef flats: Examples from the Seychelles. Estuar. Coast. Shelf Sci. 64, 223–234. doi:10.1016/j.ecss.2005.02.016.

Shi, W., Zhao, X., Han, Y., Che, Z., Chai, X., and Liu, G. (2016). Ocean acidification increases cadmium accumulation in marine bivalves: a potential threat to seafood safety. Sci. Rep. 6, 20197. doi:10.1038/srep20197.

Short, F. T., and Neckles, H. A. (1999). The effects of global climate change on seagrasses. Aquat. Bot. 63, 169–196. doi:10.1016/S0304-3770(98)00117-X.

Shults, J. M., and Galea, S. (2017). Preparing for the Next Harvey, Irma, or Maria — Addressing Research Gaps. Perspective 363, 1–3. doi:10.1056/NEJMp1002530.

Silverman, J., Schneider, K., Kline, D. I., Rivlin, T., Rivlin, A., Hamylton, S., et al. (2014). Community calcification in Lizard Island, Great Barrier Reef: A 33year perspective. Geochim. Cosmochim. Acta 144, 72–81. doi:https://doi.org/10.1016/j.gca.2014.09.011.

Song, A. M., and Chuenpagdee, R. (2015). Interactive Governance for Fisheries. Interact. Gov. Small-Scale Fish. 5, 435–456. doi:10.1007/978-3-319-17034-3.

Spalding, M. D., Burke, L., Wood, S. A., Ashpole, J., Hutchison, J., and zu Ermgassen, P. (2017). Mapping the global value and distribution of coral reef tourism. Mar. Policy 82, 104–113. doi:10.1016/j.marpol.2017.05.014.

Spalding, M. D., Ruffo, S., Lacambra, C., Meliane, I., Hale, L. Z., Shepard, C. C., et al. (2014). The role of ecosystems in coastal protection: Adapting to climate change and coastal hazards. Ocean Coast. Manag. 90, 50–57. doi:10.1016/j.ocecoaman.2013.09.007.

Steinberg, D. K., Ruck, K. E., Gleiber, M. R., Garzio, L. M., Cope, J. S., Bernard, K. S., et al. (2015). Long-term (1993-2013) changes in macrozooplankton off the western antarctic peninsula. Deep. Res. Part I Oceanogr. Res. Pap. 101, 54–70. doi:10.1016/j.dsr.2015.02.009.

Storlazzi, C. D., Elias, E. P. L., and Berkowitz, P. (2015). Many Atolls May be Uninhabitable Within Decades Due to Climate Change. Sci. Rep. 5, 14546. doi:10.1038/srep14546.

Sydeman, W. J., Garcia-Reyes, M., Schoeman, D. S., Rykaczewski, R. R., Thompson, S. A., Black, B. A., et al. (2014). Climate change and wind intensification in coastal upwelling ecosystems. Science (80-.). 345, 77–80. doi:10.1126/science.1251635.

Telesca, L., Belluscio, A., Criscoli, A., Ardizzone, G., Apostolaki, E. T., Fraschetti, S., et al. (2015). Seagrass meadows (Posidonia oceanica) distribution and trajectories of change. Sci. Rep. 5, 12505. doi:10.1038/srep12505.

Temmerman, S., Meire, P., Bouma, T. J., Herman, P. M. J., Ysebaert, T., and De Vriend, H. J. (2013). Ecosystem-based coastal defence in the face of global change. Nature 504, 79–83. doi:10.1038/nature12859.

Tittensor, D. P., Mora, C., Jetz, W., Lotze, H. K., Ricard, D., Berghe, E. V., et al. (2010). Global patterns and predictors of marine biodiversity across taxa. Nature 466, 1098–1101. doi:10.1038/nature09329.

Turner, J., Phillips, T., Marshall, G. J., Hosking, J. S., Pope, J. O., Bracegirdle, T. J., et al. (2017). Unprecedented springtime retreat of Antarctic sea ice in 2016. Geophys. Res. Lett. 44, 6868–6875. doi:10.1002/2017GL073656.

Unsworth, R. K. F., van Keulen, M., and Coles, R. G. (2014). Seagrass meadows in a globally changing environment. Mar. Pollut. Bull. 83, 383–386. doi:10.1016/j.marpolbul.2014.02.026.

van Hooidonk, R., Maynard, J. A., Manzello, D., and Planes, S. (2014). Opposite latitudinal gradients in projected ocean acidification and bleaching impacts on coral reefs. Glob. Chang. Biol. 20, 103–112. doi:10.1111/gcb.12394.

Velez, C., Figueira, E., Soares, A. M. V. M., and Freitas, R. (2016). Combined effects of seawater acidification and salinity changes in Ruditapes philippinarum. Aquat. Toxicol. 176, 141–150. doi:10.1016/j.aquatox.2016.04.016.

Vergés, A., Doropoulos, C., Malcolm, H. A., Skye, M., Garcia-Pizá, M., Marzinelli, E. M., et al. (2016). Long-term empirical evidence of ocean warming leading to tropicalization of fish communities, increased herbivory, and loss of kelp. Proc. Natl. Acad. Sci. 113, 13791–13796. doi:10.1073/pnas.1610725113.

Verges, A., Steinberg, P. D., Hay, M. E., Poore, A. G. B., Campbell, A. H., Ballesteros, E., et al. (2014). The tropicalization of temperate marine ecosystems: climate-mediated changes in

herbivory and community phase shifts. Proc. R. Soc. B Biol. Sci. 281, 20140846–20140846. doi:10.1098/rspb.2014.0846.
Veron, J. E., Hoegh-Guldberg, O., Lenton, T. M., Lough, J. M., Obura, D. O., Pearce-Kelly, P., et al. (2009). The coral reef crisis: The critical importance of <350 ppm CO2. Mar. Pollut. Bull. 58, 1428–1436. doi:10.1016/j.marpolbul.2009.09.009.
Villamayor, B. M. R., Rollon, R. N., Samson, M. S., Albano, G. M. G., and Primavera, J. H. (2016). Impact of Haiyan on Philippine mangroves: Implications to the fate of the widespread monospecific Rhizophora plantations against strong typhoons. Ocean Coast. Manag. 132, 1–14. doi:10.1016/j.ocecoaman.2016.07.011.
Waldbusser, G. G., Hales, B., Langdon, C. J., Haley, B. A., Schrader, P., Brunner, E. L., et al. (2014). Saturation-state sensitivity of marine bivalve larvae to ocean acidification. Nat. Clim. Chang. 5, 273–280. doi:10.1038/nclimate2479.
Wang, Q., Cao, R., Ning, X., You, L., Mu, C., Wang, C., et al. (2016). Effects of ocean acidification on immune responses of the Pacific oyster Crassostrea gigas. Fish Shellfish Immunol. 49, 24–33. doi:10.1016/j.fsi.2015.12.025.
Washington State Blue Ribbon Panel on Ocean Acidification (2012). Ocean Acidification: From Knowledge to Action, Washington State’s Strategic Response. Olympia, WA, USA: Washington Department of Ecology.
Weatherdon, L. V., Magnan, A. K., Rogers, A. D., Sumaila, U. R., and Cheung, W. W. L. (2016). Observed and Projected Impacts of Climate Change on Marine Fisheries, Aquaculture, Coastal Tourism, and Human Health: An Update. Front. Mar. Sci. 3, 48. doi:10.3389/fmars.2016.00048.
Widlansky, M. J., Timmermann, A., and Cai, W. (2015). Future extreme sea level seesaws in the tropical Pacific. Sci. Adv. 1. doi:10.1126/sciadv.1500560.
Wittmann, A. C., and Pörtner, H.-O. (2013). Sensitivities of extant animal taxa to ocean acidification. Nat. Clim. Chang. 3, 995–1001. doi:10.1038/nclimate1982.
York, P. H., Gruber, R. K., Hill, R., Ralph, P. J., Booth, D. J., and Macreadie, P. I. (2013). Physiological and morphological responses of the temperate seagrass Zostera muelleri to multiple stressors: Investigating the interactive effects of light and temperature. PLoS One 8. doi:10.1371/journal.pone.0076377.
York, P. H., Smith, T. M., Coles, R. G., McKenna, S. A., Connolly, R. M., Irving, A. D., et al. (2016). Identifying knowledge gaps in seagrass research and management: An Australian perspective. Mar. Environ. Res., 1–10. doi:10.1016/j.marenvres.2016.06.006.
Zhao, X., Shi, W., Han, Y., Liu, S., Guo, C., Fu, W., et al. (2017). Ocean acidification adversely influences metabolism, extracellular pH and calcification of an economically important marine bivalve, Tegillarca granosa. Mar. Environ. Res. 125, 82–89. doi:10.1016/j.marenvres.2017.01.007.
Zittier, Z. M. C., Bock, C., Lannig, G., and Pörtner, H. O. (2015). Impact of ocean acidification on thermal tolerance and acid-base regulation of Mytilus edulis (L.) from the North Sea. J. Exp. Mar. Bio. Ecol. 473, 16–25. doi:10.1016/j.jembe.2015.08.001.

3.SM.3.3 Supplementary Information to Section 3.4.13

3.SM.3.3.1 Temperature-Related Morbidity and Mortality

Detection and attribution studies show heat-related mortality in some locations has increased because of climate change (Ebi et al. 2017), alongside evidence of acclimatization and adaptation reducing mortality, particularly in high-income countries (Arbuthnott et al. 2016; Chung et al. 2017; de' Donato et al. 2015; Bobb et al. 2014; Lee et al. 2014) with future adaptation trends uncertain.

The projected risks of heat-related morbidity and mortality are generally higher under warming of 2°C than 1.5°C, with projections of greater exposure to high ambient temperatures and increased morbidity and mortality (Section 3.4.7). This indicates a transition in risk between 1.5°C and 2°C (*medium confidence*). The extent of the increase will depend on adaptation (until mid-century) and on adaptation and mitigation later in the century (Smith et al. 2014). Under 1.5°C, most risks associated with exposure to heat could be reduced through adaptation. Risks under warming of 2°C will depend on the timing of when temperature targets are met and on development choices, such as modifying urban infrastructure to reduce heat islands. The longer the delay in reaching 2°C, and the more resilient and sustainable the development pathway, the lower the expected health risks (Sellers and Ebi 2017). Confidence in these assessments of risk range from medium to high (Figure 3.20).

Heat-related mortality	White to Yellow	Begin	0
		End	1
	Yellow to Red	Begin	1
		End	3
	Red to Purple	Begin	no transition to purple
		End	no transition to purple

3.SM.3.3.2 Tourism

Changing weather patterns, extreme weather and climate events, and sea level rise are affecting global tourism investments, environment and cultural destination assets, operational and transportation costs, and tourist demand patterns (Section 3.4.9.1). Assets being affected include biodiversity, beaches, coral reefs, glaciers, and other environmental and cultural assets. 'Last chance' tourism markets are developing based on observed impacts on environmental and cultural heritage. Available evidence suggests that the transistion in risks for tourism have occurred between 0°C and 1ºC (*high confidence*), with *medium confidence* that risks transition to high risks of impacts somewhere between 1°C to 3°C.

Based on limited analyses, risks to the tourism sector are higher at 2°C than at 1.5°C, with greater impacts on climate-sensitive sun, beach and snow sports tourism markets. The degradation or loss of coral reef systems will increase the risks for coastal tourism, particularly in sub-tropical and tropical regions.

Tourism	White to Yellow	Begin	0
		End	1.5
	Yellow to Red	Begin	1.5
		End	3
	Red to Purple	Begin	no transition to purple
		End	no transition to purple

3.SM.3.3.3 Coastal Flooding

Sea level rise and coastal flooding have been observed or projected to be defined by all but two (iv, viii) of the overarching key risks identified by O'Neill et al. (2017). Even without climate change, flooding occurs. Hence it is important to determine the contribution climate change has made to this. Furthermore, the severity and extent of coastal flooding is highly dependent on the rate and timing of sea level rise based on emissions (and therefore commitment to sea level rise) (Section 3.3.9; Section 13.4 in Church et al. 2013; AR5;), plus the ability to adapt (Section 3.4.5.7 and 5.4; Wong et al. 2014; AR5).

Sea level rise has been occurring naturally for hundreds of years Church et al. 2013;Section 13.2; Kopp et al. 2016). It has and will be enhanced by man-made climate change, whilst acknowledging rates of decadal change due to natural conditions (e.g., White et al. 2005). Early signs of sea level rise departing from Holocene rates were reported since approximately 1900 (Jevrejeva et al. 2014; Dangendorf et al. 2015; Kopp et al. 2016), analogous to temperatures approximately 0.1°C above pre-industrial levels. It is very likely that global mean sea level rise was 1.7 [1.5–1.9] mm yr^{-1} between 1901 and 2010, but from 1993 to 2010 the rate was very likely higher at 3.2 [2.8 to 3.6] mm yr^{-1} (Church et al. 2013; Sections 13.2.2.1 and Section 13.2.2.2). Climate-change induced sea level rise has been detectable and attributable for a few decades (Slangen et al. 2016; Kjeldsen et al. 2015; Rignot et al. 2011; Nerem et al. 2018), occurring around 0.3°C rise above pre-industrial levels.

The ability to adapt to changing sea levels is variable between natural and human systems (Nicholls et al. 2007; Sections 6.4 and 6.6; Wong et al. 2014; AR5; Section 5.4). Adaptation may happen more effectively or be more advanced in some nations or communities over others (Section 3.4.5.7; Araos et al. 2016; Ford et al. 2015). Whilst acknowledging that sensitive environments experience the adverse effects of climate-change-induced sea level rise today, analysis suggests that impacts could be more widespread in sensitive systems and ongoing at 1.7°C of temperature rise with respect to pre-industrial levels, even when considering adaptation measures.

Risks of impacts transitioned from non-detectible to moderate between 0.1°C-0.3°C (*medium confidence*), and from moderate to high levels of risk between 0.3ºC and 0.7ºC (*high confidence*). The transition from high to very high risks is projected to occur between 1.7°C and 2.5°C (*high confidence*).

Coastal flooding	White to Yellow	Begin	0.1
		End	0.3
	Yellow to Red	Begin	0.3
		End	1.7
	Red to Purple	Begin	1.7
		End	2.5

3.SM.3.3.4 Fluvial Flooding

Research shows that flood frequency has increased, although there is limited evidence of a decrease in flood magnitude in some regions (Section 3.3.5.1). Tanoue et al. (2016) detected the increase of frequency and magnitude of flood that is attributed to climate change, and found that growing exposure of people and assets to flood according to the increase of population and economy exacerbated flood damage. Therefore, it is concluded that the current status, compared to the pre-industrial level, should be moderate.

In general, fluvial flooding at 1.5°C is projected to be lower than at 2°C, and at both levels of warming projected changes in the magnitude and frequency of flood create regionally differentiated risks (Section 3.4.2). Alfieri et al.'s (2017) study clearly points out a positive correlation between global warming and global flood risk. The projected number of the global population exposed to flood risk increases quadratically as the temperature rises from 1.5°C to 4°C, in which the population affected by river floods is increased by 100% at 1.5°C, 170% at 2°C and 580% at 4.0°C relative to the baseline period (1976–2005) (Alfieri et al. 2017). Relative changes in population affected and economic damage at 2°C warming are projected to exceed 200% in 20 and in 19 countries, respectively (Alfieri et al. 2017). Therefore, it is concluded that the transition to high risk should be at 2°C warming. Warming of 4°C from the pre-industrial level is projected to be a threefold increase of the proportion of the global population who are exposed to a 20th century 100-year fluvial flood compared to the warming of 1.6°C, while the 4.0°C warming is 14 times as high as present-day exposure (Hirabayashi et al. 2013).

The above-mentioned assessments assume the population is constant, although the variation between socio-economic differences is greater than the variation between the extent of the global warming, resulting in a change in the magnitude of the flood risks; however, these changes are not considered in this context.

Meanwhile, Kinoshita et al. (2018) indicate that potential economic loss can be halved by autonomous adaptation. However, few studies assess quantitative mitigation by adaptation, therefore transition to very high risk (red to purple) is not applicable.

Fluvial flooding	White to Yellow	Begin	0
		End	1.5
	Yellow to Red	Begin	1.5
		End	2
	Red to Purple	Begin	N/A
		End	N/A

3.SM.3.3.5 Crop Yields

Scientific literature shows that climate change resulted in changes in the production levels of the main agricultural crops. Crop yields showed contrasting patterns depending on cultivar, geographical area and response to CO_2 fertilization effect, resulting in a transition from no risk (white) to moderate risk (yellow) below recent temperatures (*high confidence*).

The projected risks for several cropping systems are generally higher under warming of 2°C than of 1.5°C (Section 3.4.6), with different impacts depending on geographical area. The most significant crop yield declines are found in West Africa, Southeast Asia, and Central and South America (Section 3.4.6), whilst less-pronounced yield reductions are expected for northern latitudes. Globally, this indicates a different adaptation capacity among the several cropping systems, thus suggesting a transition in risk from moderate (yellow) to high risk (red) between 1.5ºC and 2.5°C (*medium confidence*).

Crop yields	White to Yellow	Begin	0.5
		End	0.8
	Yellow to Red	Begin	1.5
		End	2.5

	Red to Purple	Begin	N/A
		End	N/A

3.SM.3.3.6 Arctic

High-latitude tundra and boreal forest are particularly at risk, and woody shrubs are already encroaching into the tundra (*high confidence*, Section 3.4.3). These impacts had already been detected at recent temperatures (0.7ºC) hence locating transition from undetected to moderate risk between 0ºC and 0.7ºC, but further impacts have been detected more recently and risks increase further with warming (Section 3.4.2).

Model simulations project that there will be least one sea ice-free Arctic summer per decade at 2°C, while this is one per century at 1.5°C. (*high confidence*) (Sections 3.3.8, 3.4.4.7). Further warming is projected to cause greater effects in a 2°C world than a 1.5°C world; for example, limiting warming to 1.5°C would prevent the loss of an estimated permafrost area of 2 million km^2 over future centuries compared to 2°C (*high confidence*) (Sections 3.3.2, 3.4.3, 3.5.5). A transition from high (red) to very high (purple) risk is therefore located between 1.5ºC and 2ºC (*high confidence*).

Arctic	White to Yellow	Begin	0
		End	0.7
	Yellow to Red	Begin	0.7
		End	1.5
	Red to Purple	Begin	1.5
		End	2

3.SM.3.3.7 Terrestrial Ecosystems

Detection and attribution studies show that impacts of climate change on terrestrial ecosystems have been taking place in the last few decades, indicating a transition from no risk (white) to moderate risk (yellow) below recent temperatures.

The projected risks to unique and threatened terrestrial ecosystems are generally higher under warming of 2°C than 1.5°C (Section 3.4.3; *high confidence*). Globally, effects on terrestrial biodiversity escalate significantly between these two levels of warming. Key examples of this include much more extensive shifts of biomes (major ecosystem types) and a doubling or tripling of the number of plants, animals or insects losing over half of their climatically determined geographic ranges (Section 3.4.3). This indicates a transition in risk from moderate (yellow) to high risk (red) between 1.5°C and 2°C (*high confidence*); however, since some systems and species are unable to adapt to levels of warming below 2°C, the transition to high risk is located below 2°C. By 3°C, biome shifts and species range losses escalate to very high levels and the systems have very little capacity to adapt (Section 3.4.3).

Terrestrial ecosystems	White to Yellow	Begin	0.3
		End	0.5
	Yellow to Red	Begin	0.5
		End	1.8
	Red to Purple	Begin	2.0
		End	3.0

3.SM.3.3.8 Mangroves

Recent literature is consistent with previous conclusions regarding the complex changes facing mangroves, together with increasing concern regarding the interaction between climate change (e.g., elevated air and water temperatures, drought and sea level rise) and local factors (deforestation, damming of catchments and reduced sediment and freshwater) as outlined below (Alongi, 2015; Feller et al., 2017). Decreases in the supply of sediments to deltas and coastal areas is impeding the ability of most mangroves (69% of sites) to keep pace with sea level rise through shoreward migration (Lovelock et al., 2015). At the same time, recent extremes associated with El Niño have also had large-scale impacts (e.g., extreme low sea level events; Duke et al., 2017; Lovelock et al., 2017). Shoreward migration is also challenged by the increasing amounts of coastal infrastructure preventing the relocation of mangroves (Di Nitto et al., 2014; Saunders et al., 2014). In some areas, mangroves are increasing in distribution (Godoy and De Lacerda, 2015). The total losses projected for mangrove loss (10–15%) under a 0.6 m sea level rise continue to be dwarfed by the loss of mangroves to deforestation (1–2% per annum).

However, given the scale of the dieback of mangroves in Australia’s Gulf of Carpentaria (in 2015–2016), as well as evidence that similar conditions to those of 2015–2016 (extreme heat and low tides) and the projection of greater El Niño-Southern Oscillation (ENSO) variability, (Widlansky et al., 2015; Risser and Wehner, 2017), the risks from climate change for mangroves were judged to be higher than assessed by AR5, and subsequently by Gattuso et al. (2015), leading to the transitions having greater risk of occurring (Figure 3.18). Formal attribution of recent extreme events on mangroves to climate change, however, is at an early stage (*medium agreement, limited data, hence low-medium confidence*).
See accompanying assessment by Gattuso et al. (2015) in Suplementary Material 3.SM.3.2, Supplementary information to Section 3.4.4.

Mangroves	White to Yellow	Begin	1.3
		End	1.5 (2.5)*
	Yellow to Red	Begin	2.5
		End	2.7
	Red to Purple	Begin	NA
		End	NA

3.SM.3.3.9 Warm-Water Corals

The exceptionally warm conditions of 2015–2017 drove an unprecedented global mass coral bleaching and mortality event which affected coral reefs in a large number of countries (information still being gathered at time of writing; Normile, 2016). In the case of Australia, 50% of shallow-water reef-building corals across the Great Barrier Reef died in unprecedented back-to-back bleaching events (Hughes et al., 2017). Elevated sea temperatures and record mortalities were recorded from the central to the far northern sectors of the Great Barrier Reef. Similar effects occurred in a range of regions, including the Indian Ocean, the western Pacific, Hawaii and the Caribbean Sea (Normile, 2016). The set of events has increased risk with current conditions being of high risk, and even low levels of future climate change having series implications for coral reefs. There continues to be a *high* to *very high* level of confidence as to where the transitions between risk levels due to climate change are located.

The unprecedented thermal stress along many tropical coastlines over the past three years (2015–2017) has led to extraordinary changes to coral reefs across the planet (as described above). The advent of back-to-back bleaching events, which were projected to occur around mid-century, appear to have already begun to occur as demonstrated by impacts on warm-water corals and hence coral reefs. While corals were already stressed from climate change, and are in decline in many parts of the world, the scale and impact of recent events suggests that risk levels for the transitions between risk categories need to be adjusted to represent the current status of corals and coral reefs. For this reason, expert consultation since 2015 concluded that the transition from undetectable to moderate risk has already occurred (0.2°C to 0.4°C; *high confidence*). Similarly, the transition from moderate to high levels of risks for warm-water corals occurred approximately from 0.4°C to 0.6°C (*high confidence*). In line with these changes, the transition from high to very high levels of risk are associated with increases in GMST from 0.6°C to 1.2°C (*high confidence*) above the pre-industrial period.See accompanying assessment by Gattuso et al. (2015) in Suplementary Material 3.SM.3.2.

Warm-water corals	White to Yellow	Begin	0.2
		End	0.4
	Yellow to Red	Begin	0.4
		End	0.6
	Red to Purple	Begin	0.6
		End	1.2

3.SM.3.3.10 Small-Scale Fin-Fish Fisheries (Low Latitude)

Small-scale fin-fish fisheries (low latitude) provide food for millions of people along tropical coastlines and hence play an important role in the food security of a large number of countries (McClanahan et al., 2015; Pauly and Charles, 2015). In many cases, populations are heavily dependent on these sources of protein given the lack of alternatives (Cinner et al., 2012, 2016; Pendleton et al., 2016). The climate-related stresses affecting fin fish (see Section 'Fin fish' above), however, are producing a number of challenges for small-scale fisheries based on these species (e.g., (Kittinger, 2013; Pauly and Charles, 2015; Bell et al., 2017). Recent literature (2015–2017) has continued to outline growing threats from the rapid shifts in the biogeography of key species (Poloczanska et al., 2013, 2016; Burrows et al., 2014; García Molinos et al., 2015) and the ongoing rapid degradation of key habitats such as coral reefs, seagrass and mangroves (see Sections above on 'Seagrasses (mid-latitude)', 'Mangroves' and 'Pteropods', as well as Chapter 3, Box 3.4). As these changes have accelerated, so have the risks to the food and livelihoods associated with small-scale fisheries (Cheung et al., 2010). These risks have compounded with non-climate-related stresses (e.g., pollution, overfishing, unsustainable coastal development) to drive many small-scale fisheries well below the sustainable harvesting levels required to keep these resources functioning as a source of food (McClanahan et al., 2009, 2015; Pendleton et al., 2016). As a result, projections of climate change and the growth in human populations increasingly predict shortages of fish protein for many regions (e.g., Pacific, e.g., Bell et al., 2013, 2017; Indian Ocean, e.g., McClanahan et al., 2015). Mitigation of these risks involved marine spatial planning, fisheries repair, sustainable aquaculture and the development of alternative livelihoods (Kittinger, 2013; McClanahan et al., 2015; Song and Chuenpagdee, 2015; Weatherdon et al., 2016). Threats to small-scale fisheries have also come from the increasing incidence of alien (nuisance) species as well as an increasing incidence of disease, although the literature on these threats is at a low level of development and understanding (Kittinger et al., 2013; Weatherdon et al., 2016).

As assessed by Gattuso et al. (2015), risks of impacts on small-scale fisheries are moderate today, but are expected to reach very high levels under scenarios extending beyond RCP2.6. The research literature plus the growing evidence that many countries will have trouble adapting to these changes place confidence at a high level as to the risks of climate change on low latitude in fisheries. These effects are more sensitive, hence the higher risks at lower levels of temperature change.

Small-scale fisheries are highly dependent on healthy coastal ecosystems. With the growing evidence of impacts described above, the loss of habitat for small-scale fisheries is intensifying the risks of impact from climate change. For this reason, expert consensus has judged that risks have become greater since the assessment of Gattuso et al. (2015). Therefore, the transition from undetectable to moderate levels of risk is projected to occur between 0.5°C and 0.7°C (*high confidence*), with the transition from moderate to high levels of risk occurring between 0.9°C and 1.1°C (*medium confidence*). The transition from high to very high levels of risk of impact is being judged to occur between 2.0°C and 2.5°C (*high confidence*).

See accompanying assessment by Gattuso et al. (2015) Suplementary Material 3.SM.3.2.

Small-scale fin-fish fisheries (low latitude)	White to Yellow	Begin	0.5
		End	0.7
	Yellow to Red	Begin	0.9
		End	1.1
	Red to Purple	Begin	2
		End	2.5

References

Alfieri, L., B. Bisselink, F. Dottori, G. Naumann, A. de Roo, P. Salamon, K. Wyser, and L. Feyen, 2017: Global projections of river flood risk in a warmer world. Earth's Futur., 5, 171–182, doi:10.1002/2016EF000485. http://doi.wiley.com/10.1002/2016EF000485 (Accessed March 26, 2017).

Alongi, D. M., 2015: The Impact of Climate Change on Mangrove Forests. Curr. Clim. Chang. Reports, 1, 30–39, doi:10.1007/s40641-015-0002-x. http://link.springer.com/10.1007/s40641-015-0002-x.

Araos, M., L. Berrang-Ford, J. D. Ford, S. E. Austin, R. Biesbroek, and A. Lesnikowski, 2016: Climate change adaptation planning in large cities: A systematic global assessment. Environ. Sci. Policy, 66, 375–382, doi:10.1016/j.envsci.2016.06.009. http://dx.doi.org/10.1016/j.envsci.2016.06.009.

Arbuthnott, K., S. Hajat, C. Heaviside, and S. Vardoulakis, 2016: Changes in population susceptibility to heat and cold over time: assessing adaptation to climate change. Environ. Heal., 15, S33, doi:10.1186/s12940-016-0102-7. http://www.ncbi.nlm.nih.gov/pubmed/26961541 (Accessed July 19, 2017).

Bell, J. D., and Coauthors, 2013: Mixed responses of tropical Pacific fisheries and aquaculture to climate change. Nat. Clim. Chang., 3, 591–599, doi:10.1038/nclimate1838. https://www.nature.com/nclimate/journal/v3/n6/pdf/nclimate1838.pdf (Accessed July 7, 2017).

Bell, J. D., and Coauthors, 2017: Adaptations to maintain the contributions of small-scale fisheries to food security in the Pacific Islands. Mar. Policy, doi:10.1016/j.marpol.2017.05.019.

Bobb, J. F., R. D. Peng, M. L. Bell, and F. Dominici, 2014: Heat-Related Mortality and Adaptation to Heat in the United States. Environ. Health Perspect., doi:10.1289/ehp.1307392. http://ehp.niehs.nih.gov/1307392/ (Accessed May 26, 2018).

Burrows, M. T., and Coauthors, 2014: Geographical limits to species-range shifts are suggested by climate velocity. Nature, 507, 492–495, doi:10.1038/nature12976. http://www.nature.com/doifinder/10.1038/nature12976 (Accessed April 7, 2017).

Cheung, W. W. L., V. W. Y. Lam, J. L. Sarmiento, K. Kearney, R. Watson, D. Zeller, and D. Pauly, 2010: Large-scale redistribution of maximum fisheries catch potential in the global ocean under climate change. Glob. Chang. Biol., 16, 24–35, doi:10.1111/j.1365-2486.2009.01995.x. http://doi.wiley.com/10.1111/j.1365-2486.2009.01995.x (Accessed April 11, 2017).

Chung, E. S., H.-K. Cheong, J.-H. Park, J.-H. Kim, and H. Han, 2017: Current and Projected Burden of Disease From High Ambient Temperature in Korea. Epidemiology, 28, S98–S105.

Church, J. a., and Coauthors, 2013: Sea level change. Clim. Chang. 2013 Phys. Sci. Basis. Contrib.

Work. Gr. I to Fifth Assess. Rep. Intergov. Panel Clim. Chang., 1137–1216, doi:10.1017/CB09781107415315.026.
Cinner, J. E., and Coauthors, 2012: Vulnerability of coastal communities to key impacts of climate change on coral reef fisheries. Glob. Environ. Chang., 22, 12–20, doi:10.1016/j.gloenvcha.2011.09.018. http://linkinghub.elsevier.com/retrieve/pii/S0959378011001579 (Accessed July 7, 2017).
Cinner, J. E., and Coauthors, 2016: A framework for understanding climate change impacts on coral reef social–ecological systems. Reg. Environ. Chang., 16, 1133–1146, doi:10.1007/s10113-015-0832-z. http://link.springer.com/10.1007/s10113-015-0832-z (Accessed July 11, 2017).
Dangendorf, S., M. Marcos, A. Müller, E. Zorita, R. Riva, K. Berk, and J. Jensen, 2015: Detecting anthropogenic footprints in sea level rise. Nat. Commun., 6, 7849. http://dx.doi.org/10.1038/ncomms8849.
de' Donato, F. K., and Coauthors, 2015: Changes in the Effect of Heat on Mortality in the Last 20 Years in Nine European Cities. Results from the PHASE Project. Int. J. Environ. Res. Public Health, 12, 15567–15583, doi:10.3390/ijerph121215006. http://www.ncbi.nlm.nih.gov/pubmed/26670239 (Accessed July 19, 2017).
Duke, N. C., and Coauthors, 2017: Large-scale dieback of mangroves in Australia's Gulf of Carpentaria: A severe ecosystem response, coincidental with an unusually extreme weather event. Mar. Freshw. Res., 68, 1816–1829, doi:10.1071/MF16322.
Ebi, K., N. Ogden, J. Semenza, and A. Woodward, 2017: Detecting and Attributing Health Burdens to Climate Change. Environ. Health Perspect., 125, 085004, doi:10.1289/EHP1509.
Feller, I. C., D. A. Friess, K. W. Krauss, and R. R. Lewis, 2017: The state of the world's mangroves in the 21st century under climate change. Hydrobiologia, 803, 1–12, doi:10.1007/s10750-017-3331-z. http://link.springer.com/10.1007/s10750-017-3331-z.
Ford, J. D., G. McDowell, and T. Pearce, 2015: The adaptation challenge in the Arctic. Nat. Clim. Chang., 5, 1046–1053, doi:10.1038/nclimate2723.
García Molinos, J., and Coauthors, 2015: Climate velocity and the future global redistribution of marine biodiversity. Nat. Clim. Chang., 6, 83–88, doi:10.1038/nclimate2769. http://www.nature.com/doifinder/10.1038/nclimate2769 (Accessed April 7, 2017).
Gattuso, J.-P., and Coauthors, 2015: Contrasting futures for ocean and society from different anthropogenic CO2 emissions scenarios. Science (80-.)., 349, aac4722, doi:10.1126/science.aac4722. http://www.sciencemag.org/cgi/doi/10.1126/science.aac4722.
Godoy, M. D. P., and L. D. De Lacerda, 2015: Mangroves Response to Climate Change: A Review of Recent Findings on Mangrove Extension and Distribution. An Acad Bras CiencAnnals Brazilian Acad. Sci., 87, 651–667, doi:10.1590/0001-3765201520150055. www.scielo.br/aabc%5Cnhttp://dx.doi.org/10.1590/0001-3765201520150055.
Hirabayashi, Y., R. Mahendran, S. Koirala, L. Konoshima, D. Yamazaki, S. Watanabe, H. Kim, and S. Kanae, 2013: Global flood risk under climate change. Nat. Clim. Chang., 3, 816–821, doi:10.1038/nclimate1911. http://www.nature.com/doifinder/10.1038/nclimate1911 (Accessed April 5, 2017).
Hughes, T. P., and Coauthors, 2017: Global warming and recurrent mass bleaching of corals. Nature, 543, 373–377, doi:10.1038/nature21707. http://www.nature.com/doifinder/10.1038/nature21707.
Jevrejeva, S., J. C. Moore, A. Grinsted, A. P. Matthews, and G. Spada, 2014: Trends and acceleration in global and regional sea levels since 1807. Glob. Planet. Change, 113, 11–22, doi:https://doi.org/10.1016/j.gloplacha.2013.12.004. http://www.sciencedirect.com/science/article/pii/S0921818113002750.
Kinoshita, Y., M. Tanoue, S. Watanabe, and Y. Hirabayashi, 2018: Quantifying the effect of autonomous adaptation to global river flood projections: Application to future flood risk assessments. Environ. Res. Lett., 13, 014006, doi:10.1088/1748-9326/aa9401. http://iopscience.iop.org/article/10.1088/1748-9326/aa9401.
Kittinger, J. N., 2013: Human Dimensions of Small-Scale and Traditional Fisheries in the Asia-Pacific Region. Pacific Sci., 67, 315–325, doi:10.2984/67.3.1. http://www.bioone.org/doi/10.2984/67.3.1.
——, and Coauthors, 2013: Emerging frontiers in social-ecological systems research for sustainability

of small-scale fisheries. Curr. Opin. Environ. Sustain., 5, 352–357, doi:10.1016/j.cosust.2013.06.008.
Kjeldsen, K. K., and Coauthors, 2015: Spatial and temporal distribution of mass loss from the Greenland Ice Sheet since AD 1900. Nature, 528, 396. http://dx.doi.org/10.1038/nature16183.
Kopp, R., and Coauthors, 2016: Temperature-driven global sea-level variability in the Common Era. Proc. Natl. Acad. Sci., 113, 1434–1441.
Lee, M., F. Nordio, A. Zanobetti, P. Kinney, R. Vautard, and J. Schwartz, 2014: Acclimatization across space and time in the effects of temperature on mortality: a time-series analysis. Environ. Heal., 13, 89, doi:10.1186/1476-069X-13-89. https://doi.org/10.1186/1476-069X-13-89.
Lovelock, C. E., and Coauthors, 2015: The vulnerability of Indo-Pacific mangrove forests to sea-level rise. Nature, 526, 559–563, doi:10.1038/nature15538. http://www.nature.com/doifinder/10.1038/nature15538.
——, I. C. Feller, R. Reef, S. Hickey, and M. C. Ball, 2017: Mangrove dieback during fluctuating sea levels. Sci. Rep., 7, 1680, doi:10.1038/s41598-017-01927-6. http://www.nature.com/articles/s41598-017-01927-6.
McClanahan, T. R., J. C. Castilla, A. T. White, and O. Defeo, 2009: Healing small-scale fisheries by facilitating complex socio-ecological systems. Rev. Fish Biol. Fish., 19, 33–47, doi:10.1007/s11160-008-9088-8.
McClanahan, T. R., E. H. Allison, and J. E. Cinner, 2015: Managing fisheries for human and food security. Fish Fish., 16, 78–103, doi:10.1111/faf.12045.
Nerem, R. S., B. D. Beckley, J. T. Fasullo, B. D. Hamlington, D. Masters, and G. T. Mitchum, 2018: Climate-change-driven accelerated sea-level rise detected in the altimeter era. Proc. Natl. Acad. Sci., 115, 2022–2025, doi:10.1073/pnas.1717312115. http://www.pnas.org/content/115/9/2022.
Nicholls, R. J., P. P. Wong, V. R. Burkett, J. O. Codignotto, J. E. Hay, R. F. McLean, S. Ragoonaden, and C. . Woodroffe, 2007: Coastal systems and low-lying areas. Climate Change 2007: Impacts, Adaptation and Vulnerability. Contribution of Working Group II to the Fourth Assessment Report of the Intergovernmental Panel on Climate Change, M.L. Parry, O.F. Canziani, J.P. Palutikof, P.J. Van der Linden, and C.E. Hanson, Eds., Cambridge University Press, Cambridge, UK, 315–356.
Di Nitto, D., G. Neukermans, N. Koedam, H. Defever, F. Pattyn, J. G. Kairo, and F. Dahdouh-Guebas, 2014: Mangroves facing climate change: Landward migration potential in response to projected scenarios of sea level rise. Biogeosciences, 11, 857–871, doi:10.5194/bg-11-857-2014.
Normile, D., 2016: El Niño’s warmth devastating reefs worldwide. Science, 352, 15–16, doi:10.1126/science.352.6281.15. http://www.ncbi.nlm.nih.gov/pubmed/27034348.
O’Neill, B. C., and Coauthors, 2017: IPCC Reasons for Concern regarding climate change risks. Nat. Clim. Chang., 7, 28–37, doi:10.1038/nclimate3179.
Pauly, D., and A. Charles, 2015: Counting on small-scale fisheries. Science (80-.)., 347, 242–243, doi:10.1126/science.347.6219.242-b. http://www.sciencemag.org/cgi/doi/10.1126/science.347.6219.242-b.
Pendleton, L., and Coauthors, 2016: Coral reefs and people in a high-CO2 world: Where can science make a difference to people? PLoS One, 11, 1–21, doi:10.1371/journal.pone.0164699.
Poloczanska, E. S., and Coauthors, 2013: Global imprint of climate change on marine life. Nat. Clim. Chang., 3, 919–925, doi:10.1038/nclimate1958. http://www.nature.com/articles/nclimate1958.
——, and Coauthors, 2016: Responses of Marine Organisms to Climate Change across Oceans. Front. Mar. Sci., 3, 62, doi:10.3389/fmars.2016.00062. http://journal.frontiersin.org/Article/10.3389/fmars.2016.00062/abstract (Accessed June 26, 2017).
Rignot, E., I. Velicogna, van den Broeke M. R., A. Monaghan, and J. T. M. Lenaerts, 2011: Acceleration of the contribution of the Greenland and Antarctic ice sheets to sea level rise. Geophys. Res. Lett., 38, doi:10.1029/2011GL046583. https://agupubs.onlinelibrary.wiley.com/doi/abs/10.1029/2011GL046583.
Risser, M. D., and M. F. Wehner, 2017: Attributable human-induced changes in the likelihood and

magnitude of the observed extreme precipitation during Hurricane Harvey. Geophys. Res. Lett., n/a--n/a, doi:10.1002/2017GL075888. http://dx.doi.org/10.1002/2017GL075888.
Saunders, M. I., and Coauthors, 2014: Interdependency of tropical marine ecosystems in response to climate change. Nat. Clim. Chang., 4, 724–729, doi:10.1038/NCLIMATE2274.
Sellers, S., and K. L. Ebi, 2017: Climate Change and Health under the Shared Socioeconomic Pathway Framework. Int. J. Environ. Res. Public Health, 15, 3, doi:10.3390/ijerph15010003. http://www.ncbi.nlm.nih.gov/pmc/articles/PMC5800104/.
Slangen, A. B. A., J. A. Church, C. Agosta, X. Fettweis, B. Marzeion, and K. Richter, 2016: Anthropogenic forcing dominates global mean sea-level rise since 1970. Nat. Clim. Chang., 6, 701–705, doi:10.1038/nclimate2991.
Smith, K. R., and Coauthors, 2014: Human Health: Impacts, Adaptation, and Co-Benefits. Climate Change 2014: Impacts, Adaptation, and Vulnerability. Part A: Global and Sectoral Aspects. Contribution of Working Group II to the Fifth Assessment Report of the Intergovernmental Panel on Climate Change, C.B. Field et al., Eds., Cambridge University Press, Cambridge, United Kingdom and New York, NY, USA, 709–754 http://www.ipcc.ch/pdf/assessment-report/ar5/wg2/WGIIAR5-Chap11_FINAL.pdf (Accessed March 27, 2017).
Song, A. M., and R. Chuenpagdee, 2015: Interactive Governance for Fisheries. Interact. Gov. Small-Scale Fish., 5, 435–456, doi:10.1007/978-3-319-17034-3.
Tanoue, M., Y. Hirabayashi, H. Ikeuchi, E. Gakidou, and T. Oki, 2016: Global-scale river flood vulnerability in the last 50 years. Sci. Rep., 6, 36021, doi:10.1038/srep36021. http://www.nature.com/articles/srep36021 (Accessed April 7, 2017).
Weatherdon, L. V., A. K. Magnan, A. D. Rogers, U. R. Sumaila, and W. W. L. Cheung, 2016: Observed and Projected Impacts of Climate Change on Marine Fisheries, Aquaculture, Coastal Tourism, and Human Health: An Update. Front. Mar. Sci., 3, 48, doi:10.3389/fmars.2016.00048. http://journal.frontiersin.org/Article/10.3389/fmars.2016.00048/abstract (Accessed June 26, 2017).
White, N., J. Church, and J. Gregory, 2005: Coastal and global averaged sea level rise for 1950 to 2000. Geophys. Res. Lett., 32, doi:10.1029/2004GL021391. https://agupubs.onlinelibrary.wiley.com/doi/abs/10.1029/2004GL021391.
Widlansky, M. J., A. Timmermann, and W. Cai, 2015: Future extreme sea level seesaws in the tropical Pacific. Sci. Adv., 1, doi:10.1126/sciadv.1500560. http://advances.sciencemag.org/content/1/8/e1500560.
Wong, P. P., I. J. Losada, J.-P. Gattuso, J. Hinkel, A. Khattabi, K. L. McInnes, Y. Saito, and A. Sallenger, 2014: Coastal Systems and Low-Lying Areas. Climate Change 2014: Impacts, Adaptation, and Vulnerability. Part A: Global and Sectoral Aspects. Contribution of Working Group II to the Fifth Assessment Report of the Intergovernmental Panel on Climate Change, C.B. Field et al., Eds., Cambridge University Press, Cambridge, United Kingdom and New York, NY, USA, 361–409 https://www.ipcc.ch/pdf/assessment-report/ar5/wg2/WGIIAR5-Chap5_FINAL.pdf.

3.SM.3.4 Supplementary Information to Section 3.4.7 Human health

Table 3.SM.7: Decades when 1.5°C, 2°C and higher degrees of warming are reached for multi-climate model means

Generation	Scenario	Decade 1.5°C reached	Decade 2°C reached	dT 2080–2099	dT 2090–2099
SRES	B1	2039–2048	2065–2074	2.18	2.27
SRES	A1b	2029–2038	2045–2054	3.00	3.21
SRES	A2	2032–2041	2048–2057	3.39	3.83
RCP	2.6	2047–2056	a	1.48	1.49
RCP	4.5	2031–2040	2055–2064	2.32	2.37
RCP	6.0	2036–2045	2058–2067	2.63	2.86
RCP	8.5	2026–2035	2040–2049	3.90	4.39

[a] 2°C not reached

Table 3.SM.8: Projected temperature-related risks at 1.5°C and 2°C. Abbreviations: DALY: Disability adjusted life year; RCP: Representative Concentration Pathway; SSP: Shared Socio-Economic Pathway; GMST: global mean surface temperature

Region	***Health Outcome Metric***	***Study Baseline***	***Climate Model(S)***	***Scenario***	***Time Periods of Interest***	***Impacts at Study Baseline***	***Projected Impacts at 1.5°C***	***Projected Impacts at 2°C***	***Other Factors Considered***	***Reference***
Global and 21 regions	Heat-related mortality in adults over 65 years of age	1961–1990	BCM2.0, EGMAM1, EGMAM2, EGMAM3, CM4vl	A1B	2030, 2050		In 2030 92,207 additional heat-related deaths without adaptation (ensemble mean) and 28,055 with adaptation under BCM2 scenario; the	In 2050 255,486 additional heat-related deaths without adaptation and 73,936 with adaptation under BCM2 scenario; the same regions	Population growth and aging; improved health in elderly due to economic development; three levels of adaptation (none, partial, and full)	(Hales et al. 2014)

Region	***Health Outcome Metric***	***Study Baseline***	***Climate Model(S)***	***Scenario***	***Time Periods of Interest***	***Impacts at Study Baseline***	***Projected Impacts at 1.5°C***	***Projected Impacts at 2°C***	***Other Factors Considered***	***Reference***
							Asia Pacific, Asia, North Africa / Middle East, Sub-Saharan Africa, Europe and north America at higher risk.	are at higher risk.		
Global	Extremely hot summers over land areas (>3 standard deviations anomalies)	1861–1880	26 models from CMIP5	RCP2.6, RCP4.5, RCP8.5	To 2100	Probability of an extremely hot summer (>3 standard deviations) in 1996–2005 (compared with 1951–1980) is 4.3%	Probability of an extremely hot summer is approximately 25.5% and probability of an exceedingly hot summer (>5 standard deviations) is approximately 7.1% above pre-industrial.	Extremely hot summers are projected to occur over nearly 40% of the land area.		(Wang et al. 2015)
Global	Population exposure to hot days and	1961–1990	21 CMIP5 GCMs	Temperature change based on	Up to 2100	Increasing exposure to heatwaves	The frequency of heatwave	Overall, exposure to heatwaves is		(Arnell et al. 2018)

Region	***Health Outcome Metric***	***Study Baseline***	***Climate Model(S)***	***Scenario***	***Time Periods of Interest***	***Impacts at Study Baseline***	***Projected Impacts at 1.5°C***	***Projected Impacts at 2°C***	***Other Factors Considered***	***Reference***
	heatwaves			pattern scaling		already evident	days increases dramatically as global mean temperature increases, although the extent of increase varies by region. Increases are greatest in tropical and sub-tropical regions where the standard deviation of warm season daily maximum temperature is least, and therefore, a smaller increase in temperature leads to a larger	reduced by more than 75% in all models in each region if GMSTs do not increase to 2°C; the avoided impacts vary by region.		

Region	***Health Outcome Metric***	***Study Baseline***	***Climate Model(S)***	***Scenario***	***Time Periods of Interest***	***Impacts at Study Baseline***	***Projected Impacts at 1.5°C***	***Projected Impacts at 2°C***	***Other Factors Considered***	***Reference***
							increase in heat wave frequency.			
Japan, Korea, Taiwan, USA, Spain, France, Italy	Heat-related mortality for 65+ age group	1961–1990	BCM2	A1B	2030, 2050		In 2030 heat-related excess deaths increased over baselines in all countries, with the increase dependent on the level of adaptation.	In 2050 heat-related excess deaths are higher than for 2030, with the increase dependent on the level of adaptation.	Three adaptation assumptions: 0, 50, and 100%	(Honda et al. 2014)
Australia (five largest cities) and UK	Temperature-related mortality	1993–2006	UKCP09 from HadCM3, OzClim 2011	A1B, B1, A1FI	2020s, 2050s, 2080s	For England and Wales, the estimated % change in mortality associated with heat exposure is 2.5% (95% CI: 1.9–3.1) per 1°C rise in temperature above the	In the 2020s heat-related deaths increase from 1503 at baseline to 1511 with a constant population and 1785 with the projected population. In Australia,	In the 2050s heat-related deaths further increase to 2866 with a constant population and to 4012 with the projected population. In Australia, the numbers	Projected population change	(Vardoulakis et al. 2014)

Region	***Health Outcome Metric***	***Study Baseline***	***Climate Model(S)***	***Scenario***	***Time Periods of Interest***	***Impacts at Study Baseline***	***Projected Impacts at 1.5°C***	***Projected Impacts at 2°C***	***Other Factors Considered***	***Reference***
						heat threshold (93rd percentile of daily mean temperature). In Australian cities, the estimated overall % change in mortality is 2.1% (95% CI: 1.3, 2.9).	the numbers of projected deaths are 362 and 475, respectively, with a baseline of 214 deaths.	of projected deaths are 615 and 970, respectively.		
Australia	Temperature-related morbidity and mortality; days per year above 35°C	1971–2000	CSIRO	2030 A1B low and high; 2070 A1FI low and high	2030, 2070	4–6 dangerously hot days per year for un-acclimatized individuals	Sydney – from 3.5 days at baseline to 4.1–5.1 days in 2030; Melbourne – from 9 days at baseline to 11–13 days in 2030.	Sydney – 6–12 days and Melbourne – 15–26 days in 2070.		(Hanna et al. 2011)
Brisbane, Sydney and Melbourne, Australia	Temperature-related mortality	1988–2009	62 GCMs, with spatial downscaling and bias	A2, A1B, B1	2050s, 2090s		In 2030 net temperature-related mortality	In 2050 there are further net temperature		(Guo et al. 2016)

Region	*Health Outcome Metric*	*Study Baseline*	*Climate Model(S)*	*Scenario*	*Time Periods of Interest*	*Impacts at Study Baseline*	*Projected Impacts at 1.5°C*	*Projected Impacts at 2°C*	*Other Factors Considered*	*Reference*
			correction				(heat/cold) increases in Brisbane under all scenarios, increases in Sydney under A2, and declines in Melbourne under all scenarios.	-related mortality (heat/cold) increases in Brisbane under all scenarios, increases in Sydney under A2 and A1B, and further declines in Melbourne under all scenarios.		
Brisbane, Australia	Years of life lost due to temperature extremes (hot and cold)	1996–2003		Added 1–4°C to observed daily temperature to project for 2050	2000, 2050	In 2000, 3077 temperature-related years of life lost for men, with 616 years of life lost due to hot temperatures and 2461 years of life lost due to	For 1°C above baseline, years of life lost increase by 1014 (840 to 1178) for hot temperature s and decrease by 1112 (–1,337 to –	For 2°C above baseline, years of life lost increase by 2450 (2049 to 2845,) for hot temperature s and decrease by 2069 (–2484		(Huang et al. 2012)

Region	***Health Outcome Metric***	***Study Baseline***	***Climate Model(S)***	***Scenario***	***Time Periods of Interest***	***Impacts at Study Baseline***	***Projected Impacts at 1.5°C***	***Projected Impacts at 2°C***	***Other Factors Considered***	***Reference***
						cold. The numbers for women are 3495 (total), 903 (hot), and 2592 (cold).	871) for cold temperatures.	to –1624) for cold temperatures.		
Quebec, Canada	Heat-related mortality	1981–1999	Ouranos Consortium; SDSM downscaled HADCM3	A2 and B2 (projected impacts the same)	2020 (2010–2039), 2050 (2040–2069), 2080 (2070–2099)		2% increase in summer mortality in 2020.	4–6% increase in summer mortality in 2050.		(Doyon et al. 2008)
USA, 209 cities	Heat- and cold-related mortality	1990 (1976–2005)	Bias corrected (BCCA) GFDL-CM3, MIROC5	RCP6.0	2030 (2016–2045), 2050 (2036–2065), 2100 (2086–2100)		In 2030 a net increase in premature deaths, with decreases in temperature-related winter mortality and increases in summer mortality; the magnitude varied by region and city with an overall	In 2050 a further increase in premature deaths, with decreases in temperature-related winter mortality and increases in summer mortality; the magnitude varied by region and city with an	Held population constant at 2010 levels; mortality associated with high temperatures decreased between 1973–1977 and 2003–2006	(Schwartz et al. 2015)

Region	***Health Outcome Metric***	***Study Baseline***	***Climate Model(S)***	***Scenario***	***Time Periods of Interest***	***Impacts at Study Baseline***	***Projected Impacts at 1.5°C***	***Projected Impacts at 2°C***	***Other Factors Considered***	***Reference***
							increase of 11,646 heat-related deaths.	overall increase of 15,229 heat-related deaths.		
Washington State, USA	Heat-related mortality	1970–1999	PCM1, HadCM	Average of PCM1-B1 and HadCM-A1B; humidex baseline; number and duration of heatwaves calculated	2025, 2045, 2085		Under moderate warming in 2025, 96 excess deaths in Seattle area.	Under moderate warming in 2045, 156 excess deaths in Seattle area.	Holding population constant at 2025 projections	(Jackson et al. 2010)
Boston, New York and Philadelphia, USA	Heat-related mortality	1971–2000	CMIP5 bias corrected (BCSD)	RCP4.5, RCP8.5	2010–2039, 2040–2069, 2070–2099	Baseline heat-related mortality is 2.9–4.5/100,000 across the three cities	In the 2020s under both RCPs, heat-related mortality increased to 5.9–10/ 100,000.	In the 2050s heat-related mortality increased to 8.8–14.3/100,000 under RCP4.5 and to 11.7 to 18.9/100,000 under RCP8.5.	Population constant at 2000	(Petkova et al. 2017)
Europe	Heat-related mortality	1971–2000	SMHI RCA4/HadGE	RCP4.5, RCP8.5	2035–2064, 2071–209		2035–2064 excess heat	2071–2099 excess heat		(Kendrovski et al. 2017)

Region	***Health Outcome Metric***	***Study Baseline***	***Climate Model(S)***	***Scenario***	***Time Periods of Interest***	***Impacts at Study Baseline***	***Projected Impacts at 1.5°C***	***Projected Impacts at 2°C***	***Other Factors Considered***	***Reference***
			M2 ES r1 (MOHC)				mortality to be 30,867 and 45,930.	mortality to be 46,690 and 117,333 attributable deaths/year.		
Europe: London, UK and Paris, France	Heat-related mortality	Present climate	(HAPPI)	Climate stabilization at 1.5°C and 2°C		Model of 2003 heat event resulted in about 735 excess deaths for Paris and about 315 for London	Compared with 2°C stabilization, mortality event is 2.4 times less likely in London and 1.6 times less likely in Paris.	22% increase in mortality in Paris and 15% increase in mortality in London, compared with 1.5°C stabilization.		(Mitchell 2018)
UK	Temperature -related mortality	1993–2006	9 regional model variants of HadRm3-PPE-UK, dynamically downscaled	A1B	2000–2009, 2020–2029, 2050–2059, 2080–2089	At baseline, 1974 annual heat-related deaths and 41,408 cold-related deaths	In the 2020s in the absence of adaptation, heat-related deaths projected to increase to 3281 and cold-related deaths to increase to 42,842.	In the 2050s in the absence of adaptation, heat-related deaths projected to increase 257% by the 2050s to 7040 and cold-related mortality to decline	Population projections to 2081	(Hajat et al. 2014)

Region	***Health Outcome Metric***	***Study Baseline***	***Climate Model(S)***	***Scenario***	***Time Periods of Interest***	***Impacts at Study Baseline***	***Projected Impacts at 1.5°C***	***Projected Impacts at 2°C***	***Other Factors Considered***	***Reference***
								about 2%.		
Netherlands	Temperature -related mortality	1981–2010	KNMI' 14; G-scenario is a global temperature increase of 1°C and W-scenario an increase of 2°C		2050 (2035–2065)	At baseline, the attributable fraction for heat is 1.15% and for cold is 8.9%; or 1511 deaths from heat and 11,727 deaths from cold	Without adaptation, under the G scenario, the attributable fraction for heat is 1.7–1.9% (3329–3752 deaths) and for cold is 7.5–7.9% (15,020–15,733 deaths). Adaptation decreases the numbers of deaths, depending on the scenario.	Without adaptation, under the W scenario, the attributable fraction for heat is 2.2–2.5% (4380-5061 deaths) and for cold is 6.6–6.8% (13,149–13,699 deaths). Adaptation decreases the numbers of deaths, depending on the scenario.	Three adaptation scenarios, assuming a shift in the optimum temperature, changes in temperature sensitivity, or both; population growth and declining mortality risk per age group	(Huynen and Martens 2015)

Region	***Health Outcome Metric***	***Study Baseline***	***Climate Model(S)***	***Scenario***	***Time Periods of Interest***	***Impacts at Study Baseline***	***Projected Impacts at 1.5°C***	***Projected Impacts at 2°C***	***Other Factors Considered***	***Reference***
Korea	Burden of disease from high ambient temperatures	2011	CMIP5	RCP4.5, RCP8.5	2030, 2050	DALY for all-cause mortality in 2011 was 0.49 (DALY/1000) DALY for cardio-and cerebrovascular disease was 1.24 DALY/1000	In 2030 DALY for all-cause mortality, 0.71 (DALY/1000) DALY for cardio-and cerebrovascular disease is 1.63 (1.82) DALY/1000	In 2050 DALY for all-cause mortality, 0.77 (1.72) (DALY/1000) DALY for cardio-and cerebrovascular disease is 1.76 (3.66) DALY/1000		(Chung et al. 2017)
Beijing, China	Heat-related mortality	1970–1999	Downscaled and bias corrected (BCSD) 31 GCMs in WCRP CMIP5; monthly change factors applied to daily weather data to create a projection	RCP4.5, RCP8.5	2020s (2010–2039), 2050s (2040–2069), 2080s (2070–2099)	Approximately 730 additional annual heat-related deaths in 1980s	In the 2020s under low population growth and RCP4.5 and RCP8.5, heat-related deaths projected to increase to 1012 and 1019, respectively. Numbers of deaths are higher with	In the 2050s under low population growth and RCP4.5 and RCP8.5, heat-related deaths projected to increase to 1411 and 1845, respectively.	Adults 65+ years of age; no change plus low, medium and high variants of population growth; future adaptation based on Petkova et al., (2013) , plus shifted mortality 5%, 15%, 30%,	(Li et al. 2016c)

Region	***Health Outcome Metric***	***Study Baseline***	***Climate Model(S)***	***Scenario***	***Time Periods of Interest***	***Impacts at Study Baseline***	***Projected Impacts at 1.5°C***	***Projected Impacts at 2°C***	***Other Factors Considered***	***Reference***
							medium and high population growth.		50%	
Beijing, China	Cardiovascular and respiratory heat-related mortality	1971–2000	Access 1.0, CSIRO Mk3.6.0, GFDL-CM3, GISS E2R, INM-CM4	RCP4.5, RCP8.5	2020s, 2050s, 2080s	Baseline cardiovascular mortality 0.396 per 100,000; baseline respiratory mortality 0.085 per 100,000	Cardiovascular mortality could increase by an average percentage of 18.4% in the 2020s under RCP4.5, and by 16.6% under RCP8.5. Statistically significant increases are projected for respiratory mortality.	Cardiovascular mortality could increase by an average percentage of 47.8% and 69.0% in the 2050s and 2080s under RCP4.5, and by 73.8% and 134% under RCP8.5. Similar increases are projected for respiratory mortality.		(Li et al. 2015)
Africa	Five thresholds for number of hot days per year	1961–2000	CCAM (CSIRO) forced by coupled GCMs:	A2	2011–2040, 2041–2070, 2071–2100	In 1961–1990, average number of hot days	In 2011–2040, annual average number of hot days	In 2041–2070, annual average number of hot days	Projected population in 2020 and 2025	(Garland et al. 2015)

Region	*Health Outcome Metric*	*Study Baseline*	*Climate Model(S)*	*Scenario*	*Time Periods of Interest*	*Impacts at Study Baseline*	*Projected Impacts at 1.5°C*	*Projected Impacts at 2°C*	*Other Factors Considered*	*Reference*
	when health could be affected, as measured by maximum apparent temperature		CSIRO, GFDL20, GFDL 21, MIROC, MPI, UKMO. CCAM was then downscaled. Bias corrected using CRU TS3.1 dataset			(maximum apparent temperature > 27°C) ranged from 0 to 365, with high variability across regions	(maximum apparent temperature > 27°C) projected to increase by 0–30 in most parts of Africa, with a few regions projected to increase by 31–50.	(maximum apparent temperature > 27°C) projected to increase by up to 296, with large changes projected in southern Africa and parts of northern Africa.		

Table 3.SM.9: Projected air quality-related health risks at 1.5°C and 2°C. Abbreviations: DALY: disability adjusted life year; RCP: Representative Concentration Pathway; SSP: Shared Socio-Economic Pathway; CV: cardiovascular

Region	*Health Outcome Metric*	*Study Baseline*	*Climate Model(S) and Air Pollution Models*	*Scenario*	*Time Periods of Interest*	*Impacts at Study Baseline*	*Projected Impacts at 1.5°C*	*Projected Impacts at 2°C*	*Other Factors Considered*	*Reference*
Global	PM 2.5 and O3-related mortality	2000	14 global models participating in ACCMIP CESM	RCP2.6, RCP4.5, RCP6.0 RCP8.5	2000, 2030, 2050, 2100	Global O3 mortality 382,000 (121,000–728,000) deaths year -1; global mortality burden of PM2.5 1.70 (1.30–2.10) million deaths year-1	PM2.5-related mortality peaks in 2030 (2.4–2.6 million deaths/year – except for RCP6.0)	O3-related mortality peaks in 2050 (1.84–2.6 million deaths per year)	Population projected from 2010–2100	(Silva et al. 2016)
Global and Europe and France	PM2.5-related CV- and O3-related respiratory mortality	2010	IPSL-cm5-MR, LDMz-INCA, CHIMERE	RCP4.5 (for Europe and France)	2010, 2030–2050	Global CV mortality 17,243,000	In 2030 in Europe PM2.5-related CV mortality decreases by 3.9% under CLE and 7.9% under MFR. In 2030 O3-related respiratory mortality decreases by 0.3% under	In 2050 4.5% decrease in PM2.5-related CV mortality under CLE and 8.2% MFR.	Population 2030–sensitivity analysis	(Likhvar et al. 2015)

Region	***Health Outcome Metric***	***Study Baseline***	***Climate Model(S) and Air Pollution Models***	***Scenario***	***Time Periods of Interest***	***Impacts at Study Baseline***	***Projected Impacts at 1.5°C***	***Projected Impacts at 2°C***	***Other Factors Considered***	***Reference***
							MFR.			
UK	O3-related morbidity and mortality	2003	EMEP-WRF	A2, B2	2003, 2030	O3-attributable mortality and morbidity in 2003: 11,500 deaths and 30,700 hospitalizations	With no threshold for O3, increase of premature mortality and hospitalization of 28% (under B2 + CLE scenario) – greatest health effects; A2 premature morbidity and mortality projections: 22%. With 35 ppbv, 52% increase in mortality and morbidity (under B2+CLE).	Increases in temperatures by 5°C, projected O3 mortality will increase from 4% (no O3 threshold) to 30% (35 ppbv O3 threshold).	Population projections increase, +5°C scenario	(Heal et al. 2013)
Poland	PM2.5 mortality	2000	ECHAM5-RegCM3, CAMx	A1B	1990s 2040s, 2090s	39,800 premature deaths related to PM2.5 air	0.4°C –1°C in 2040; 6% decrease in PM2.5-related	2°C –3°C in the 2090s; 7% decrease in PM25-related		(Tainio et al. 2013)

Region	***Health Outcome Metric***	***Study Baseline***	***Climate Model(S) and Air Pollution Models***	***Scenario***	***Time Periods of Interest***	***Impacts at Study Baseline***	***Projected Impacts at 1.5°C***	***Projected Impacts at 2°C***	***Other Factors Considered***	***Reference***
						pollution	mortality in 2040s.	mortality in 2090s.		
Korea	O3 summer mortality	2001–2010	ICAMS	RCP2.6 RCP4.5, RCP6.0, RCP8.5	1996–2005, 2016–2025, 2046–2055		In the 2020s summer mortality to increase by: 0.5%, 0.0%, 0.4%, and 0.4% due to temperature change. In the 2020s, due to O3 concentration change, mortality to increase by 0.0%, and 0.5%.	In the 2050s summer mortality to increase by: 1.9%, 1.5%, 1.2% and 4.4% due to temperature change. In the 2050s, due to O3 concentration change, mortality to increase by 0.2%, 0.4% and 0.6%.	Current mortality trends expected to increase, temperature effects compared	(Lee et al. 2017)

Region	***Health Outcome Metric***	***Study Baseline***	***Climate Model(S) and Air Pollution Models***	***Scenario***	***Time Periods of Interest***	***Impacts at Study Baseline***	***Projected Impacts at 1.5°C***	***Projected Impacts at 2°C***	***Other Factors Considered***	***Reference***
US (12 metropolitan areas)	O3 inhalation exposures	2000	APEX, CESM, MIP5, WRF, CMAQ	RCP4.5, RCP6, RCP8.5	1995–2005, 2025–2035	At least one exceedance/year	Comparing 2030 to 2000, almost universal trend with at least three exceedances (of DM8H exposure above the 60 ppb and 70 bbp thresholds).	Health implications increase as population exposures to O3 increases based on the degree of radiative forcing in 2100.	Population projections using IPCC SRES and adapted for US	(Dionisio et al. 2017)

Table 3.SM.10: Projected vectorborne disease risks at 1.5°C and 2°C. Abbreviations: DALY: disability adjusted life year; RCP: Representative Concentration Pathway; SSP: Shared Socio-Economic Pathway

Region	***Health Outcome Metric***	***Study Baseline***	***Climate Model(S)***	***Scenario***	***Time Periods of Interest***	***Impacts at Study Baseline***	***Projected Impacts at 1.5°C***	***Projected Impacts at 2°C***	***Other Factors Considered***	***Reference***
Malaria										
China	Malaria vectors Anopheles dirus, A. minimus, A. lesteri, A. sinensis	2005–2008	BCC-CSM1-1, CCCma_CanESM2, CSIRO-Mk3.6.0 from CMIP5	RCP2.6, RCP4.5, RCP8.5	2020–2049, 2040–2069		In the 2030s environmentally suitable areas for *A. dirus* and *A. minimus* increase by an average of 49% and 16%, respectively.	In the 2050s environmentally suitable areas for *A. dirus* and *A. minimus* decrease by 11% and 16%, respectively. An increase of 36% and 11%, in environmentally suitable area of *A. lesteri* and *A. sinensis*.	Land use, urbanization	(Ren et al. 2016)
Northern China	Spatial distribution of malaria	2004–2010	GCMs from CMIP3	B1, A1B, A2	2020, 2030, 2040, 2050	Average malaria incidence 0.107% per annum in northern China	In 2020 malaria incidence increases 19–29%, and increases	In 2040 malaria incidence increases 33–119% and 69–182% in	Elevation, GDP, water density index held constant	(Song et al. 2016)

							43–73% in 2030, with increased spatial distribution.	2050, with increased spatial distribution.		
Sub-Saharan Africa	Malaria	2006–2016	21 CMIP5 models	RCP4.5, RCP8.5	2030, 2050, 2100		In 2030 under RCP8.5, many parts of western and central Africa will have no malaria, but significant malaria hotspots will be along the Sahel belt, eastern and southern parts of Africa.	Climate change will redistribute the spatial pattern of future malaria hotspots, especially under RCP8.5.	Various environmental variables	(Semakula et al. 2017)
Aedes										
Global	Global niche models for autochthonous Chikungunya virus transmission	Current climate	CESM 1 bcg, FIO ESM, GISS e2-r, INM CM4 and MPI-ESM-lr	RCP4.5, RCP8.5	2021–2040, 2041–2060, 2061–2080	Current distribution of Chikungunya transmission	In 2021–2040 climatically suitable areas projected to increase in multiple regions,	In 2041–2060 greater geographic expansion.		(Tjaden et al. 2017)

							including China, sub-Saharan Africa, the US and continental Europe.			
North America, United States	Climate suitability for Aedes albopictus vector for dengue, Chikungunya and vectorborne zoonoses, such as West Nile virus (WNV), Eastern equine encephalitis virus, Rift Valley fever virus, Cache Valley virus and LaCrosse	1981–2010	8 RCMs: CanRCM4, CRCM5, CRCM 4.2.3, HIRHAM5, RegCM3, ECPC, MM5I, WRF	RCP4.5, RCP8.5, A2	2020s (2011–2040), 2050s (2041–2070)	Index of precipitation and temperature suitability was highly accurate in discriminating suitable and non-suitable climate	In 2011–2040 under RCP4.5, climate suitability increases across US, with the magnitude and pattern dependent on parameter projected and RCM.	In 2041–2070 under RCP4.5, areal extent larger than in earlier period; under RCP8.5, areal extent larger.	Climatic indicators of Ae. albopictus survival; overwintering conditions (OW); OW combined with annual air temperature (OWAT); and an index of suitability	(Ogden et al. 2014a)

	virus									
Mexico	Dengue	1985–2007	National Institute of Ecology; added projected changes to historic observations	A1B, A2, B1	2030, 2050, 2080	National: 1.001/100.000 cases annually Nuevo Leon: 1.683/100.000 cases annually Queretaro: 0.042/100.000 cases annually Veracruz: 2.630/100.000 cases annually	In 2030 dengue incidence increases 12–18%.	In 2050 dengue incidence increases 22–31%.	At baseline, population, GDP, urbanization, access to piped water	(Colón-González et al. 2013)
Europe, Eurasia and the Mediterranean	Climatic suitability for Chikungunya outbreaks	1995–2007	COSMO-CLM, building on ECHAM5	A1B and B1	2011–2040, 2041–2070, 2071–2100	Currently, climatic suitability in southern Europe. The size of these regions will expand during the 21st century	In 2011–2040 increases in risk are projected for Western Europe in the first half of the 21st century.	In 2041–2070 projected increased risks for Central Europe.		(Fischer et al. 2013)

Europe	Potential establishment of Ae. albopictus	Current bioclimatic data derived from monthly temperature and rainfall values	Regional climate model COSMO-CLM	A1B, B1	2011–2040, 2041–2070, 2071–2100		In 2011–2040 higher values of climatic suitability for Ae. albo pictus increases in Western and Central Europe	Between 2011–40 and 2041–2070 for southern Europe, only small changes in climatic suitability are projected. Increasing suitability at higher latitudes is projected for the end of the century.		(Fischer et al. 2011)
Europe	Dengue fever risk in 27 EU countries	1961–1990	COSMO-CLM (CCLM) forced with ECHAM5/MPIOM	A1B	2011–2040, 2041–2070, 2071–2100	Number of dengue cases are between 0 and 0.6 for most European areas, corresponding to an incidence of less than 2	In 2011–2040 increasing risk of dengue in southern parts of Europe.	In 2041–2070 increased dengue risk in many parts of Europe, with higher risks towards the end of the century.	Socio-economic variables, population density, degree of urbanization and log population	(Bouzid et al. 2014)

						per 100,000 inhabitants		Greatest increased risk around the Mediterranean and Adriatic coasts and in northern Italy.		
Tanzania	Distribution of infected Aedes aegypti co-occurrence with dengue epidemics risk	1950–2000	CMIP5		2020, 2050	Currently high habitat suitability for Ae. aegypti in relation to dengue epidemic, particularly near water bodies	Projected risk maps for 2020 show risk intensification in dengue epidemic risks areas, with regional differences.	In 2050 greater risk intensification and regional differences.		(Mweya et al. 2016)
West Nile virus										
Europe, Eurasia, and the Mediterranean	Distribution of human WNV infection	Monthly temperature anomalies relative to 1980–1999, environme	NCAR CCSM3	A1B	2015–2050		In 2025 progressive expansion of areas with an elevated probability for WNV	In 2050 increases in areas with a higher probability of expansion.	Prevalence of WNV infections in the blood donor population	(Semenza et al. 2016)

		ntal variables for 2002–2013					infections, particularly at the edges of the current transmission areas.			
Lyme disease and other tick-borne diseases										
North America (mainly Ontario and Quebec, Canada, and northeast and midwest, United States)	Capacity of Lyme disease vector (*Ixodes scapularis*) to reproduce under different environmental conditions	1971–2010	CRCM4.2.3, WRF, MM5I, CGCM3.1, CCSM3	A2	1971–2000, 2011–2040, 2041–2070	In 1971–2010 reproductive capacity increased in North America; increase consistent with observation	In 2011–2040 mean reproductive capacity increased, with projected increases in the geographic range and number of ticks.	In 2041–2070 further expansion and numbers of ticks projected. R_0 values for *I. scapularis* are projected to increase 1.5–2.3 times in Canada. In the US values are expected to double.		(Ogden et al. 2014b)

Southeastern New York, United States	Emergence of *I. scapularis*, leading to Lyme disease	1994–2012			2050	19 years of tick and small mammal data (mice, chipmunks)	In the 2020s the number of cumulative degree-days enough to advance the average nymphal peak by 4–6 days, and the mean larval peak by 5–8 days, based on 1.11°C – 1.67°C increase in mean annual temperature.	In the 2050s the nymphal peak advances by 8–11 days, and the mean larval peak by 10–14 days, based on 2.22°C – 3.06°C increase in mean annual temperature.		(Levi et al. 2015)
Other										
Venezuela	Chagas disease: number of people exposed to changes in the geographic	1950–2000	CSIRO3.0	A1B, B1	2020, 2060, 2080		In 2020 decreasing population vulnerability.	In 2060 effects more pronounced, with less of a change under B1.	MaxEnt model of climatic niche suitability	(Ceccarelli and Rabinovich 2015)

	range of five species of triatomine species									
Colombia	Visceral leishmaniasis caused by the trypanosomatid parasite *Leishmania infantum*	Present	CSIRO, Hadley	A2A, B2A	2020, 2050, 2080		In 2020 shift in the altitudinal distribution in the Caribbean coast and increase in the geographic area of potential occupancy under optimistic scenarios.	In 2050 even greater geographic area of potential occupancy, with a greater impact under A2.	MaxEnt model; three topographical variables	(González et al. 2014)

References

Arnell, N. W., J. A. Lowe, B. Lloyd-Hughes, and T. J. Osborn, 2018: The impacts avoided with a 1.5°C climate target: a global and regional assessment. Clim. Change, 147, 61–76, doi:10.1007/s10584-017-2115-9.

Bouzid, M., F. J. Colón-González, T. Lung, I. R. Lake, and P. R. Hunter, 2014: Climate change and the emergence of vector-borne diseases in Europe: case study of dengue fever. BMC Public Health, 14, 781, doi:10.1186/1471-2458-14-781.

Ceccarelli, S., and J. E. Rabinovich, 2015: Global Climate Change Effects on Venezuela's Vulnerability to Chagas Disease is Linked to the Geographic Distribution of Five Triatomine Species. J. Med. Entomol., 52, 1333–1343, doi:10.1093/jme/tjv119.

Chung, E. S., H.-K. Cheong, J.-H. Park, J.-H. Kim, and H. Han, 2017: Current and Projected Burden of Disease From High Ambient Temperature in Korea. Epidemiology, 28, S98–S105.

Colón-González, F. J., C. Fezzi, I. R. Lake, P. R. Hunter, and Y. Sukthana, 2013: The Effects of Weather and Climate Change on Dengue. PLoS Negl. Trop. Dis., 7, e2503, doi:10.1371/journal.pntd.0002503.
Dionisio, K. L., C. G. Nolte, T. L. Spero, S. Graham, N. Caraway, K. M. Foley, and K. K. Isaacs, 2017: Characterizing the impact of projected changes in climate and air quality on human exposures to ozone. J. Expo. Sci. Environ. Epidemiol., 27, 260, doi:10.1038/jes.2016.81.
Doyon, B., D. Belanger, and P. Gosselin, 2008: The potential impact of climate change on annual and seasonal mortality for three cities in Québec, Canada. Int. J. Health Geogr., 7, 23, doi:10.1186/1476-072x-7-23.
Fischer, D., S. M. Thomas, F. Niemitz, B. Reineking, and C. Beierkuhnlein, 2011: Projection of climatic suitability for Aedes albopictus Skuse (Culicidae) in Europe under climate change conditions. Glob. Planet. Change, 78, 54–64, doi:10.1016/j.gloplacha.2011.05.008.
——, S. M. Thomas, J. E. Suk, B. Sudre, A. Hess, N. B. Tjaden, C. Beierkuhnlein, and J. C. Semenza, 2013: Climate change effects on Chikungunya transmission in Europe: geospatial analysis of vector's climatic suitability and virus' temperature requirements. Int. J. Health Geogr., 12, 51, doi:10.1186/1476-072X-12-51.
Garland, R. M., M. Matooane, F. A. Engelbrecht, M. J. M. Bopape, W. A. Landman, M. Naidoo, J. van der Merwe, and C. Y. Wright, 2015: Regional Projections of Extreme Apparent Temperature Days in Africa and the Related Potential Risk to Human Health. Int. J. Environ. Res. Public Health, 12, 12577–12604, doi:10.3390/ijerph121012577.
González, C., A. Paz, and C. Ferro, 2014: Predicted altitudinal shifts and reduced spatial distribution of Leishmania infantum vector species under climate change scenarios in Colombia. Acta Trop., 129, 83–90, doi:10.1016/j.actatropica.2013.08.014.
Guo, Y., S. Li, D. L. Liu, D. Chen, G. Williams, and S. Tong, 2016: Projecting future temperature-related mortality in three largest Australian cities. Environ. Pollut., 208, 66–73, doi:10.1016/j.envpol.2015.09.041.
Hajat, S., S. Vardoulakis, C. Heaviside, and B. Eggen, 2014: Climate change effects on human health: Projections of temperature-related mortality for the UK during the 2020s, 2050s and 2080s. J. Epidemiol. Community Health, 68, 641–648, doi:10.1136/jech-2013-202449.
Hales, S., S. Kovats, S. Lloyd, and D. Campbell-Lendrum, 2014: Quantitative risk assessment of the effects of climate change on selected causes of death, 2030s and 2050s. S. Hales, S. Kovats, S. Lloyd, and D. Campbell-Lendrum, Eds. Geneva, Switzerland, 115 pp.
Hanna, E. G., T. Kjellstrom, C. Bennett, and K. Dear, 2011: Climate Change and Rising Heat: Population Health Implications for Working People in Australia. Asia-Pacific J. Public Heal., 23, 14s–26s, doi:10.1177/1010539510391457.
Heal, M. R., C. Heaviside, R. M. Doherty, M. Vieno, D. S. Stevenson, and S. Vardoulakis, 2013: Health burdens of surface ozone in the UK for a range of future scenarios. Environ. Int., 61, 36–44, doi:10.1016/j.envint.2013.09.010.
Honda, Y., and Coauthors, 2014: Heat-related mortality risk model for climate change impact projection. Environ. Health Prev. Med., 19, 56–63, doi:10.1007/s12199-013-0354-6.
Huang, C. R., A. G. Barnett, X. M. Wang, and S. L. Tong, 2012: The impact of temperature on years of life lost in Brisbane, Australia. Nat. Clim. Chang., 2, 265–270, doi:10.1038/Nclimate1369.
Huynen, M. M. T. E., and P. Martens, 2015: Climate Change Effects on Heat- and Cold-Related Mortality in the Netherlands: A Scenario-Based Integrated Environmental Health Impact Assessment. Int. J. Environ. Res. Public Health, 12, 13295–13320, doi:10.3390/ijerph121013295.
Jackson, J. E., and Coauthors, 2010: Public health impacts of climate change in Washington State: projected mortality risks due to heat events and air pollution. Clim. Change, 102, 159–186, doi:10.1007/s10584-010-9852-3.
Kendrovski, V., M. Baccini, G. Sanchez Martinez, T. Wolf, E. Paunovic, and B. Menne, 2017: Quantifying Projected Heat Mortality Impacts under 21st-Century Warming Conditions for Selected European Countries. Int. J. Environ. Res. Public Health, 14, 729, doi:10.3390/ijerph14070729.
Lee, J. Y., S. Hyun Lee, S.-C. Hong, and H. Kim, 2017: Projecting future summer mortality due to ambient ozone concentration and temperature changes. Atmos. Environ., 156, 88–94.

Levi, T., F. Keesing, K. Oggenfuss, and R. S. Ostfeld, 2015: Accelerated phenology of blacklegged ticks under climate warming. Philos. Trans. R. Soc. London B Biol. Sci., 370.

Li, T. T., J. Ban, R. M. Horton, D. A. Bader, G. L. Huang, Q. H. Sun, and P. L. Kinney, 2015: Heat-related mortality projections for cardiovascular and respiratory disease under the changing climate in Beijing, China. Sci. Rep., 5, doi:10.1038/srep11441.

——, R. M. Horton, D. A. Bader, M. G. Zhou, X. D. Liang, J. Ban, Q. H. Sun, and P. L. Kinney, 2016: Aging Will Amplify the Heat-related Mortality Risk under a Changing Climate: Projection for the Elderly in Beijing, China. Sci. Rep., 6, doi:10.1038/srep28161.

Likhvar, V., and Coauthors, 2015: A multi-scale health impact assessment of air pollution over the 21st century. Sci. Total Environ., 514, 439–449, doi:https://doi.org/10.1016/j.scitotenv.2015.02.002.

Mitchell, D., 2018: Extreme heat-related mortality avoided under Paris Agreement goals. Nat. Clim. Chang.,.

Mweya, C. N., S. I. Kimera, G. Stanley, G. Misinzo, L. E. G. Mboera, and N. Ntinginya, 2016: Climate Change Influences Potential Distribution of Infected Aedes aegypti Co-Occurrence with Dengue Epidemics Risk Areas in Tanzania. PLoS One, 11, e0162649, doi:10.1371/journal.pone.0162649.

Ogden, N. H., R. Milka, C. Caminade, and P. Gachon, 2014a: Recent and projected future climatic suitability of North America for the Asian tiger mosquito Aedes albopictus. Parasit. Vectors, 7, 532, doi:10.1186/s13071-014-0532-4.

——, M. Radojevic, X. Wu, V. R. Duvvuri, P. A. Leighton, and J. Wu, 2014b: Estimated effects of projected climate change on the basic reproductive number of the Lyme disease vector Ixodes scapularis. Environ. Health Perspect., 122, 631–638, doi:10.1289/ehp.1307799.

Petkova, E. P., J. K. Vink, R. M. Horton, A. Gasparrini, D. A. Bader, J. D. Francis, and P. L. Kinney, 2017: Towards More Comprehensive Projections of Urban Heat-Related Mortality: Estimates for New York City under Multiple Population, Adaptation, and Climate Scenarios. Environ. Health Perspect., 125, 47–55, doi:10.1289/Ehp166.

Ren, Z., and Coauthors, 2016: Predicting malaria vector distribution under climate change scenarios in China: Challenges for malaria elimination. Sci. Rep., 6, 20604, doi:10.1038/srep20604.

Schwartz, J. D., and Coauthors, 2015: Projections of temperature-attributable premature deaths in 209 US cities using a cluster-based Poisson approach. Environ. Heal., 14, 85, doi:ARTN 85 10.1186/s12940-015-0071-2.

Semakula, H. M., and Coauthors, 2017: Prediction of future malaria hotspots under climate change in sub-Saharan Africa. Clim. Change, 143, 415–428, doi:10.1007/s10584-017-1996-y.

Semenza, J. C., A. Tran, L. Espinosa, B. Sudre, D. Domanovic, and S. Paz, 2016: Climate change projections of West Nile virus infections in Europe: implications for blood safety practices. Environ. Heal., 15, S28, doi:10.1186/s12940-016-0105-4.

Silva, R. A., and Coauthors, 2016: The effect of future ambient air pollution on human premature mortality to 2100 using output from the ACCMIP model ensemble. Atmos. Chem. Phys., 16, 9847–9862, doi:10.5194/acp-16-9847-2016.

Song, Y., Y. Ge, J. Wang, Z. Ren, Y. Liao, and J. Peng, 2016: Spatial distribution estimation of malaria in northern China and its scenarios in 2020, 2030, 2040 and 2050. Malar. J., 15, 345, doi:10.1186/s12936-016-1395-2.

Tainio, M., K. Juda-Rezler, M. Reizer, A. Warchałowski, W. Trapp, and K. Skotak, 2013: Future climate and adverse health effects caused by fine particulate matter air pollution: case study for Poland. Reg. Environ. Chang., 13, 705–715, doi:10.1007/s10113-012-0366-6.

Tjaden, N. B., J. E. Suk, D. Fischer, S. M. Thomas, C. Beierkuhnlein, and J. C. Semenza, 2017: Modelling the effects of global climate change on Chikungunya transmission in the 21st century. Sci. Rep., 7, 3813, doi:10.1038/s41598-017-03566-3.

Vardoulakis, S., K. Dear, S. Hajat, C. Heaviside, B. Eggen, and A. J. McMichael, 2014: Comparative Assessment of the Effects of Climate Change on Heat-and Cold-Related Mortality in the United Kingdom and Australia. Environ. Health Perspect., 122, 1285–1292, doi:10.1289/ehp.1307524.

Wang, L., J. B. Huang, Y. Luo, Y. Yao, and Z. C. Zhao, 2015: Changes in Extremely Hot Summers over the Global Land Area under Various Warming Targets. PLoS One, 10, doi:ARTN e0130660 10.1371/journal.pone.0130660.

3.SM.3.5 Supplementary information to Key Economic Sectors

Table 3.SM.11: Key Economic Sectors (Energy, Tourism, Transport, Water)

Projected Risks at 1.5°C and 2°C

Sector (Sub-Sector)	*Region*	*Metric*	*Baselines*	*Climate Model(S)*	*Scenario*	*Time Periods of Interest*	*Impacts at Baseline*	*Projected Impacts at 1.5°C*	*Projected Impacts at 2°C*	*Other Factors Considered*	*Reference*
Energy (thermal and hydro plants; cooling demand)	Global	Cooling demand (absolute growth in annual cooling degree days; CDD); hydroclimate risk to power production	1971–2000	5 GCMS GFDL-ESM2M; HadGEM2-ES; IPSL-CM5A-LR; MIROC-ESM-CHEM; NorESM1-M	RCP8.5 SSP1–3	1.5°C (2002–2048), 2.0°C (2014–2065)			Increased CCD, especially in tropical areas. Increased risk to thermal and hydro power plants in Europe, North America, South and Southeast Asia, and southeast Brazil.		(Byers et al. 2018)
Energy (wind)	Europe	Daily wind power output (transformed from daily near	2006–2015	HAPPI		1.5°C (2106–2115		Great potential for wind energy in northern		Limited spatial resolution	(Hosking et al. 2018)

		surface wind speeds)							Europe, especially in the UK.				
Energy (electricity demand)	US	Electric sector models: GCAM-USA ReEDS IPM			MIT IGSM-CAM	REF CS3 REF CS6 POL4.5 CS3 POL3.7 CS3 TEMP 3.7 CS3	2015–2050			Increase in electricity demand by 1.6–6.5% in 2050.			(McFarland et al. 2015)
Energy (demand)	Global	Economic and end-use energy model Energy service demands for space heating and cooling				RCP2.6 (2°C) RCP8.5 (4°C) RCP8.5 constant after 2020 (1.5°) SSP1 SSP2 SSP3	2050–2100		Economic loss of 0.31% in 2050 and 0.89% in 2100 globally	GDP negative impacts in 2100 are highest (median: –0.94%) under 4.0°C (RCP8.5) scenario compared with a GDP change (median: −0.05%) under 1.5°C scenario			(Park et al. 2018)
Energy (heating and cooling	Global and regional	Degree days above or below 18°C	1961–1990	21 CMIP5			2100		Cooling energy demand: 31% impacts				(Arnell et al. 2018)

demand)								avoided; heating energy demand: 27% impacts avoided, relative to 2°C.			
Energy (hydropower)	US (Florida)	Conceptual rainfall-runoff (CRR) model: HYMOD MOPEX	1971–2000	CORDEX (6 RCMs) CMIP5, bias corrected	RCP4.5	2091–2100			Based on a min/max temperature increase of 1.35°C −2°C, overall stream flow to increase by an average of 21% with pronounced seasonal variations, resulting in increases in power generation (72% winter, 15% autumn) and decreasing (–14%) in summer		(Chilkoti et al. 2017)

Energy (hydropower)	Global	Gross hydropower potential; global mean cooling water discharge	1971–2000	5 bias-corrected GCMs	RCP2.6, RCP8.5	2080			Global gross hydropower potential expected to increase (+2.4% RCP2.6; +6.3% RCP8.5). Strongest increases in central Africa, Asia, India and northern high latitudes. 4.5–15% decrease in global mean cooling water discharge with largest reductions in US and Europe.	Socio-economic pathways	(van Vliet et al. 2016)

Energy (hydropower)	Brazil	Hydrological model for natural water inflows (MGB)	1960–1990	HadCM3 Eta-CPTEC-40		2011–2100		A decrease in electricity generation of about 15% and 28% for existing and future generation systems starting in 2040.		Other water use and economic development scenarios	(de Queiroz et al. 2016)
Energy (hydropower)	Ecuador	CRU TS v.3.24 monthly mean temperature, precipitation and potential evapotranspiration (PET) conceptual hydrological model assessing runoff and hydropower electricity model	1971–2000	CMIP5 bias corrected using PET	RCP8.5, RCP4.5, RCP2.6	2071–2100			Annual hydroelectric power production to vary between −55 and +39% of the mean historical output. Inter-GCM range of projections is extremely large (−82%−+277%).	ENSO impacts	(Carvajal et al. 2017)

Energy (wind)	Europe	Near surface wind data: wind energy density means; intra and inter annual variability	1986–2005	21 CMIP5 Euro-CORDEX	RCP8.5, RCP4.5	2016–2035, 2046–2065, 2081–2100		No major differences in large scale wind energetic resources, interannual or intraannual variability in near term future (2016–2035).	Decreases in wind energy density in eastern Europe, increases in Baltic regions (−30% vs. +30%). Increase of intraannual variability in northern Europe, decrease in southern. Interannual variability not expected to change.	Changes in wind turbine technology	(Carvalho et al. 2017)
Energy (wind)	Europe	Near surface wind speed wind power simulated energy mix scenario		Euro-CORDEX	RCP4.5, RCP8.5	2050		Changes in the annual energy yield of the future European wind farms fleet as a whole will remain within ±5%.			(Tobin et al. 2016)

Energy (wind)	Europe	Potential wind power generation		ENSEMBLES 15 RCM 6 GCM	SRES A1B				In Europe changes in wind power potential will remain within ±15% and ±20%.		(Tobin et al. 2015)
Energy (solar)	Europe	Mean photovoltaic (PV) power generation potential (PVPot); surface wind velocity (SWV); radiation (RSDS); surface air temp (TAS)	1970−1999	Euro-CORDEX	RCP4.5, RCP8.5	2070−2099			Solar PV supply by the end of 2100 should range from −14_+2% with largest decreases in northern countries.	Solar spectrum distribution and the air mass effect	(Jerez et al. 2015)
Energy (solar)	Global	Energy yields of PV systems		CMIP5	RCP8.5	2006−2049		Decreases in PV outputs in large parts of the world, but notable exceptions with positive trends in large parts of Europe, southeast of North America and the			(Wild et al. 2015)

								southeast China.			
Energy (electricity: wind, solar PV, hydro, thermal)	Europe	Wind power production; PV power generation potential; gross hydropower potential (VIC model); thermoelectric power generation (VIC-RBM models)	1971–2000	Euro-CORDEX (ensemble of 3 RCMs and 3 GCMs)	RCP4.5, RCP8.5	+1.5°C (2004-2043) +2.0°C (2016–2059) +3.0°C (2037–2084)		Impacts remain limited for most countries. PV and wind power potential may reduce 10%, hydro and thermal may reduce 20%.	At 2.0°C impacts across sub-sectors remain limited, negative impacts double at 3°C. Impacts more severe in southern Europe.	No spatial distribution accounted for in analysis	(Tobin et al. 2018)
Energy (hydropower)	Suriname	VHM hydrological model	1960–1990	CMIP5	RCP2.6, RCP4.5, RCP6.0, RCP8.5	1.5°C (2070–2100)		40% decrease in hydropower potential (RCP2.6).	50% decrease in hydropower potential (RCP4.5); 80% decrease in hydropower potential at 3°C GMST (RCP8.5).		(Donk et al. 2018)
Tourism	Europe	Climate Index for Tourism; Tourism Climatic Index (three variants)		Euro-CORDEX	RCP4.5, RCP8.5	+2°C			Varying magnitude of change across different indices;		(Grillakis et al. 2016)

									improved climate comfort for majority of areas for May to October period; June to August period climate favourability projected to reduce in Iberian peninsula due to high temperature s.		
Tourism	Southern Ontario, Canada	Weather-visitation models (peak, shoulder, off-season)				1°C –5°C warmin g		Each additional degree of warming experienced annual park visitation could increase by 3.1%, annually.		Social variables, for example, weekends or holidays	(Hewer et al. 2016)
Tourism	Europe	Natural snow	1971–20	Euro-CORDEX	RCP2.6,	+2°C			Under a	Tourism	(Damm et al. 2017)

		conditions (VIC); monthly overnight stay; weather value at risk	00		RCP4.5, RCP8.5	periods: 2071–2100 2036–2065 2026–2055			+2°C global warming, up to 10 million overnight stays are at risk (+7.3 million nights), Austria and Italy are most affected.	trends based on economic conditions	
Tourism	Sardinia (Italy) and the Cap Bon peninsula (Tunisia)	Overnight stays; weather/climate data (E-OBS)	1971–2000	EU-FP6 ENSEMBLES (ECH-REM, ECH-RMO, HCH-RCA and ECH-RCA)		2041–2070			Climate-induced tourism revenue gains, especially in the shoulder seasons during spring and autumn; threat of climate-induced revenue losses in the summer months due to increased heat stress.	GDP, prices, holidays, events	(Köberl et al. 2016)

Tourism	Iran (Zayandehroud River route)	Physiologically equivalent temperature (PET)	1983–2013	HADCM3	B1, A1B	2014–2039		The PET index shows a positive trend with a reduction in number of climate comfort days (18 < PET < 29), particularly in the western area.			(Yazdanpanah et al. 2016)
Tourism	Portugal	Arrivals of inbound tourists; GDP						Increasing temperatures are projected to lead to a decrease of inbound tourism arrivals between 2.5% and 5.2%, which is expected to reduce Portuguese GDP between 0.19% and			(Pintassilgo et al. 2016)

								0.40%.			
Transportation (shipping)	Arctic Sea (North Sea route; NSR)	Climatic losses; gross gains; net gains		PAGE-ICE	RCP4.5, RCP8.5 SSP2	2013–2200		Large-scale commercial shipping is unlikely possible until 2030 (bulk) and 2050 (container) under RCP8.5.	The total climate feedback of NSR could contribute 0.05% to global mean temperature rise by 2100 under RCP8.5, adding $2.15 trillion to the net present value of total impacts of climate change over the period until 2200. The climatic losses offset 33% of the total economic gains from NSR under RCP8.5 with the biggest	Business restrictions	(Yumashev et al. 2017)

									losses set to occur in Africa and India.		
Transportation (shipping)	Arctic Sea	Sea ice ship speed (in days); sea ice thickness (SIT)	1995–2014	CMIP5	RCP2.6, RCP4.5, RCP8.5	2045–2059, 2075–2089			Shipping season 4–8 under RCP8.5, double that of RCP2.6. Average transit times decline to 22 days (RCP2.6) and 17 days (RCP8.5).		(Melia et al. 2016)
Transportation (shipping)	Arctic Sea (NSR)	Mean time of NSR transit window; sea ice concentration	1980–2014	CMIP5	RCP4.5, RCP8.5	2020–2100			Increase in transit window by 4 (RCP4.5) and 6.5 (RCP8.5) months.		(Khon et al. 2017)
Water	Europe	Runoff discharge snowpack based on hydrological models: E-HYPE Lisflood WBM		CMIP5 CORDEX (11) Bias corrected to E-OBS	RCP2.6, RCP4.5, RCP8.5	1.5°C 2°C 3°C		Increases in runoff affect the Scandinavian mountains; decreases in runoff in Portugal.	Increases in runoff in Norway, Sweden and north Poland; decreases in runoff around		(Donnelly et al. 2017)

		LPJmL							Iberian, Balkan and parts of French coasts.		
Water	Global (8 river regions)	River runoff Glob-HM Cat-HM		HadGEM2-ES IPSL-CM5A-LR; MIROCESM-CHEM; GFDL-ESM2; NorESM1-M;	RCP8.5	1°C 2°C 3°C 1971–2099		Projected runoff changes for the Rhine decrease, Tagus decrease and Lena increase with global warming.	Increased risk of decreases in low flows for Rhine (−11% at 2°C to −23% at 3°C); risk of increases in high flows increases for Lena +17% (2°C) to +26% (3°C).		(Gosling et al. 2017)

References

Arnell, N. W., J. A. Lowe, B. Lloyd-Hughes, and T. J. Osborn, 2018: The impacts avoided with a 1.5°C climate target: a global and regional assessment. Clim. Change, 147, 61–76, doi:10.1007/s10584-017-2115-9.

Byers, E., and Coauthors, 2018: Global exposure and vulnerability to multi-sector development and climate change hotspots. Environ. Res. Lett.,.

Carvajal, P. E., G. Anandarajah, Y. Mulugetta, and O. Dessens, 2017: Assessing uncertainty of climate change impacts on long-term hydropower generation using the CMIP5 ensemble---the case of Ecuador. Clim. Change, 144, 611–624, doi:10.1007/s10584-017-2055-4.

Carvalho, D., A. Rocha, M. Gómez-Gesteira, and C. Silva Santos, 2017: Potential impacts of climate change on European wind energy resource under the CMIP5 future climate projections. Renew. Energy, 101, 29–40, doi:10.1016/j.renene.2016.08.036.

Chilkoti, V., T. Bolisetti, and R. Balachandar, 2017: Climate change impact assessment on hydropower generation using multi-model climate ensemble. Renew. Energy, 109, 510–517, doi:10.1016/j.renene.2017.02.041.

Damm, A., J. Köberl, F. Prettenthaler, N. Rogler, and C. Töglhofer, 2017: Impacts of +2°C global warming on electricity demand in Europe. Clim. Serv., 7, 12–30, doi:10.1016/j.cliser.2016.07.001.

Donnelly, C., W. Greuell, J. Andersson, D. Gerten, G. Pisacane, P. Roudier, and F. Ludwig, 2017: Impacts of climate change on European hydrology at 1.5, 2 and 3 degrees mean global warming above preindustrial level. Clim. Change, 143, 13–26, doi:10.1007/s10584-017-1971-7.

Gosling, S. N., and Coauthors, 2017: A comparison of changes in river runoff from multiple global and catchment-scale hydrological models under global warming scenarios of 1°C, 2°C and 3°C. Clim. Change, 141, 577–595, doi:10.1007/s10584-016-1773-3.

Grillakis, M. G., A. G. Koutroulis, K. D. Seiradakis, and I. K. Tsanis, 2016: Implications of 2°C global warming in European summer tourism. Clim. Serv., 1, 30–38, doi:10.1016/j.cliser.2016.01.002.

Hewer, M., D. Scott, and A. Fenech, 2016: Seasonal weather sensitivity, temperature thresholds, and climate change impacts for park visitation. Tour. Geogr., 18, 297–321, doi:10.1080/14616688.2016.1172662.

Hosking, J. S., D. MacLeod, T. Phillips, C. R. Holmes, P. Watson, E. Shuckburgh, and D. Mitchell, 2018: Changes in European wind energy generation potential within a 1.5°C warmer world. Environ. Res. Lett.,.

Jerez, S., and Coauthors, 2015: The impact of climate change on photovoltaic power generation in Europe. Nat. Commun., 6, 10014, doi:10.1038/ncomms10014.

Khon, V. C., I. I. Mokhov, and V. A. Semenov, 2017: Transit navigation through Northern Sea Route from satellite data and CMIP5 simulations. Environ. Res. Lett., 12, 24010.

Köberl, J., F. Prettenthaler, and D. N. Bird, 2016: Modelling climate change impacts on tourism demand: A comparative study from Sardinia (Italy) and Cap Bon (Tunisia). Sci. Total Environ., 543, 1039–1053, doi:10.1016/j.scitotenv.2015.03.099.

McFarland, J., and Coauthors, 2015: Impacts of rising air temperatures and emissions mitigation on electricity demand and supply in the United States: a multi-model comparison. Clim. Change, 131, 111–125, doi:10.1007/s10584-015-1380-8.

Melia, N., K. Haines, and E. Hawkins, 2016: Sea ice decline and 21st century trans-Arctic shipping routes. Geophys. Res. Lett., 43, 9720–9728, doi:10.1002/2016GL069315.

Park, C., S. Fujimori, T. Hasegawa, J. Takakura, K. Takahashi, and Y. Hijioka, 2018: Avoided economic impacts of energy demand changes by 1.5 and 2 °C climate stabilization. Environ. Res. Lett., 13, 45010.

Pintassilgo, P., J. Rosselló, M. Santana-Gallego, and E. Valle, 2016: The economic dimension of climate change impacts on tourism: The case of Portugal. Tour. Econ., 22, 685–698, doi:10.1177/1354816616654242.

de Queiroz, A. R., L. M. Marangon Lima, J. W. Marangon Lima, B. C. da Silva, and L. A. Scianni, 2016: Climate change impacts in the energy supply of the Brazilian hydro-dominant power system. Renew. Energy, 99, 379–389, doi:10.1016/j.renene.2016.07.022.

Tobin, I., and Coauthors, 2015: Assessing climate change impacts on European wind energy from ENSEMBLES high-resolution climate projections. Clim. Change, 128, 99–112, doi:10.1007/s10584-014-1291-0.

——, and Coauthors, 2016: Climate change impacts on the power generation potential of a European mid-century wind farms scenario. Environ. Res. Lett., 11, 34013.

Tobin, I., W. Greuell, S. Jerez, F. Ludwig, R. Vautard, M. T. H. van Vliet, and F.-M. Bréon, 2018: Vulnerabilities and resilience of European power generation to 1.5 °C, 2 °C and 3 °C warming. Environ. Res. Lett., 13, 44024.

van Vliet, M. T. H., L. P. H. van Beek, S. Eisner, M. Fl??rke, Y. Wada, and M. F. P. Bierkens, 2016: Multi-model assessment of global hydropower and cooling water discharge potential under climate change. Glob. Environ. Chang., 40, 156–170, doi:10.1016/j.gloenvcha.2016.07.007.

Wild, M., D. Folini, F. Henschel, N. Fischer, and B. Müller, 2015: Projections of long-term changes in solar radiation based on CMIP5 climate models and their influence on energy yields of photovoltaic systems. Sol. Energy, 116, 12–24, doi:https://doi.org/10.1016/j.solener.2015.03.039.

Yazdanpanah, H., H. Barghi, and A. Esmaili, 2016: Effect of climate change impact on tourism: A study on climate comfort of Zayandehroud River route from 2014 to 2039. Tour. Manag. Perspect., 17, 82–89, doi:10.1016/j.tmp.2015.12.002.

Yumashev, D., K. van Hussen, J. Gille, and G. Whiteman, 2017: Towards a balanced view of Arctic shipping: estimating economic impacts of emissions from increased traffic on the Northern Sea Route. Clim. Change, 143, 143–155, doi:10.1007/s10584-017-1980-6.

3.SM.4 Supplementary information to Cross-Chapter Box 6 Food Security

Table 3.SM.12: Projected health risks of undernutrition and dietary change at 1.5°C and 2°C. Abbreviations: DALY: disability adjusted life year; RCP: Representative Concentration Pathway; SSP: Shared Socio-Economic Pathway

Region	***Health Outcome Metric***	***Study Baseline***	***Climate Model(S)***	***Scenario***	***Time Periods of Interest***	***Impacts at Study Baseline***	***Projected Impacts at 1.5°C***	***Projected Impacts at 2°C***	***Other Factors Considered***	***Reference***
Global and 21 regions	Undernutrition	1961–1990	BCM2.0, EGMAM1, EGMAM2, EGMAM3, CM4vl	A1B	2030, 2050		In 2030 95,175 additional undernutrition deaths without adaptation and (ensemble mean) 131,634 with adaptation under the low growth scenario and 77,205 under the high growth scenario; Asia and sub-Saharan Africa at highest risk.	In 2050 risks are generally lower in most regions because of underlying trends, with 84,695 additional undernutrition deaths without adaptation, 101,484 with adaptation under the low growth scenario and 36,524 under the high growth scenario.	Population growth; improved population health; crop models include adaptation measures	(Hales et al. 2014)

Global and 17 regions	Undernourished population; DALY (disability) caused by underweight of a child under 5 years of age	2005–2100	5 models from ISIMIP (GFDL-ESM2, NorESM1-M, IPSL-CM5A-LR, HadGEM2-ES, MIROC-ESM-CHEM)	RCP2.6 and 8.5 with SSP2 and SSP3	2005–2100	Baseline assumed no climate change (no temperature increase from present)	In 2025 under SSP3, global undernourished population is 530–550 million at 1.5°C. Global mean DALYs of 11.2 per 1000 persons at 1.5°C.	In 2050 under SSP3, global undernourished population is 540–590 million at 2.0°C. Global mean DALYs of 12.4 per 1000 persons at 2°C.	Population growth and aging; equity of food distribution	(Hasegawa et al. 2016)
Global divided into 17 regions	DALYs from stunting associated with undernutrition	1990–2008	12 GCMs from CMIP5	Six scenarios: RCP2.6 + SSP1, RCP4.5 + SSPs 1–3, RCP8.5 + SSP2, SSP3	2005–2050	57.4 million DALYs in 2005	In 2030 DALYs decrease by 36.4 million (63%), for RCP4.5, SSP1, and by 30.4 million (53%) and 16.2 million (28%) for RCP8.5, SSP2 and SSP3, respectively.	By 2050 DALYs decrease further to 17.0 million for RCP4.5, SSP1, and to 11.6 million for RCP8.5, SSP2. DALYs increase to 43.7 million under RCP8.5, SSP3.	Future population and per capita GDP from the SSP database	(Ishida et al. 2014)

References

Hales, S., S. Kovats, S. Lloyd, and D. Campbell-Lendrum, 2014: Quantitative risk assessment of the effects of climate change on selected causes of death, 2030s and 2050s. S. Hales, S. Kovats, S. Lloyd, and D. Campbell-Lendrum, Eds. Geneva, Switzerland, 115 pp.
Hasegawa, T., S. Fujimori, K. Takahashi, T. Yokohata, and T. Masui, 2016: Economic implications of climate change impacts on human health through undernourishment. Clim. Change, 136, 189–202, doi:10.1007/s10584-016-1606-4.
Ishida, H., and Coauthors, 2014: Global-scale projection and its sensitivity analysis of the health burden attributable to childhood undernutrition under the latest scenario framework for climate change research. Environ. Res. Lett., 9, 064014, doi:10.1088/1748-9326/9/6/064014.